Thirty Sixth Edition

Photovoltaics International

THE TECHNOLOGY RESOURCE FOR PV PROFESSIONALS

LONGi Green Energy Technology Supply of low-cost and high-efficiency multi-GW mono wafers
Fraunhofer ISE Solar cell demand for bifacial and singulated-cell module architectures
University of New South Wales Current state of high-efficiency perovskite solar cells
ECN Cell modifications for preventing potential-induced degradation in c-Si PV systems
GCL System Integration Technology Advanced cell and module design for solar LCOE optimization: Is the white glass–glass module the future?
TUV Rheinland Understanding the energy yield of PV modules

Second Quarter, May 2017

www.pv-tech.org

Photovoltaics International

Published by:
Solar Media Ltd.,
3rd Floor, America House, 2 America Square
London EC3N 2LU, UK
Tel: +44 (0) 207 871 0122
Fax: +44 (0) 207 871 0101
E-mail: info@pv-tech.org
Web: www.pv-tech.org

Publisher: David Owen

Head of Content: John Parnell
Managing Editor: Ben Willis
Commissioning Editor: Adam Morrison
Sub-Editor: Steve D. Brierley
Senior News Editor: Mark Osborne
Reporters: Andy Colthorpe, Tom Kenning, Danielle Ola

Design: Tina Davidian
Production: Daniel H Brown, Sarah-Jane Lee

Sales Director: David Evans
Account Managers: Adam Morrison, Graham Davie, Lili Zhu, Matthew Bosnjak

Cover image: Raw ingot for 8.4 inch monocrystalline wafers during cooling.

Image courtesy of LONGi Green Energy Technology

Printed by Buxton Press

Photovoltaics International
Thirty Sixth Edition
Second Quarter, May 2017
Photovoltaics International is a quarterly journal published in February, May, August and December.

Distributed in the USA by Mail Right International, 1637 Stelton Road B4, Piscataway, NJ 08854.

ISSN: 1757-1197

USPS Information
USPS Periodical Code: 025 313

Periodicals Postage Paid at New Brunswick, NJ
Postmaster: Send changes to: Photovoltaics International, Solar Media Ltd., C/o 1637 Stelton Road, B-4, Piscataway, NJ 08854, USA

Foreword

SNEC, with its more than 200,000 visitors, is perhaps the trade show where identifying trends among the masses is the most difficult. One that stood out over the noise this year was the lengthening list of module manufacturers offering bifacial panels. Bifacial modules are beginning to make their mark commercially (Trina Solar has already dealt with its first 20MW order) but as with any fledgling technology, new applications are always around the corner.

In this issue of *Photovoltaics International* Fraunhofer ISE (p. 48) presents a concept for a bifacial, shingled cell technology that it claims tracks a cost-effective route to a 400W module using existing industrial-scale concepts.

One trend now much more than a notion is the ongoing switch to monocrystalline cell technology. Recent findings from our market research team's PV Manufacturing & Technology Quarterly report has forecast a 49% market share for mono in 2018 before seizing the majority share among c-Si cells in 2019. Mono wafer production giant LONGi discusses a number of approaches across manufacturing processes and materials that it believes will see further reductions in cost and improvements in efficiency in the near term (p.38).

Meanwhile the University of New South Wales (p.66) pulls together and critically assesses the raft of research on perovskite PV technology. While the potential of the new thin-film material is plain to see, the UNSW highlights some key areas where further innovation will be required to push the technology into a commercially viable position.

Another highlight, provided by ECN Solar Energy (p.84), reviews potential mitigation options at a cell level to reduce the impact of the increasingly notorious PID problem. Headaches from PID-related issues are on the rise, with reports of PID presenting in modules installed in hot and humid emerging markets as early as one year into operation. While the ECN team primarily focusses on n-PERT cells, they also review options for other cell architectures.

Following the success of our PV CellTech conference, we're also introducing our new PV ModuleTech event focusing on the technology that turns completed cells into supplied modules in the commercial market. Conference chair and head of our market research team, Finlay Colville, explains more about the motivation for the event against the backdrop of progressively more diverse, and complex, module technology options (p.19).

Whichever way these morphing cell and module technology trends turn, we'll make sure *Photovoltaics International* is on hand to guide you through the process.

John Parnell
Head of Content
Solar Media Ltd

Photovoltaics International

Photovoltaics International's primary focus is on assessing existing and new technologies for "real-world" supply chain solutions. The aim is to help engineers, managers and investors to understand the potential of equipment, materials, processes and services that can help the PV industry achieve grid parity. The Photovoltaics International advisory board has been selected to help guide the editorial direction of the technical journal so that it remains relevant to manufacturers and utility-grade installers of photovoltaic technology. The advisory board is made up of leading personnel currently working first-hand in the PV industry.

Editorial Advisory Board

Our editorial advisory board is made up of senior engineers from PV manufacturers worldwide. Meet some of our board members below:

Prof Armin Aberle, CEO, Solar Energy Research Institute of Singapore (SERIS), National University of Singapore (NUS)

Prof Aberle's research focus is on photovoltaic materials, devices and modules. In the 1990s he established the Silicon Photovoltaics Department at the Institute for Solar Energy Research (ISFH) in Hamelin, Germany. He then worked for 10 years in Sydney, Australia as a professor of photovoltaics at the University of New South Wales (UNSW). In 2008 he joined NUS to establish SERIS (as Deputy CEO), with particular responsibility for the creation of a Silicon PV Department.

Dr. Markus Fischer, Director R&D Processes, Hanwha Q Cells

Dr. Fischer has more than 15 years' experience in the semiconductor and crystalline silicon photovoltaic industry. He joined Q Cells in 2007 after working in different engineering and management positions with Siemens, Infineon, Philips, and NXP. As Director R&D Processes he is responsible for the process and production equipment development of current and future c-Si solar cell concepts. Dr. Fischer received his Ph.D. in Electrical Engineering in 1997 from the University of Stuttgart. Since 2010 he has been a co-chairman of the SEMI International Technology Roadmap for Photovoltaic.

Dr. Thorsten Dullweber, R&D Group Leader at the Institute for Solar Energy Research Hamelin (ISFH)

Dr. Dullweber's research focuses on high efficiency industrial-type PERC silicon solar cells and ultra-fineline screen-printed Ag front contacts. His group has contributed many journal and conference publications as well as industry-wide recognized research results. Before joining ISFH in 2009, Dr. Dullweber worked for nine years in the microelectronics industry at Siemens AG and later Infineon Technologies AG. He received his Ph. D. in 2002 for research on Cu(In,Ga)Se2 thin-film solar cells.

Dr. Wei Shan, Chief Scientist, JA Solar

Dr. Wei Shan has been with JA Solar since 2008 and is currently the Chief Scientist and head of R&D. With more than 30 years' experience in R&D in a wider variety of semiconductor material systems and devices, he has published over 150 peer-reviewed journal articles and prestigious conference papers, as well as six book chapters.

Chen Rulong, Chief Technology Officer, Solar Cell R&D Department, Wuxi Suntech

Chen Rulong graduated from Changchun Institute of Optics and Fine Mechanics, majoring in applied optics. He began working in the field of R&D on solar cells from 2001. He is a visiting fellow at the University of New South Wales in Australia and an expert on the IEC Technical Committee 82, which prepares international standards on PV energy systems.

Florian Clement, Head of Group, MWT solar cells/printing technology, Fraunhofer ISE

Dr. Clement received his Ph.D in 2009 from the University of Freiburg. He studied physics at the Ludwigs-Maximilian-University of Munich and the University of Freiburg and obtained his diploma degree in 2005. His research is focused on the development, analysis and characterization of highly efficient, industrially feasible MWT solar cells with rear side passivation, so called HIP-MWT devices, and on new printing technologies for silicon solar cell processing.

Sam Hong, Chief Executive, Neo Solar Power

Dr. Hong has more than 30 years' experience in solar photovoltaic energy. He has served as the Research Division Director of Photovoltaic Solar Energy Division at the Industry Technology Research Institute (ITRI), and Vice President and Plant Director of Sinonar Amorphous Silicon Solar Cell Co., the first amorphous silicon manufacturer in Taiwan. Dr. Hong has published three books and 38 journal and international conference papers, and is a holder of seven patents. In 2011 he took office as Chairman of Taiwan Photovoltaic Industry Association.

Matt Campbell, Senior Director, Power Plant Products, SunPower

Matt Campbell has held a variety of business development and product management roles since joining the SunPower, including the development of the 1.5MW AC Oasis power plant platform, organized SunPower's power plant LCOE reduction programmes, and the acquisition of three power plant technology companies. Campbell helped form a joint venture in Inner Mongolia, China for power plant project development and manufacturing. He holds an MBA from the University of California at Berkeley and a BBA in Marketing, Finance, and Real Estate from the University of Wisconsin at Madison.

Ru Zhong Hou, Director of Product Center, ReneSola

Ru Zhong Hou joined ReneSola as R&D Senior Manager in 2010 before being appointed Director of R&D in 2012. Before joining ReneSola he was a researcher for Microvast Power Systems, a battery manufacturer. His work has been published in numerous scientific journals. He has a Ph.D. from the Institute of Materials Physics & Microstructures, Zhejiang University, China.

Contents

FUSION TALESUN CLOUD MANAGEMENT CENTER

(PV POWER PLANT O&M SERVICES)

- Full-scale inline optical and electrical dual-channel PV power plant management
- Providing complete smart data control and analysis
- Complete life-cycle monitoring, maintenance of systems and components

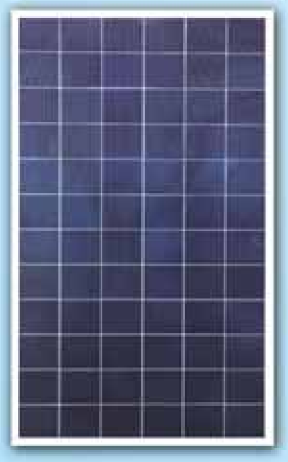

MBB SOLAR PANEL PRODUCT

(HIGH EFFICIENCY, RELIABILITY, INCREASED KWH AND LOWER LCOE)

- Greater light capture
- Less resistance losses from grid pattern multi busbars
- Additional 30% silver cost reduction
- Improved module reliability

扫一扫 与我们互动

SUZHOU TALESUN SOLAR TECHNOLOGIES CO., LTD.

E:sales@talesun.com | W: www.talesun.com | T:+86 512 8235 5888 | F: +86 512 8235 5588

Contents


MEYER BURGER
Just imagine: photovoltaics got it off the ground.
Flying around the globe powered only by solar energy! We are proud to be part of a project which achieved such impressive success.
We invest all our efforts into clean, sustainable technologies. Our ambitious people make a better future come true for all mankind. We know how to efficiently turn the infinite power of the sun into energy by spanning the entire process chain from the wafer through cell production to the complete solar module.
“Meyer Burger is on track into a decarbonized future.”
André Borschberg & Bertrand Piccard, co-founders of Solar Impulse
Meyer Burger provided the premium technology, which was used to connect the over 17,000 high-efficiency solar cells to the 269.5 m² wing panel of the Solar Impulse airplane, which collects up to 340 kWh of solar energy per day.
www.meyerburger.com
SOLARIMPULSE
www.solarimpulse.com
© Solar Impulse | Revillard | Rezo.ch

Product Reviews

Alfartec

Alfartec's BlueSky-MT240 solar simulator provides long light pulse and good spectral matching

Product Outline: Alfartec's BlueSky-MT240 solar simulator is based on LED and halogen technologies, making it ideal for production, research and certification. Its long flash duration and short cycle time are suitable for all module technologies.

Problem: When testing PV modules, one of the important points is to have enough light intensity with LED at low price in the IR region. A limitation of most flashers is the limited illumination time due to the xenon flashtubes. Therefore a system using LED illumination instead, combined with halogen lamps, would allow the best spectral coverage of the solar spectrum, at reasonable costs.

Solution: The idea behind the BlueSky-MT240 solar simulator is to provide the long light pulse and good spectral matching needed by actual and future cell technologies. LEDs and halogen lamps are also extremely long-lasting light sources, so no service except calibration is needed for several years of normal operation. Using LEDs and halogen lamps, the MT240 has a wide range spectrum, from 350nm to 1200nm, which enables highly accurate solar module efficiency measurements for all solar technologies.

Applications: PV module solar simulation tester for R&D, testing houses and volume production lines.

Platform: The system can illuminate in continuous light so the cycle time can be reduced on a production line between each module or cell measurement. The halogen lamps provide better accuracy on the spectrum range than for an LED tester in the IR region from 900nm to 1200nm. This system can be used for any technology of module and cell providing a minimum of pulse duration of 100ms to continuous light.

Availability: Currently available.

Agfa

Agfa's 'UNIQOAT' is a single layer backsheet with high reflectivity

Product Outline: Agfa Specialty Products' 'UNIQOAT' is a polyester-based backsheet product that eliminates the risk of backsheet delamination as it is manufactured as a single layer backsheet.

Problem: In the design of a PV solar module, one of the performance targets is the maximization of the light capture by the cells. In a completed module about one quarter of the radiation is not reaching the cells and cannot contribute to the generation of electrical power. The sunrays that enter a module via the gap between the cells are lost for power generation unless the backsheet can reflect them to reach the cells. Today, the most used polyester-based backsheet structures feature two or three film layers that are laminated together using an adhesive component. Such a laminate structure is the weakest link in a solar module because the adhesion strength between its layers is lower than the bonding strength between the other components in the module.

Solution: Agfa's UNIQOAT backsheet achieves a high level of reflectivity and thereby offers increased module power output, according to the company. UNIQOAT eliminates the risk of backsheet delamination because it is conceived and manufactured as a single layer. During the extrusion process the hydrolysis and UV resistant polyester is surface-modified to face the challenges to which it will be exposed and to actively contribute to more reliable and durable solar modules.

Applications: PV module lamination.

Platform: UNIQOAT backsheets are offered to the market in three product types depending on thickness and weathering properties: UNIQOAT 315, UNIQOAT XR 315 for extra reflectivity and UNIQOAT XR 330F for additional protection.

Availability: Available since April 2017.

HT-SAAE

HT-SAAE offers high-efficiency small format PV module with 250W output

Product Outline: Shanghai Aerospace Automobile Electromechanical Co., (HT-SAAE) has introduced a new lineup of high-efficiency monocrystalline PV modules under its 'HyperC' Series brand. The modules adopt PERC technology and can reach output power of 300W and above for a 60-cell module.

Problem: High-efficiency PV modules are increasingly being used for residential rooftop PV systems as incentives typically have declined under feed-in tariffs. Smaller area rooftop installations can be limited in the number of modules installed in overall system design due to the larger 60-cell module format. Providing smaller modules such as 50-cell formats can potentially provide greater system size and therefore adoption to maximize self-consumption and FiT payments where applicable.

Solution: The HyperC Series PV modules feature 5BB (busbar) cell technology, anti-PID cells and high reliability encapsulation material. The two products come with lower series resistance, higher cell conversion efficiency and higher power output per unit, according to the company. HT-SAAE also developed the HyperC PV module in a smaller 50-cell format) as relatively compact and light product offering for smaller area residential rooftops with a length and width ratio of 2:1 that fits easier with smaller roofs. Although relatively compact, the maximum power output can still reach 250W.

Applications: Residential rooftops including small area rooftops in a 50-cell module format.

Platform: The HyperC includes techniques developed and deployed with the company's 'HIGHWAY' series such as PERC cell technology with 5BB and lower series resistance with output power of 300W and above for a 60-cell module.

Availability: Currently available.

Product Reviews

PLANT PV

PLANT PV launches 'Silver-on-Aluminum' paste that provides a 1% increase in power output for c-Si cells

Product Outline: PLANT PV's 'Silver-on-Aluminum' paste is claimed to lead to a 1% increase in relative power output for c-Si solar cells.

Problem: Conventional silicon solar cells have a rear tabbing layer that does not form a back-surface field and lowers the open-circuit voltage and fill factor of the solar cell. Commercial solar cells typically lose between 0.05-0.15% (absolute) because of this.

Solution: PLANT PV has developed novel particles that are mixed with silver to form a paste that during co-firing prevents silver/aluminum inter-diffusion, while strengthening the underlying aluminum layer. This allows for the full formation of the back-surface field and aluminum-silicon eutectic layer. PLANT PV recently demonstrated a 0.15% absolute efficiency gain over cells using conventional rear-tabbing pastes on multi-crystalline silicon solar cells at Fraunhofer ISE in Germany. Greater gains are said to be achieved for monocrystalline wafers.

Applications: The Ag-on-Al paste is a drop-in replacement for conventional rear tabbing pastes and only requires the PV cell maker to change the print order of the rear aluminum paste and tabbing paste during production.

Platform: Silver-on-Aluminum paste provides cell manufacturers with the ability to print the paste directly onto dried aluminum film, allowing them to cover the entire back of the wafer with aluminum paste and obtain the beneficial passivation of a continuous aluminum back-surface field.

Availability: PLANT PV is now entering into testing with select customers.

Heraeus

HeraGlaze from Heraeus provides SiO2 diffusion barrier coating for multicrystalline silicon ingot production

Product Outline: Heraeus Photovoltaics has introduced 'HeraGlaze,' a high-purity SiO2 diffusion barrier coating for enhanced crucible performance. It is the first product of Heraeus Photovoltaics beyond solar cell metallization pastes.

Problem: Multicrystalline ingot/wafer manufacturers require new ways of increasing the bulk lifetime of the wafer to reduce the solar cell efficiency gap with monocrystalline cells. This has become a growing issue with the adoption of mono-PERC processes.

Solution: HeraGlaze is used in the first step of the cell manufacturing process, when silicon blocks are melted into a single silicon ingot. This early process is crucial for the quality of the ingots and thus of the final product – the wafers. The product comes as a slurry, which is applied on the porous surface of the crucibles. This can be done through retrofitting or upgrading of existing crucibles, meaning no additional expenditures on new crucibles are required. HeraGlaze acts as a barrier preventing thermally induced impurities such as iron being transferred from the crucible into the silicon ingot during the melting and crystallization of silicon. The higher wafer yield is achieved by increasing the usable section of a silicon ingot.

Applications: HeraGlaze is a high-purity SiO2 diffusion barrier coating for multicrystalline silicon ingot production.

Platform: With HeraGlaze the wafer yield is increased by up to 4% and cell efficiency is improved by 0.1%, according to Heraeus. Assuming an annual wafer production of 50GW today, HeraGlaze would be able to deliver close to an additional 2GW per year without increasing wafer production capacity.

Availability: Available since March 2017.

Heraeus

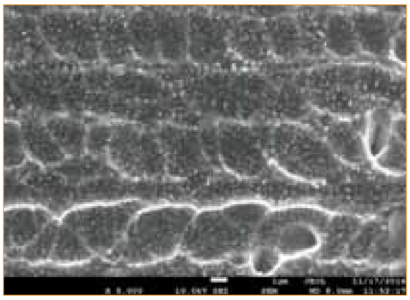

Heraeus SOL9641A series frontside silver paste was specifically designed for black silicon wafers

Product Outline: Heraeus Photovoltaics has launched a specifically designed frontside silver paste to provide improved contact ability diamond wire cut wafer with 'Black Silicon' texture

Problem: As the PV industry continuously improves cost-to-performance ratio for the p-type multicrystaline cells, the diamond wire cut wafer with 'black silicon' texture is the new avenue to achieve improvements. However, the nano-structured Black-Silicon surface prepared by special texturing process (such as RIE and MCCE) boots efficiency gain, but also gives challenges to metallization paste contact ability.

Solution: Heraeus SOL9641A series frontside silver paste was specially re-designed for black-silicon texturing. It features unique glass chemistry for contacting unique silicon surface and fine-tuned organic media matching nano-structured surface morphology. This has resulted in well-balanced metallization contact and Voc. After low temperature firing the microstructure of the fired finger has an increased densified structure including the Ag-Silicon interface, enhancing adhesion, grid resistivity and solder ability.

Applications: The SOL9641A is used with multicrystalline Black-Silicon cell and is tailored for ultra-fine-line printability for screen printing that can print defect-free through a less than 30µm screen opening.

Platform: SOL9641A has a wide firing window, which makes the paste specifically suitable for the application on PERC solar cells. The patent-pending paste technology provides excellent adhesion, which is almost two times higher than SOL9631 Series.

Availability: Available since April 2017.

Product Reviews

Singulus Technologies

Singulus Technologies 'GENERIS' PVD system produces heterojunction cells above 22% conversion efficiencies

Product Outline: Singulus Technologies' 'GENERIS' PVD inline sputtering system for heterojunction (HJ) cells is claimed to produce conversion efficiencies of more than 22%, as well as reducing manufacturing costs.

Problem: Sputter damage to the amorphous silicon passivation layers is caused by plasma photons in the range of 2.5 to 4.15eV, which cause carrier lifetime degradation in HJ cells. Charge carrier mobility and electron density need to be optimized to minimize free carrier absorption in the ITO film. To reach high efficiencies, the hetero-interface state density should be minimalized.

Solution: The GENERIS physical vapour deposition(PVD) system is a horizontal inline sputter tool designed for special requirements in high-efficiency cell production. On top of the silicon layers, an antireflective TCO is deposited by PVD and the charge collection is made by a screen-printed metallic contact. A heterojunction cell performance of 22.3% was achieved in cooperation with a research institute, according to the company.

Applications: The GENERIS PVD system is suited for challenging transparent conductive oxides layers like ITO and AZO to match the key requirements of heterojunction cell technology.

Platform: With the GENERIS PVD sputtering system, contact layers can be deposited on the front and rear of the Si wafers without the need to turn the wafers between coating processes and without vacuum interruption. By using rotatable sputtering cathodes, highest target utilization is achieved and offers lowest production costs.

Availability: Available since April 2017.

DuPont

DuPont Photovoltaic's 'Solamet' PV20A offers more than 0.1% improvement in cell efficiency

Product Outline: 'Solamet' PV20A, the newest addition to DuPont's photovoltaic metallization paste range, is designed for both Lightly Doped Emitter (LDE) and Passivated Emitter Rear Cell (PERC) p-type solar cell construction.

Problem: Continued conversion efficiency gains for p-type solar cells are required. Solar cells fabricated with a LDE can achieve a significant gain in open-circuit voltage (Voc) due to a reduction in the front surface area and improved emitter recombination.

Solution: Solamet PV20A provides further aspect ratio improvement and superior contact, resulting in a more than 0.1% improvement in efficiency compared to other metallization pastes, according to the DuPont. The metallization paste was developed to enable exceptional ultrafine line printing and contact performance with lower firing temperature, and is ideally suited to maximize efficiency for the most demanding conventional and PERC architectures while also ensuring reliable production performance.

Applications: LDE and PERC p-type solar cells.

Platform: Solamet PV20A uses DuPont's proprietary tellurium technology. Solamet PV20A is already being used by Taiwan Solar Energy Company (TSEC), which has demonstrated 21.15% cell efficiencies and module power output as high as 305Watts (60-cell) in its V-Series mono PERC modules. Another adoption comes from REC Group, with its TwinPeak 2 Series, 60-cell multicrystalline solar panel, rated up to 295Wp.

Availability: Available since April 2017.

Heraeus

Heraeus launches front side silver pastes for 'knotless screen' printing

Product Outline: Heraeus Photovoltaics has introduced specially developed metallization pastes for 'knotless screen' printing of solar cells. The new SOL9641AX/BX series is designed to realize the full advantages of knotless printing screens.

Problem: Different from the conventional metal wire mesh, the knotless screen with so-called 'zero degree mesh,' can give more room for silver paste to go through the mesh compared to conventional screens, while conventional screens usually need adjustment printability. However, specially developed metallization pastes are required to maximize the key benefits of knotless screen printing to obtain higher aspect ratio on ultra-fine-line fingers.

Solution: The SOL9641AX and SOL9641BX have been built on two product platforms, 9641A and 9641B. Both 9641AX and 9641BX provide conversion efficiency gains by only the switch in screens, which gives great cost advantage. Compared to conventional paste, 9641AX and 9641BX can achieve much better aspect ratio (AR) for fired fingers (0.3 AR versus 0.5 AR), which results a gain in Isc and FF, therefore providing efficiency improvements; Heraeus said a 0.1% efficiency gain can be achieved.

Applications: SOL9641AX is suitable for black silicon, while SOL9641BX has a wide process window for PERC and ultra-lightly-doped-emitters. The pastes are compatible with both monocrystalline and multicrystalline wafers.

Platform: SOL9641AX/BX features a unique paste rheology, enabling a higher aspect ratio on ultra-fine-line fingers, which can print defect-free through a less than 26μm screen opening in high throughput mass production.

Availability: Available since April 2017.

Independent module testing under field conditions.

The key to reliable yield estimates and investment success.

Why should modules be tested under field conditions?
Real field tests help you adapt your PV modules to actual conditions. This way, you can improve module durability and reliability, maximizing energy production.
Recognized test procedures underpin the long-term stability of a project and lower investment risks. Real field-testing by a third party not only helps you convince EPCs, investors and lenders, but also provides you with useful R&D data and strengthens your market position.

Why TÜV Rheinland?
For more than 35 years, we have researched, developed and applied methods for evaluating modules and components under field conditions and in our laboratories. We operate a growing number of test sites in different climate conditions including dry/hot sites in North America and the MENA region, a Central European moderate climate site and a tropical site in Asia.
Make your PV project a success with TÜV Rheinland.

www.tuv.com/solar

TÜVRheinland®
Precisely Right.

Product Reviews

InnoLas Solutions

InnoLas Solutions ILS-TTnx laser system offers high-throughput PERC cell contact opening

Product Outline: InnoLas Solutions' new high throughput laser workstation for various applications offers throughput of up to 6,000 wafers per hour (wph).

Problem: In the past the throughput of laser machines typically was limited to 3,000 to 4,000wph while modern solar cell production lines are increasing their output above 4,000wph. This means laser machines are increasingly becoming a bottleneck in the fabrication of high efficiency solar cells. Should a solar cell production line be operating at a throughput of 5,000wph and the throughput of the laser machine is limited to less than 4,000wph, it could require two laser machines to be deployed. This would increase the capex required for the production line but the second tool would be underutilized.

Solution: The InnoLas Solutions, ILS-TTnx enables an increase in the throughput beyond 4,000wph without increasing the tool footprint. The compact design of the ILS-TTnx saves factory space and lowers the overall cost of ownership.

Applications: The ILS-TTnx laser workstation is suitable for various process applications such as laser contact opening (LCO) for PERC solar cells, laser doped selective emitter (LDSE) and front side LCO for the upcoming copper plating on silicon (PoSi) metallization technology.

Platform: The ILS-TTnx can reach a throughput of up to 6,000 wph and beyond. The machine can be configured as fully automatic stand alone platform with cassette-to-cassette operation, or integrated into any inline production system such as e.g. a screen printing line.

Availability: Available since April 2017.

3D-Micromac

3D-Micromac's latest microCELL OTF laser systems has throughput of 8,000wph

Product Outline: 3D-Micromac launched the second generation of its high-performance microCELL OTF laser systems at SNEC 2017. The high-performance production solution for Laser Contact Opening (LCO) of PERC cells achieves a throughput of 8,000 wafers per hour (wph).

Problem: Solar cell manufacturers are under pressure to increase cell efficiency while simultaneously reducing manufacturing costs. In the LCO process the protection of the sensitive front side of the cell is especially important. Scratching and contaminants impair the cell or can increase light-induced degradation (LID).

Solution: The industry-proven microCELL OTF systems produce a selective opening on backside-passivated multi- and monocrystalline solar cells to allow more light to be absorbed by the solar cell. The newly introduced second-generation system provides a throughput of more than 8,000wph, double the throughput of the previous generation. This is facilitated by dual-lane wafer handling and on-the-fly laser processing. The new tool generation meets customers' requirements for inline integration into two- or three-line metallization machinery since the throughput of the single laser process step now matches that of the other process steps, ensuring that the laser process is not the bottleneck in material flow.

Applications: Besides PERC, the tool can also be used for laser-doped selective emitter processes.

Platform: The system offers precise surface structuring, low operating costs and highest availability, according to the company. The contactless cell handling enables processing without surface defects and microcracks.

Availability: Available since April 2017.

4JET

4JET's high volume system lowers costs for back end processing of CIGS panels

Product Outline: 4JET microtech has developed a high-throughput solution that enables laser edge deletion, busbar exposure and via drilling operations of CIGS glass substrates. Each of the new Mass Production Combi Tool (MPCT) units can process 100MW of typical CIGS substrates per annum.

Problem: In relation to large-scale CIGS thin-film fabs, up to now the three process steps would require at least five process lines with a total of up to 15 machines to carry out the backend processing of CIGS panels.

Solution: The 4JET microtech MPCT system cuts down the number of units required to only three and provides for approximately 30% savings in capex, 50% shorter ramp-up times and a 30% smaller factory footprint, according to the company. The high-precision laser edge deletion module allows a reduction in panel edge dead zones, enhancing module efficiencies (1Wp per 150Wp module). This is achieved by processing substrates on vacuum tables and smart image processing. The busbar exposure module is equipped with a quick exchange blade system and process validation capabilities. The glass drilling module enables freeform shaping of vias including an edge chamfer for low-stress wire attachments.

Applications: Combination of three processes within one tool for thin-film solar cell modules such as CIGS or perovsike modules, which include edge deletion for isolation at the outer perimeter of the module, busbar exposure for subsequent string connection process and glass drilling for connection of the junction box.

Platform: The MPCT is said to provide yields of 99.8% and machine uptime of >95%.

Availability: Currently available.

Market Watch

News

Suniva asks Trump for 78 cents price floor on imported modules

Bankrupt US manufacturer Suniva has filed an anticipated petition requesting a minimum import price (MIP) of 78 cents on Chinese modules.

The Section 201 request, the first in the US for 16 years, asks the US International Trade Commission (US ITC) to consider whether imports have been the major factor in the US solar manufacturing industry's woes. If it agrees, it will make a recommendation to the White House with any action ultimately the decision of President Trump.

The tariffs would be applied to any module not produced in the US unless catered for in the design of any trade remedies. According to the petition, seen by PV Tech, the floor price would fall to 72 cents in the second year, 69 cents in year three and 68 cents in year four.

Credit Dave Newman/Flickr

Suniva has threatened to spark a new US-China trade ware with its minimum import price request.

A similarly structured price floor on cells would start at 40 cents per cell falling to 33 cents by year four.

The complaint is not a revival or renewal of the longstanding anti-dumping and anti-subsidy cases, however, it's something different all-together. The so-called Section 201 case has different procedures, thresholds and decision making processes.

Unlike in some jurisdictions for anti-dumping cases where the complaint must be shown to come from a body that is representative of a majority or at least large collective of that country's domestic industry, a 201 complaint can come from one company typical of that industry, one trade body, a union or even a more informal group of workers.

Trade

Price of Chinese module imports to India dropped 8% in Q1 2017

The price of Chinese module imports to India has dropped 8% over the last quarter and 29% year-on-year, according to new price indices calculated by consultancy firm Bridge to India.

The consultancy has analysed import prices for modules and inverters, as well as costs of utility-scale and rooftop EPC, by interviewing up to 10 leading project developers, EPC firms and module suppliers.

Looking specifically at multi-crystalline PV module imports from China for orders of minimum 50MW in size, Bridge to India calculated cost, insurance and freight (CIF) to India, not including any further port or inland transportation costs.

Module prices have been falling steeply due to oversupply combined with quarterly demand fluctuations in China.

European Commission confirms 18-month extension of solar trade duties

The European Commission has confirmed that it will extend its anti-dumping and anti-subsidy duties on cells and modules imported from China by 18 months, a reduction from the 24 months first proposed, according to trade body SolarPower Europe.

The Commission has also agreed to a gradual phase-out of the measures.

EU member states had already passed the 18-month extension of the punitive trade duties in February, having rejected the originally proposed 24-month extension in January.

James Watson, chief executive of SolarPower Europe, said: "As expected following the pressure exerted on the Commission by the member states, it has decided to prolong the anti-dumping and anti-subsidy measures for 18 months. We consider this an improvement."

Last month, SolarWorld vice president Milan Nitzschke welcomed a revamp of the MIP but was disappointed not to see an extension beyond even the two years initially proposed.

Credit European Commission

The European Commission has confirmed another 18 months of trade duties on Chinese solar imports.

Four Chinese PV manufacturers withdraw from MIP

Chinese PV manufacturers Jetion Solar, Hareon Solar, GCL Technology and Talesun have now been fully withdrawn from the Minimum Import Price (MIP) undertaking, according to the European Commission.

Jetion Solar, Hareon Solar and GCL Technology had already notified the commission in October 2016 that they wished to withdraw from the undertaking, while Talesun followed suit in January this year.

The news follows the commission's decision to extend its solar trade duties by 18 months, while launching an interim review into the effectiveness of its anti-dumping and anti-subsidy measures.

Credit GCL System Integration

China's predicted installs 2017 remain a matter of debate, leading to varying forecasts for the year.

Global Trends

2017 global PV demand forecasts as high as 85GW

Global PV demand for 2017 could be as high as 85GW according to market research firm GTM.

The figures published on Tuesday coincided with that of rival firm IHS Markit, which has predicted a lower tally of 79GW.

The latter's prediction of negligible growth on its 2016 figure of 78GW is attributed to poor performance in the three largest markets of China, the US and Japan.

GTM Research has forecast that by the end of 2017, India will have overtaken Japan to become the third-largest PV end market demonstrating that India can hardly be considered an emerging market.

China has proven to be a difficult market to forecast with state-level proclamations capable of shifting the industry on its axis.

Both firms expect recent deployment growth in China to tail off with IHS going further and betting on a fall in installations during 2017.

Solar will drop below two cents in 2017: GTM

A solar power project is likely to register a per-kWh price below two US cents at some stage during 2017, according to analyst firm GTM Research.

As part of its 2017 market forecast, the company suggested that an impending tender round in Saudi Arabia was the most likely contender following on from a 2.3 cents tender for the Sweihan project under similar conditions in Abu Dhabi.

"Similar to the conditions that brought record low bids in Sweihan, namely a long project timeline, an escalating or split tariff, near-zero land cost, permitting costs, taxes, and most significantly, highly attractive financing terms, the first Saudi tender could create a perfect storm for another record-setting bid that could dip below two cents," Ben Attia, research associate at GTM Research and lead author of the report told PV Tech.

The Saudi Arabian market has long been "the next big thing" but substantial tenders failed to emerge. A target of 9.5GW of renewable power capacity by 2023 replaced a goal to invest US$109 billion in solar over the course of 20 years.

Global clean energy investment drops as US and China scale back on renewables

Global clean energy investment in the first quarter of 2017 was down 17% compared to Q1 2016, as market leaders China and the US scaled back support for wind and solar farms.

The latest figures from Bloomberg New Energy Finance (BNEF) reveal that despite the lower year-on-year figures, Q1 2017 was only down 7% on Q4 2016. Regardless of a tepid start to the year for the global clean energy market, this quarter saw higher than normal equity raising from public markets and venture capital.

Some good news for the quarter was marked by a US$1.4 billion public market share sale by Tesla, and US$650 million investment by Enel for its 754MW Villanueva project in Mexico.

"Q1 this year reflects, once again, the declines in average capital costs per megawatt for wind and solar," said Jon Moore, CEO of BNEF. "This trend means that year by year it's possible to finance equivalent amounts of capacity in these technologies for fewer dollars."

Overall the US and China saw a slow-down in their clean energy investment, with the latter down 11% to just US$17.2 billion in Q1 and the former down 24% with just US$9.4 billion.

Market Leaders

China installed 7.21GW of solar in Q1 2017, curtailment issues remain

China added 7.21GW of solar PV in the first quarter of the year, roughly 70MW more than in Q1 2016, according to figures from China's National Energy Administration (NEA).

Of this capacity, 4.78GW were utility-scale solar and 2.43GW were distributed PV installs.

However, NEA noted continued grid constraints and curtailment of solar energy generation in several states particularly Xinjiang (39%), Gansu (19%) and Ningxia (10%).

The country's cumulative deployment stood at 84.63GW by the end of Q1, of which 72GW is utility-scale. Last year, China added 34.24GW.

Beijing-based Asia Europe Clean Energy Advisory (AECEA) released a chart showing that demand is likely to stay strong until a feed-in tariff (FiT) deadline is reached. After this levels of deployment levels remain relatively uncertain.

Japan could strip FiT for a quarter of approved clean energy pipeline

Japan may remove feed-in tariff (FiT) support for a significant number of clean energy projects certified before July last year, because they missed a deadline to secure grid access, according to provisional estimates from the Ministry of Economy, Trade and Industry (METI).

Out of the 3.15 million clean energy projects with a combined total of 106.5GW capacity that had secured approval for the subsidy by the end of June 2016, an estimated 456,000 projects, with a combined capacity of 27.7GW, have missed the 1 April deadline and could soon lose access to this support mechanism.

This means roughly 26% of certified capacity and 14.5% of individual projects could be affected.

However, projects that received certification after 1 July 2016 still have nine months to secure grid access.

In March, Toshimitsu Fujiki, a director at METI, announced that Japan would be lowering its FiT payments once again, while a multi-gigawatt pipeline of unbuilt large-scale PV projects would be cancelled and lose their rights to the FiT at the beginning of April.

Some 57GW of large-scale PV projects were registered for the FiT in the first two or three years of the scheme's introduction after 2012, with would-be developers taking advantage of relatively relaxed rules on what constituted a project's planning documents.

India to add nearly 10GW solar in 2017 – Mercom

Mercom Capital Group has forecasted India to add 9,812MW of solar PV this year, well up from its previous projection of 9,020MW in January.

This would also be a 130% increase on the 4.3GW India installed last year, and the Asian country is widely expected to become the world's third largest PV market during 2017.

The consultancy's latest quarterly market said that overall deployment had reached 12.8GW by the end of Q1 this year. Meanwhile, the pipeline of utility-scale projects under development stands at roughly 12.6GW, with around 6.1GW of tenders awaiting auctions.

The pipeline is still primarily being driven by the flagship programme National Solar Mission (NSM), which has seen significant capacities tendered. State-level policies and tenders were the second main driver.

Southern states are dominating the pipeline with Karnataka, Andhra Pradesh and Telangana all having more than 2GW in development or ready for auction.

Trump halts Clean Power Plan litigation

The US Court of Appeals for the District of Columbia has granted the Trump administration's request to freeze the ongoing litigation over the Clean Power Plan.

The federal court's decision to pause the legal battle over whether the Plan was causing the Environmental Protection Agency (EPA) to act beyond its legal powers leaves many concerned that the freeze may be for good. The stalling of legal action, without a Supreme Court decision on the CPP, also puts the Plan at risk of being revoked completely.

For now, the litigation has been halted for at least 60 days. The plan itself has been suspended since February 2016 when the Supreme Court put the regulations on hold whilst under review.

A coalition of 28 states led by coal bastion West Virginia originally took the EPA to court over the Plan, asserting that the former had gone too far in targeting existing coal-fired and natural gas plants in an effort to reduce emissions.

But now, that lawsuit has been suspended for two months after Trump requested a delay on the ruling, despite the objections of two dozen states and scores of environmental groups who were awaiting a final decision on the regulation.

Credit Adani Solar

India's solar boom looks set to continue in 2017, with projections of nearly 10GW this year.

Module tech under the microscope

John Parnell, Head of Content, Solar Media

ABSTRACT
From 400W panels, multi-busbars, glass-glass, new materials and fresh designs, module technology is more advanced and more varied than at any other time. Having pulled together a throng of senior PV technology experts for our PV CellTech conference, PV Tech's head of market research, Finlay Colville, discusses the need to match these advances with a dedicated event this November.

It's always nice when someone tells you directly that you can't do something to set out and prove them wrong.

Photovoltaics International, its sister title PV-Tech.org and their publisher Solar Media were told in the early phases of planning the inaugural PV CellTech conference, that pulling together a string of CTOs and R&D heads from the some of the biggest firms in the cell processing supply chain would not be possible. Following the event's second outing in March 2017, we have now done it twice.

Dr. Pierre Verlinden, Chief Scientist at Trina Solar, Qi Wang, Chief Scientist at JinkoSolar and Dr. Markus Fischer, Director of R&D Processes at Hanwha Q CELLS, are among the names that have joined us since. In November his year, we'll be putting together a similarly stellar line-up catering for everything the PV manufacturing supply involves once the cell is complete.

"There hasn't been this type of event before," says Finlay Colville, chair of both conference and head of market research at PV Tech. "Our experience from doing the PV CellTech event in the last couple of years is that this is a high-tech industry so showing data to back up the claims and predict future trends is absolutely critical and I'm convinced that module suppliers will gravitate towards this event as being an excellent forum to talk about their products."

The motivation for the conference is rooted in the additional complexity, sophistication and sheer variety of technologies that could theoretically differentiate identical sets of cells rolling off the same production line.

"Similar to cells, modules have really moved on in the last four to five years. It used to be that module assembly was a very low-tech, low-barrier-to-entry part of the value chain. A lot of the work was manual. Now modules are 60-, 72- even 90-cell [formats]. We will have 72-cell modules exceeding 400W by the end of next year. Multi-busbars on the modules have really driven another level of power increases and there is a significantly greater level of automation on the production lines as well," explains Colville.

"We're starting to see glass-glass, new types of glass, new materials, bifacial modules…Actually keeping track of that – which manufacturers are genuinely producing state-of-the-art modules in terms of power performance and reliability and consistency with the cells they are using – is a huge issue now compared to a few years ago. Back then everyone's module factory was the same and a lot of people were buying cells from just a small group of players."

Changes

These changes in technology are not trifling either. These are not niche developments springing up in isolated pockets. Recent research by Colville has shown that by 2018 the ratio of mono versus multi modules will be around 50:50 (see Figure 1).

The International Technology Roadmap for Photovoltaic (ITRPV) forecasts a less dramatic but more varied shift in the make-up of chosen encapsulants out to 2025. Likewise for module interconnection materials, backsheets, frame materials, metalization, busbars…the list goes on.

Bifacial modules are waiting in the pipeline to begin grabbing significant share from markets where conditions on the ground, literally, make the additional expense pay back for investors. Trina Solar and SolarWorld are already bringing these to market.

Marketing

While there is never any shortage of people willing to line up and explain why their product is in fact the best, PV ModuleTech shifts the onus on to the technology and bold claims will be backed by data.

As the number of routes to increased power and efficiency grows, with differing side effects for other performance and reliability indicators, the event will look to provide a more transparent approach to assessing the relative merits of these.

"If you look now at how module suppliers back up their claims of being the best there really are very few platforms on offer. Obviously they have marketing collateral that they bring out through their websites, through trade shows, datasheets, brochures, but that is all done in-house. It's not done in an independent platform or forum. The trade shows and the related exhibitions are always 100% marketing platforms as well, so really an independent event to provide

Finlay Colville at the inaugural PV CellTech conference in Malaysia.

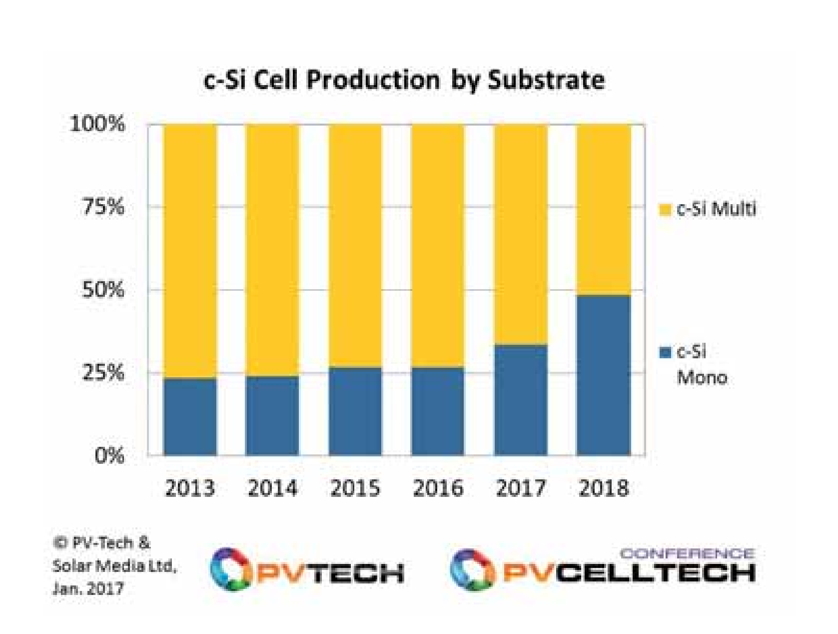

Source: PV Tech & Solar Media Ltd.

The changing balance of mono versus multicrystalline silicon production in the coming year.

that third-party voicing of why modules are performing in a certain way and how the quality, reliability and consistency is there is something that almost all module suppliers would jump at; the industry is dying to get qualified, technology-driven data analysis from an independent source about how modules are put together, the materials used in them and the performance.

"It's a perfect platform for the module makers to the show the industry, their supply chain and also the people buying modules from them, the data that backs up the claims with regard to specifications, performance, materials, reliability, testing, to take away the typical marketing claims and pull in the data and the technology surrounding the modules," adds Colville.

"PV CellTech was designed to fill this gap between the big solar exhibitions that have side events that are unregulated and badly attended and the highly academic events like PV SEC and IEEE that are largely there for the academic community to talk about blue-sky research or what is going on in the universities and research institutes.

"If you look at the module side, there is nothing like this and again we have this gap between the big exhibitions demonstrating modules and the module research spoken about at the academic conferences. Again, it's about identifying the overlapping technology with the commercial manufacturing. The key questions are what is happening in the real world and what are the technical issues important to the commercial success of module design and supply?"

> "The key questions are what is happening in the real world and what are the technical issues important to the commercial success of module design and supply?"

How we put it together

Finlay Colville explains the approach used to ensure PV ModuleTech connects the dots between technology and real-world commercial success.

"Fundamentally, it's a dedicated upstream conference specific to modules. What we're doing internally at PV Tech is a number of surveys and internal research to really identify the top 10 or so categories that are important for module supply. Then we've identified leading experts in each of those ten categories to form a technical advisory board. It is the technical advisory board that then sets the agenda and also determines which companies are the best ones to be invited to stand up and talk about their modules or technology or materials. The next stage is ensuring that we have a senior level technology driven senior executive to talk. It's not a platform for sales and marketing people to convince the audience why supplier a is better than suppliers b,c and d. We make sure we find the right person from within the company as the speaker. So, in terms of the speakers, it is invite only. That means it's altogether a different type of event to one where you have sales and marketing people, often region-specific, basically trying to convince the whole audience that they are the best."

Benchmarking

As end-market demand and manufacturing capacity have ballooned in recent years, the legacy systems for ensuring a manufacturer was legitimate have become obsolete. Most manufacturers with anything approaching a reasonable amount of capacity are able to make claims that, on paper at least, put them shoulder to shoulder with the largest and most sophisticated manufacturers. This is, in part, the motivation for the conference.

"There isn't a benchmarking process that dives into quality and performance supported by data. There are numerous ranking systems by third-parties that have never built a module, never supplied a module and are not in the module supply arena. There are many ranking systems that use weird and wonderful algorithms to generate a top ten, but rarely have these ranking systems been of any use. We've had companies going bankrupt within 12 months of appearing in some ranking systems," Colville points out.

"So it's really about having an absolutely independent platform for companies to explain, whether or not they are supplying 50MW of very high-spec modules for the Japanese residential market or it's a company supplying multi-gigawatt volumes to utility-scale companies. These are very different types of companies and they will have absolutely mastered what's important in terms of the module design. But ranking systems try to commoditise and standardise the industry as opposed to really breaking out which modules are best for which environment."

Commodity no more

It is becoming an increasingly difficult argument to consider solar panels as an undifferentiated commodity. Whether it's the increasing data from older assets, whch offers the ability to identify lost revenue from underperforming plants, or simply the growing choice on offer for different end-uses in different geographies, investors are better educated on solar technology than they have previously been.

"The recent pace of technology change in the last few years means a lot of the investment community are asking suppliers, 'Are your modules mono- or multi-? Are they 60- or 72-cells? Are your modules in the US market next year coming out in 400W? Is your module production being specified for residential markets or have you got dedicated 1500V modules to be used specifically for harsher environments in India and the Middle East?'

HT-SAAE 航天机电

High-Efficiency Poly-Crystalline PV Modules

Hyper Black

Leaving The Past Behind

Black silicon cell
Nano texture method leads to higher cell efficiency
Uniformity in the cell's overall appearance

5BB cell
Lower series resistance
Higher module efficiency

Microcrack protected /PID protected
Triple EL tested for high quality control
Applied anti-PID cell and high reliability encapsulation material

280W
Output power can reach 280W and above for 60-cell module

19.8%
Cell efficiency level for mass production up to 19.8% and above

9.6%
Output power increase of 9.6% per unit area (compared with 260W)

4.8%
A 4.8% BOS reduction per Watt (compared with 260W)

*48pcs,60pcs,72pcs modules and other options available

Solar Silk Road, Paving The Way

To The Future

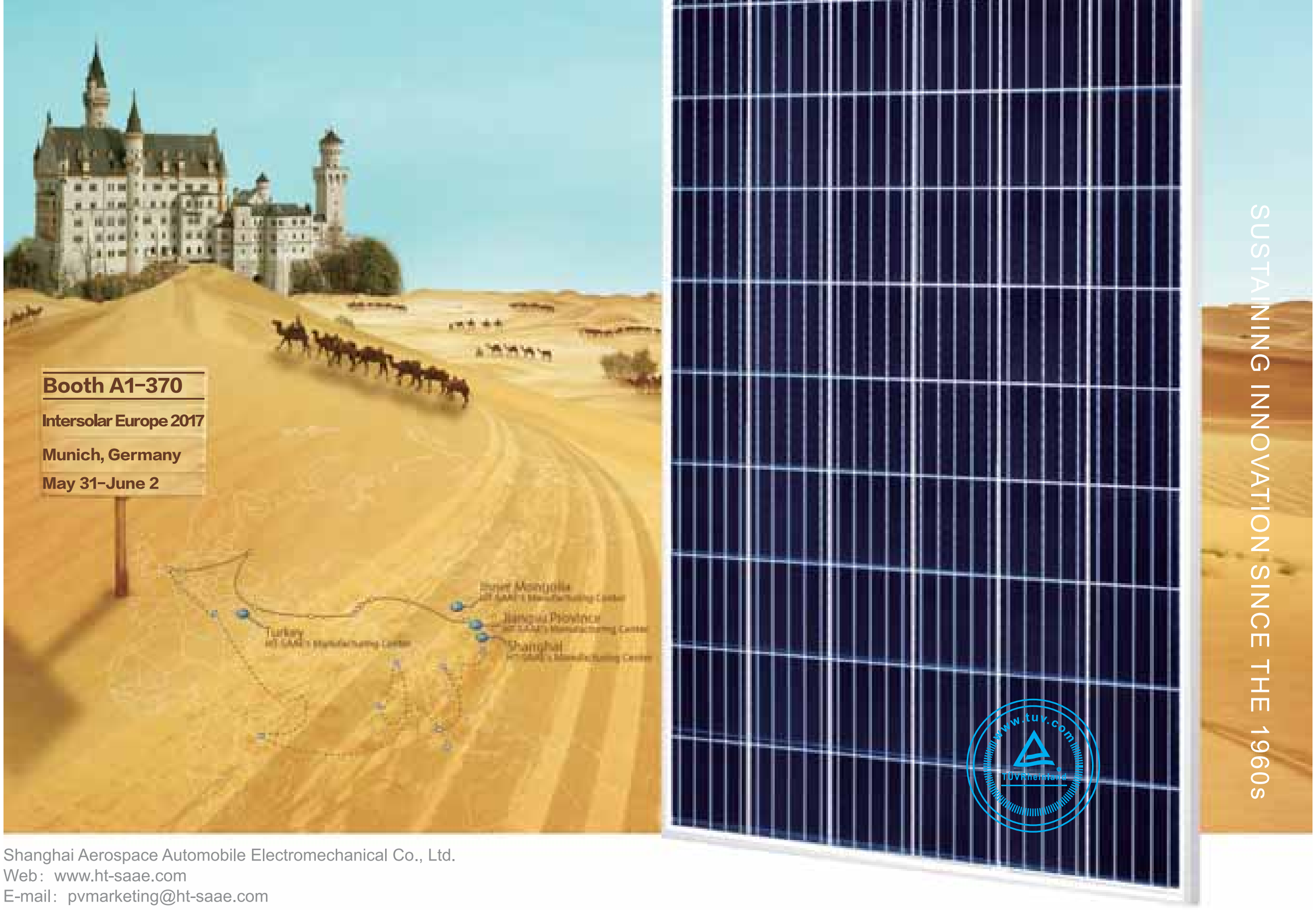

Shanghai Aerospace Automobile Electromechanical Co., Ltd.
Web：www.ht-saae.com
E-mail：pvmarketing@ht-saae.com

FORTUNE 世界 500	Bloomberg TIER 1	60YS Based on nearly 60 years experience in solar technology R&D by CASC	10 million+ 10 million+ USD R&D investment per year	1.8 billion+ Corporate's total assets is over 1.8 billion US dollars	100+ Over 100 independent intellectual property rights for cell & module	600+ Established over 600 PV power plants in China and overseas

* All above information on technical parameters is for reference only. HT-SAAE reserves the right to modify.

PV ModuleTech will follow the same successful format as PV CellTech, providing an independent forum for in-depth exploration of emerging technologies.

> "We've got the investment community asking those questions because they realise that a module is not a module. It's not a standard product across all manufacturers."

"We've got the investment community asking those questions because they realise that a module is not a module. It's not a standard product across all manufacturers," says Colville. "The module suppliers and the whole supply chain of materials and equipment are having to address which are the best modules and why. Not only on the roof or on the ground, but also across different countries, and I think that the investment guys absolutely want to know who has got the modules that will allow the company to grow globally and not be just confined to certain smaller parts of the market or just certain countries because their modules are not going to operate in warmer or more humid environments."

Networking

Part of the attraction of drawing together such a large group of senior PV technology executives is the focused networking opportunity on offer.

"PV ModuleTech will be a dedicated two-day event not in China, not in the US; we've chosen Malaysia again, and over the two days, the only issue on the table is modules. Module quality, module performance, module materials, equipment, certification…That means you end up with a few hundred of the top people globally driving the module improvements, that are behind the certification, the people that are producing the vast amount of modules being used. When you have the key stakeholders together in the same place for a couple of days so the scope for networking and business opportunities is absolutely immense. We saw that at PV CellTech, because of that environment, and we expect the same again."

PV ModuleTech will be held in Kuala Lumpur, Malaysia, on 7-8 November. Further details are available at moduletech.solarenergyevents.com

What they said about PV CellTech

"The PV CellTech conference was a fantastic opportunity to discuss PV manufacturing issues, opportunities and prospects with key players and prepare this industry for the TW level." Dr. Pierre Verlinden, VP, Chief Scientist and Vice-Chair of State Key Lab Technology Dept, Trina Solar.

"A very well organised event with an impressive selection of speakers and topics covered." Stuart Wenham, Centre Director, University of New South Wales.

"It was absolutely amazing to me to see such a good conference with outstanding talks along with a networking opportunity with all the most important experts who are driving and dominating the PV industry. All the family members got together and it felt like a family event every single minute." Dr. Christian Buchner, Vice President, Business Unit PV, SCHMID Group

"The PV CellTech conference presentations gave an excellent overview about the current most discussed topics in cell processing. Having assembled key representatives of most of the leading c-Si cell manufacturers and institutes provided a great overview about today's activities and about the roadmap to the future of c-Si PV." Dr. Markus Fischer, Vice President R&D Processes, Hanwha Q CELLS.

"In two days I was able to hear perspectives from top cell producers, technology leaders, major equipment suppliers and leading academics on critical topics to the industry. What a unique opportunity to gain a great perspective on the progress within the industry, its challenges and the bright future ahead. This was an outstanding and worthwhile event." Peter Cousins, VP R&D, SunPower.

"It was truly one of the best PV conferences I have participated in. Also a great start for more successful future events." Homer Antoniadis, CTO, DuPont Photovoltaic Solutions.

Fab & Facilities

Global solar PV manufacturing capacity expansion plans rebound in Q1

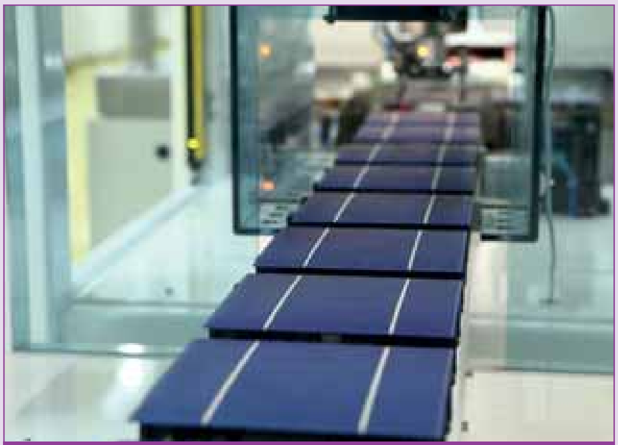

Credit JA Solar

Manufacturing expansion announcements rebounded strongly in the first quarter of this year.

Preliminary analysis of global solar PV manufacturing capacity expansion announcements in the first quarter of 2017 by Photovoltaics International sister website, PV Tech, shows a strong rebound compared to the significantly subdued environment experienced in the second half of 2016.

Although capacity expansion announcements in January remained subdued and followed the low level of activity set in the second half of 2016, February proved to be the third highest month since 2014, and the highest February in more than three years.

March did not maintain that momentum but still posted strong figures, becoming the second highest March figures in more than three years.

As a result, the first quarter of 2017 was the third highest for capacity expansion announcements since the start of the PV industry's second major manufacturing expansion phase in 2014.

As previously reported, January, 2017 capacity expansion plans remained subdued, indicating the potential for an end to the latest global expansion phase, after seven months of low activity, primarily due to fears of overcapacity and the fact that global module ASPs declined by around 25% in the second half of 2016.

See page 28 for an in-depth report on the latest capacity expansion trends.

Expansion plans and new facilities

JA Solar shifting more solar cell capacity to p-type mono PERC

JA Solar is continuing to expand manufacturing capacity in 2017 after guiding total shipments to be in the range of 6GW to 6.5GW, up from 5.2GW in 2016.

JA Solar exited 2016 with an in-house annual ingot/wafer manufacturing capacity of 2.5GW, up from 1GW in 2015. In-house solar cell capacity reached 5.5GW, up from 3.6GW at the end of 2015 and in-house PV module capacity also reached 5.5GW at the end of 2016, up from 3.6GW.

The company guided further in-house expansions in 2017, which would mean adding 500MW of ingot/wafer production to reach 3GW and 1.5GW of solar cell capacity to reach an in-house production level of 7GW by the end of 2017.

However, in-house PV module capacity expansions include only a 500MW increase to 6GW by the end of 2017. Management noted in a recent earnings call that its OEM partnership in Vietnam provided an additional 1GW of module assembly capacity to achieve a balanced cell and module nameplate capacity of 7GW in 2017.

JA Solar had module shipments of 4,606.6 in 2016, up from 3,672.9MW in the previous year, a 25.4% increase.

Credit Tata Power Solar

Tata Power Solar has almost doubled its module manufacturing capacity in Bangalore.

Tata Power Solar nearly doubles manufacturing capacity in Bangalore

Integrated PV firm Tata Power Solar has doubled its module manufacturing capacity and raised its cell capacity by 65% at its plant in Bangalore, southern India.

The firm has also modernised and fully automated the whole facility, while claiming to have reached full capacity in record time and ahead of global benchmarks.

Tata's second expansion in three years, made to keep up with increasing demand, brings the facility from 200MW to 400MW in modules and 180MW to 300MW in cells.

At the firm's Delhi offices in January, Ashish Khanna, executive director and CEO, Tata Power Solar, told PV Tech: "This industry requires continuous investment in technologies, unlike many other industries. If you look at automobiles then [investments] are incremental, but solar is one where, if you are in the manufacturing area, you have to continuously invest in technologies. Otherwise you are not at the helm of the technologies or the product will die its own death."

Hanwha Q CELLS holding off new in-house capacity expansions in 2017

Hanwha Q CELLS is allocating only US$50 million to capital expenditures in 2017, indicating there would be no new in-house capacity expansions in 2017.

Hanwha Q CELLS noted in reporting


PVMODULETECH
CONFERENCE
7 - 8 November 2017
KUALA LUMPUR, MALAYSIA
PV-Tech and Solar Media Ltd. announce PV ModuleTech, a new conference dedicated to understanding the critical parameters behind the technology, quality & reliability of PV modules supplied to the global market today.
• Technologies & drivers for glass/glass, 1500V, bifacial, 60/72-cell modules
• Materials, equipment advances for low-cost module manufacturing
• Environmental testing, PID, LID, module certification
• Benchmarking quality & performance of module suppliers
moduletech.solarenergyevents.com
To get involved either as a speaker, partner or attendee please email:
marketing@solarmedia.co.uk
PVTECH
Photovoltaics International
SOLAR MEDIA
EVENTS | PUBLISHING | RESEARCH

Credit BYD

BYD's module factory in Brazil is now open, with a nameplate capacity of 200MW.

fourth quarter and full-year 2016 financial results that its capital expenditures in 2017 would be around US$50 million, which would include manufacturing technology upgrades and certain unspecified R&D related expenditures.

With in-house annualized production capacities of 1,550MW for ingot capacity, 950MW of wafer capacity in China and 4,150MW of cell and module capacity (2.4GW in China and 1.75GW in Malaysia) at the end of 2016, capital expenditures of US$50 million would be required primarily for facility and equipment maintenance.

In contrast, Hanwha Q CELLS allocated US$23.0 million in the third quarter of 2016 to capital expenditures and US$137.7 million in total capital expenditures in 2016. The spending amounted to small incremental capacity expansions and upgrades to p-type multi-PERC cells. All of the 1.75GW at the Malaysia plant had been converted to PERC by the end of 2016.

However, Hanwha Q CELLS does have access to solar cell and module supply of up to 1,550MW from Hanwha Q CELLS Korea Corporation, an affiliate of the company, which has also upgraded around 1GW to P-type multi-PERC and around 500MW of cell capacity to p-type mono PERC.

BYD officially opens 200MW module assembly plant in Brazil

China's BYD has officially opened its first solar module assembly plant in Brazil with a nameplate capacity of 200MW.

BYD initially announced plans for a manufacturing facility in Brazil that would include an all-electric commercial bus chassis production line as well as a 200MW module assembly plant in July 2014.

The R$150 million (US$45 million) module assembly plant, located in the city of Campinas in the south eastern region of Brazil is already producing modules for downstream PV projects in Brazil and is expected to generate around 360 jobs. It will produce BYD's double-glass modules.

Local content rules for downstream PV power plants are intended to build a PV manufacturing sector in Brazil.

Recently, Canadian Solar opened a 350MW to 400MW module assembly plant in Sorocaba, state of Sao Paulo that is being operated by electronics subcontractor Flextronics International (Flex).

Essel and GCL to start site development at Indian PV fab within two months

A consortium between Essel Infra, an arm of Indian conglomerate Essel group, and China's GCL Poly Energy Holdings will start initial site development of a major solar PV manufacturing plant in the Indian state of Andhra Pradesh within two months.

Preliminary approval has been received, but the partners are waiting for more detailed approval from the government, an Essel representative told Photovoltaics International sister website PV Tech under condition of anonymity.

Phase one will be 1GW in capacity involving both cells and modules, but later phases are expected to include materials processing including polysilicon ingot and wafers. Plans for a total 5GW by 2020 were announced when a memorandum of understanding was first signed between the Andhra Pradesh government and the consortium back in January 2016.

On the downstream side, Essel Infra has won a new portfolio of 600MW solar PV in recent auctions, said the representative, and the firm is "aggressively pursuing" a target of 1.5GW of power purchase agreement (PPA) signings within 2017.

Tool manufacturers

Singulus expects to double sales in 2017 as order backlog increased over 300%

Specialist PV manufacturing equipment supplier Singulus Technologies expects to double sales in 2017 after its new order backlog in 2016 reached €109.9 million, a 310% increase over the previous year.

Singulus reported 2016 sales of €68.8 million, down from €83.7 million in 2015. The company said that doubling of sales guidance was based on expectations of follow-on orders with China-based China National Building Materials (CNBM), which owns Germany-based CIGS thin-film producer, AVANCIS, which is establishing production plants in China.

Singulus noted in its 2016 annual report that around 50% of the first-phase order from CNBM had been shipped and assembled. The company expects further orders in the 300MW range from CNBM in 2017. Interest for further large CIGS production lines from other companies based in China were also promising, according to the company.

The company also said it expected further orders for its crystalline silicon wet-chemical equipment (Silex II) for n-type mono heterojunction (HJ) solar cells within its solar division in 2017.

Total new order intake in 2016 was €152.1 million, up from €96.3 million in 2015, driven by the major orders from CNBM of over €110 million, the largest single order in the history of the company.

Intevac's order backlog boosted by recent solar ion implant orders

Specialist semiconductor and PV equipment supplier Intevac reported first quarter 2017 financial results that included a 40% increase in new orders, driven by the largest single order in its Thin-film Equipment segment that includes a 12 system follow-on order in March for its solar 'ENERGi' implant tools.

Revenue in the first quarter of 2017 was US$30.4 million, including US$21.5 million of Thin-film Equipment segment revenue. However, the segment sales are not expected to include the solar ion implant order until later in the year, after tools are shipped to a customer in China planning to ramp n-type mono IBC (interdigitated back contact) solar cells and modules, including bifacial modules.

Management said in its first-quarter earnings call that the solar ion implant order was valued at around US$23 million. The company had not disclosed the value of the order when it was announced in March 2017.

Intevac's Thin-film Equipment segment sales have been increasing significantly since the third quarter of 2016, partially driven by new solar orders for implant and PVD tools. Intevac reported total new orders in the quarter of US$35 million.

Meyer Burger's sales increased 40% in 2016 on back of new technology buy cycle

Leading PV manufacturing equipment supplier Meyer Burger reported a significant increase in revenue in 2016, due to the start of a major technology upgrade and capacity expansion cycle by PV manufacturers primarily in the ingot/wafer and solar cell segments.

Meyer Burger reported 2016 sales of CHF453.1 million (US$456.1 million), up 40% from the previous year. Sales in 2016 were the second highest since the capacity expansion boom ended in 2012, when sales topped CHF645.2 million.

Incoming orders in 2016 were fuelled by strong demand for upgrade technologies such as diamond wire saws and PERC cell technologies, which has extended through the first quarter of 2017.

On a geographical basis, sales in Asia accounted 72% of total sales in 2016, up from 63% in 2015. Europe remained stable at 23% of total sales, compared to 22% in 2015. The US only accounted for 5% of sales in 2016, compared to 15% in the previous year.

Meyer Burger reported an order backlog for 2016 of CHF 244.5 million (US$246.1 million), down slightly from CHF 257.5 million in 2015.

Singulus confirms SILEX II system acceptance from Hevel Solar in Russia

Specialist PV manufacturing equipment supplier Singulus Technologies said it received a Final Acceptance Test (FAT) from Russia-based Hevel Solar for its SILEX II system, used for wet-chemical processing of heterojunction (HJ) solar cells.

Recently, Hevel Solar announced that it had fabricated its first HJ solar cell and that the cell had achieved a conversion efficiency of 21.75%. Hevel noted that the cell efficiency was measured under standard testing conditions in-house and not verified by a third party.

Singulus and Meyer Burger had been key HJ equipment suppliers to Hevel Solar as it switched its manufacturing lines from a-Si thin-film solar modules to HJ technology.

The SILEX II platform is said to use newly developed ozone-based cleaning steps in shorter process times with low usage of chemicals.

Company news

Beamreach Solar's pilot line up for sale after bankruptcy

Bankrupt US solar module start-up Beamreach Solar's pilot production line in Milpitas, California is being offered for sale by Silicon Valley Disposition Inc. (SVD).

The 72,000 square foot facility is equipped with a turnkey line, said to have cost over US$22 million in the 2014/15 period.

According to a previous Greentech Media report, Beamreach Solar accumulated around US$250 million in costs over the lifetime of the company, which was formerly known as Solexel for the majority of its life.

The company re-launched at Intersolar North America in 2016, offering an integrated industrial and commercial rooftop system that claimed a design that enabled higher flat rooftop module density and fast installation using a lightweight PV module.

SVD and Onyx are immediately offering the facility as a Turnkey/In-place sale, rather than through an auction.

Credit Meyer Burger

Meyer Burger's 2016 revenue saw a significant increase compared to 2015.

PV manufacturing capacity expansion announcement plans and analysis for Q1 2017

Mark Osborne, Senior News Editor, Photovoltaics International

ABSTRACT
Our preliminary analysis of global solar PV manufacturing capacity expansion announcements in the first quarter of 2017 shows a strong rebound compared with the significantly subdued environment seen in the second half of 2016. A key driver over the period was plans announced by the majority of the 'Silicon Module Super League' (SMSL) members, which are profiled separately in this report.

Although capacity expansion announcements in January remained subdued and followed the low level of activity seen in the second half of 2016, February proved to be the third busiest month since 2014 and the strongest February in more than three years. March did not maintain that momentum but still posted strong figures, the second highest March figures in more than three years.

As a result, the first quarter of 2017 was the third highest for capacity expansion announcements since the start of the PV industry's second major manufacturing expansion phase in 2014.

As previously noted, January 2017 capacity expansion plans remained subdued, indicating the potential for an end to the latest global expansion phase, after seven months of low activity, primarily due to fears of overcapacity and the fact that global module average shipment prices (ASPs) declined by around 25% in the second half of 2016.

Hanwha Q CELLS

Despite a slow start to the year, PV manufacturers have had a busy first quarter setting out new expansion plans.

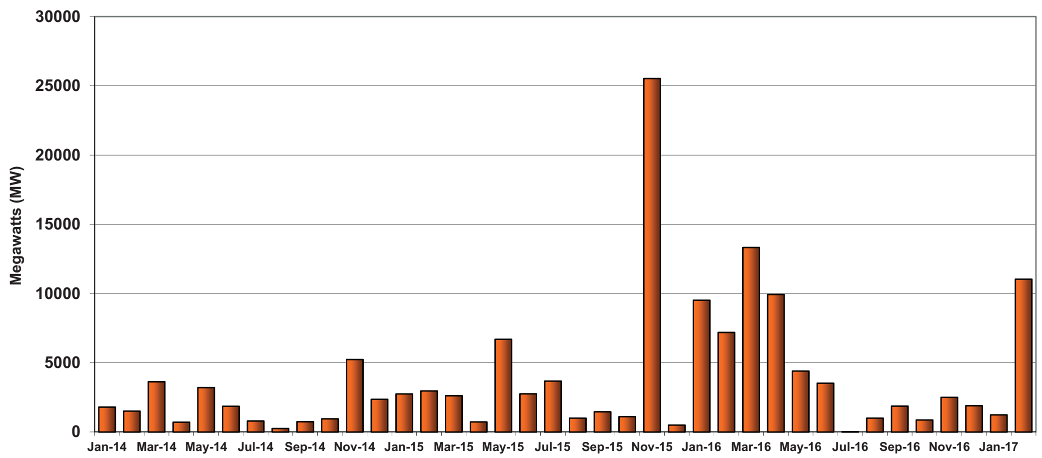

Figure 1. Combined total (c-Si cell, module & thin-film) expansion announcements by month (MW).

A total of 1,235MW of thin-film, solar cell and module assembly expansion plans were announced in January 2017. This included a total of around 370MW of thin-film announcements, 450MW of solar cell and 415MW of module assembly plans.

This low January total was boosted by rare CIGS thin-film plans from China and contrasts with 1,900MW of expansions announced in December 2016.

> "The first quarter of 2017 was the third highest for capacity expansion announcements since the start of the PV industry's second major manufacturing expansion phase in 2014"

February rebound

The significant rebound in capacity expansion plans in February 2017 led to a total of 11,040MW of announcements. This included 6,740MW of solar cell plans and 4,300MW of module assembly plans. Photovoltaics International's preliminary review indicates no new capacity announcements were made in the thin-film sector or for integrated cell and

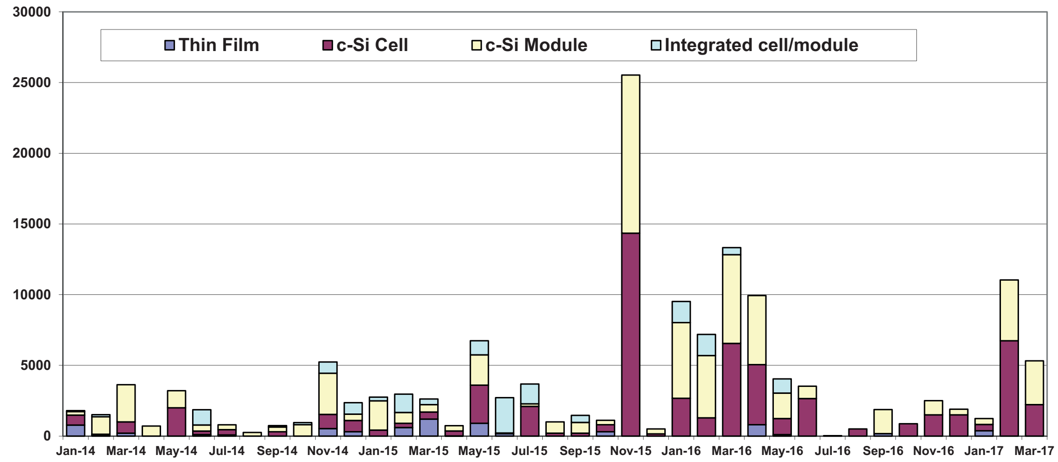

Figure 2. Capacity expansion announcements by product type monthly since January 2014 (MW).

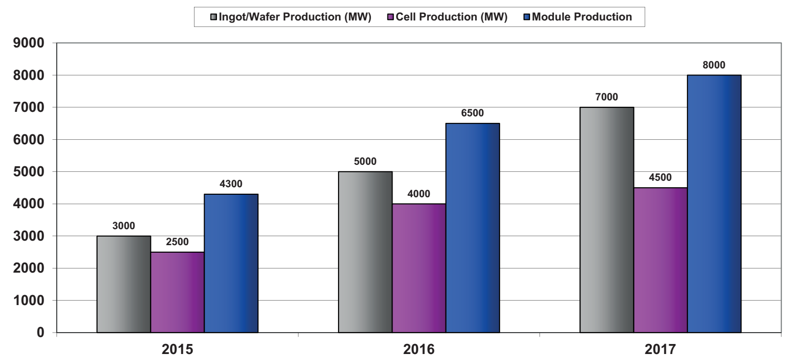

Figure 3. JinkoSolar manufacturing capacity in 2017 (MW).

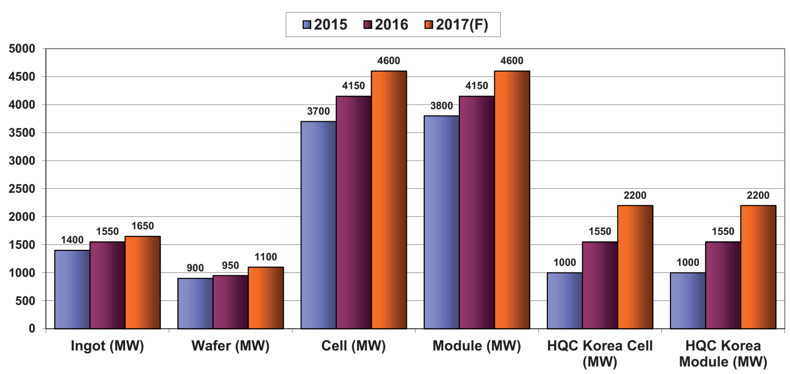

Figure 4. Hanwha Q CELLS manufacturing capacity expansions (MW).

module manufacturing plants.

There were two key trends at play. Firstly, several large announcements were actually phased expansions over specified and non-specified time frames.

A key announcement was that US manufacturer SunPower had signed a new joint venture partnership in China to produce both solar cells (p-type mono PERC) and modules for its P-Series technology with its existing China-based supply chain partners Dongfang Electric Company (DEC) and Tianjin Zhonghuan Semiconductor (TZS); that proposal included a manufacturing capacity expansion from 1.1GW to 5GW.

The second key trend was the start of expansion plan updates from 'Silicon Module Super League' (SMSL) members. JinkoSolar was the first SMSL to announce plans to expand in-house solar cell production by 500MW in 2017 and module assembly capacity by 1,500MW.

Also of note in February was the confirmation that Panasonic would take over the formerly SolarCity now Tesla facility in Buffalo, New York State, previously known as Riverbend, now dubbed 'Gigafactory 2'.

However, as the 1GW facility plans had been announced back in June 2014 it does not count as a new announcement from a capacity perspective and is not included in the preliminary new announcements for February.

Perhaps more important is that its seems increasingly possible that Panasonic's expected US$250 million investment in Gigafactory 2 is only related to module assembly and not HIT solar cell production. This would change the status of the facility from being the largest integrated production plant in the US to being the largest module assembly plant, should it be ramped at some time in the future to 1GW-plus of module capacity only.

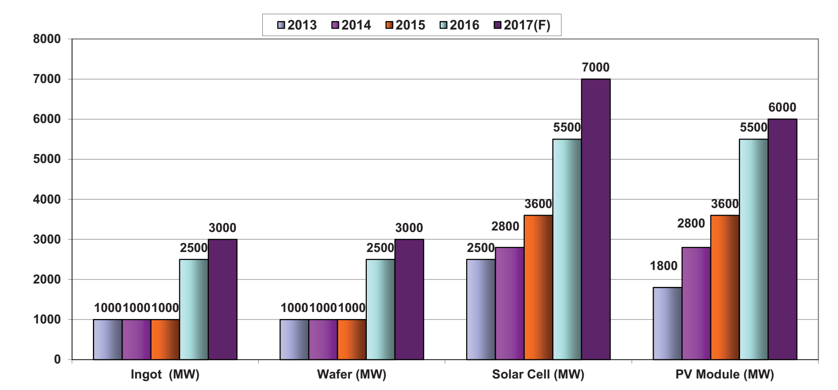

Figure 5. JA Solar in-house manufacturing capacity (MW).

March still strong

Preliminary figures for March 2017 indicate that a total of 5,320MW of new capacity expansion plans were announced. Following on from February, only solar cell and module assembly expansions were announced. This included 2,220MW of solar cell plans and 3,100MW of module assembly plans.

Momentum in capacity expansions was sustained primarily by three SMSL members (Hanwha Q CELLS, JA Solar and Canadian Solar) reporting on plans for 2017 as part of their fourth-quarter and full-year financial results.

SMSL update

The Silicon Module Super League (SMSL) is our table of the top-ranking module suppliers that collectively are driving many of the trends shaping the market. In the latest quarter they once again played a prominent role.

JinkoSolar

Leading SMSL member JinkoSolar said that it would be expanding in-house ingot/wafer, solar cell and module assembly capacity this year.

The company expects to expand in-house ingot/wafer production from 5GW at the end of 2016 to 7GW by the end of 2017. Around 1GW of the wafer expansion will be monocrystalline based.

The company is still limiting in-house solar cell capacity expansions, adding only 500MW in 2017 to take nameplate capacity from 4GW at the end of 2016 to 4.5GW by the end of 2017.

However, the company noted that it is further migrating cell capacity to PERC technology, having reached 1.4GW of in-house PERC capacity in 2016. The company plans to have reached 2GW of PERC capacity by the end of 2017. JinkoSolar is planning to expand module assembly capacity by 1,500MW, reaching 8GW in 2017.

Hanwha Q CELLS

Caption for fig 4, in here Figure 4. Hanwha Q CELLS manufacturing capacity expansions (MW).

Hanwha Q CELLS and Hanwha Q CELLS Korea are adding a combined 1.2GW of p-type multi/mono PERC

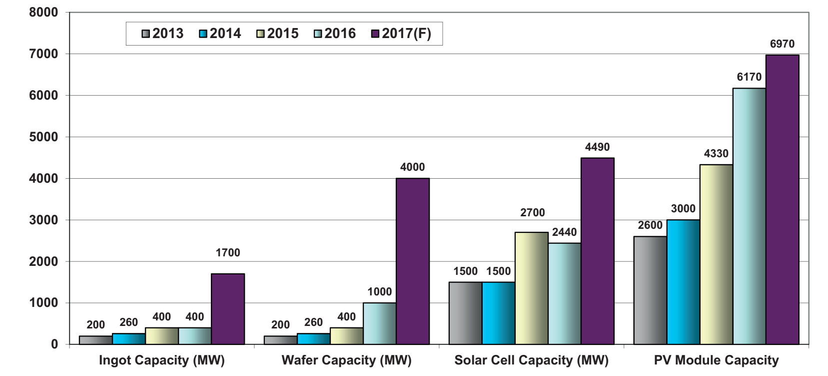

Figure 6. Canadian Solar manufacturing capacity expansions (MW).

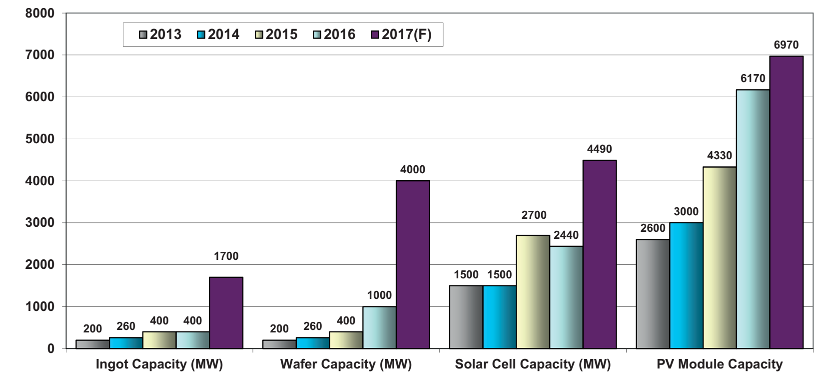

Figure 7. LONGi PV manufacturing capacity goals (MW).

capacity in 2017, including 500MW via PERC upgrades and more mono migration at its facilities in Malaysia and South Korea.

Hanwha Q CELLS also announced plans for an integrated (wafer/cell/module) p-type multi/mono PERC plant in Turkey with a nameplate capacity of 500MW as part of local content rules for developing PV power plants in the country. However, the establishment of plant could be several years away as it seeks government approvals.

JA Solar

JA Solar is continuing to expand manufacturing capacity in 2017 after guiding total shipments to be in the range of 6GW to 6.5GW, up from 5.2GW in 2016.

JA Solar exited 2016 with an in-house annual ingot/wafer manufacturing capacity of 2.5GW, up from 1GW in 2015. In-house solar cell capacity reached 5.5GW, up from 3.6GW at the end of 2015, and in-house PV module capacity also reached 5.5GW at the end of 2016, up from 3.6GW.

The company guided further in-house expansions in 2017, which would mean adding 500MW of ingot/wafer production to reach 3GW and 1.5GW of solar cell capacity to reach an in-house production level of 7GW by the end of 2017.

However, in-house PV module capacity expansions include only a 500MW increase to 6GW by the end of 2017. Management noted in a recent earnings call that its OEM partnership in Vietnam provided an additional 1GW of module assembly capacity to achieve a balanced cell and module nameplate capacity of 7GW in 2017.

JA Solar's 1.2GW Malaysian solar cell facility, which had predominantly produced p-type multi cells, will shift around two thirds of capacity to p-type mono-PERC cells in 2017, according to the company. This equates to a shift of around 800MW of p-type multi-PERC cell production to p-type mono-PERC.

Canadian solar

Canadian Solar is placing a major bet on pushing ahead with the migration to p-type multi PERC cell technology using diamond-wire saw (DWS) and 'Black Silicon' texturing under its 'ONYX' label, instead of increasing p-type mono PERC capacity as many companies are.

The company noted that its in-house ingot capacity, which stood at a mere 400MW at the end of 2016, would be ramped to 1,700MW by the end of 2017. In-house wafer capacity would also be significantly expanded from 1,000MW in 2016 to 4,000MW by the end of this year. Wafer capacity is expected to reach 2,000MW by the end of June 2017.

These specific expansions would enable Canadian Solar to benefit from a PERC transition, providing higher efficiency cells and modules, while reducing silicon kerf losses and manufacturing cost by avoiding the use of slurries with DWS technology.

With respect to its solar cell manufacturing capacity, which stood at 2,440MW at the end of 2016, Canadian Solar said that it had restored production at two cell lines totalling 240MW at its Funing cell facility in China, which was completely destroyed by a tornado in 2016. An additional 480MW of cell capacity will be ramped in March 2017, while a further 720MW will come on stream in June 2017, providing a combined 1,440MW of p-type multi-PERC cell capacity.

Canadian Solar also noted that its newest 850MW solar cell plant in Southeast Asia was completed in February 2017, with production starting to ramp in March 2017.

As a result, total in-house cell manufacturing capacity is expected to reach 4,490MW by 30 June 2017. The company noted in an SEC filing that this level of nameplate capacity would remain through to the end of 2017. With the completed ramp of its Southeast Asia plant, and without further expansions at its Funing facility, Canadian Solar's in-house cell capacity would stand at approximately 4,730MW.

Having given PV module shipment guidance for 2017, Canadian Solar expects shipments to be between 6.5GW and 7GW this year. Therefore, the company is expanding in-house module assembly capacity from 6,170MW at the end of 2016 to 6,970MW by the end of June 2017.

Combined, SMSL members (JinkoSolar, Canadian Solar, JA Solar and Hanwha Q CELLS) have announced 3,700MW of solar cell expansions and 4,000MW of module assembly expansions for 2017.

With Trina Solar going private before being required to provide fourth-quarter and full-year financial results, the company has yet to make public any new expansion plans for 2017. However, indicative of intent, Trina Solar in January 2017 became a JV partner with LONGi Green Energy


FIRST SOLAR NOVA AWARD 2015
BEST IN CLASS SUPPLIER
VON ARDENNE
PIA|nova®
SCALA
GC60V
XEA|nova®
XENIA
ADVANCED COATING EQUIPMENT FOR HIGH-PERFORMANCE PHOTOVOLTAICS
If you are looking for coating equipment with low cost of ownership for thin-film photovoltaics or crystalline solar cells, VON ARDENNE is your partner of choice.
Our PIA|nova® and GC60V coating systems deposit functional layers on glass for thin-film solar modules.
The XEA|nova® is designed for the deposition of high-performance contact layers on silicon wafers.
The coating systems SCALA and XENIA are suited for both applications.
Learn more at Intersolar Europe: booth 140, hall A2.
www.vonardenne.biz


PVTECH
PV Tech Institutional Licence
Photovoltaics International
Fully searchable knowledge vault
COVERING THE LATEST DEVELOPMENTS IN LAB TO FAB TECHNOLOGIES AND PROCESSES
Helping reduce R&D costs and ensure you have immediate access to the latest research on the technologies impacting the market now
700+
technical papers covering cutting edge technology and advancements in global solar manufacturing
Print and digital access to Photovoltaics International
THE ONLY PUBLICATION TO BRING YOU THE PERFECT BLEND OF MARKET NEWS AND ANALYSIS ALONG WITH THE LATEST TECHNICAL PAPERS AND PRODUCT REVIEWS
PVI
The technical resource read by and referred to by 98% of the module producing community
(Source PV Tech survey)
Contact:
Digital Marketing Manager:
Lindsey Guest | lguest@pv-tech.org +44 (0) 207 871 0122
pv-tech.org/pvi

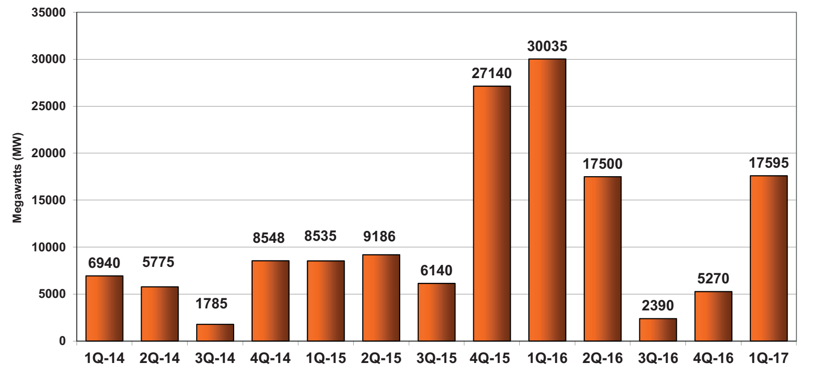

Figure 8. All manufacturing capacity expansion announcements (thin-film, cell, module, integrated) by quarter (MW).

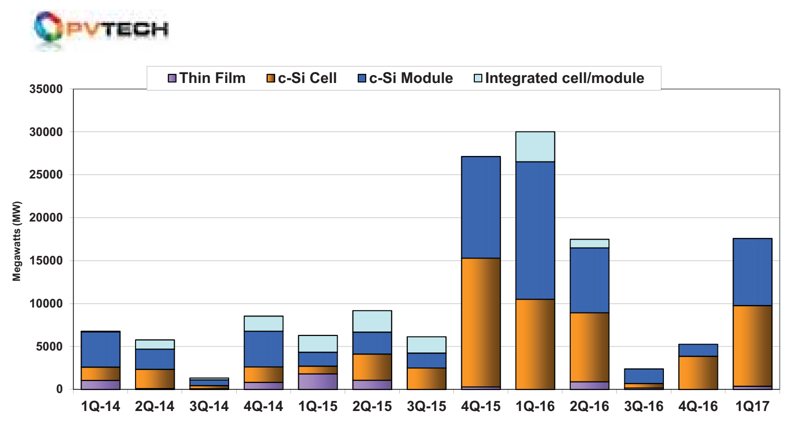

Figure 9. Capacity expansion announcements by product type quarterly (MW).

Technology's previously announced 5GW monocrystalline silicon ingot pulling production plant in Lijiang City, Yunnan Province, China.

LONGi

New SMSL member in 2017 is LONGi Green Energy Technology, which has become the leading fully integrated, high-efficiency monocrystalline module manufacturer in recent years.

LONGi has come a long way very quickly. Annual revenue in 2013, which came solely from selling mono c-Si wafers, was around US$330 million but skyrocketed to approximately US$1.67 billion in 2016, almost a 94% increase over the previous year, which had itself generated a revenue growth of around 61%.

The significant increase was due to aggressive capacity expansions at the ingot/wafer, cell and module segments that were perfectly timed with China's downstream end-market growth that resulted in 34.54GW being installed in the country in 2016.

With intense expansion activity in the polysilicon, ingot and wafer segments supported by several key partnerships, LONGi also plans to expand in the solar cell and module segments, including through overseas production.

Having reached around 2.5GW of cell capacity and 5GW of module capacity in 2016, LONGi Solar is expected to add a further 1.5GW of cell capacity in 2017. This is comprised of ongoing expansions at its 2GW nameplate mono-PERC cell facility in Taizhou, China, and establishment of a 500MW solar cell and module facility in India.

LONGi's vertically integrated ingot/wafer/cell/module facility in Kuching, Malaysia, includes around 500MW of dedicated cell and module production. At the end of 2017, LONGi expects to have approximately 4GW of mono cell production capacity in-house and 6.5GW of in-house module assembly capacity.

LONGi had around 800MW of domestic mono-PERC cell production in 2016, achieving average cell conversion efficiencies of 21%. This is likely to be expanded to around 1.4GW in 2017, with 300MW from its Malaysian facility providing total mono-PERC cell capacity of around 1.7GW. Average cell conversion efficiencies are expected to reach 21.3% in 2017.

By the end of 2018, LONGi expects mono-PERC cell capacity to reach around 5GW, with domestic capacity at 4.5GW and overseas mono-PERC cell capacity at 500MW.

Should module shipments in 2017 be in the range of 4.3GW to 4.5GW, as guided by LONGi, then the company would become a new member of the SMSL, having achieved shipments of 2.34GW in 2016.

Surprise strong quarter

Preliminary total global PV manufacturing capacity expansion announcements in the first quarter of 2017 were 17,595MW, which just beat the second quarter of 2016, when total expansion plans topped 17,500MW.

The first quarter included 370MW of thin-film announcements, 9,140MW of solar cell and 7,815MW of module assembly. No integrated plant announcements were recorded for the quarter.

The quarter was also notable for a number of possible module assembly expansions, although these lacked meaningful information.

Almost all of the solar cell expansions were for high-efficiency upgrades such as p-type multi PERC, p-type mono PERC, n-type mono heterojunction and bifacial cells. Indeed, 2,100MW was attributed to n-type mono IBC/bifacial cells, due to confirmations to *Photovoltaics International* that Jolywood (Suzhou) Sunwatt had started construction of a new cell production plant in February.

On a geographical basis, China expansions dominated, followed by South Korea and the Philippines. Expansions were also announced in India, Malaysia, Taiwan, Germany, Italy and US.

Conclusion

Although capacity expansion announcements in the second half of 2016 proved subdued, annual updates by SMSL members and some top 15-ranked PV manufacturers resulted in a rebound in the first quarter of 2017. Linked to this recovery was the migration to high-efficiency solar cells whether in new-build lines or upgrades. However, the rebound was also driven by some speculative long-range phased expansion plans, mainly related to modules.

Materials

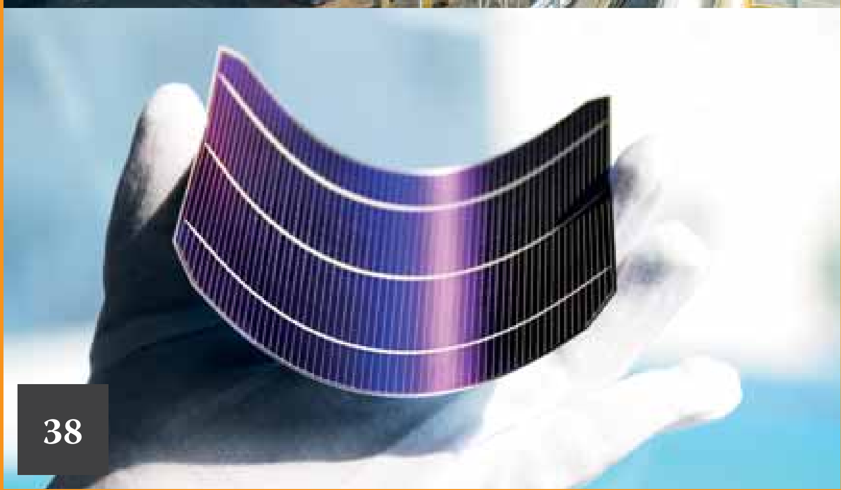

News

Wacker edges GCL in polysilicon leadership

Wacker Chemie narrowly beat GCL-Poly's production figures in 2016, partly a consequence of its new Tennessee plant.

Since Wacker Chemie opened its new 20,000MT polysilicon plant in Charleston, Tennessee in 2016, there was a good chance that the German-headquartered chemicals firm could overtake incumbent market leader, GCL-Poly.

While Wacker ramped the new Charleston facility to full-production and kept its German plants at full capacity throughout the year, GCL-Poly cut production in the second half of the year and extended maintenance periods to reduce inventory on weaker domestic demand.

As a result, according to the latest polysilicon market analysis by Bernreuter Research, Wacker indeed beat GCL-Poly's production and capacity figures in 2016, the second time only since 2012 that the company was the market leader.

However, the battle at the top of polysilicon leadership table proved to be a close call, as GCL-Poly has dominated the sector since 2013.

Wacker's polysilicon production exceeded 70,000MT in 2016. Meanwhile, GCL-Poly's polysilicon production capacity was held at 70,000MT in 2016 and production reached 69,345MT, representing a decrease of 6.7%, compared to 74,358MT in 2015.

Bernreuter believes that Wacker could remain in the leadership position for a few years until GCL-Poly can ramp further Siemens reactor capacity at its subsidiary, Jiangsu Zhongneng Polysilicon's facility in Xinjiang, China.

Polysilicon

GCL-Poly to spend US$823 million on expanding polysilicon production by 40,000MT

GCL-Poly Energy Holdings has announced plans to invest around US$823 million to expand production by 40,000MT and relocate and upgrade a further 20,000MT of capacity.

The new polysilicon plant in Xinjiang, China, will comprise 40,000MT of new-built facilities and 20,000MT of relocated production from GCL-Poly's existing facilities in Xuzhou, China, providing a single plant capacity of 60,000MT.

GCL-Poly has an existing capacity of 70,000MT of Siemens-based polysilicon production in operation. The company has also built an FBR (granular) polysilicon technology plant and is purchasing SunEdison's FBR plant in Korea. Technical difficulties have prevented either facility from ramping production.

A first-phase 20,000MT plant in Xinjiang would be completed by the second quarter of 2018. A second phase expansion of 20,000MT would be completed by the end of 2018.

Daqo shifting polysilicon supply

China-based polysilicon producer Daqo New Energy is responding to the need for higher specification polysilicon demand by increased adoption of high-efficiency mono wafers, notably being required for Passivated Emitter Rear Contact (PERC) solar cells.

"In particular, we are seeing a shift in industry trend, with rising demand and increasing manufacturing capacities for high-efficiency mono crystalline solar wafers and solar cells," noted Gongda Yao, founder and CEO of Daqo New Energy. "This has translated to increased demand for high-purity semiconductor-grade polysilicon, which only very few Chinese domestic manufacturers are able to supply."

Such is the demand for polysilicon that meets monocrystalline wafers and cells that Daqo expects to shift around 50% of its 18,000MT annual capacity to mono-spec requirements. The company also noted that PV manufacturers were willing to offer pre-payments to secure supply, due to limited supply compared to demand.

Wacker's polysilicon volumes drop on weaker China demand in Q1

Major polysilicon producer Wacker has said polysilicon shipment volumes fell substantially in the first quarter of 2017, while revenue declined around 10%. The China market had been relatively weak with only a slight rebound in demand at the end of the quarter.

Wacker's first quarter polysilicon segment sales were €268.1 million, down 10% from the previous quarter when sales reached €297.2 million, which included special income of €13.3 million from advance payments retained and damages received from solar-sector customers.

EBITDA amounted to €70.5 million, up 79% from the prior year period, driven by the completion and ramp of its new polysilicon plant in Charleston, Tennessee, and significant reduction in capex requirements.

However, relative to the fourth quarter of 2016, EBITDA was down around 19%, due to inventory build, which was forced by polysilicon spot market price declines on weaker than expected demand in Asia and notably China. EBITDA margin was negative 11.8%.

REC Silicon rides polysilicon demand fluctuations in Q1

Polysilicon producer REC Silicon ASA reported a slump in polysilicon sales in the first quarter of 2017 as market demand weakness resumed after strong demand in the fourth quarter of 2016.

REC Silicon reported first quarter revenues of US$57.5 million, down from US$80.4 million in the previous quarter. EBITDA was US$4.6 million, compared to US$4.9 million in the previous quarter. Silicon gas sales volumes in the quarter were stronger than expected, at 820MT, exceeding guidance by 9.4%, although ASPs declined 8.8% in the quarter. Total polysilicon production in the quarter was 3,127MT. FBR-based polysilicon production was 2,416MT. Total polysilicon inventory increased by 618MT. Polysilicon sales volume was 2,509MT in the first quarter of 2017, down 34% from the previous quarter.

The company had a cash balance of US$80.9 million at the end of the first quarter, up US$15.2 million from the end of the prior quarter. Capacity utilisation was around 50%, while FBR production costs were US$10.7/kg.

QSTec produces first polysilicon at Qatar plant

Polysilicon start-up Qatar Solar Technologies (QSTec) has finally started production at its plant in Qatar.

QSTec had secured financing for the construction of the 8,000MT plant back in May 2012. Since then the company has acquired major stakes in SolarWorld and centrotherm photovoltaics.

SolarWorld is expected to be a key captive customer of the polysilicon, while centrotherm, which provided much of the technology for the polysilicon plant, would be responsible for further expansions of more than 50,000MT, sometime in the future.

"The first polysilicon produced from our facility in Qatar represents a major milestone for QSTec and has paved the way for a solar manufacturing base to be established within the region," said QSTec's Chairman and CEO, Dr. Khalid K. Al Hajri.

Ingots and Wafers

Heraeus Photovoltaics launches first product outside solar cell metallization pastes

Heraeus Photovoltaics has launched its first commercial product outside its solar cell metallization paste domain.

The company has targeted the multicrystalline silicon ingot manufacturing sector, accounting for more than 80% of the current wafer market with a high-purity SiO_2 diffusion barrier coating dubbed HeraGlaze for enhanced crucible performance.

HeraGlaze comes in a slurry form, which is applied on the porous surface of the crucibles carrying polysilicon chunks that are melted and formed into silicon ingots in a DSS furnace. This can be done directly at the production site of the customer.

HeraGlaze acts as a high-purity SiO_2 diffusion barrier and prevents thermally induced impurities such as iron that are transferred from the crucible into the silicon ingot during the melting and crystallization process. The higher wafer yield is achieved by increasing the usable section of a silicon ingot.

According to Heraeus Photovoltaics the wafer yield is increased by up to 4% and cell efficiency is improved by 0.1%. With an assumed an annual wafer production of 50GW today, the adoption of HeraGlaze would deliver close to an additional 2GW per year of ingot/wafer output without increasing wafer production capacity.

Credit Heraeus Photovoltaics

Heraeus Photovoltaics is targeting ingot production with its first non-metallization product.

Comtec mono wafer sales decline

High-efficiency monocrystalline wafer producer Comtec Solar Systems Group reported a net loss of US$146 million in 2016, after previously announced write-down on assets at its Malaysian manufacturing facilities that were being sold to leading mono wafer supplier, LONGi Green Energy Technology.

Comtec reported 2016 revenue of RMB810.0 million (US$117.5 million), down from US$158 million in 2015, a 25.8% decline as the company is redirecting its business to the downstream sector.

The company reported a net loss margin of 124.3%, compared to 39.8% for the prior year.

Monocrystalline wafer sales were US$44.4 million in 2016, compared to around US$90 million in 2015. Monocrystalline solar ingot sales were US$4.3 million in 2016, compared to US$0.52 million in 2015.

The company was impacted by cell and module customers in the Philippines, Malaysia, Japan and the US reducing production and closing manufacturing lines.

These included SunPower and Mission Solar Energy.

However, Comtec has secured a major wafer deal with Jolywood(Taizhou) Sunwatt Co for 68 million pieces of its A-grade n-type super monocrystalline wafers.

Credit Trina Solar

QSTec has begun producing polysilicon at its new plant in Qatar.

Company News

Longi changes name

Leading integrated monocrystalline PV manufacturer Xi'an LONGi Silicon Materials has officially changed its name in China.

The new full company name is LONGi Green Energy Technology Co., Ltd., dropping the traditional location name where the company is headquartered as well as the familiar 'Silicon Materials' aspect, which the company was well known for.

Having in recent years acquired solar cell and module manufacturer, LERRi Solar, and expanded downstream to build PV power plants, LONGi's original focus on monocrystalline ingot/wafer production remains an important business unit but does not reflect its more fully-integrated business model that includes both upstream and downstream operations.

Supply of low-cost and high-efficiency multi-GW mono wafers

Yichun Wang & **Tian Xie**, LONGi Green Energy Technology Co., Ltd., Xi'an City, PR China

ABSTRACT

This paper begins with a brief review of the Chinese PV industry, especially the mono crystalline silicon market. In the situation of a booming mono market, the mono wafer manufacturers are optimizing their capacity in order to guarantee a steady supply and to satisfy increasing customer demand. In addition, these manufacturers strive to drive down the cost of mono wafers and increase wafer performance through continuing technological development, especially in the areas of silicon ingot pulling and wafer slicing. With advanced pulling technology, mono silicon wafers can be produced with a low oxygen concentration and a long minority carrier lifetime, both of which are essential for excellent wafer performance. The development of diamond wire saw technology in recent years, compared with traditional slurry slicing, has dramatically reduced the slicing cost; it is also the perfect solution for thin wafer slicing, which directly reduces the silicon material cost per wafer. Alternatively, in order to facilitate the mono PV industry development, some of the leading companies are promoting various wafer product standards, such as the M2 wafer from LONGi. It is believed that all the above endeavours could boost the mono wafer market and help achieve grid parity.

Introduction

In the Chinese PV market, multicrystalline silicon firmly holds a large market share compared with monocrystalline silicon, entirely as a result of the development of the Chinese PV industry. Dating back to around 2008, silicon casting technology has been successfully developed in China, with multi wafer factory production capacity reaching GW scale. Because multicrystalline silicon casting was extremely productive (five times greater than mono pulling furnace manufacturing), the Chinese PV market began moving to multi and attracted enormous investment. This staggering expansion lasted for several years, which led, as we know, to a tremendous overcapacity and to the Chinese PV industry facing a period of severe disarray. Factories across the industry started to shut down their mono production lines or convert them to multi, since multi was lower in cost and higher in productivity. Thousands of factories were facing a crisis and even closed. The mono proportion of the market, of course, declined dramatically: by 2013 there were only four or five independent mono wafer factories left in the market.

> "Low-cost high-performance wafers are becoming increasingly important to solar cell manufacturers and the wafer suppliers upstream."

With the constant efforts by the mono wafer companies to expand mono production and technology R&D, the cost of mono wafers has fallen rapidly over the last few years. In addition, diamond wire saw technology (initially developed for mono wafers) has dramatically brought down the cost of mono wafers even further. Moreover, with the Chinese PV market becoming more mature in terms of understanding both investment and technology perspectives, along with the evolution of related industries, the Chinese PV market focus is shifting to high-efficiency solar cells, which could significantly reduce costs and yield greater financial profit. As a result, low-cost high-performance wafers are becoming increasingly important to solar cell manufacturers and the wafer suppliers upstream.

Growth of the monocrystalline market

After more than ten years of rapid growth, the Chinese PV industry has now entered a period of steady growth. Nevertheless, the technology related to monocrystalline silicon wafer production is still in a period of rapid innovation and development. Emerging solar cell technologies – such as p-type passivated emitter rear cell (PERC), n-type passivated emitter, rear totally diffused (PERT), heterojunction with intrinsic thin layer (HIT) and interdigitated back contact (IBC) – are gradually becoming sufficiently mature for mass production. Compared with multicrystalline solar cells, monocrystalline solar cells are demonstrating increasingly outstanding efficiencies: for example, Kaneka announced that its new HJ-IBC solar cell achieved an efficiency of 26.3%, which is a record-breaking efficiency for a Si solar cell [1].

On another note, the cost of mono solar wafers is being reduced through process technology and material innovations, especially in the areas of ingot growing and wafer slicing. In addition, considering the price decline of auxiliary materials, the non-silicon cost gap between mono wafers and multi wafers is getting smaller and smaller, and is expected to level out, or even reverse, in the next three to five years. Consequently, the latest mono solar cells are outstanding, with the advantages of high efficiency and low cost, and the mono wafer market is exhibiting aggressive growth.

The number of monocrystalline silicon solar module installations in China has steadily increased in recent years, and a market share of over 60% is forecast for 2018. It is expected that the mono cell market in 2017 might be limited by mono wafer supply, and serious mono wafer shortage is becoming an obstacle to mono cell market scaling.

Expansion of mono wafer production capacity

Given the current situation, mono wafer manufacturers are optimizing their production capacity planning in order to guarantee a steady supply and to satisfy growing market demand. Furthermore, it is believed that the increased production and sales volume will help dilute R&D spending and management/administration costs, as well as reducing supply chain and logistics costs.

LONGi is one of the largest mono wafers providers in China; Fig. 1 shows its expansion plan, which is aggressive and anticipates a 5GW year-on-year increase. In 2019 the estimated production capacity will reach 25GW for monocrystalline silicon ingots and wafers.

LONGi's capacity expansion optimization has a number of advantages. First, the increasing production of monocrystalline ingots and wafers could meet the surging market demand and help the development of the mono market. Second, the capacity expansion could reduce the average cost of operation. Third, the wide distribution of LONGi manufacturing sites could spread the business risk, and utilize the low-cost resources in specific locations in order to reduce production costs further. Last, but not least, the production at the Yunnan site, which is currently under construction, will largely use hydroelectric power; thus it will be possible to realize a smaller carbon footprint for wafer production and enhance the environmental performance of the PV industry.

Capacity expansion is one way in which mono wafer manufacturers are coping with the developing mono market; the other important aspect is technology innovation, which could improve mono wafer performance, indirectly bringing down the cost. Besides recharge CZ (RCZ), large-crystal silicon recharging, wafer dimension optimization and so on, some areas of investigation are minority-carrier lifetime, oxygen concentration, diamond wire sawing and thinner wafers.

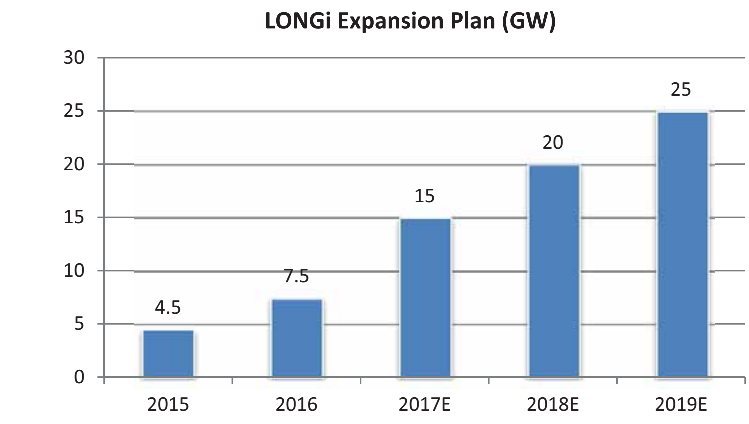

Figure 1. LONGi's plan for wafer production capacity expansion.

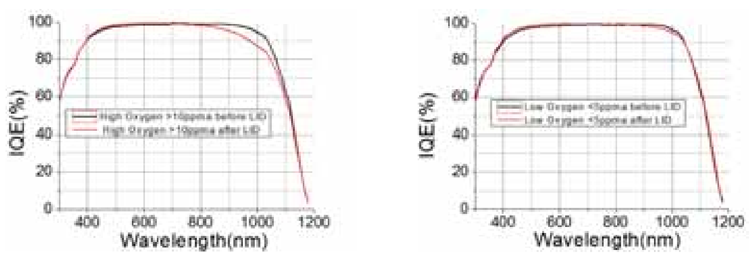

Figure 2. LONGi IQE charts for high-oxygen and low-oxygen wafers.

Pulling technology development – oxygen control and improved minority-carrier lifetime

With the development of the PV industry, the achievement of grid parity requires a higher conversion efficiency for solar cells; this imposes higher intrinsic quality requirements on crystalline silicon material, especially with regard to minority-carrier lifetime, impurity content, density of defects, etc. The minority-carrier lifetime is directly related to the conversion efficiency of solar cells [2]. Impurities and defects are the two main factors affecting minority-carrier lifetime. In monocrystalline silicon wafers, oxygen is the main impurity [3]; therefore, for the future high-efficiency solar cells, one key challenge is decreasing the oxygen content. From experimental investigations, the degradation of mono solar cell efficiency is correlated to oxygen precipitation.

In general, silicon solar cells do not respond to wavelengths of ultraviolet light below around 0.35μm and to wavelengths of infrared light above 1.15μm; the peak value of the spectral response is in the range 0.8~0.9μm. Depending on the solar cell manufacturing process and the resistivity of the material, when the resistivity is low, the spectral response peak value is around 0.9μm. In essence, the spectral response to long wavelengths mainly depends on the minority-carrier lifetime and on the diffusion length in the bulk. In the case of short wavelengths, the response is mainly determined by the minority-carrier lifetime in the diffusion layer and by the recombination velocity at the front surface.

The internal quantum efficiency (IQE) will be reduced in the long-wavelength regions after an extended period of light exposure; an example of such a phenomenon is light-induced degradation (LID). The LID effect is closely related to oxygen concentration. Fig. 2 shows that the decrease in IQE for wafers with low oxygen concentration after 48h LID is smaller than that for wafers with high oxygen concentration.

A sensitivity model of the surface recombination and bulk lifetime in a high-efficiency back-contact (IBC) solar cell demonstrates that solar cell performance becomes more sensitive to bulk lifetime as the front-surface diffusion recombination is reduced. This means that, at the same surface current density, the solar cell efficiency increases with higher minority-carrier lifetime, and when the surface current density is low, the increase in efficiency could be much greater [3].

Materials

Measurements of external quantum efficiency (EQE) of the solar cells with different oxygen densities after different anneals have revealed that wafers with the highest density of oxygen produce the worst performance [4].

One study of the impact of different improvements on the efficiency of PERCs has indicated that the long-lifetime wafer, i.e. 1ms wafer, is one of the key factors of the high-efficiency solar cell roadmap; other factors include metallization technology, multi-wire, thin fingers and selective emitters [5]. In that study, the impact of rapid thermal annealing (RTA) was investigated; the RTA was performed in a belt-type firing furnace, as used for the metallization of screen-printed silicon solar cells. By varying the peak temperatures and the cooling rates of the RTA treatment, significant differences in the lifetimes after complete degradation, after dark annealing and after permanent recovery were observed. It was possible to improve the permanently recovered lifetime much more dramatically, from 1.1ms to 1.54ms, which means that the long-lifetime wafers undergo a far better permanent recovery on the basis of high bulk minority-carrier lifetime. The LID of long-lifetime wafers is minimized after the RTA process. Long-lifetime wafers are therefore the industry requirement for high-efficiency solar cells.

To sum up, a low oxygen concentration and a long minority-carrier lifetime are the two key issues for high-efficiency solar cells at the wafer level; much R&D work and many studies focus on such challenges in the PV industry. The upgraded pulling technology is stable and its implementation is ongoing in order to reduce the oxygen concentration and to improve the lifetime of wafers in mass production.

Today it is possible to produce monocrystalline silicon ingots with a long lifetime, low oxygen concentration and high-quality uniformity across the whole ingot. For example, Fig. 3 shows the performance of LONGi's n-type ingot sample with an advanced controlled crystal pulling process: a minority-carrier lifetime (MCL) of over 10ms (90% of the ingot) is achieved, with a peak value of around 24ms. The wafer resistivity is 1–7Ω·cm.

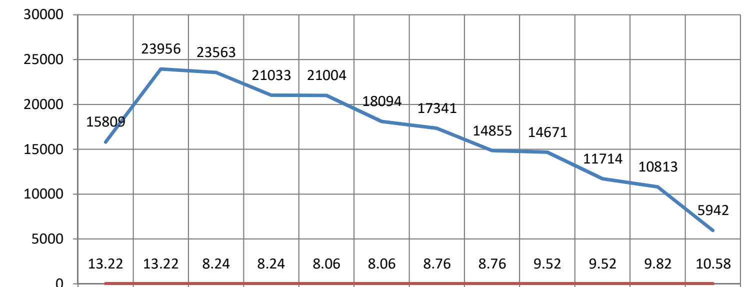

	Seed End A	Seed End B	Brick 2 A	Brick 2 B	Brick 3 A	Brick 3 B	Brick 4 A	Brick 4 B	Brick 5 A	Brick 5 B	Tail End A	Tail End B
MCL (µs)	15809	23956	23563	21033	21004	18094	17341	14855	14671	11714	10813	5942
Oi(ppma)	13.22	13.22	8.24	8.24	8.06	8.06	8.76	8.76	9.52	9.52	9.82	10.58

Figure 3. Oxygen concentration and MCL for LONGi's n-type ingot sample.

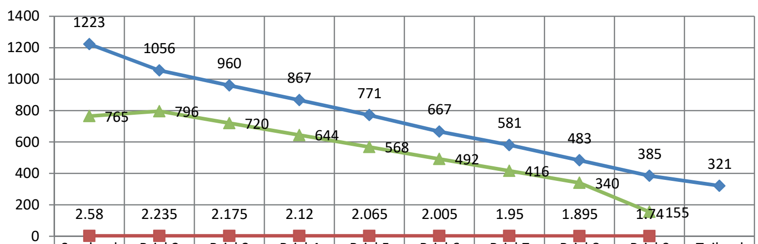

	Seedend	Brick2	Brick3	Brick4	Brick5	Brick6	Brick7	Brick8	Brick9	Tailend
LT-A	1223.179	1055.556	960.1481	866.9231	770.963	666.52	580.8462	483.35	384.9375	321.3333
Res	2.58	2.235	2.175	2.12	2.065	2.005	1.95	1.895	1.74	
Ave	765	796	720	644	568	492	416	340	155	

Figure 4. Oxygen concentration and MCL for LONGi's p-type ingot sample.

In contrast, Fig. 4 shows the performance of LONGi's p-type ingot sample with an advanced controlled crystal pulling process: an MCL of above 300µs (over 100% of the ingot) is achieved, with a peak value of greater than 1ms.

As shown above, mono manufacturers can supply ingot/wafer products that have improved performance. Several technical issues still need to be dealt with, however, and are currently under investigation.

Ring patterns on thin mono wafer surfaces have been observed using photoluminescence (PL) tests, and also ring patterns on the fabricated solar cell using electroluminescence (EL) tests; this raises worries of reduced cell efficiency. Through research and investigation, it has been determined that the ring patterns are formed during the process of ingot pulling, and that they are inherent and inevitable [6].

Slicing technology development – diamond wire slicing

Monocrystalline solar cell development is mainly committed to achieving grid parity, which requires focusing on high efficiency and low cost. Innovations in materials, solar cell structures, manufacturing processes and so on are what drive the PV industry to move forwards. On the other hand, efforts to keep costs down are another key to PV industry scaling.

Wafer cost can be divided into silicon cost and non-silicon cost. Most technology innovations and upgrades today are aimed at reducing the non-silicon cost contribution. Room for further reducing the non-silicon cost, however, is becoming less and less; thus it is beneficial to look at the silicon cost segment.

Diamond wire slicing is the process of using wire of various diameters and lengths, impregnated with diamond particles of various sizes, to cut through materials. This type of sawing produces less kerf and waste material than traditional methods, such as the slurry slicing method. Unlike slurry saws, which use bare wire and contain the cutting material in the cutting fluid, diamond wire saws just use water (or some other fluid) for lubrication, cooling the cut and removing debris. Monocrystalline silicon is composed of silicon atoms in an extended orderly arrangement, with no grain boundaries or hard spots; hence the monocrystalline wafer is suited to the diamond wire sawing technique. Diamond wire saw technology has therefore become a perfectly matched option for mono wafer slicing, and significantly reduces costs.

Compared with the slurry slicing method, diamond wire slicing can cut wafers that have smooth surfaces with shallow regions of damage; moreover, the wafers produced have better strength, thus supporting thinner wafers. The diamond wire slicing method also brings the added benefit of lower metal concentration on the silicon wafer surface.

> "The trend for thinner wafers is the future for the solar industry."

Thinner wafers

The industry has up to now been concentrating on aspects other than silicon, and the non-silicon cost has kept on decreasing dramatically in recent years. The trend for thinner wafers, however, is the future for the solar industry. The thinner wafer solution is becoming increasingly important, since it directly addresses the reduction of the silicon cost of wafers. In order to bring down the cost, and facilitate the development of the solar industry, the market has been promoting thinner wafers in recent years, driven by some of the leading companies. LONGi, for example, passes on the benefit of reduced silicon costs of wafers to the customers, i.e. thinner wafers at a lower price.

At the moment, multi-wire cutting is widely used for solar cell wafering: thousands of wafers can be produced in a single-pass cut. In order to produce more wafers from a single ingot, silicon wafer thinning is necessary. Wafer thinning technology could directly bring down the average wafer cost, since less kerf is produced and more wafers are created.

For typical cell technology, however, the performance of thin wafers is inherently inferior in terms of efficiency: thinner wafers yield lower IQEs in the long-wavelength region. To maintain a high efficiency for wafers of thicknesses below 200μm, a lower back-surface recombination is necessary [7]. Screen-printed p-type cells with an Al back-side field (BSF) can scale to a minimum wafer thickness of around 170–180μm. For thicknesses below that, optical and back-surface recombination losses significantly degrade the efficiency; innovations with regard to materials, processes, device structures, etc. (for example, the PERL-type cell) are therefore required in order to continue scaling the wafer thickness.

Compared with the traditional solar cell structure, the new HIT solar cell reaps many more benefits from thinner wafers, notably higher efficiencies. The world-class HIT solar cell has so far demonstrated a laboratory conversion efficiency of 25.6% [8].

For thin wafers, several challenges still exist. Although wafer strength is initially outstanding, the bending strength is reduced with decreasing wafer thickness; further studies have shown that bending strength can be improved after the texturing process. In addition, thin mono wafers with micro-cracks and/or V-shape chips have shown higher probability of breakage. With improved manufacturing processes and inspection tool upgrades, however, the potential for wafer breakage can be minimized.

Besides the wafer quality being improved with pulling technologies, the same is true with slicing technologies upgraded by diamond wire. Wafer thicknesses down to 110μm have been achieved in an R&D setting. Recently, the most technically challenging issues for thin wafers have been resolved, resulting in the creation of extra-thin (down to 100μm) wafers; Fig. 5 shows the first 100μm wafer manufactured by LONGi in 2014. In contrast, a wafer thickness of 150μm is currently possible in mass production,

	Wafer thickness	2013	2015	2017
p-type	200μm	60%	3%	X
	190μm	30%	55%	35%
	180μm	10%	40%	55%
	<180μm	X	2%	10%
n-type	200μm	100%	50%	0%
	180μm	X	30%	90%
	<180μm(110μm)	X	X	10%

Table 1. LONGi wafer shipment statistics.

Dimensions	Diameter [mm]	Length [mm]	Area [cm^2]	Increased area [cm^2]
8 inch	200.00	156.00	238.95	-
M2	210.00	157.75	244.32	5.37 (2.25%)

Table 2. Wafer dimension comparison.

Figure 5. A flexible solar cell made from a LONGi 100μm wafer.

with all the wafer capacity being easily converted to thinner wafer thicknesses according to a particular customer's request.

As Table 1 shows, the thin wafers manufactured by LONGi have been in increasing demand since 2013; in 2017 it is expected that over 65% of the company's wafer products will be thin wafers, i.e. with thicknesses of 180μm and below. The shipment data of LONGi, a supplier of mono wafers, indicate that the market is moving to thin wafers.

Promotion of an industry standard – the M2 wafer

To help and facilitate the development of the PV industry, planning work has been under way to create a wafer product standard, especially from a wafer manufacturer's perspective. At the end of 2013, LONGi's M2 mono wafer was introduced; on the basis of the product's technology and market performance, it has been widely accepted by customers and is becoming the industry standard. Furthermore, mono wafer companies are actively promoting wafer-thinning technology, so that the cost of the mono wafer can be reduced even further and such wafers can thus be more competitive in the market. In consequence, the PV industry could become a more important player in the field of energy and could achieve grid parity.

The larger-wafer products – M2 mono wafers (Table 2) – have several advantages. First, the unified single crystalline product specifications help to reduce costs in the upstream and downstream industry chains. Second, with virtually no changes necessary to the production line, single-cell power output is increased and the value of a single cell is improved. Third, solar module power is enhanced, and the single-solar-module performance to price ratio is improved.

> "There has been a significant increase in the monocrystalline market share, which clearly indicates that there is a growing demand for high-efficiency wafers."

Conclusion

Innovations in structure technology, manufacturing processes and materials are being introduced, all of which lead to a lower cost for monocrystalline compared with multicrystalline, with a wide scope for even further reductions. Meanwhile, as manufacturing technologies continue to be studied, they are reaching the level of maturity suitable for mass production, especially with regard to oxygen control, improved minority-carrier lifetime, decreased degradation, M2 wafer standardization, etc. As a result, the quality of monocrystalline solar cells will be further improved in terms of conversion efficiency, with a 2% advantage over multicrystalline solar cells.

Looking to the future, there has been a significant increase in the monocrystalline market share, which clearly indicates that there is a growing demand for high-efficiency wafers along with high expectations.

References

[1] Yoshikawaet, K. et al. 2017, "Silicon heterojunction solar cell with interdigitated back contacts for a photoconversion efficiency over 26%", *Nature Energy*, Vol. 2, Article no. 17032.

[2] Steinkemperet, H. et al. 2016, *Prog. Photovolt: Res. Appl.* [DOI: 10.1002/pip.2790].

[3] Cousins, P. et al. 2010, *Proc. 35th IEEE PVSC*, Honolulu, Hawaii, USA, p. 275.

[4] Chen, L. et al. 2011, *Sol. Energy Mater. Sol. Cells*, Vol. 95, pp. 3148–3151.

[5] Walter, D.C. et al. 2014, *Appl. Phys. Lett.*, Vol. 104, p. 042111.

[6] Voronkovet, V.V. et al. 2000, "On the properties of the intrinsic point defects in silicon: A perspective from crystal growth and wafer processing", *physica status solidi (b)*, Vol. 222, p. 218.

[7] MEMC workshop, 2010.

[8] Panasonic 2016, PVCellTech, Kuala Lumpur, Malaysia.

About the Authors

Yichun Wang received a B.S. in electrical engineering in 2007 from Northwestern University, China, and an M.S. in electrical engineering in 2010 from the University of Kentucky, USA. She joined LONGi Green Energy Technology Co., Ltd. in 2014, and is currently the application engineering and customer service manager in the silicon wafer business group, where her responsibilities include technical/product quality support and supervising technical collaboration projects with global institutes and corporations.

Tian Xie received his Ph.D. in physics in 2004 from Hiroshima University, Japan. He is the director of the quality management department at LONGi Green Energy Technology Co., Ltd., where his primary responsibility is overseeing the quality management, customer service, product design and sales groups at the company.

Enquiries

Yichun Wang
Tel: +86 186 8185 6911

Email: wangyc@longi-silicon.com

Cell Processing

News

Neo Solar Power to shift all production to monocrystalline PERC

Neo Solar Power is phasing out multicrystalline production in favour of mono.

Credit Neo Solar Power

Neo Solar Power (NSP) is to phase out production of multicrystalline products and switch completely to monocrystalline production.

It joins Germany's SolarWorld, which recently became the first major PV manufacturer to announce a shift away from multicrystalline wafer, cell and module production in favour of monocrystalline production using PERC cell technology and also offer bi-facial modules.

Overcapacity in multicrystalline production and slim ASP margins are commercial factors behind NSP and SolarWorld's recent production shift as well as increasing scale with the higher efficiency monocrystalline products to reduce costs as demand for mono products is growing and is in a relatively shorter supply.

According to NSP, using p-type mono PERC over p-type multi increases module power by 15%, although total module costs per watt increased by 9.2%.Therefore, the module cost per watt decreased by around 3% to 4% when using P-type mono PERC, compared to p-type multi PERC.

The company has relocated around 100MW of mono cell production from its 500MW cell plant in Malaysia to Vietnam and migrate around 500MW of capacity in Taiwan to mono-PERC.

Overall timelines for the migration of all capacity to mono was not disclosed.

New Technologies

IFC to invest US$60 million in Jinko Malaysia as company upgrades to PERC cell technology

The International Finance Corporation (IFC) has said that it will invest up to US$60 million in JinkoSolar subsidiary, Jinko Malaysia.

Jinko Malaysia will use the IFC funding for a US$100 million plan to upgrade its existing solar cell production lines to PERC, which will boost energy conversion and cut down on system costs.

The investment from IFC will come in two segments, including a US$40 million IFC A Loan from IFC's own account, along with US$20 million from the Managed Co-Lending Portfolio Programme.

Jinko Malaysia, a subsidiary of JinkoSolar, will use the IFC funding for a US$100 million plan to upgrade its existing solar cell production lines to passivated emitter rear cells (PERC), which will boost energy conversion and cut down on system costs.

Yingli Green expects volume production of n-PERT IBC cells in 2018

Yingli Green Energy and industrial technology partners, Dutch research centre ECN and equipment manufacturer Tempress, a subsidiary of Amtech Systems, have fabricated their first interdigitated back contact (IBC) n-type solar cells on six-inch monocrystalline wafers at the manufacturer's pilot line in China.

Yingli Green said that its long-standing n-PERT 'PANDA' process was adapted to the IBC cell architecture to provide a lower-cost route to IBC cell efficiencies that deploy fine-line screen printing technology for patterning and metallisation with support from the new production process co-developed by ECN and Tempress.

Pilot production was managed in less than three months, according to the partners.

The companies aim to produce n-PERT IBC cells that have an efficiency of 22% by the end of 2017, while the development and production of commercial modules using the cells was expected for 2018.

The IBC n-PERT cell architecture also enables high-efficiency bi-facial module production.

Efficiencies

1366 Technologies pushes 'Direct Wafer' cell efficiencies with Hanwha Q CELLS to 19.9%

US-Based wafer producer 1366 Technologies and Hanwha Q CELLS have jointly achieved cell conversion efficiencies of 19.9%, up from 19.6% announced in December 2016.

1366 Technologies said that its 'Direct

Yingli is expecting volume production of IBC n-PERT cells by next year.

Credit Yingli Solar

GEMÜ®

VALVES, MEASUREMENT AND
CONTROL SYSTEMS

Resistant, easy to fit, high flow rate
GEMÜ C60/C67 CleanStar®

Advantages:

- *Good flow capability thanks to high-flow bodies*
- *Made from resistant materials*
- *Various connections available*
- *Specifically designed for cleanroom media*
- *Outstanding price-performance ratio*

*www.**gemu-group**.com*

Wafer' (156mm x 156mm) multicrystalline wafers and Hanwha Q CELLS' 'Q.ANTUM' PERC solar cell process efficiency milestone was independently confirmed by the Fraunhofer ISE CalLab.

1366 Technologies noted its Direct Wafer process had a high-purity growth environment, better wafer microstructure and the ability to modify the dopant concentration between the front and back of a wafer improves electron harvesting as unique features that boost cell conversion efficiencies.

Frank van Mierlo, CEO of 1366 Technologies said: "Our efficiency is improving at a rate that's nearly double that of the rest of the industry. Late last year, we exceeded the cell efficiency of the high-performance multi (HPM) reference group in a head-to-head comparison, and we continue to make progress. This latest milestone demonstrates the rapid gains still possible with our Direct Wafer process because our technology is not limited by the inherent weaknesses of ingot-based wafer manufacturing."

Hevel's first heterojunction solar cell achieves 21.75% conversion efficiency

Russia-based integrated PV manufacturer Hevel Group has claimed its first fabricated heterojunction (HJ) solar cell has achieved a conversion efficiency of 21.75%.

Hevel noted that the cell efficiency was measured under standard testing conditions in-house and not verified by a third party.

Leading PV manufacturing equipment supplier Meyer Burger landed a US$22.5 million order from Hevel to convert to HJ and bifacial cell production and 'SmartWire' module assembly.

The switch, which was announced back in June 2016, would provide a nameplate capacity of 160MW, according to the company.

Hevel's HJ modules are expected to be used in downstream PV power plant projects in Russia. The company claimed a project pipeline of around 500MW, which includes grid connected and off grid PV plants.

SunPower hits average cell conversion efficiencies of 25% at Fab 4

SunPower has reached a production average cell conversion efficiency of 25% at its Fab 4 facility in the Philippines, the highest in the industry.

The company also highlighted that its Fab 4 facility was expected to complete ramping to its nameplate capacity of 350MW in 2017.

SunPower's management also said that it expected to spend around US$100 million in capital expenditures to upgrade its Fab 3 (800MW) solar cell facility in Malaysia to its next-generation n-type monocrystalline IBC cell technology (X Series) that is being ramped at Fab 4. Total capex for 2017 was said to be around US$120 million.

With the ramping of Fab 4 and planned upgrades at Fab 3, SunPower could be expected to rely more heavily on its P-Series modules, which uses sourced solar cells and assembled at its consolidated module assembly plant in Mexico.

Fraunhofer ISE touts n-type multicrystalline cell with record 21.9% conversion efficiency

Fraunhofer ISE has claimed a new record conversion efficiency of 21.9% for a 20mm x 20mm n-type multicrystalline cell using process match wafer and its TOPCon (Tunnel Oxide Passivated Contact) developed technology.

Fraunhofer ISE said the record was achieved by combining n-type high performance multicrystalline silicon that shows a higher tolerance to impurities, especially iron, with its TOPCon technology that has metal contacts applied to the wafers rear side without patterning, which enables majority charge carriers to pass and prevents the minority carriers from recombining, boosting efficiency.

TOPCon technology is deployed as a full-area passivated back contact, without any patterning. The thickness of the intermediate passivation layer is only one or two nanometers thick, allowing the charge carriers to 'tunnel' through it, preventing recombination and limiting losses.

Fraunhofer ISE trumps own multi-junction solar cell conversion efficiency record

Fraunhofer ISE has surpassed its record solar cell conversion efficiency for an III-V/Si multi-junction solar cell it set in November 2016 – achieving a cell conversion efficiency of 31.3%, up from 30.2%.

Fraunhofer ISE had worked together with the Austrian semiconductor

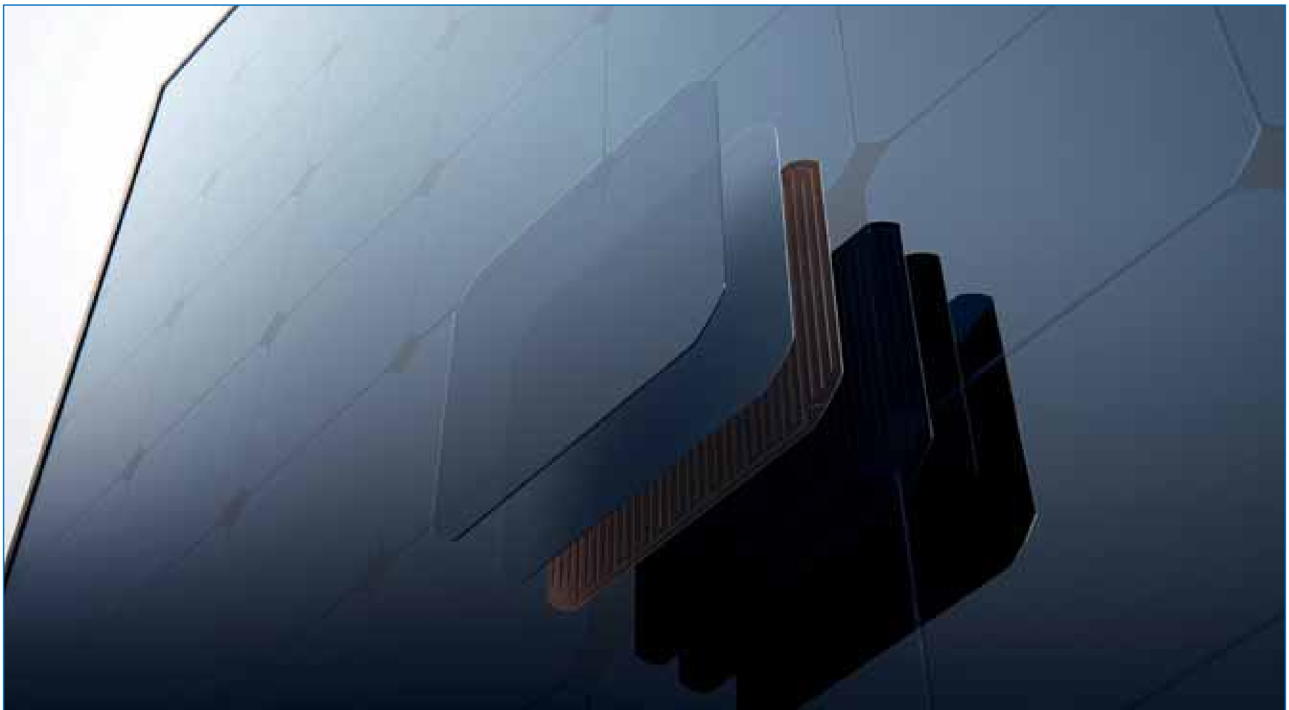

Credit SunPower

SunPower has hit an average 25% cell conversion efficiency at its Philippines facility.

Credit Innolas

InnoLas Solutions has secured new orders for its ILS-TTnx high-throughput laser platform.

equipment company EV Group (EVG).

EVG supplies a direct wafer bonding tool to transfer III-V semiconductor materials only a few nanometres thick to conventional silicon substrate that creates a monolithic solar cell. Potentially, processing costs would be reduced for using III-V materials.

Tool Orders

Meyer Burger bags PERC cell upgrade order valued at US$15 million

Meyer Burger Technology has secured an order for its MAiA 2.1 upgrade cell coating platform for PERC technology from an existing customer in Asia valued at around CHF 15 million (US$15.06 million).

Delivery and commissioning of the equipment is scheduled to begin in the second quarter of 2017.

3D-Micromac half-cell cutting tool orders top 1.5GW

PV manufacturing equipment specialist 3D-Micromac said it had booked over 1.5GW of orders related to its microCELL TLS (Thermal Laser Separation) high-throughput half-cell cutting tools since the beginning of the year.

The TLS process is said to provide higher mechanical strength, better edge quality as well as lower power reduction compared to laser scribing and other cleaving approaches.

The company claims module power gain of more than 1.0W has been achieved compared to conventional scribe and break methods, in addition to the 5-7W per module gain of half-cell module technology.

InnoLas launches ILS-TTnx high-throughput laser platform with confirmed orders

PV laser technology equipment specialist InnoLas Solutions has secured new orders for its ILS-TTnx high-throughput laser platform that was officially launched at SNEC 2017 in Shanghai, China, in April.

The company said the new order intake included a number of key PV manufacturers in Asia, including leading companies in China.

Innolas noted that new order inflow in the first quarter of 2017 had been over €10 million with the expectation of significant growth during the year, due to the high demand for the Laser Contact Opening (LCO) process for PERC and the increasing interest in the Laser Doped Selective Emitter (LDSE) process for advanced p-type solar cells.

Aurora Solar secures new volume order from leading solar cell producer

Inline measurement equipment specialist Aurora Solar Technologies (AST) has secured a new order from the world's largest solar cell producer, expanding the use of its Decima 3T and Veritas servers for high-efficiency solar cell production. Recently, AST secured a major order from LG Electronics and launched the first system that measures bifacial solar cells.

AST noted that the order included 10 'Decima 3T' inline measurement tools in combination with Aurora's 'Veritas' servers for visualization and control that will span several production lines.

The order is expected to ship in June and July 2017.

RENA Technologies wins large orders from Asia for mono c-Si wafer texturing

RENA Technologies has secured several major orders from Asia-based PV cell manufacturers for its alkaline texturing and junction isolation tools in the first quarter of 2017.

The orders equated to the production capacity of more than 4.5GW of monocrystalline silicon solar cells, which included the RENA BatchTex 'N400' texturing tools that enables high throughput alkaline texturing, as well as the RENA 'InOxSide+' inline systems that combines junction isolation and rear side smoothing for high efficiency solar cells.

The monocrystalline solar cell equipment orders come on the back of a major order in September, 2016 from LONGi Solar, formerly LERRI Solar, for the same equipment for the equivalent of 2GW of monocrystalline PERC solar cell production.

INDEOtec to supply Saudi Arabia's KAUST with heterojunction solar cell deposition system

INDEOtec SA has secured a new order for a combined OCTOPUS II – PECVD/PVD deposition system for high-efficiency and heterojunction solar cell development from the King Abdullah University of Science and Technology (KAUST) in Saudi Arabia.

The company has won a series of orders for the OCTOPUS II as research builds momentum for next-generation heterojunction solar cells.

The OCTOPUS II cluster tool enables double-sided HJ cell passivation and junction layer deposition for heterojunction cell architectures.

Company news

NSP sales decline on migration away from multicrystalline cell production

Neo Solar Power (NSP) is feeling the impact of its shift away from multicrystalline cell production to become a differentiated producer of high-efficiency monocrystalline PERC and heterojunction (HJ) cells and modules as sales continue to decline through the first quarter of 2017.

NSP reported March sales of NT$661 million (US$21.57 million), down 10.2% from the previous month and down 63.37% from the prior year period.

Unaudited sales in the first quarter of 2017 were approximately NT$2,162 million (US$70.56 million), down 68% from the prior year period.

Market Watch

Fab & Facilities

Materials

Cell Processing

Thin Film

PV Modules

Solar cell demand for bifacial and singulated-cell module architectures

Nico Wöhrle, **Elmar Lohmüller**, **Max Mittag**, **Anamaria Moldovan**, **Puzant Baliozian**, **Tobias Fellmeth**, **Karin Krauss**, **Achim Kraft** & **Ralf Preu**, Fraunhofer Institute for Solar Energy Systems ISE, Freiburg, Germany

ABSTRACT

The pursuit of achieving higher power output of silicon-based PV modules demands creative improvements in module design in order to reduce geometrical, optical and electrical cell-to-module (CTM) losses. A suitable method, which has been known since Dickson's patent in 1956 (but has been mostly under the radar of the manufacturing industry), is the shingling of singulated solar cell stripes. This technology offers three advantages in comparison to modules with standard-sized solar cells. First, blank cell spacing in the module is minimized, thus increasing the power-generating area per module area. Second, the active cell area is busbar-less, which leads to reduced shading losses. Third, because of the smaller area of the solar cell stripes, the generated current per cell is less, which results in a reduction in the overall series resistance of the cell interconnection within the module. To boost the power output of such a shingled module even further, the introduction of bifacial properties is suggested. To make this bifacial shingled module technology visible on the industry's radar, a practical concept is essential; this paper presents, step by step, Fraunhofer ISE's approach for a bifacial shingled module. Suitable bifacial cell concepts – such as passivated emitter and rear (PERC), passivated emitter, rear totally diffused (PERT), and passivated emitter, rear locally diffused (PERL) – are briefly introduced. The PERL cells are based on the PassDop approach, in which the rear-side passivation layer stack also acts as a doping source during local laser doping. Furthermore, next-generation bifacial cell concepts based on selective and/or passivated contacts, such as in the already established silicon heterojunction technology (SHJ) and the tunnel oxide passivated contact (TOPCon) approaches, developed at Fraunhofer ISE, are presented. Laser-assisted cutting as the singulation technology for realizing the cell stripes, and the challenge of charge-carrier recombination at the cutting edges, are discussed. A bifacial simulation model is presented for the singulated shingle solar cells, covering the question of the impact of different recombination factors, bifacial gains and optimizations of the cell layout. Finally, the module assembly, as well as a detailed calculation of module output power and a comparison with standard module layouts, is presented. This comparison emphasizes the advantages offered by bifacial shingled modules, with the potential to achieve a module power of 400W with a power density of 240W/m^2 and beyond, for irradiance intensities of 1,000W/m^2 and 100W/m^2 from the front and rear sides respectively.

Introduction

The first appearance of a shingled solar cell interconnection pattern (see Fig. 1) dates back to 1956 with a US patent filed by Dickson [1] for Hoffman Electronics Corporation, which is just two years after the first publication of a silicon solar cell by Chapin et al. [2]. In the years that followed, further patents were filed containing concepts of shingling solar cells serving various module designs and applications – for example, Nielsen [3] for Nokia Bell Labs, Myer [4] for Hughes Aircraft Company, Baron [5] for Trw Inc, Gochermann and Soll [6] for Daimler-Benz Aerospace AG, Yang et al. [7] for Silevo LLC, and the most recent patent applications by Morad et al. [8–10] for SunPower Corporation in 2016. Besides the patents, there are a number of items in the literature that have been devoted to this topic in the last few years, with publications by Zhao et al. [11], Glunz et al. [12] and Beaucarne [13]. Recently, the first widely available commercial shingled module was introduced by SunPower [14] as their top-of-the-line product; according to the data sheet, these modules feature a backsheet and are therefore not bifacial.

The idea of singulated solar cells interconnected by a shingling design is therefore by no means new. The early publications of shingling approaches were mostly motivated by particular design requirements, such as modules that were curved, triangular [4] or dome shaped [6]. Later publications started to make use of the potential for achieving

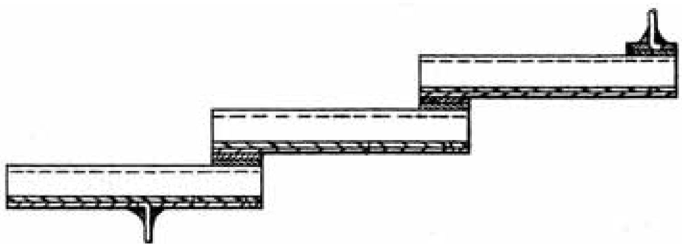

Figure 1. First published illustration of the shingling scheme for monofacial silicon solar cells, taken from Dickson's patent [1] (the descriptive labels in the original image have been removed for reasons of clarity).

higher module power densities with this technique than with standard-module cell interconnection, for example in the limited available space on the vehicle for the 'World Solar Challenge' in 1996 [11]. Consequently, a few large module manufacturers [7,14] seem to have rediscovered the potential of shingling technology to reduce cell-to-module (CTM) losses. The International Technology Roadmap for Photovoltaic (ITRPV) 2017 projects a world market share of 7% for shingled interconnection technology by 2027 [15].

> "The opportunity is at hand for combining bifacial solar cell technology with shingle cell module technology."

Another line of technological evolution spreading in the PV industry is the concept of bifacially illuminated solar cells, which has been extensively covered in a recent article by Kopecek and Libal [16]. As the demand for modules with high power density is large, the opportunity is at hand for combining bifacial solar cell technology with shingle cell module technology, with bifacial cells profiting from additional light coming from the rear side. The busbars on the front and rear sides for the shingle cells are covered by an active area from the adjacent cells, leading to a virtually busbar-free cell string.

The approach for such a bifacial shingle module is presented in three stages. First, eligible bifacial cell concepts – including passivated emitter and rear (PERC [17]), passivated emitter, rear totally diffused (PERT [18]), and passivated emitter, rear locally diffused (PERL [19]) – will be discussed. For this study, the PERL concept is based on the PassDop approach [20–22], in which the rear-side passivation layer stack – i.e. the layer stack consisting of aluminium oxide (AlO_x) and boron-doped silicon nitride (SiN_x:B) – also serves as a doping source for local laser doping. Furthermore, cell concepts with selective and/or passivated contacts that are based on silicon heterojunction (SHJ [23]) or hybrid PERC structures with tunnel oxide passivated contacts (TOPCon [24]) on the rear side will be discussed. Second, physically and technically relevant challenges for the transition from standard cells

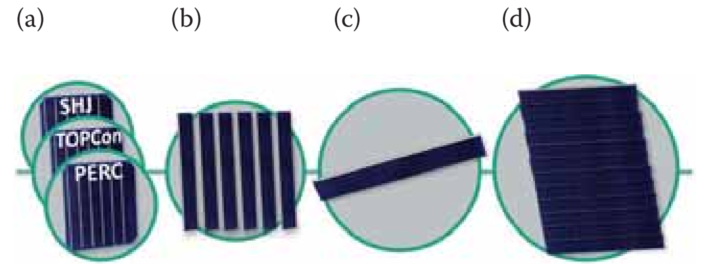

Figure 2. Schematic of the different process steps in the fabrication of shingle modules, starting from bifacial cells on a standard-sized wafer with an edge length of 156mm. (a) Six shingle solar cells are placed on the large-area wafer. The cell concept is modular; silicon heterojunction (SHJ), TOPCon and PERC examples are shown here. (b) The individual shingle cells are singulated into cell stripes. (c) A magnified single shingle cell. (d) Cell stripes are shingled onto each other to form a string.

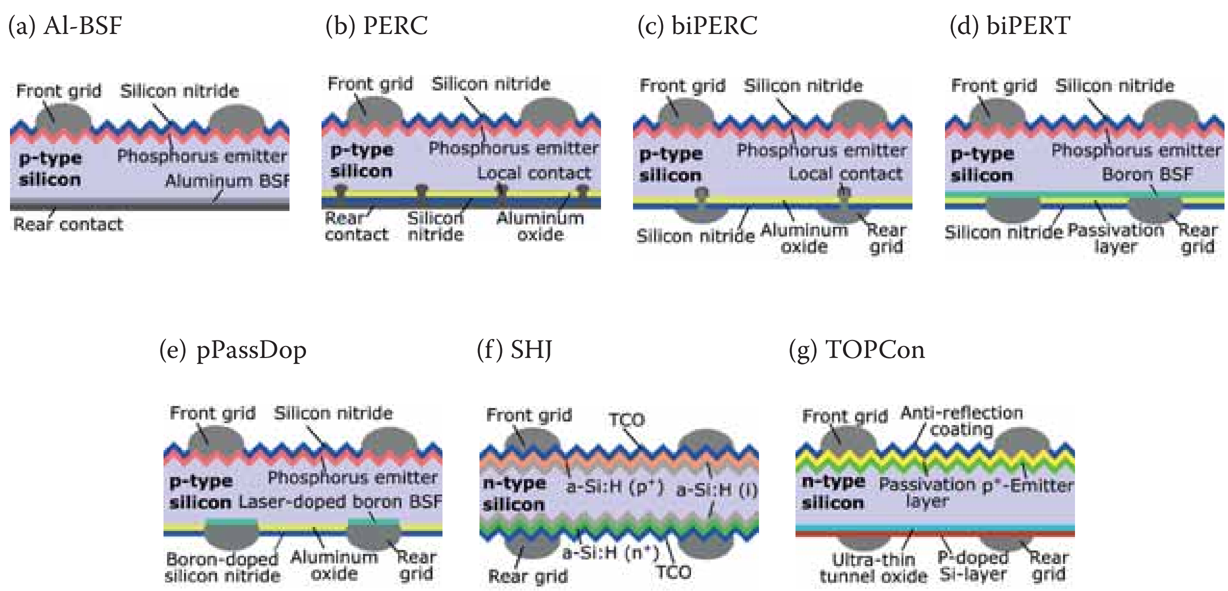

Figure 3. Schematic cross sections of seven different silicon solar cell types with homogeneous emitter. (a) Aluminium back-surface field (Al-BSF) cell. (b) Monofacial PERC with local rear-side contacts. (c) Bifacial PERC with finger grid on the rear side. (d) Bifacial PERT concept with full-area rear-side BSF. (e) Bifacial pPassDop concept with local laser-boron-doped BSF. (f) Silicon heterojunction (SHJ) cell with doped amorphous silicon emitter and a transparent conducting oxide (TCO) as anti-reflection layer. (g) Bifacial TOPCon cell with passivated rear-side contacts (the bifacial rear side shown is only a concept at the moment).

Cell Processing

to stripe cells will be addressed, including a discussion of edge recombination effects with a suitable full-cell simulation model realized with the Quokka3 tool [25]. Third, module integration strategies and CTM-loss calculations are provided.

As a name convention, the term 'output power density' P_{out} (mW/cm^2) will always be used instead of 'energy conversion efficiency' η (%) for measurement data referring to bifacial illumination, as that unit is less ambiguous. The scale chosen is such that, with a monofacial irradiation of 1,000W/m^2, the respective numerical values for P_{out} and η are identical.

Approach

To achieve a module output power P_{module} of 400W with power densities of 240W/m^2 and beyond for a standard 60-cell module with a size of 1.68m × 1.00m (irradiation intensities of 1,000W/m^2 and 100W/m^2 from the front and rear sides respectively), the approach proposed here is to apply shingling technology in order to use the module area as efficiently as possible. By shingling the solar cells, three CTM-related types of loss are minimized, namely 1) losses due to inactive module area; 2) shading losses due to busbar contacts; and 3) series resistance losses due to cell interconnection. To also benefit from the additional rear-side illumination from bifacial solar cell architectures, the proposed shingle solar cell and module technology is also bifacial in nature. The authors foresee a large potential for this bifacial shingling approach in cases where the 'old idea' of shingled modules can be merged with state-of-the art bifacial solar cell concepts.

To raise interest with regard to industrial mass production, standard-sized solar cell manufacturing sequences, with only minor adaptations, should be utilized for the manufacturing of shingle solar cells. Thus, the most obvious industrial solar cell concept to be used is the bifacial passivated emitter and rear cell (biPERC) technology, utilizing p-type Czochralski-grown silicon (Cz-Si) wafers. Fig. 2 illustrates four different typical stages of the fabrication of shingle solar cells and module strings, starting from a standard wafer with an edge length of 156mm. The general approach here is to create a certain number (six in this example) of shingle solar cells on a large-area wafer.

After metallization and contact formation, the cell stripes are singulated by a laser-assisted cutting process. Subsequently, the single cell stripes are interconnected by shingling the cells onto each other. Since singulation into stripe cells results in an increased contour-to-area ratio, edge passivation becomes important and needs to be considered. This design approach will be called the *shingled passivated edge, emitter and rear (SPEER)* solar cell concept. A true indication of strength of the module assembly of shingle cells is the modularity of the chosen cell concept to be utilized; the shingle module concept can therefore directly profit from progress in solar cell efficiency, while keeping the same module platform, and thus the same module manufacturing process.

Apart from the SPEER solar cells (which can be based on PERC, PERT or PERL structures), approaches with passivated contacts (SHJ, TOPCon) are within the scope of the work currently being pursued at Fraunhofer ISE. The shingle solar cells that are based on passivated contact approaches are called the *shingled passivated edge, emitter, rear and contact (SPEERCon)* solar cell concept.

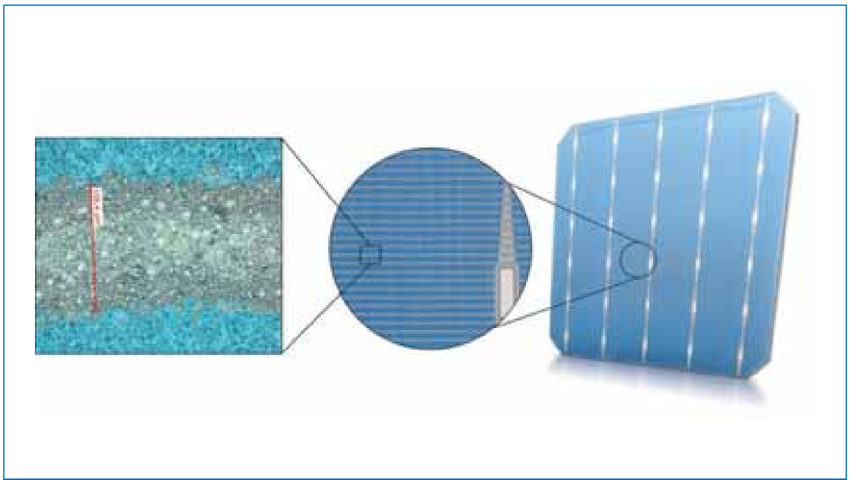

Figure 4. Bifacial PERC solar cell with a screen-printed aluminium rear finger grid with a finger width approaching 100µm [34]. The indicated selection has a measured width of 108.4µm, while the underlying LCO features a width of 30–35µm.

Eligible bifacial cell concepts

At the moment, aluminium back-surface field (Al-BSF) solar cells (see Fig. 3(a)), with a market share of around 80% in 2016 [15], still dominate the industrial production of crystalline silicon solar cells. However, the passivated emitter and rear cell (PERC) [17] (see Fig. 3(b)) allows higher energy conversion efficiency as a result of its dielectrically passivated rear side. The market share for PERC has gradually increased, to about 15%, in the last few years, and is expected to win significant market share over Al-BSF technology in the future [15]. Besides the dielectric rear-side passivation, one of the main features distinguishing PERC from Al-BSF cells is the local contacts on the rear side. On the Fraunhofer ISE PV-TEC pilot line [26], the baseline PERC process has yielded energy conversion efficiencies of 21.0% to 21.5% on p-type Cz-Si with a homogeneous emitter and a 156mm edge length [27–29].

A bifacial solar cell can harvest additional light coming from the rear side (depending on albedo) [16], if an appropriate module concept, such as a glass-glass module, is used. Bifacial cell and module technology therefore offers a higher energy yield potential in cases where the energy conversion efficiency of the front side of the cells is not significantly influenced by the bifacial approach, and is thus on a similar level to their monofacial cell counterparts. Hence, reducing the metallized rear-side area from a full-area metallization, as commonly employed for PERC cells, to a metallization grid is a logical technological adaptation (Fig. 3(c)). With a metallization grid on the rear side instead of a full-area metallization, the bifacial application is enabled, and the adapted cell structure is referred to as *biPERC*.

The potential of PERC-like bifacial cell architectures was shown on cells in the laboratory back in the 1990s [30–32]. Industrial large-area p-type biPERC cells with a screen-printed aluminium rear-side grid were first realized on multicrystalline silicon in 2016, achieving an efficiency of η = 17.8% [33]. Subsequently, biPERC solar cells utilizing p-type

Cell type	Cell area [cm^2]	Material	Finger width rear side [µm]	Monofacial illumination	V_{oc} [mV]	j_{sc} [mA/cm^2]	*FF* [%]	η_{mean} [%]	η_{max} [%]	Bifaciality factor [%]
biPERC*	243	p-type Cz-Si	100	Front	660	39.5	79.3	20.7	20.7	76.8
				Rear	654	30.7	79.6	15.9	16.4	
			150	Front	660	39.5	79.8	20.8	20.9	72.1
				Rear	652	28.8	80.1	15.0	15.5	
			200	Front	661	39.5	79.9	20.9	21.0	66.0
				Rear	651	26.6	80.3	13.8	14.2	
Monofacial PERC*			–	Front	656	39.8	80.0	20.9	21.1	–
biPERT*	243	p-type Cz-Si	200	Front	654	39.5	79.3	20.4	20.5	68.1
				Rear	642	26.1	79.9	13.9	13.9	
			50	Front	635	39.2	79.7	19.8	19.9	86.4
				Rear	632	33.7	80.3	17.1	17.2	
Monofacial PERT*			–	Front	656	39.8	80.0	20.9	21.1	–
pPassDop*	244	p-type Cz-Si	65	Front	638	39.1	79.4		19.8	88.9
				Rear	635	34.6	79.8		17.6	
Monofacial TOPCon*	4	n-type FZ-Si	–	Front	725	42.5	83.3		25.7	–
Bifacial SHJ†	244	n-type FZ-Si	50	Front	738	38.9	81.5		23.4	93.6
				Rear	738	35.7	83.2		21.9	

* Fraunhofer ISE solar cells; † Meyer Burger solar cells

Table 1. Open-circuit voltage V_{oc}, short-circuit current density j_{sc}, fill factor *FF*, energy conversion efficiency η, and bifaciality factor η_{rear}/η_{front} for various solar cell groups.

Cz-Si have been reported to achieve conversion efficiencies of up to η = 21.0% [34,35] (measured on a black non-conductive chuck). Beyond enabling the bifacial application, a further advantage of biPERC solar cells compared with PERC cells is a reduced consumption of aluminium paste.

When the full-area rear metallization is reduced to an aluminium grid with thin finger contacts, there are challenges associated with aligning the laser contact opening (LCO) and with the screen-printing step. Fig. 4 shows the rear view of a screen-printed aluminium finger grid, with finger widths approaching 100µm and a successful alignment with the underlying LCO. In this case, the rear features a very smooth surface, typical of monofacial PERC devices. The rear capping layer thickness has been reduced in order to serve as an anti-reflection coating, although it has not yet been fully optimized, as can be deduced from its optical appearance.

Table 1 shows the current–voltage (I–V) parameters for monofacial illumination, measured with contact bars on a black non-conductive chuck, of different solar cells featuring different rear-side finger widths. The results for optional monofacial reference cells are also shown for comparison. The monofacial reference for the biPERC cells features a thicker rear capping layer and a full-area aluminium metallization serving as a reflector, increasing the optical generation and thus the short-circuit current density j_{sc}. The biPERC cells feature a reduced capping layer thickness that serves as an anti-reflection coating. As can be seen, the bifacial and the monofacial cells achieve similar efficiency levels of around 21%, where lower j_{sc} and *FF* for the bifacial cell are compensated by V_{oc} gains. The higher V_{oc} is due to the lower recombination-active local contacts for the line-shaped aluminium fingers than in the case of full-area aluminium metallization [36]. By reducing the finger width from 200µm to 100µm, the mean front efficiency η_{front} drops moderately, from 20.9% to 20.7%, as a result of an increased finger resistance. In contrast, the mean rear efficiency η_{rear} increases significantly, from 13.8% to 15.9%. The bifaciality factor, defined by the ratio of η_{rear} and η_{front}, hence increases from 66.0% to 76.8%.

Compared with a biPERC device, the bifacial passivated emitter, rear totally diffused (biPERT) solar cells exhibit a full-area BSF on the rear side; the idea here is to exploit the additional conductivity by increasing the separation of the contacts (Fig. 3(d)). In the case of a p-type base, the presence of the BSF reduces the need for heavy base doping; in consequence, a lighter-doped material, which is less prone to light-induced boron–oxygen-related degradation, can be used. Moreover, the BSF enables the use of alternative pastes for the rear contact, for example silver-aluminium or even pure silver pastes, the latter typically being used for front-side contacts on phosphorus-doped emitters.

Recent developments have put the PERT approach back into the spotlight. Chemical vapour deposition (CVD) technology enables the application of a borosilicate glass (BSG) layer and a capping layer prior to the conventional tube furnace diffusion in a $POCl_3$ atmosphere. During this (co-)diffusion process [36–38], both the BSF and emitter are formed. Furthermore, the remaining rear stack of BSG and capping remains on the wafer, acting also as a passivation and anti-reflection layer. The use of firing-through pastes means that LCO prior to metallization can be omitted, thus also removing the need for alignment between the laser and screen printer.

The biPERT section in Table 1 shows the I–V-related parameters obtained by exploiting the benefits of co-diffusion. The base doping of these cells is of the order of 4Ωcm, showing that light-induced degradation due to boron–oxygen complexes is significantly reduced. The cells are fully solderable and resemble the appearance of the biPERC cell shown in Fig. 4. Because of the thinner rear-side fingers with biPERT, higher bifaciality factors (in this example 86.4%) can be achieved than with biPERC.

One of the first proofs-of-concept for the 'pPassDop' PERL approach on solar cells with an edge length of 156mm yields η_{front} = 19.8% [39] (see Fig. 3(e) and Table 1). This solar cell achieves a high bifaciality of about 89% because of the rear-side grid with thin contact fingers of only around 65µm in width. The applied 'pPassDop' layer stack consisting of AlO_x/SiN_x:B on the cell's rear side serves as both surface passivation and doping source. Laser processing is used to locally introduce boron atoms from the 'pPassDop' layer stack into the silicon, which results in a boron-doped BSF underneath the rear screen-printed and fired contacts. A special alignment procedure ensures that the rear grid with finger widths of about 65µm is placed over the entire wafer on top of the ~40µm-wide laser-doped and opened lines.

Silicon heterojunction (SHJ) technology (Fig. 3(f)) is also a promising candidate because of its already bifacial design (bifaciality factors above 90%), excellent passivation quality, and high-efficiency potential of up to 25.1% for lab-scale solar cells [40]. Large-area bifacial SHJ cells (with busbar-less metallization) are available on the market, with efficiencies of up to 23.4% [41], and can thus also serve as a candidate for stripe cells. To close the efficiency gap between PERC-like structures and SHJ while maintaining low-cost processing, next-generation hybrid PERC structures with tunnel oxide passivated contacts (TOPCon) are already being developed on lab-scale solar cell sizes with an optional bifacial design; the design concept is illustrated in Fig. 3(g). The monofacial TOPCon cells currently achieve record efficiency values of 25.6% on a lab scale [42]. The TOPCon approach is currently being transferred to large-area wafers and a bifacial structure, and is expected to be market ready in the near future.

Technology-specific challenges

Despite the solar cell concepts for shingling technology being quite diverse, they will all face the separation process step, the potential need for edge passivation, and finally the integration into a module.

Separation

The quality of the separation of the solar cell stripes is closely related to edge recombination, as the separation process may induce damage to the edge and leaves a surface with a process-dependent damage density and roughness. In the case of SPEER and SPEERCon cells, edge recombination becomes significant because of the high contour-to-area ratio (see next section). The most common method used so far for silicon solar cell separation has been laser scribing, followed by mechanical cleavage [12]. For example, the pulsed laser source engraves about one-third of the cell thickness (usually from the rear side) in the scribing phase [43]; the complete separation of the rest of the solar cell occurs mechanically in the final cleaving step. Fig. 5 shows an example of a cross section of an

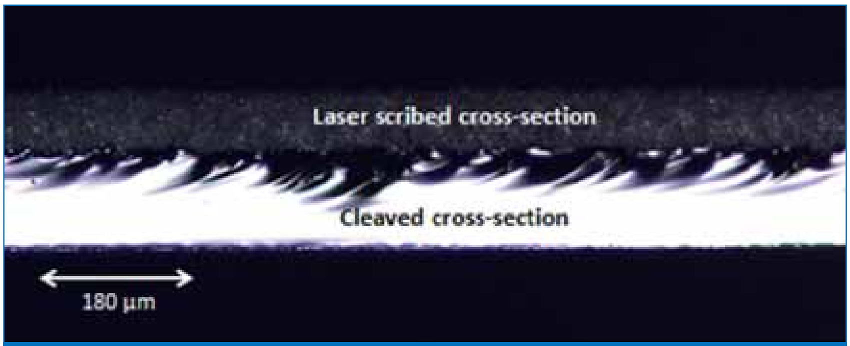

Figure 5. A light-microscope image of a laser-scribed and mechanically cleaved edge of a silicon solar cell.

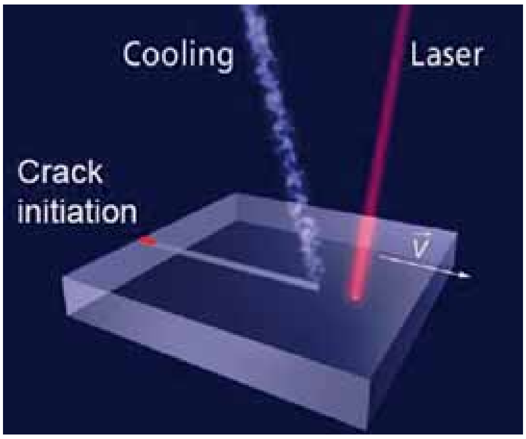

Figure 6. An illustration of the TLS process, showing the crack initiation, laser heating and fluid cooling steps leading to the substrate separation. (Image taken from Lewke [45].)

	Contour/area [1/cm]	$j_{02,edge}$ [nA/cm^2]
25 × 156mm^2 stripe	0.93	12.1
50 × 156mm^2 stripe	0.53	6.9
156 × 156mm^2 cell	0.26	3.3

Table 2. Example calculations for contour-to-area ratio and resulting $j_{02,edge}$ (after Dicker [47]), showing that a 25mm-wide stripe has a fourfold influence on $j_{02,edge}$ recombination, compared with a regular square cell (in the case of an unpassivated edge).

	S_{eff} [cm/s]	$j_{02,edge}$ [nA/cm]
Unpassivated edge	10^6	13
Passivated edge	10	0

Table 3. Applied recombination levels for the cell edges, representing unpassivated and passivated edges.

edge to illustrate the difference in the surface morphology remaining in the scribed and cleaved areas.

Recently, with the increase in half- and quarter-cell production demand [15], thermal laser separation (TLS) [43,44] was proposed as a candidate for future silicon substrate dicing [44]. TLS is a kerf-free, laser-based dicing technology that is based on crack guiding by means of thermally induced mechanical stress [43] (see Fig. 6). This technology is widely used in the semiconductor industry [44]. Briefly, TLS is a two-step process [43], starting with an initial scribe (less than 50μm deep) using a laser source to induce a crack. The second step is the crack guidance. The laser-induced substrate heating creates a compressive stress, followed by a subsequent fluid cooling, which incites tensile stress.

The TLS method of separating silicon wafers has been reported to show a higher edge quality; in initial TLS tests performed on PERC solar cells to obtain half-cells it has been found that this method leads to improved electrical and mechanical properties compared with conventional laser-scribed and cleaved half-cells [44,45]. There have been statements to the effect that the half-cells separated by the TLS process have shown a $1\%_{rel}$ reduction in maximal power, whereas the half-cells separated by conventional laser scribing and cleaving have shown a $1.2\%_{rel}$ power reduction.

To gain a deeper understanding of the TLS parameters [43,44] and their effects on the quality of the edges of the separated stripe cells, further development within the PV production research community is expected. An optimized process should be aimed at creating a very smooth surface as a good basis for subsequent passivation. The introduction of such a laser process into the process chain for the separation of the cell stripes could decrease the recombination of the stripes' edge regions, which will be discussed in the next section.

Edge passivation

As mentioned in the previous section, the singulated solar cell stripes have a larger contour-to-area ratio than standard (pseudo-)square cells, which is illustrated in Table 2 for 2.5cm- and 5cm-wide stripes. Moreover, (pseudo-)square cells undergo a passivation process which also covers the edges, while the stripes are singulated after metallization and contact formation, leaving the edges initially blank. This poses the question of potential losses through recombination at those edges, which can be divided into three subregions:

1. Surfacing bulk region, implicating ideal surface recombination (ideality factor n = 1). This can be accounted for with modelling by using an effective surface recombination velocity between $S_{eff} \approx 8$cm/s for excellent passivation (e.g. reported by Saint-Cast et al. [46]) and $S_{eff} = 10^6$cm/s for an unpassivated surface (with high defect density, reported by Glunz and Dicker [12,47]).
2. Surfacing heavily doped emitter region, implicating ideal surface recombination.

3. Surfacing space charge region (SCR), implicating non-ideal surface recombination activity (ideality factor $n \approx 2$). Dicker parameterized this recombination for a single recombining edge using the second diode in the two-diode model, naming it $j_{02,edge}$ [47]. This recombination current density comprises a determined constant of 13nA/cm scaling with the contour-to-area ratio, so that $j_{02,edge}$ = contour/area·13nA/cm². A very similar value has been recently found by Fell et al. [48]. This yields the $j_{02,edge}$ values given in Table 2 for the example stripes.

Figure 7. 3D model of a bifacial SPEER solar cell.

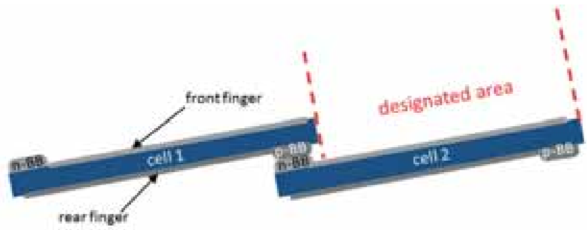

Figure 8. Shingling scheme of two solar cells, whereby the bottom busbar of cell 1 is placed onto the top busbar of cell 2.

For the examined cells, Dicker [47] concluded that the surfacing bulk region recombination and the SCR recombination contribute equally to the total edge recombination, whereas the emitter region surface recombination has a negligible influence because of its small extent.

In the particular case presented here, it is desired to calculate the worst case of all four edges of the stripe cell being recombination active. To model these effects, the newly developed Quokka3 tool (currently in beta stage, with release planned in 2017) will be used. Because a lumped skin approach (an expression originally coined by Cuevas et al. [49]) is used for non-neutral regions, the mesh fineness can be reduced to a minimum. In consequence, this allows the modelling of much larger domains, in this case an entire cell stripe, resulting in a generalized model without spatial simplifications such as potential or series resistance distributions (as opposed to the usual one-cell approach). With the

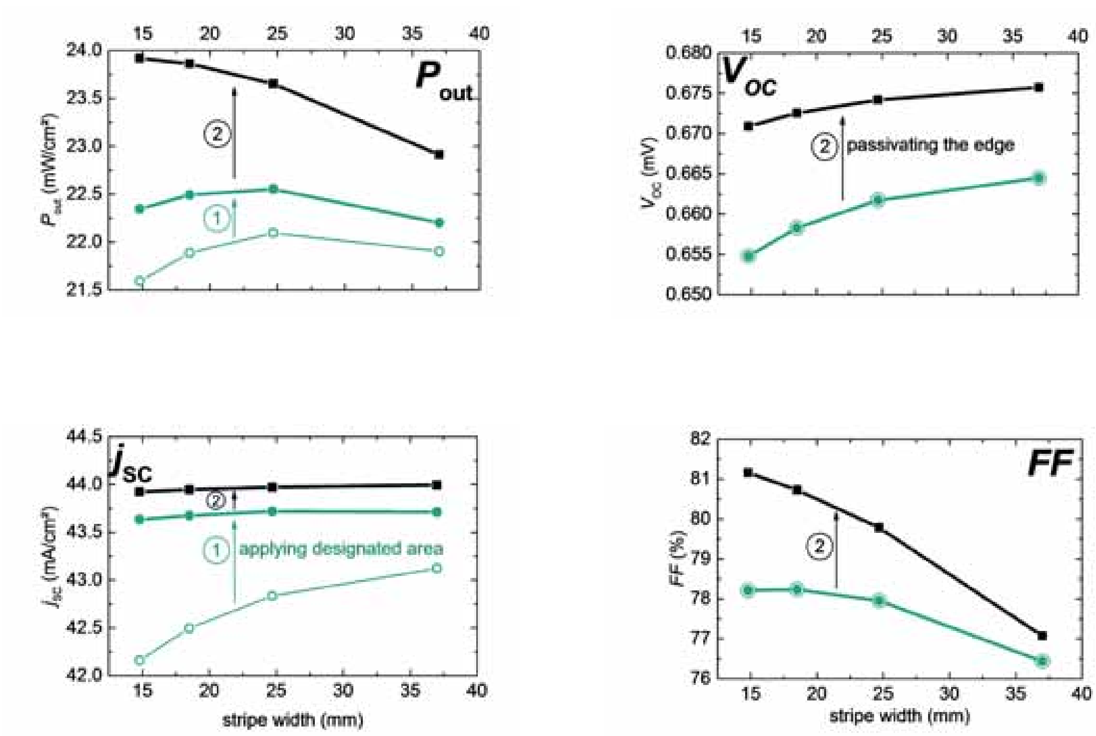

Figure 9. Simulated *I–V* parameters of the stripe cells for various cell stripe widths, for illumination intensities of 1,000W/m^2 and 100W/m^2 on the front and rear sides respectively. The lower light-green plot shows the parameters for the full stripe area calculation with maximum recombination at the edges. In step 1, j_{sc} is calculated only for the designated area (see Fig. 8), which excludes the busbar adjacent area because it is covered by the next shingle cell in the module layout. Step 2 includes an excellent edge passivation.

latest addition of a vertical resistance and full injection dependence on the skin parameterization [25], the skins can be described by lumped parameters without errors, compared with, for example, explicitly accounting for doping profiles. The cell stripe CAD model is depicted in Fig. 7.

> "The goal of the cell optimization is to find the ideal cell stripe width and determine the impact of edge recombination."

The input parameters are extracted from a bifacial PERC solar cell that has been processed on the Fraunhofer ISE PV-TEC pilot line, yielding a front-side efficiency of 21% under 1,000W/m² AM1.5g illumination and with a bifaciality of 75% (see Table 1); these parameters are then applied to the stripe cell, which is based on the same processes. The goal of the cell optimization is to find the ideal cell stripe width and determine the impact of edge recombination. Three scenarios are therefore simulated while varying the stripe width, beginning with a stripe cell with a highly recombinational edge (S_{eff} and j_{02} as shown in Table 3).

As shown in Fig. 8, the busbar, as well as the adjacent area, is covered by an active area of the overlying cell; thus, only the marked designated area is relevant in the determination of the j_{sc}. In step one ('1' in Fig. 9), this effect due to shingling in the module is included in the simulated *I–V* parameters. The second step ('2' in Fig. 9) introduces an excellent edge passivation, assuming S_{eff} = 10cm/s and $j_{02,edge}$ = 0nA/cm. All the results shown were calculated for a bifacial illumination with a front irradiance of 1,000W/m² and a rear irradiance of 100W/m² (which is presumed to be a candidate for a coming standard for bifacial *I–V* measurements).

Step 1 has a major effect on j_{sc}, but the dependence on the stripe width vanishes as the continuous shading of the busbar is diminished. Moreover, j_{sc} shifts by around 1mA/cm², to 43.7mA/cm², which reflects one aspect of the advantages of shingling technology. Step 2, the edge passivation, manifests its effect mainly in *FF* and V_{oc}. Reduced SCR recombination at the edges $j_{02,edge}$ leads to a jump in *FF* by 2–3%$_{abs}$ for small stripes; the reduced base edge recombination S_{eff} increases V_{oc} by 10–15mV for small stripes. Both effects are pronounced for small stripes as a result of their higher contour-to-area ratio.

Step 1 increases the overall power output P_{out} of the stripe cell from 22 to 22.5mW/cm² at an ideal stripe width of 25mm, and reduces the sensitivity to variations in stripe width. Step 2 increases P_{out} to 23.6mW/cm² at a stripe width of 25mm. It increases further with smaller stripe widths, but this is not a suitable approach for cell interconnection, as will be shown in the next section. Overall, with a gain of more than 1mW/cm² it is well worth considering an additional process step for edge passivation. The implementation of such an edge passivation technique, which is in the best case also suitable for mass production, is currently a high-priority line of investigation in the ongoing work at Fraunhofer ISE.

Module integration and CTM loss analysis

As described above (see Fig. 8), the electrical interconnection of solar cells in shingled modules is achieved by overlapping and directly connecting the n and p sides of adjacent solar cells. To increase electrical performance, an electrically conductive adhesive (ECA) or solder paste may be used between the cell stripes [13]. The depth of the overlap is observed to be between 1 and 2mm. A trade-off in overlap between manufacturing requirements (cell lay-up

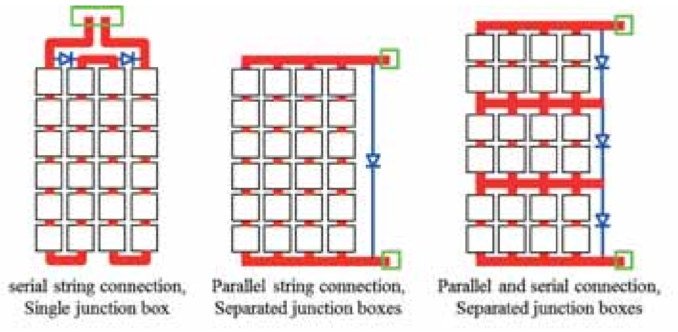

Figure 10. Different module topologies with serial, parallel and combined string interconnection, and single and separate junction boxes.

precision) and costs (shaded cell parts do not generate power, but still have to be purchased) needs to be examined, which is crucial for the module's power/price ratio. The same argument is valid for the size of the shingled cells: although smaller cell stripes decrease some electrical losses because of lower current generation, as shown in the previous modelling, they increase manufacturing requirements, the proportion of overlapped area, and edge recombination losses.

Since all cells are directly connected, a string of significant length without gaps or compensating

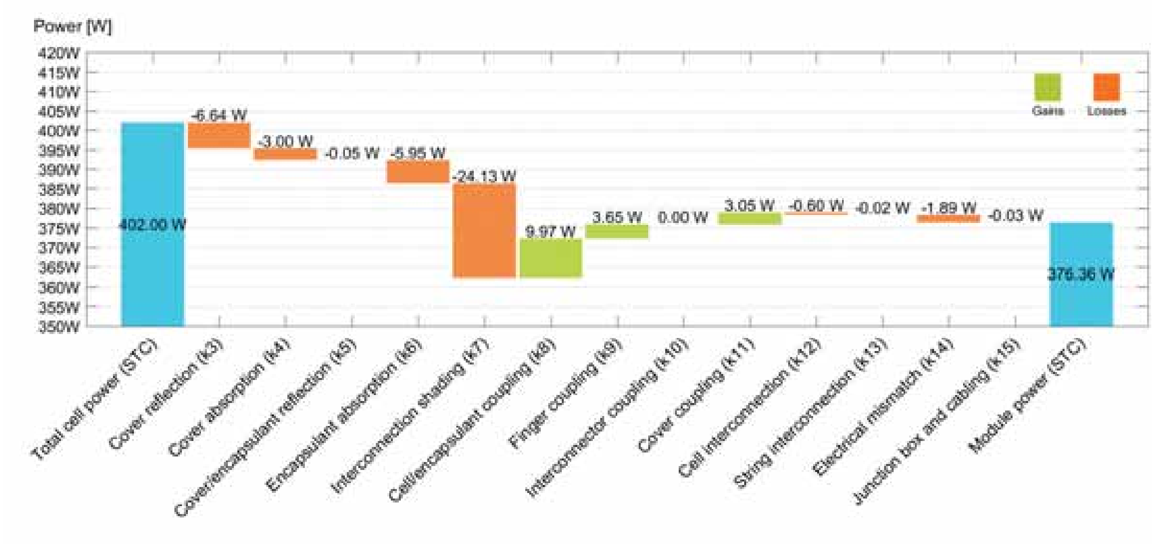

Figure 11. CTM analysis for a shingled module with bifacial PERC cells.

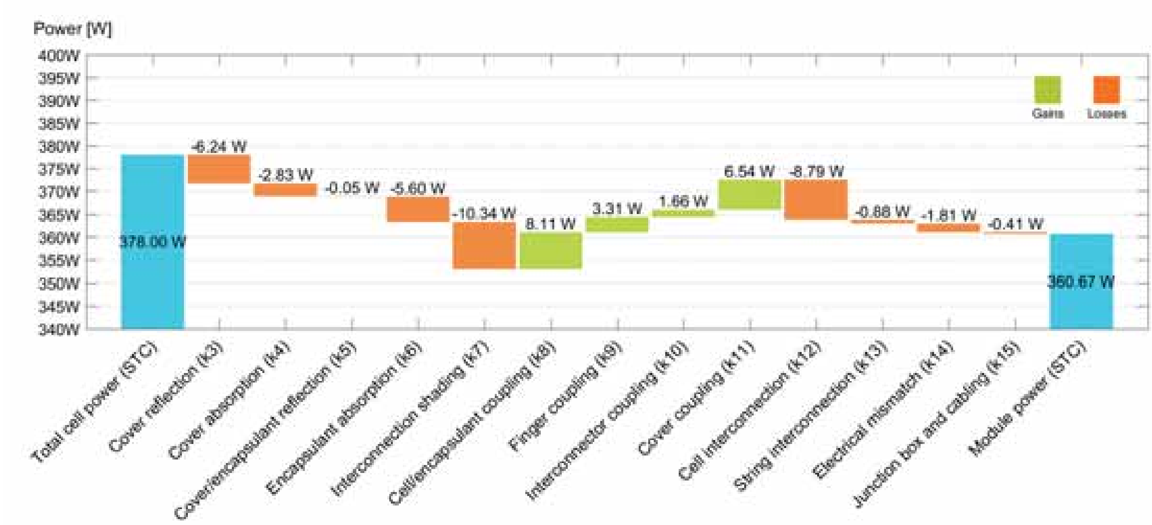

Figure 12. CTM analysis (power) for a conventional module using biPERC solar cells.

elements is formed. At changing temperatures, thermomechanical stress occurs within the cell interconnection and the cell metallization. While the stress from external loads (e.g. snow) may be reduced by placing the solar cells in the neutral plane of double-glass modules, the thermomechanical stress resulting from different coefficients of thermal expansion cannot be avoided.

The direct overlapping of the cell stripes eliminates the cell gaps, and therefore increases the active module area proportion. Two options are possible to take advantage of the resulting gains: 1) reduce the module size, keeping the module power constant and saving on module area and materials; or 2) keep the module area constant and increase power and efficiency. For typical set-ups, either approximately 9% more power than a conventional module can be generated, or the module area can be reduced.

As a result of the increased number of (smaller) solar cells in shingled modules, the module voltage increases if a conventional module topology that connects strings of solar cells in series (Fig. 10) is used. To be compatible with existing inverters, and so as not to exceed electrical limitations, electrical properties similar to conventional PV modules are desirable. New module topologies featuring strings connected in parallel, or using combinations of parallel and serial cell and string interconnection, are therefore necessary and have been discussed in the literature [8,50,51]. Shingling requires new solutions for string interconnection, junction boxes and bypass diode placement.

"Shingling requires new solutions for string interconnection, junction boxes and bypass diode placement."

Shingled modules are a concept that is certainly capable of producing increased module efficiency and module power. A detailed CTM analysis using SmartCalc.CTM by Fraunhofer ISE [52] (also presented in another article in this issue of *Photovoltaics International*. p.97) reveals important gains and losses as well as several major differences with conventional modules.

First, a few remarks on the CTM-loss calculations have to be made. Shingling is the only crystalline module concept in which the active cell area may be shaded by another active area. The overlapping cell area usually has a higher efficiency, since the overlapped cell area features metallization patterns for interconnection.

Let us assume that two cells of the same power are completely overlapped, and that the lower cell is fully shaded and therefore produces no electrical power. Now, only one 'power unit' remains after this overlapping. Since the reference area has also changed, the efficiency remains the same ($CTM_{efficiency} = 1$). Because initially (before overlapping) two power producing cells were present, the CTM factor for *power* has changed and is now $CTM_{power} = 0.5$. With shingling, therefore, the CTM factors for power and efficiency do not correspond as they do with other module concepts.

Usually, the absolute power loss is higher for a shingled module than for a conventional one, but so is the sum of the initial cell powers, since more cells are needed to cover the module and the overlapping areas. Figs. 11 and 12 illustrate the higher absolute CTM losses for shingled modules. Nevertheless, shingled modules are capable of achieving higher module powers and efficiencies than conventional modules [53].

Shingled modules do not include interconnection ribbons; thus, there are no electrical losses associated with ribbons, but contact and bulk resistance losses in the ECA occur. Optical gains and losses remain practically unchanged from those of conventional modules, with the exception of backsheet reflections (k11) and potential reflective gains from interconnection ribbons (k10). Electrical mismatch losses are heavily dependent on the manufacturing equipment and the homogeneity of the cell stripes [54].

SmartCalc.CTM was used to analyse the CTM ratio of a shingled module using the modelled bifacial PERC cells described above; results of the analysis are shown in Fig. 11. The module features six strings of 67 shingled cells with dimension 25mm

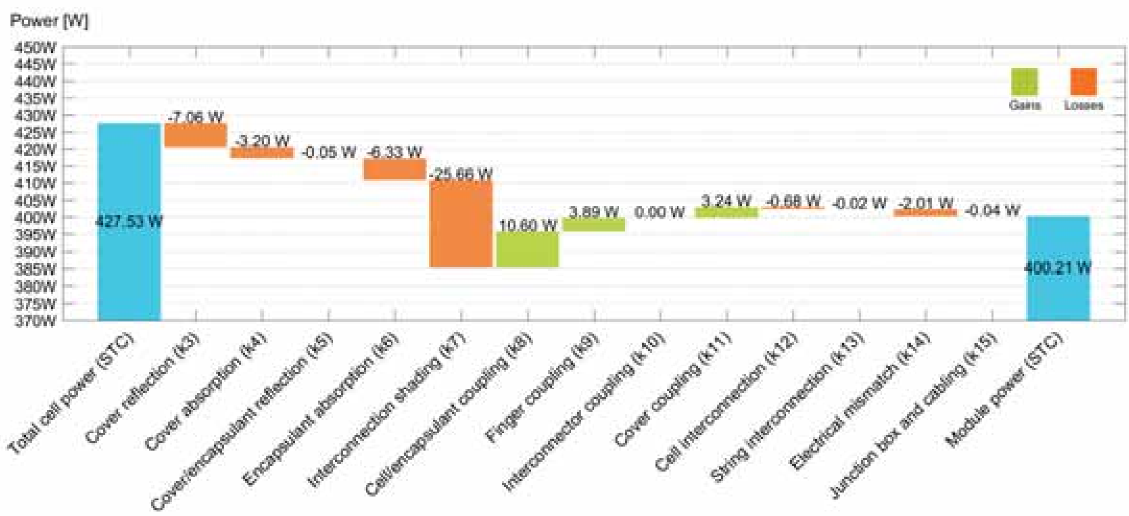

Figure 13. CTM analysis (power) for a shingled module with 400Wp (257W/m^2).

× 156mm. Each cell has a power of 1W (P_{out} = 23.2mW/cm^2 at 1,000W/m^2 front-side and 100W/m^2 rear-side irradiance), which corresponds to the black line in Fig. 9 at 25mm, calculated using a full area instead of a designated area. Commercially available module materials – such as EVA, AR-coated glass and a polymer backsheet – are used. The overlap of the cells is set to 2mm; reducing this value would greatly reduce the total power loss from cell to module, but not the final module power. A module with SPEER cells would produce 376W (P_{out} = 21.9mW/cm^2).

Full-size biPERC solar cells were used in a conventional module set-up (H-pattern, ribbon interconnection, 205mm pseudo-square, 6W per bifacial cell), and a comparative CTM analysis of both module concepts was performed. Results of the ribbon-interconnected PERC cells are shown in Fig. 12. A conventional ribbon-interconnected module – featuring solar cells with the same biPERC technology as the previous SPEER cells – would only produce 361W.

Since an overlap of the shingled cells of 2mm was chosen, a larger number of cells is necessary for the shingled module (402Wp, Fig. 11). At this point, cost considerations become important and further module optimization is supported with SmartCalc.CTM.

To obtain a module power with the conventional module set-up that is similar to the power that can be achieved with the shingle concept, an increase in the initial cell performance is necessary for H-pattern biPERC cells. Bifacial H-pattern cells with 24.2mW/cm^2 at 1,100W/m^2 irradiance (an increase of 1.0mW/cm^2 compared with the SPEER cells for shingling) would be required to also achieve a module power of 376W. As the approach here features stripe cells based on the specific process technology for large-area cells, the power of the shingled module will automatically surpass that of the conventional module technology by around this margin, even if the cell efficiencies improve.

The next step to reaching the target of 400W per module (at an area of a common 60-cell module) is to perform an estimation of the necessary cell power to achieve this goal. A detailed CTM analysis is shown in Fig. 13.

A parameter sweep of the electrical cell characteristics reveals that SPEER cells with 1.06Wp (P_{out} = 24.7mW/cm^2) are required if a shingled module set-up as described above is used. Dividing that output power by 1.1 (irradiance factor), and neglecting the bifaciality factor, the approximate front-side efficiency for such a cell would be η = 22.5%. This is a number which, according to the ITRPV roadmap [15], is to be expected for mass-cells produced by 2021, and has in fact already been achieved for full-size pseudo-square PERC record cells ([55], η = 22.61%). Furthermore, if the next-generation cell concepts discussed above, such as SHJ, are integrated in shingled modules, then powers exceeding 400W in standard-size modules can definitely be expected.

Summary

PV modules with shingled cell technology have a history almost as old as the silicon solar cell itself. With bifacial PERC or PERC-like solar cells, industrially available concepts are at hand that now put shingling technology into an attractive position. A cost-effective cell concept can be boosted by the bifacial shingled module concept towards achieving the module power benchmark of 400W, for a conventional ('60-cell') module size with 1,000W/m^2 front and 100W/m^2 rear irradiance, by reducing CTM losses and benefitting from bifacial irradiance gains.

Some of the challenges faced on the path to realizing a bifacial shingled module have been highlighted:

1. Achievement of a monofacial cell efficiency of 22.5% (standard test conditions, 1,000W/m^2 irradiance) in mass production, which is supposed to be reached by PERC/PERT/PERL R&D in the next two years as a result of industry self-interest.

2. Provision of suitable cell separation techniques and/or reduction in edge recombination through appropriate passivation methods.

3. Development of reliable shingled cell interconnection and precise module assembly to guarantee durability and minimum mismatch in the module.

> "It is the authors' belief that the combination of shingling and bifacial technology offers the greatest and most accessible levers for power output increases in solar modules."

The modularity of the shingling module concept, together with the availability of the presented hybrid PERC (TopCon) or silicon heterojunction concepts, furthermore implies the possibility of even higher module powers, which are basically a bonus when the module concept for biPERC has been developed. Overall, this is encouraging in the development of a product suitable for the industrial and consumer markets, because it is the authors' belief that the combination of shingling and bifacial technology offers the greatest and most accessible levers for power output increases in solar modules. The recent appearance of the first shingled modules from large manufacturers seems to support the considerations discussed in this paper.

Acknowledgements

The experiments in this work were conducted within the framework of the 'PV-BAT400' project (Contract No. 0324145), supported by the German Federal Ministry for Economic Affairs and Energy. The authors would like to thank all the people in the PMZ, PTQ and SEC teams at Fraunhofer ISE for their support and making this study possible.

References

[1] Dickson, D.C., Jr. 1960, "Photovoltaic semiconductor apparatus or the like", US Patent 2938938 (May 31).

[2] Chapin, D.M., Fuller, C.S. & Pearson, G.L. 1954, "A new silicon p-n junction photocell for converting solar radiation into electrical power", *J. Appl. Phys.*, Vol. 25, No. 5, p. 676.

[3] Nielsen, R.J. & Leif, R. 1963, "Satellite solar cell assembly", US Patent 3116171 (Dec. 31).

[4] Myer, J.H. 1968, "Photovoltaic generator", US Patent 3369939 (Feb. 20).

[5] Baron, W.R. 1969, "Solar cells with flexible overlapping bifurcated connector", US Patent 3459597 (Aug. 5).

[6] Gochermann, H. & Soll, J. 1996, "Shingle-type solar cell generator prodn. – allowing formation of curved or domed product", German Patent 3942205 (Feb. 1).

[7] Yang, B. et al. 2015, "High efficiency solar panel", US Patent 14/563,867 (Apr. 2).

[8] Morad, R. et al. 2016, "Shingled solar cell module", US Patent 14/605,695 (Nov. 1).

[9] Morad, R. et al., "Shingled solar cell module", US Patent 14/572,206 (Jul. 26).

[10] Morad, R. et al. 2016, "Shingled solar cell module", US Patent 14/594,439 (Jul. 19).
[11] Zhao, J. et al. 1997, "20000 PERL silicon cells for the '1996 World Solar Challenge' solar car race", *Prog. Photovolt: Res. Appl.*, Vol. 5, No. 4, pp. 269–276.
[12] Glunz, S.W. et al. 2002, "High-efficiency silicon solar cells for low-illumination applications", *Proc. 29th IEEE PVSC*, New Orleans, Louisiana, USA, pp. 450–453.
[13] Beaucarne, G. 2016, "Materials challenge for shingled cells interconnection", *Energy Procedia*, Vol. 98, pp. 115–124.
[14] SunPower Corporation 2017, "SunPower introduces new solar panel: The performance series" [https://us.sunpower.com/blog/2015/11/12/sunpower-introduces-performance-series-solar-panel/].
[15] ITRPV 2017, "International technology roadmap for photovoltaic (ITRPV): 2016 results", 8th edn (Mar.) [http://www.itrpv.net/Reports/Downloads/].
[16] Kopecek, R. & Libal, J. 2017, "Quo vadis bifacial PV?", *Photovoltaics International*, 35th edn.
[17] Blakers, A.W. et al. 1989, "22.8% efficient silicon solar cell", *Appl. Phys. Lett.*, Vol. 55, No. 13, pp. 1363–1365.
[18] Zhao, J., Wang, A. & Green, M.A. 2001, "24.5% efficiency PERT silicon solar cells on SEH MCZ substrates and cell performance on other SEH CZ and FZ substrates", *Sol. Energy Mater. Sol. Cells*, Vol. 66, Nos. 1–4, pp. 27–36.
[19] Wang, A., Zhao, J. & Green, M.A. 1990, "24% efficient silicon solar cells", *Appl. Phys. Lett.*, Vol. 57, No. 6, pp. 602–604.
[20] Norouzi, M.H. et al. 2017, "Development and characterization of multifunctional PassDop layers for local p+-laser doping", *Energy Procedia* [forthcoming].
[21] Norouzi, M.H. et al. 2017, "Development and characterization of AlO_x/SiNx:B layer systems for surface passivation and local laser doping", *IEEE J. Photovolt.* [forthcoming]
[22] Suwito, D. et al. 2010, "Industrially feasible rear passivation and contacting scheme for high-efficiency n-type solar cells yielding a V_{oc} of 700 mV", *IEEE Trans. Electron Dev.*, Vol. 57, No. 8, pp. 2032–2036.
[23] Wolf, S.D. et al. 2012, "High-efficiency silicon heterojunction solar cells: A review", *Green*, Vol. 2, No. 1.
[24] Feldmann, F. et al. 2014, "Passivated rear contacts for high-efficiency n-type Si solar cells providing high interface passivation quality and excellent transport characteristics", *Sol. Energy Mater. Sol. Cells*, Vol. 120, pp. 270–274.
[25] Fell, A., Schubert, M.C. & Glunz, S.W. 2017, "The concept of skins for (silicon) solar cell modelling", *Sol. Energy Mater. Sol. Cells* [forthcoming].
[26] Biro, D. et al. 2006, "PV-TEC: Photovoltaic technology evaluation center – Design and implementation of a production research unit", *Proc. 21st EU PVSEC*, Dresden, Germany, pp. 621–624.
[27] Werner, S. et al. 2017, "Key aspects for fabrication of p-type Cz-Si PERC solar cells exceeding 22% conversion efficiency", *Proc. 33rd EU PVSEC*, Amsterdam, The Netherlands.
[28] Saint-Cast, P. et al. 2016, "Analysis and outlook of near-industrial PERC solar cells", *Photovoltaics International*, 34th edn, pp. 52–59.
[29] Saint-Cast, P. et al. 2017, "Analysis of the losses of industrial-type PERC solar cells", *physica status solidi (a)*, Vol. 214, No. 3, p. 1600708.
[30] Hezel, R. & Jaeger, K. 1989, "Low-temperature surface passivation of silicon for solar cells", *J. Electrochem. Soc.*, Vol. 136, No. 2, pp. 518–523.
[31] Aberle, A.G. & Hezel, R. 1997, "Progress in low-temperature surface passivation of silicon solar cells using remote-plasma silicon nitride", *Prog. Photovolt: Res. Appl.*, Vol. 5, No. 1, pp. 29–50.
[32] Hübner, A., Aberle, A.G. & Hezel, R. 1997, "20% efficient bifacial silicon solar cells", *Proc. 14th EU PVSEC*, Barcelona, Spain, pp. 92–95.
[33] Krauß, K. et al. 2016, "biPERC silicon solar cells enabling bifacial applications for industrial solar cells with passivated rear sides", *physica status solidi (a)*, Vol. 213, No. 1, pp. 68–71.
[34] Wöhrle, N. et al. 2017, "Understanding the rear-side layout of p-doped bifacial PERC solar cells with simulation driven experiments", *Energy Procedia* [forthcoming].
[35] Dullweber, T. et al. 2016, "PERC+: Industrial PERC solar cells with rear Al grid enabling bifaciality and reduced Al paste consumption", *Prog. Photovolt: Res. Appl.*, Vol. 24, No. 12, pp. 1487–1498.
[36] Fellmeth, T. et al. 2017, "Co-diffused bi-facial PERT solar cells", *Energy Procedia* [forthcoming].
[37] Meier, S. et al. 2017, "Fast co-diffusion process for bifacial n-type solar cells", *Solar RRL*, Vol. 1, No. 1, p. 1600005.
[38] Meier, S. et al. 2016, "Co-diffusion for p-type PERT solar cells using APCVD BSG layers as boron doping source", *Proc. 32nd EU PVSEC*, Munich, Germany.
[39] Lohmüller, E. et al. 2017, "Bifacial p-type PERL solar cells with screen-printed pure Ag metallization and 89% bifaciality", *Proc. 33rd EU PVSEC*, Amsterdam, The Netherlands.
[40] Adachi, D., Hernández, J.L. & Yamamoto, K. 2015, "Impact of carrier recombination on fill factor for large area heterojunction crystalline silicon solar cell with 25.1% efficiency", *Appl. Phys. Lett.*, Vol. 107, No. 23, p. 233506.
[41] Strahm, B. 2017, "Heterojunction solar cells", 7th nPV worksh., Freiburg, Germany.
[42] Benick, J. et al. 2017, "High-efficiency multicrystalline n-type silicon solar cells", *Energy Procedia* [forthcoming].
[43] Röth, J. et al. 2015, "Thermal laser separation (TLS) dicing process study – A new technology for cutting silicon solar cells for high-efficiency half-cell modules", *Proc. 31st EU PVSEC*, Hamburg, Germany.
[44] Eiternick, S. et al. 2015, "High quality half-cell processing using thermal laser separation", *Energy Procedia*, Vol. 77, pp. 340–345.
[45] Lewke, D. 2015, "Thermal laser separation – TLS: Wafer-dicing der Zukunft" [www.iisb.fraunhofer.de/content/dam/iisb2014/en/Documents/events/jahrestagung-2015/jt-2015-lewke.pdf].
[46] Saint-Cast, P. et al. 2010, "High-efficiency c-Si solar cells passivated with ALD and PECVD aluminum oxide", *IEEE Electron Device Lett.*, Vol. 31, No. 7, pp. 695–697.

Metallization & Interconnection Workshop 2017

7th Workshop on Metallization and Interconnection for Crystalline Silicon Solar Cells

REGISTER NOW!
www.metallizationworkshop.info

October 23-24, 2017 | Konstanz | Germany

- Advance in metallization has been main technological progress in PV technology over the last 10 years

- New solar cell interconnection is likely to become the next key area for PV performance improvement

Do you want to understand evolutions in those fields and anticipate what it can mean for your activities?

Join the prime event for experts in Metallization and Interconnection of Crystalline Silicon Solar Cells!

sponsors

Applied Materials, Besi, Dow, Dow Corning, Heraeus, imec, ISC International Solar Energy Research Center Konstanz, Longsun 中希电子科技, MacDermid Enthone Electronics Solutions, Samsung SDI, sunlab

supporters

csem, DHBW, ECN

media partners

naturblau, Photovoltaics International, PV Tech

[47] Dicker, J. 2003, "Analyse und Simulation von hocheffizienten Silizium-Solarzellenstrukturen für industrielle Fertigungstechniken" (in German), Dissertation, Faculty of Physics, University of Konstanz, Germany.

[48] Fell, A. et al. 2017, "A detailed analysis of edge related losses in half-cells", *Proc. 33rd EU PVSEC*, Amsterdam, The Netherlands.

[49] Cuevas, A. et al. 2015, "Skin care for healthy silicon solar cells", *Proc. 42nd IEEE PVSC*, New Orleans, Louisiana, USA, pp. 1–6.

[50] SunPower Corp, "SunPower Performance Series P17: Technical product datasheet".

[51] Zhao, J. et al. 1997, "Improved efficiency silicon solar cell module", *IEEE Electron Device Lett.*, Vol. 18, No. 2, pp. 48–50.

[52] Mittag, M. 2017, "Systematic PV-module optimization with the cell-to-module (CTM) analysis software 'SmartCalc.CTM'", *Photovoltaics International*, 36th edn.

[53] Mittag, M. "Cell-to-Module (CTM) Analysis for photovoltaic modules with shingled solar cells", *Proc. 44th IEEE PVSC*, Washington DC, USA.

[54] Mittag, M. 2017, "Progress on unified cell-to-module (CTM) determination methodology: Systematic calculation of module power", *Proc. 44th IEEE PVSC*, Washington DC, USA.

[55] Clover, I. 2016, "Trina Solar sets new 22.61% mono PERC efficiency record", *pv magazine* (Dec.).

About the Authors

Nico Wöhrle studied physics at the University of Freiburg, Germany, and was awarded his diploma degree in 2012 for his work at Fraunhofer ISE on the optical simulation of silicon solar cells. He received his Ph.D. from the University of Freiburg in 2016, with a topic involving the simulation of PERC solar cells. He is currently a researcher at Fraunhofer ISE, where he focuses on the simulation and modelling of solar cells, as well as on the conceptual development of p-type PERC solar cells.

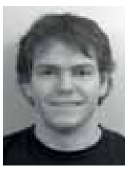

Elmar Lohmüller studied physics at the University of Tübingen, Germany, and at Nelson Mandela Metropolitan University, Port Elizabeth, South Africa. He received his diploma degree in 2010 for his work at Fraunhofer ISE on the development of p-type MWT-PERC solar cells, followed by his Ph.D. from the University of Freiburg in 2015 for his contributions to the development of n-type MWT solar cells. He is currently a researcher at Fraunhofer ISE, with a focus on the development of p-type PERC solar cells.

Max Mittag studied industrial engineering and management at the Freiberg University of Mining and Technology. In 2010 he completed his diploma thesis at Fraunhofer ISE and joined the PV module department. His current work includes CTM efficiency analysis and the development of new PV module concepts.

Anamaria Moldovan studied chemistry at the University of Zurich, Switzerland, and in Freiburg, Germany, receiving her diploma degree in 2011 for her work at Fraunhofer ISE on wet chemical cleaning. She was awarded her Ph.D. by the University of Freiburg in 2016 for her investigations of cleaning and conditioning for high-efficiency silicon solar cells. She is currently a researcher at Fraunhofer ISE, focusing on the development of wet chemical and plasma processes for solar cells with passivated contacts.

Puzant Baliozian obtained a B.Sc. in physics in 2014 from the American University of Beirut. In 2016 he received his M.Sc. in renewable energy engineering and management from the University of Freiburg for his thesis work completed at Fraunhofer IPM in the field of magnetocaloric energy conversion. He is currently a Ph.D. candidate at Fraunhofer ISE, where his main area of research is the development of p-type SPEER solar cells.

Tobias Fellmeth studied physics at the University of Konstanz, Germany, and received his diploma degree in 2009 for his work at Fraunhofer ISE on the development and characterization of MWT concentrator solar cells. He was awarded his Ph.D. by the University of Tübingen in 2014 for his studies of silicon-based, low-concentrator solar cells. He is currently a scientist at Fraunhofer ISE, where he focuses on the development of bifacial p-type PERC solar cells.

Karin Krauss studied physics at the Albert Ludwig University of Freiburg and received her diploma degree in 2012. Since 2013 she has been working towards her Ph.D. at Fraunhofer ISE. She joined the PV production technology and quality assurance division at Fraunhofer ISE in 2011, where her research interests involve multicrystalline silicon solar cells and light-induced degradation.

Achim Kraft studied electrical engineering at the University of Applied Science in Hanover, Germany, and renewable energies at the University of Applied Science in Berlin. He received his master's in renewable energies, before joining Fraunhofer ISE in 2012 as a Ph.D. student. He was awarded his Ph.D. in the field of plated-copper front-side metallizations for silicon solar cells by the Albert Ludwig University of Freiburg in 2015. Since then he has focused on solar cell interconnection technologies and processes as head of the interconnection technologies team in the module research group at Fraunhofer ISE.

Ralf Preu is director of the PV production technology division at Fraunhofer ISE in Freiburg, Germany, and also teaches PV at the University of Freiburg. He studied physics at the Universities of Freiburg and Toronto, and economics at the University of Hagen, Germany. He holds a Ph.D. in electrical engineering, and joined Fraunhofer ISE in 1993. His work in different fields in PV includes system monitoring, and silicon solar cell and module technology, characterization and simulation, but his main focus is R&D in advanced silicon solar cell technology and its transfer to industrial production.

Enquiries

Nico Wöhrle
Fraunhofer Institute for Solar Energy Systems ISE
Heidenhofstraße 2
79110 Freiburg, Germany

Tel: +49 (0)761 4588 5964
Email: nico.woehrle@ise.fraunhofer.de

Thin Film

News

Dieter Manz to step aside as CEO

Dieter Manz, the founder and CEO of tool maker Manz, will step aside taking a role on the company's supervisory board.

The company's current CTO, Eckhard Hörner-Marass, will replace him as CEO.

Earlier this year the company secured the largest order in its history, for two of its turnkey CIGS thin-film production lines, in a deal worth US$282 million.

"At the start of 2017 we reached a major milestone by finalizing our strategic cooperation with Shanghai Electric and the Shenhua Group in the solar field and securing the associated orders which are the largest orders in our company's history. This lays the foundation for a sustainable profitable development of our company, and it opens up huge growth and revenue potential for the future," Manz said.

Manz will continue to be the main shareholder in the company.

Credit Manz AG

Dieter Manz, front-left, is to step down as CEO of the company he founded in 1987.

First Solar

First Solar selling power plants to boost liquidity in 2017

Leading thin-film PV manufacturer First Solar reported first quarter results ahead of expectations, primarily due to the sale and entire revenue recognition of its Moapa PV power plant project.

Selling PV projects, whether completed or at an early stage of development is expected to become a key strategy for First Solar over the next several years as it gambles its business success or failure on transitioning from its small-area Series 4 CdTe thin-film module format to the large-area, Series 6 at a cost of around US$1 billion.

With the ramp-down of Series 4 production having started late last year and expected to continue through 2018 and at least to mid-2019, revenue from Series 4 module sales will decline ahead of the Series 6 transition, compounded by continued ASP pressures.

Selling PV projects and potentially its 50% stake in its JV yieldco, 8Point3 as previously announced by the company would provide further liquidity while spending US$1 billion in capex over the next two years. First Solar ended the first quarter of 2017 with US$2.4 billion in cash and cash equivalents.

First Solar shipped 2.7GW of modules in 2016

First Solar has reported lower than guided total thin-film module shipments in 2016 but beat revenue guidance.

First Solar reported fourth quarter 2016 sales of US$480 million and US$3.0 billion for 2016, slightly higher than previous guidance of US$2.8 billion to US$2.9 billion for 2016.

Module shipments were 2.7GW, compared to previous guidance of 2.8GW to 2.9GW.

First Solar reported a fourth quarter 2016 loss per share of US$6.92, compared to earnings per share of US$1.63 in the prior quarter. The fourth quarter was said to have been impacted by pre-tax charges of US$729 million, primarily related to the previously announced restructuring actions.

First Solar guided GAAP revenue in 2017 to be in the range of US$2.8 billion to US$2.9 billion, up from previous guidance of US$2.5 billion to US$2.6 billion, primarily due to stronger than expected module volumes booked.

Module shipments are expected to be in the range of 2.4GW to 2.6GW as the company ramps down Series 4 module capacity.

Credit First Solar

First Solar is looking to sell PV projects as it prepares to transition to a new module technology.

First Solar wants to exit JV yieldco 8point3 with SunPower

First Solar has said it wants to sell its share in its joint venture (JV) yieldco with SunPower to free up funds to support its switch to manufacturing its large-area Series 6 CdTe modules.

SunPower also said that it and First Solar would coordinate a review of a possible sale to a third party.

8point3 it has agreed to waive the buying negotiation period with respect to First Solar's 179MW Switch Station project, which allows First Solar to find a potential third party to purchase the plant.

It also noted that First Solar has formally offered its 280MW California Flats and 40MW Cuyama projects, currently included in the Right of First Offer (ROFO) portfolio, to the yieldco, yet these could also be sold outside the JV yieldco partnership, should the yieldco not purchase them.

Credit Singulus

Singulus has won an order from China for its CIGS production equipment.

CIGS

Singulus wins new CIGS thin-film equipment order from China

Specialist PV manufacturing equipment supplier Singulus Technologies said it received a new order worth over €20 million from a customer in China.

The new equipment order was for its VISTARIS vacuum sputtering systems as well as its TENUIS II system for wet chemical buffer layer deposition. Singulus said that the payment for the order was expected soon.

The customer was said to be a subsidiary of a major public energy company and producer of solar modules in China. Delivery and equipment commissioning timelines were not disclosed.

Last year, Singulus signed a contract worth around €110 million (US$123 million) for CIGS thin-film production equipment for two 150MW production plants to be built in China using technology from AVANCIS for CNBM's entry into BIPV and BAPV markets.

Focus on latest advances of CIGS thin-film module production

International CIGS thin-film experts will convene in Stuttgart on 30 May 2017, at the annual IW-CIGSTech workshop to discuss present and future technical and industrial advances in this solar technology, hosted by the Centre for Solar Energy and Hydrogen Research (ZSW) and the Helmholtz-Zentrum Berlin fuer Materialien und Energie (HZB).

IW-CIGSTech has been an established annual fixture on the solar calendar since 2010, as the leading international workshops dedicated to CIGS thin-film solar cell technology. An all-day event, it offers an intriguing mix of topics at the crossroads of science, engineering and industrial applications.

Speakers from the industry's leading companies and renowned scientists will participate at this year's event. On the agenda are lectures, discussions and poster presentations that cover the wide scope of technological approaches and analytical methods. The progresses of module development and manufacturing processes will be reported. Besides glass-based module technologies ways to produce high efficiency flexible modules are highlighted.

CIGS (copper, indium, gallium and selenium) efficiency is increasing fast reaching values comparable to silicon-based cell technologies. As a consequence manufacturing costs are dropping. CIGS technology has now attained a level of maturity that merits large investments.

CIGS thin-film modules have become a hot topic for the solar industry, with several major module and equipment manufacturers expanding their funding for projects in this field. Production capacities of GW scale are announced by several players, including Solar Frontier, CNBM (Avancis) and Shanghai Electric (Manz).

Further details are available at www.iw-cigstech.org

Perovskite

Microquanta claims 15.24% perovskite mini-module efficiency record

China-based thin-film PV firm Hangzhou Microquanta Semiconductor has claimed a new efficiency record for perovskite mini-modules of 15.24%, certified by Newport PV Lab in Montana, US.

The tested mini-module has an aperture size of more than $16cm^2$.

Microquanta said that by passing the 15% efficiency milestone for the first time, with previous records around the 12% mark, it has moved significantly closer towards commercialization of perovskite solar cells. It also claimed that perovskite mini-modules are desirable since they can reduce the manufacturing cost of current c-Si based solar cells by between 60-80%

Professor Yang Yang, from engineering institute, UCLA, said: "In the past, perovskite solar cell is more or less like an academic research project, but with the new results from those young scientists, it has [moved] one giant step closer to the commercial applications."

Professor Jenny Nelson, Royal Society fellow of the Physics Department, Imperial College London, said: "Perovskite semiconductors are one of the most exciting materials for solar photovoltaic energy conversion, as they have led to remarkably high power conversion efficiencies in spite of being made by relatively simple, low cost techniques.

"Until now, one of the bottlenecks in bringing perovskite solar panels to market has been the drop in performance in a module, where many cells are linked together, compared to a single cell. Before this breakthrough the best performance of a perovskite mini-module was 12.1%, and now Microquanta have pushed the record to 15.2%."

Microquanta was established in Huangzhou in 2015.

Current status of high-efficiency perovskite solar cells

Anita W.Y. Ho-Baillie, Australian Centre for Advanced Photovoltaics, School of Photovoltaic and Renewable Energy Engineering, University of New South Wales, Sydney, Australia

ABSTRACT

Organic-inorganic lead halide perovskite solar cells have become the fastest advancing solar cell technology in the last few years. Due to the excellent optical absorption of perovskites, a thin film that is 400 times thinner than a silicon solar cell is sufficient for photovoltaic energy generation. This material is highly versatile, as efficient cells can be produced using a diverse range of solar cell architectures, deposition methods and material compositions. It can be deposited using a solution process and requires low material usage and processing temperature to become photoactive. In addition, its bandgap can be tuned by varying its composition making it suitable to be used as a component in tandem solar cell. Therefore there is an immense interest in the technology, resulting in rapid progress and a large number of research contributions to this field. This paper documents the evolution of the state-of-the-art record devices and provides a summary of future directions for the research of this new class of solar cell technology.

Organic metal halide perovskite solar cell cells rose to prominence after the first demonstration in solid-state form with an energy conversion efficiency of 9.7% in mid-2012 [1]. The history of metal halide perovskite can be tracked back to 1839 when the distinctive crystal structure was named [2]. The first reports of organic- inorganic halide perovskites appeared in 1884 and 1892 followed by reports of methyl-ammonium lead halide ($CH_3NH_3PbI_3$) and formamidinium lead halide (HC(NH2)2PbI3) in 1978 and in 1995, which are now commonly used in state of the perovksite solar cells [3, 4]. Studies of the materials were focused on investigating their prospects for transistors and light emitting diodes (LEDs) in the 1990s [5-10] until in 2006 when the connection between perovskite and solar cells was publicized in a conference presentation in Japan [11] Due to the excellent optical absorption of perovskites, a thin film of less than 0.5 micrometer is sufficient for an efficient solar cell. This is 400 times thinner than a silicon solar cell. This means that solar cells would no longer be limited to rigid structures such as rooftop panels. The material is highly versatile, as efficient cells can be produced using a diverse range of solar cell architectures, deposition methods and material compositions. It can be deposited using a solution process, and requires low material usage and processing temperature to become photoactive. In addition, its bandgap can be tuned by varying its composition making it suitable to be used as a component in a tandem solar cell. Since 2012 there has been an immense interest in developing metal halide perovskite as a new class of photovoltaic technology resulting in rapid progress and a large number of research contributions to this field [12-13].

The performance of the best certified organic-inorganic halide perovskite solar cells has improved by more than 150% relative and 8% absolute (Figure 1) over the last few years making it the fastest advancing photovoltaic technology. There has been a move from the widely researched $CH_3NH_3PbI_3$ ($MAPbI_3$) [14-15] towards mixed perovskites by incorporating $HC(NH_2)_2^+$ (FA^+) to take advantage of lower bandgap and therefore higher current but is often compromised by the addition of Br^- ions for better perovskite phase stability [16-19]. The addition of Cs [20] and most recently Rb [21-22] also produce cells with excellent efficiencies (although not certified) and stability.

Many of these world record cells (Table 1 and Figure 2) demonstrated use the "standard architecture" fabricated on fluorine doped tin oxide (FTO) coated glass which is then coated with hole-blocking or compact titanium dioxide (c-TiO_2) layer overlaid by meso-porous (mp-) TiO_2 to form a "meso-structure" on which a perovskite absorber layer is deposited. The most commonly used hole transport layer (HTM) on these high performing devices are 2,2',7,7'-tetrakis(N,N-di-p-methoxyphenylamine)9,9'-spirobifluorene (spiro-OMeTAD) and Poly[bis(4-phenyl)(2,4,6-trimethylphenyl)amine] (PTAA). Although the details of the 22.1% device are yet to be published, the spectral response shown in Figure 2b shows very good long wavelength response (similar to the 20.1% device mostly likely due to the use of lower bandgap perovskite absorber). The latest devices appear to use less absorptive substrates resulting

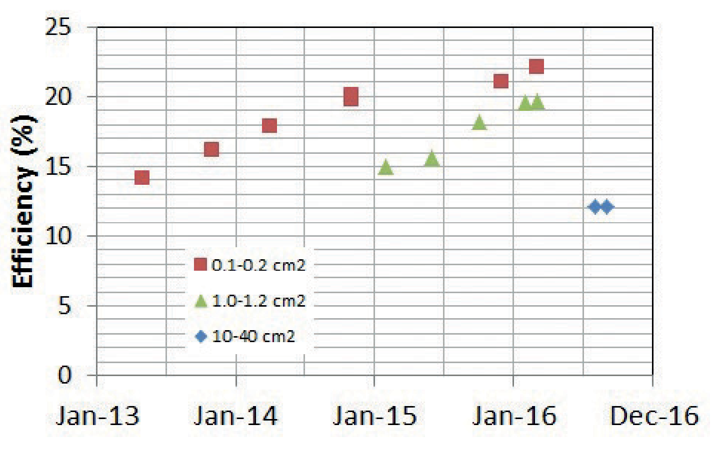

Figure 1. Evolution of certified perovskite solar cell performance.

Certification Time	Publication Time	Eff. (%)	Area (cm^2)	V_{OC} (V)	J_{SC} (mA/cm^2)	Fill factor (%)	Comments	Ref.
May 13	Jul 13	14.1	0.209	1.00	21.3	0.66	Sequential solution process for perovskite. Glass/FTO/c-TiO_2/mp-TiO_2/$MAPbI_3$/spiro-OMeTAD/Au	[14]
Nov 13	Jul 14	16.2	0.094	1.11	19.6	0.74	Solvent engineering during solution process of perovskite. Glass/FTO/c-TiO_2/mp-TiO_2/$MAPbI_{1-X}Br_X$/PTAA/Au	[15]
Apr 14	Jan 15	17.9	0.096	1.11	21.8	0.74	Compositional engineering of perovskite. Glass/FTO/c-TiO_2/mp-TiO_2/ $(FAPbI_3)_{0.85}(MABr_3)_{0.15}$/ PTAA/Au	[16]
Nov 14	Nov 2015	19.7	0.096	1.13	22.5	0.78	Incorporate excess PbI_2 into perovskite. Glass/FTO/c-TiO_2/mp-TiO_2/ $(FAPbI_3)_{0.85}(MAPbBr_3)_{0.15}$/ PTAA/Au	[17]
Nov 14	May 2015	20.1	0.096	1.06	24.7	0.77	Intramolecular exchange for perovskite. Glass/FTO/c-TiO_2/mp-TiO_2/ $(FAPbI_3)_{0.85}(MAPbBr_3)_{0.15}$/ PTAA/Au	[18]
Dec 15	Sep 2016	21.0	0.105	1.13	23.8	0.78	Polymer-templated nucleation Glass/FTO/c-TiO_2/mp-TiO_2/ $(FAI)_{0.81}(PbI_2)_{0.85}(MAPbBr_3)_{0.15}$/Spiro-OMeTAD/Au	[19]
Mar 2016	N/A	22.1	0.095	1.10	25.0	0.80	Details not yet published	[23]

Table 1. Independently certified efficiencies for small perovskite solar cells.

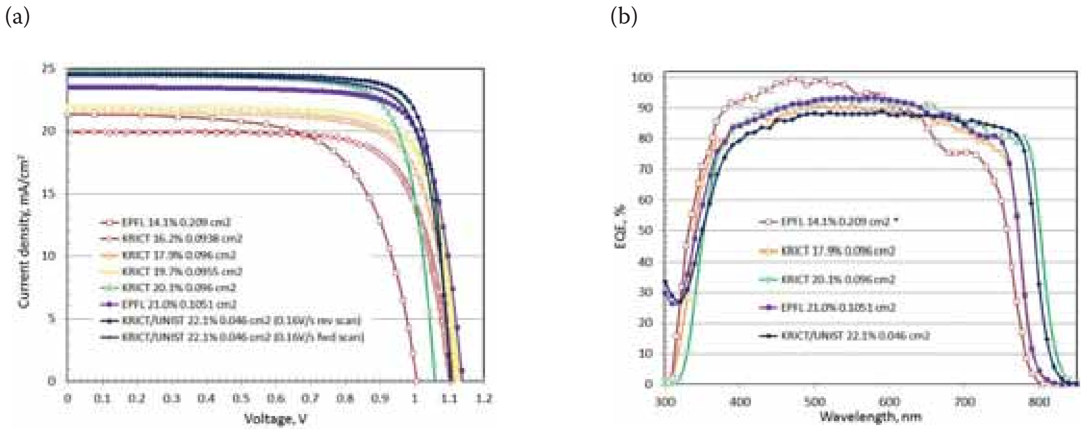

Figure 2. (a) Current density – voltage; (b) quantum efficiency of certified small area perovskite solar cells. (*Denotes normalized data while others are as measured.)

in better short wavelength responses.

Larger cells

Since 2015, there has been an increase in activity on $1cm^2$ cell demonstrations (Table 2 and Figure 3) rather than tiny (0.1 to 0.2 m^2) devices, initiated by National Institute for Materials Science, Tsukuba, Japan (NIMS). Interestingly, many of these cells adopted an "inverted" cell architecture using inorganic inter-layers. The 15% $1cm^2$ cell [24] reported has an improvement in carrier extractions after doping the inorganic inter-layers. Improvement in the 18.2% $1cm^2$ cell [25] came from the use of PCBM dissolved in toluene as an "anti-solvent" for the perovskite nucleation process, which was reported to also form a "perovskite–fullerene graded heterojunction". For the 19.6% cell [26] demonstrated by a team at École Polytechnique Fédérale de Lausanne (EPFL), a physical vacuum-based process is used that effectively removes the perovskite solvent for rapid nucleation instead of the use of an anti-solvent to reduce the solubility of the perovskite precursor for rapid nucleation. Another scalable process for improving the perovskite crystallization process over a large area has also been developed by a team at the University of New South Wales (UNSW) who demonstrated a slightly larger device of $1.2cm^2$ at 18% [27].

In the second half of 2016, cells and modules that are more realistic in size (>$10cm^2$) started to be certified (Table 3 and Figure 4) as fabrication, cell interconnection and encapsulation techniques matured. A mini-module of the size of $36cm^2$, fabricated by Shanghai Jiao Tong University in conjunction with NIMS, achieved an efficiency of 12.1% [23]. The largest certified single perovskite cell of $16cm^2$ was fabricated by UNSW using a scalable solution process in conjunction with the use of a metal grid. This large area cell does not require any isolation of the device into thin strips followed by series interconnection as is commonly found in large area thin modules. This eliminates the use of laser ablation, physical scribing or chemical etching and metal deposition, which require high-precision alignment. This demonstration is relevant to large area tandem cell applications.

Planar perovskite

Simpler planar devices (Table 4) with "standard" polarity that eliminate the use of the mp-TiO_2 are starting to catch up in conversion efficiencies, as new strategies are developed to overcome conspicuous hysteresis found in these devices in general. This probably made the certifying of these devices difficult at the early stages of development.

The first of such planar devices was developed by Liu et al. [32] with the

Certification Time	Publication Time	Eff. (%)	Area (cm^2)	V_{OC} (V)	J_{SC} (mA/cm^2)	Fill factor (%)	Comments	Ref.
Feb 15	Oct 15	15.0	1.10	1.09	20.6	0.67	Doping of inorganic interlayers Glass/FTO/NiMgLiO (p-type)/$MAPbI_3$/PCBM/Ti(Nb) O_x/Ag	[24]
Jun 15	N/A	15.6	1.02	1.07	19.3	0.75	Details not yet published	[23]
Oct 15	Sep 16	18.2	1.02	1.08	21.5	0.78	Perovskite–fullerene graded heterojunction Glass/FTO/NiO/$(FAPbI_3)_{0.85}(MAPbBr_3)_{0.15}$/PCBM/Ti(Nb) O_x/Ag	[25]
Feb 16	May 16	19.6	1.00	1.14	22.6	0.76	Vacuum flash-assisted solution process Glass/FTO/c-TiO_2/mp-TiO_2/ $(FAPbI_3)_{0.85}(MAPbBr_3)_{0.15}$/ spiro-OMeTAD/Au	[26]
Mar 16	N/A	19.7	0.99	1.10	24.7	0.72	Details not yet published	[23]
Sep 16	N/A	18.0	1.20	1.13	21.4	0.75	Scalable solution process for improving large area perovskite crystallization Glass/FTO/c-TiO_2/mp-TiO_2/ $(FAPbI_3)_{0.85}(MAPbBr_3)_{0.15}$/ spiro-OMeTAD/Au	[27]

Table 2. Independently certified efficiencies for $1cm^2$ perovskite solar cells.

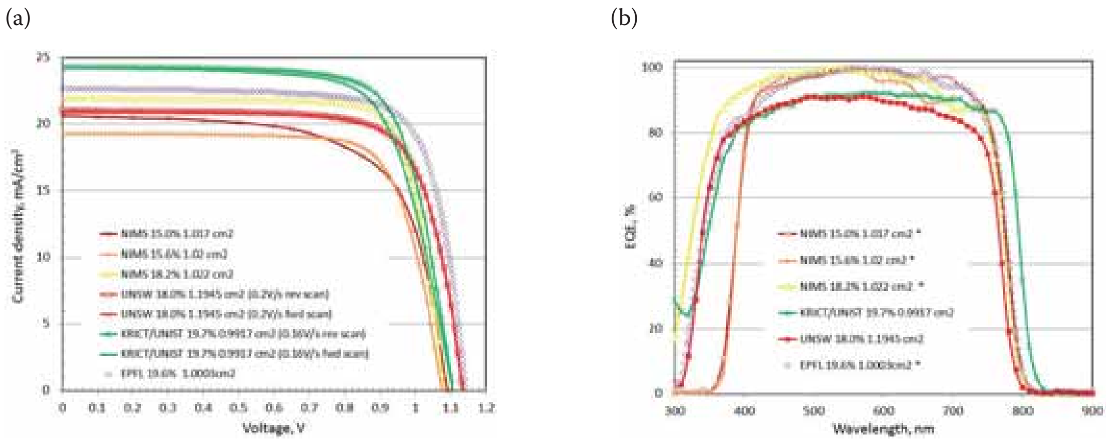

Figure 3. (a) Current density – voltage; (b) quantum efficiency of certified 1 cm^2 and slight larger 1.2 cm^2 perovskite solar cells. (*Denotes normalized data while others are as measured.)

Certification Time	Description	Eff. (%)	Area (cm^2)	V_{OC} (V)	J_{SC} (mA/cm^2)	Fill factor (%)
Aug 16	10 cells in series	12.1	36.13	0.84	20.2	0.72
Sep 16	Single cell	12.1	15.99	1.13	17.3	0.62
Sep 16	Four cells in parallel	11.5	15.95	1.14	16.7	0.60

Table 3. Independently certified efficiencies for >$10cm^2$ perovskite solar cells and module.

$CH_3NH_3PbI_3$ perovskite layer deposited by dual source thermal evaporation. This 15.4% efficiency device is the first of its kind as a physical deposition is used instead of the typically used solution process such as spin coating to deposit the perovskite layer. A 18% planar cell that uses atomic layer deposited (ALD) SnO_2 as the blocking layer and $(FAPbI_3)0.85(MAPbBr_3)0.15$ as the absorber layer for the first time was reported by Baena et al. [33]. A more efficient (19.3%) planar $CH_3NH_3PbI_3$ device was reported by Zhou et al. [34], which replaces the FTO glass with ITO glass coated with polyethyleneimine ethoxylated (PEIE), which is then overlaid by a yttrium-doped c-TiO_2.

Since then, more creditable certified efficiencies have been reported. The first of which, interestingly, is on a device that uses a less conventional perovskite material that intercalates phenylethylammonium (C8H9NH3 or "PEA") between the 3D perovskite layers resulting in a quasi-2D structure with layered perovskites through van der Waals interactions. The Glass/FTO/c-TiO_2/$PEA_2(MA)_{n-1}PbnI_{3n+1}$/spiro-OMeTAD/Au cell where n=60 [28] is certified to be 15.3% efficient. The increased stability can be due to the higher energy required to remove the PEAI from the perovskite to initiate decomposition. The devices also overcome hysteresis commonly seen in current-voltage curve of planar devices. It was suggested that the introduction of these multilayered structures might alter – e.g., suppress – electronic and ionic motion across the film thereby reducing the hysteresis. New treatments of TiO_2 have led to great improvements in efficiencies to 19.4% [29] and 20.1% [30]. The latter, which reports a solution process for SnO_2 allowing almost 20% cell efficiency to be achieved, is most useful as SnO_2 by ALD is not always easily accessible. This will likely generate more lab-scale developments using SnO_2 to eliminate the UV-instability associated with TiO_2 previously reported [35].

In terms of hole-transport layers, Spiro-OMeTAD and PTAA are still heavily used in the state-of-the-art devices despite their limitations in terms of stability (especially when additives are incorporated) and being the possible cause of device degradation when in contact with perovskite [36]. Opportunities exist for the less researched inverted devices and for engineering interface layers (carrier

Certification Time	Publication Time	Eff. (%)	Area (cm^2)	V_{OC} (V)	J_{SC} (mA/cm^2)	Fill factor (%)	Comments	Ref.
Jul 15	Feb 16	15.3	0.05	1.10	19.0	0.74	Quasi-2D perovskite Glass/FTO/c-TiO_2/$PEA_2(MA)_{n-1}Pb_nI_{3n+1}$/spiro-OMeTAD/Au	[28]
?	Aug 16	19.4*	0.11	1.10	22.4	0.79	Mortification of TiO2 using [BMIM]BF4 Glass/FTO/c-TiO2/$MAPbI_3$/PTAA/Au	[29]
Apr 16	Nov 16	19.9	0.07	1.07	24.3	0.77	Low temperature solution processed SnO_2 nanoparticle Glass/FTO/SnO_2/$(FAPbI_3)_{0.97}(MABr_3)_{0.03}$/Spiro-OMeTAD/Au	[30]
Nov 16	Feb 17	20.1	0.05	1.17	21.7	0.79	Chlorine-capped TiO2 colloidal nanocrystal Glass/ITO/c-TiO2-Cl/$Cs_{0.05}FA_{0.81}MA_{0.14}PbI_{2.55}Br_{0.45}$/Spiro-OMeTAD/Au	[31]

Table 4. Independently certified or independently verified (for the second entry) efficiencies for planar perovskite solar cells.(*Verified by National Center of Supervision and Inspection on Solar Photovoltaic Product Quality.)

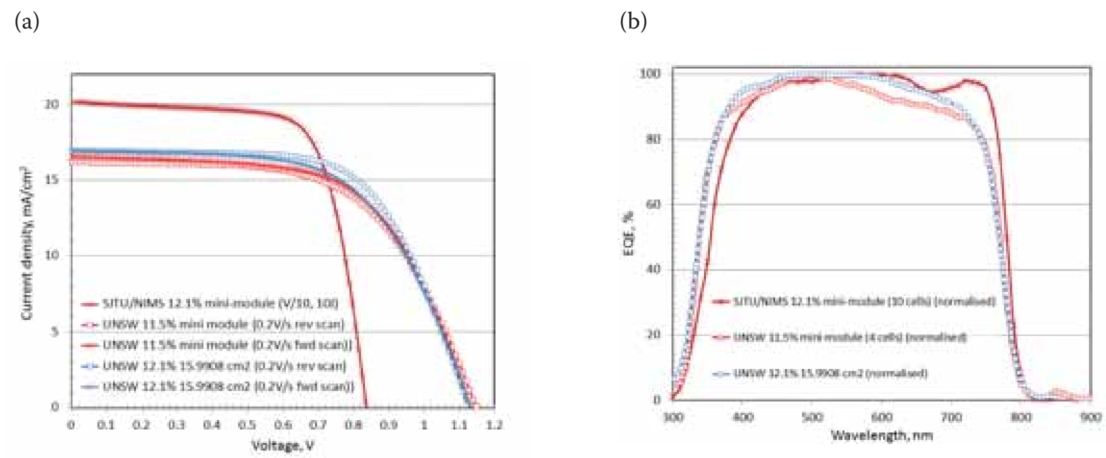

Figure 4. (a) Current density – voltage; (b) quantum efficiency of certified 10 cm2 and larger perovskite solar cells and modules. (*Denotes normalized data while others are as measured.)

transport or carrier blocking layers) with the aim of improving the voltage outputs of larger bandgap cells for tandem applications. Demonstrations of highly efficient devices that eliminate precious metals such as gold and silver are also important to reduce the cost of state-of-the-art devices.

Perovskite outlook

Given the many photovoltaic enabling properties of metal halide perovskites and the versatility of this new photovoltaic technology, flexible, device-integrated, building-integrated, vehicle-intergraded devices are some of the applications worthy to be explored. The bandgap tuneability of perovskite by varying its compositions opens up opportunities for chromaticity control as well as tandem applications. Semi-transparent or semi-opaque modules can be used as energy-generating glazing or facades for buildings.

One of the key questions related to commercializing perovskite solar cells is the cost of manufacturing. Answers to this question are important for commercial decisions on the level of investments and for setting performance and quality (e.g., lifetime) targets for the technology to be a viable product. A recent cost analysis by Chang et al. [37] shows that for a perovskite module at a cost of around USD 120/m² to be competitive in 2015 with incumbent photovoltaic technologies at a levelized cost of electricity (LCOE) of US$ 0.19/kWh, a module power conversion efficiency of 18% and a lifetime of 20 years are required. Further analysis shows that to meet the SunShot LCOE target of US$0.09/kWh in 2020, the manufacturing (including moduling and balance of system) cost needs to be reduced to around US$ 50/m² if the same module power conversion efficiency (18%) and the same lifetime (20 years) are maintained.

In conclusion, new innovations are required to overcome commercial barriers such as (i) small device size, which can be addressed relatively easily as scalable processes are constantly being developed, and (ii) the lack of longevity with current devices. The latter is more challenging. The presence of lead, albeit small but in readily soluble form, can still make it difficult for this new technology to enter into the market if potential health hazards to users in possible instances of leakage are considered.

Nevertheless, the outlook of perovsktie solar cells remains positive. The versatility of the material, the ease of fabrication and the photovoltaic-enabling attributes of the materials make it very easy for researchers, even those new to the field, to establish a baseline process for a reasonably efficient perovskite solar cell. This is the main reason for the phenomenal growth in research activities in this field. Not only can researchers experiment with new ideas, they also can experiment with old ideas that may have been previously too hard to execute. Building on the rapid progress in the last few years, and together with the growing number of research activities, pathways to overcome these challenges and barriers will be discovered.

References

[1] Kim, H.-S., et al., "Lead Iodide Perovskite Sensitized All-Solid-State Submicron Thin Film Mesoscopic

Solar Cell with Efficiency Exceeding 9%", *Scientific Reports*, 2012. 2: p. 591.

[2] Rose, G., "Description of some New Minerals from the Urals", Pogendorff Annalen der Physik und Chemie (in german) 1839. 48: p. 551-572.

[3] Wang, S., et al., "Synthesis and Characterization of [NH2C(I):NH2]3MI5 (M = Sn, Pb): Stereochemical Activity in Divalent Tin and Lead Halides Containing Single .ltbbrac.110.rtbbrac. Perovskite Sheets". *Journal of the American Chemical Society*, 1995. 117(19): p. 5297-5302.

[4] Topsöe, H., "Crystallographic-Chemical Investigations of Homologous Compounds. Z. Kristallogr. 1884, 8, 246–296 (in German). 1884. 8: p. 246-296.

[5] Poglitsch, A. and D. Weber, "Dynamic Disorder in Methylammonium trihalogenoplumbates (II) Observed by Millimeter-wave Spectroscopy", *The Journal of Chemical Physics*, 1987. 87(11): p. 6373-6378.

[6] Ishihara, T., J. Takahashi, and T. Goto, "Exciton State in Two-dimensional Perovskite Semiconductor (C10H21NH3)2PbI4", *Solid State Communications*, 1989. 69(9): p. 933-936.

[7] Onoda-Yamamuro, N., T. Matsuo, and H. Suga, "Dielectric Study of CH3NH3PbX3 (X = Cl, Br, I)", *Journal of Physics and Chemistry of Solids*, 1992. 53(7): p. 935-939.

[8] Mitzi, D.B., et al., "Conducting Tin Halides with a Layered Organic-based Perovskite Structure", *Nature*, 1994. 369(6480): p. 467-469.

[9] Mitzi, D.B., et al., "Conducting Layered Organic-inorganic Halides Containing <110>-Oriented Perovskite Sheets", *Science*, 1995. 267(5203): p. 1473-1476.

[10] Kagan, C.R., D.B. Mitzi, and C.D. Dimitrakopoulos, "Organic-Inorganic Hybrid Materials as Semiconducting Channels in Thin-Film Field-Effect Transistors", *Science*, 1999. 286(5441): p. 945-947.

[11] Kojima, A.T., K.; et al., "Novel Photovoltaic Solar Cell sensitized by Lead Halide Compounds (II)", J. Soc. Photogr. Imaging Jpn. 69 Supplement: p. 28-29 (In Japanese).

[12] M.A. Green, A. Ho-Baillie and H.J. Snaith (2014), "The Emergence of Perovskite Solar Cells", *Nature Photonics*, vol. 8, no. 7, pp. 506 – 514.

[13] MA Green, AWY Ho-Baillie (2017), "Perovskite Solar Cells: The Birth of a New Era in Photovoltaics", *ACS Energy Lett.*, 2017, 2, pp 822–830.

[14] Julian Burschka, Norman Pellet, Soo-Jin Moon, Robin Humphry-Baker, Peng Gao, Mohammad K. Nazeeruddin, & Michael Grätzel, *Nature*, 499, 316–319 (18 July 2013).

[15] N. J. Jeon, J. H. Noh, Y. C. Kim, W. S. Yang, S. Ryu, S. I. Seok, "Solvent-engineering for high performance inorganic-organic hybrid perovskite solar cells", *Nature Materials* 13, 897 (2014).

[16] N. J. Jeon, J. H. Noh, W. S. Yang, Y. C. Kim, S. Ryu, J. Seo & S. I. Seok, Nature 517, 476–480

[17] Y.C. Kim, N.J. Jeon, J.H. Noh, W.S. Yang, J. Seo, J.S. Yun, A. Ho---Baillie, S. Huang, M.A. Green, J. Seidel, Tae Kyu Ahn, S.I. Seok, "Beneficial Effects of PbI2 Incorporated in Organo---Lead Halide Perovskite Solar Cells", Advanced Energy Materials, 1502104 (2015)

[18] W.S. Yang, J.H. Noh, N.J. Jeon, Y.C. Kim, S. Ryu, J. Seo, S.I. Seok, "High-performance photovoltaic perovskite layers fabricated through intramolecular exchange", Science, 348, 1234-1237 (2015)

[19] Dongqin Bi, Chenyi Yi, Jingshan Luo, Jean-David Décoppet, Fei Zhang, Shaik Mohammed Zakeeruddin, Xiong Li, Anders Hagfeldt and Michael Grätzel, DOI: 10.1038/NENERGY.2016.142

[20] M. Saliba et al., "Cesium-containing Triple Cation Perovskite Solar Cells: Improved Stability, Reproducibility and High Efficiency", *Energy Environ. Sci.*, 2016, 9, 1989.

[21] M. Saliba, et al., "Incorporation of rubidium cations into perovskite solar cells improves photovoltaic performance", *Science* 10.1126/science.aah5557 (2016).

[22] M. Zhang , J. S. Yun, Q. Ma, J. Zheng, C. F. J. Lau, X. Deng, J. Kim, D. Kim, J. Seidel , M. A. Green, S. Huang, and A. W. Y. Ho-Baillie (2017), "High-Efficiency Rubidium-Incorporated Perovskite Solar Cells by Gas Quenching", ACS Energy Lett., 2017, 2 (2), pp 438–444.

[23] M.A. Green, A. Ho-Baillie et al. 2017, "Solar Cell Efficiency Tables (Version 50)", Prog. Photovolt: Res. Appl. July.

[24] W. Chen et al., "Efficient and stable large-area perovskite solar cells with inorganic charge extraction layers", 10.1126/science.aad1015.

[25] Y. Wu et al., "Perovskite solar cells with 18.21% effciency and area over 1 cm^2 fabricated by heterojunction engineering", DOI: 10.1038/NENERGY.2016.148.

[26] X. Li et al., "A vacuum flash-assisted solution process for high-efficiency large-area perovskite solar cells", 10.1126/science.aaf8060.

[27] Wilson Da Silva (2016), "Trendy solar cells hit new world efficiency record", UNSW Media Office 02 Dec 2016. http://newsroom.unsw.edu.au/news/science-tech/trendy-solar-cells-hit-new-world-efficiency-record. Last assessed May 4, 2017.

[28] L. Quan et al., "Ligand-Stabilized Reduced-Dimensionality Perovskites", J. Am. Chem. Soc. 2016, 138, 2649–2655.

[29] D. Yang et al., "Surface optimization to eliminate hysteresis for record efficiency planar perovskite solar cells", Energy Environ. Sci., 2016, 9, 3071

[30] Q. Jiang et al., "Enhanced electron extraction using SnO_2 for high-efficiency planar-structure HC(NH2)2PbI3-based perovskite solar cells", DOI: 10.1038/NENERGY.2016.177.

[31] Tan et al. 2017, "Efficient and stable solution-processed planar perovskite solar cells via contact passivation", *Science* 355, 722–726 (2017).

[32] M. Liu, M. Johnston & H. J. Snaith, 2013, "Efficient planar heterojunction perovskite solar cells by vapour deposition", *Nature* 501, 395–398.

[33] J. P. C. Baena, et al., "Highly efficient planar perovskite solar cells through band alignment engineering", Energy Environ. Sci., 2015, 8, 2928-2934.

[34] H. Zhou et al. 2014, "Interface engineering of highly efficient perovskite solar cells", *Science* 345, 542.

[35] T. Leijtens, et al. 2013, "Overcoming ultraviolet light instability of sensitized TiO_2 with meso-superstructured organometal tri-halide perovskite solar cells", *Nature Communications* 4, Article number: 2885.

[36] J. Kim, N. Park, J. S. Yun, S. Huang, M. A. Green, A. W. Y. Ho-Baillie, 2017, "Long-term Stability and Thermal Degradation of Planar $CH_3NH_3PbI_3$ and HC(NH2)2PbI3 Perovskite Solar Cells with the Hole Transfer Materials of Spiro-OMeTAD and PTAA", Solar Energy Materials and Solar Cells 162, 41-46.

[37] Nathan L. Chang, Anita Wing Yi Ho-Baillie, Paul A. Basore, Trevor L. Young, Rhett Evans and Renate J. Egan, "A manufacturing cost estimation method with uncertainty analysis and its application to perovskite on glass photovoltaic modules", Prog. Photovolt: Res. Appl. (2017). DOI: 10.1002/pip.2871.

About the Author

Anita Ho-Baillie is a senior research fellow at the University of New South Wales (UNSW), Australia. Her research interests in the field of photovoltaics include silicon solar cells, novel thin-film materials and tandem solar cells. She currently leads the perovskite solar cell research group at UNSW, which achieved world record energy conversion efficiencies for the largest perovskite solar cells independently certified in 2016.

PV Modules

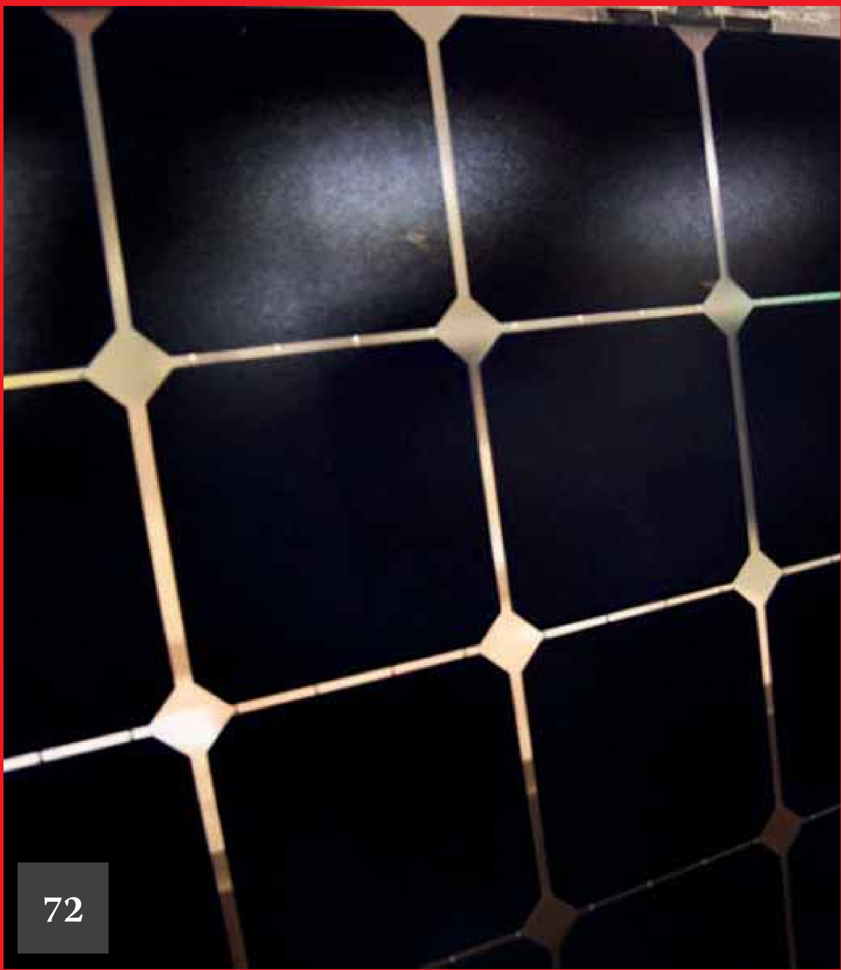

LONGi is the fastest growing PV manufacturer in the industry

Credit LONGi

LONGi has become the fastest growing PV manufacturer in the industry.

Leading integrated high-efficiency monocrystalline module manufacturer LONGi Green Energy Technology recently reported record total shipments and revenue for 2016, making it the fastest growing PV manufacturer in the industry.

Ahead of releasing full-year 2016 financial results, LONGi Green Energy Technology (formerly Xi'an LONGi Silicon Materials Co), which includes its solar cell and module manufacturing subsidiary, LONGi Solar (formerly LERRI Solar), undertook a major rebranding exercise that was intended to bring both its historical monocrystalline silicon ingot and wafer operations and previously acquired cell and module operations (LERRI, in 2014) under the LONGi name, as well as position the parent company as a 'green energy' business, reflecting the move downstream to also build PV power plants.

LONGi has come a long way very quickly. Annual revenue in 2013, which came solely from selling mono c-Si wafers, was around US$330 million but skyrocketed to approximately US$1.67 billion in 2016, almost a 94% increase over the previous year, which had itself generated a revenue growth of around 61%.

The significant increase was due to aggressive capacity expansion at the ingot/wafer, cell and module segments that were perfectly timed with China's downstream end-market growth that resulted in 34.54GW being installed in the country in 2016.

Bifacial Technology

'World's first' full-size IBC bifacial module displayed at SNEC

The Solar Energy Research Institute of Singapore (SERIS) at the National University of Singapore (NUS) has developed the world's first full-sized Interdigitated Back Contact (IBC) bifacial solar module using International Solar Energy Research Center (ISC) Konstanz, 'ZEBRA' solar cells.

The 60-cell bifacial module uses six-inch n-type mono wafers with ISC Konstanz fabricated ZEBRA cells with conversion efficiencies of up to 22%. The module is claimed to produce as much as 30% more power than an equivalent conventional IBC module, due to the bifacial nature of the solar cells and the layout with a double-glass structure to ensure ground-reflected light capture. The module is claimed to have a bifaciality of 75% and capable of producing up to 400 Watts.

Dr Wang Yan, Director of SERIS' PV Module Cluster said: "With SERIS' new module design, panels with 350 Watts front-side power can be made with sixty 23% efficient screen-printed IBC cells. Considering an additional 20% of power via the panel's transparent rear surface, each 60-cell IBC bifacial module will produce a stunning 400 Watts of power in the real world."

A key driver for bifacial module LCOE competitiveness with conventional modules is the double-glass structure that could offer a longer warranty period of 30 years or more, while generating more electricity of the lifetime of the module.

Bifacial modules emerged as a key technology theme at SNEC this year with a host of manufacturers launching new products.

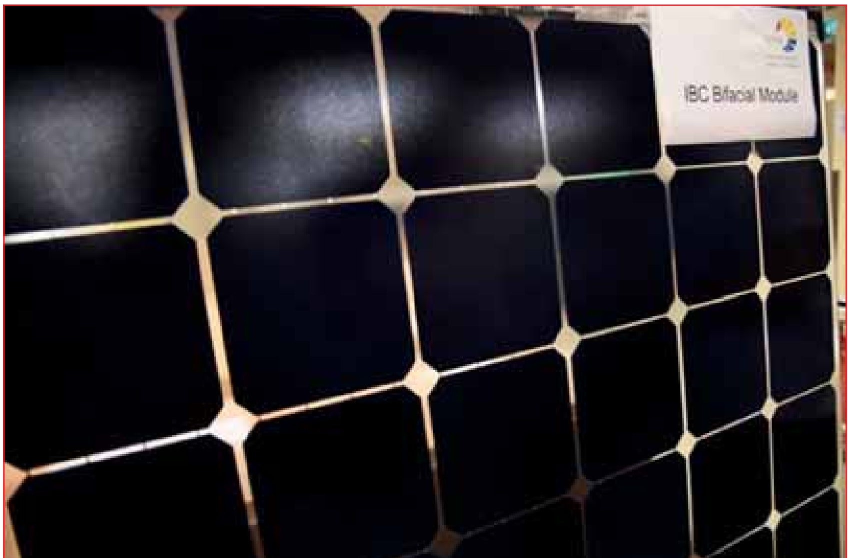

Credit SERIS

SERIS displayed the "world's first" IBC bifacial solar module at SNEC in China April.

Trina Solar wins its first order for bifacial modules

Trina Solar has secured the second largest order for bifacial modules, according to analysis by Photovoltaics International sister website PV Tech. The shipment occurred in April 2017 and is Trina Solar's first order for its bifacial modules.

Trina Solar said that it had won a 20MW module supply contract for its recently launched 'DUOMAX' bifacial module built with p-type mono-PERC (Passivated Emitter Rear Cell) technology using glass/glass encapsulation for a project located in Golmud, Qinghai, China.

According to PV Tech's analysis this is the second largest order for bifacial modules to date. Yingli Green previously supplied its bifacial modules for a 50MW PV power plant in China, the largest project to date for bifacial modules. US-headquartered heterojunction (HJ) cell manufacturer Sunpreme had supplied a project in the US with 13MW of HJ modules, previously making it the second largest order for bifacial modules, according to PV Tech's analysis.

Credit SunPower.

SunPower has signed a JV to begin producing its P-Series modules in China.

LONGi Solar launches mono PERC bifacial module

Mono module manufacturer LONGi unveiled a PERC bifacial module at the SNEC exhibition in Shanghai in April. The 72-cell version of the Hi-MO2 panel has a power output of 360-365W. According to LONGi, the front side cells will operate with a 21% efficiency. The rear side of the module will have an efficiency not less than 75% of the front.

LONGi confirmed in a statement that it had reached "mass production" of the Hi-MO2 modules making it more than an attention-grabbing release scheduled to coincide with a trade show.

"Hi-MO2 extends the strengths of mono PERC to the backside of the module, and can achieve higher power and higher energy yield without increasing costs, which will help decrease the LCOE, and bring more value for PV power plant investors," said Li Wenxue, president of LONGi Solar.

Jinergy plans production of bifacial heterojunction solar modules

High-efficiency PV module manufacturer Jinergy has said it will begin mass production of its n-type monocrystalline bifacial heterojunction (HJ) modules, which were showcased at its Technology Developer Forum ahead of SNEC 2017 in April.

The new bifacial HJT module is said to use solar cells with conversion efficiencies of around 23%, featuring excellent performance in weak light, a temperature coefficient of -0.28%/°C, and ultra-low degradation with n-type silicon wafer substrates. The module also benefit from an efficiency gain of between 8%-20% due to the bifaciality, depending on the albedo surface reflecting light to the back-side cell.

Liyou Yang, general manager of Jinergy, said: "We hope to cut the cost through breakthrough of key technologies and mass production. Currently, the mass production cost of HJT module is US$0.7/W and Jinergy aims to reduce the cost to under US$0.4/W within three years."

Jinergy expects to enter volume production at its module manufacturing base in Jinzhong, Shanxi Province, China in 2017.

Module manufacturing

SunPower enters major China manufacturing JV for P-Series solar modules

US-headquartered high-efficiency PV module producer SunPower has officially signed a joint venture partnership in China to produce both solar cells and modules for its P-Series technology.

The JV was signed in late February between its existing China-based supply chain partners Dongfang Electric Company (DEC) and Tianjin Zhonghuan Semiconductor (TZS) and includes a manufacturing capacity expansion from 1.1GW to 5GW.

Dongfang Huansheng Photovoltaic Company (DZS), the solar PV manufacturing subsidiary of DEC, currently manufactures high-efficiency monocrystalline PERC solar cells in a 1.1GW facility in Yixing, China, according to confirmation from SunPower.

Obsolete module manufacturing lines taint Indian capacity figures

India's solar manufacturers have said that roughly 2.25GW of module manufacturing capacity that was previously deemed functional is either obsolete or too old to be counted as operational, according to consultancy firm Mercom Capital Group.

As of December 2016, Mercom had put the installed figures at 2,815MW of cells and 8,008MW of modules. Of this, 1,448MW of cell and 5,246MW of module capacity were deemed operational.

Since then manufacturers have told Mercom that the true operational module manufacturing capacity stands at roughly 3GW – around 2.25GW less than previously projected. This is due to some manufacturers reporting defunct manufacturing lines as operational.

India's manufacturers have been struggling for some time, especially since the plunge in prices for products coming out of China midway through last year. Mercom reports that Indian modules that aren't part of local content rules typically cost about 10% more than Chinese modules. Furthermore, projects with the latest record low tariffs at Rewa in Madhya Pradesh of INR2.97/kWh (with escalation) will only be viable with cheaper Chinese modules.

Company news and results

SolarWorld reduces losses on higher shipments in Q1

Integrated PV module manufacturer SolarWorld used increased total product shipments in the first quarter of 2017 to limit losses as global solar panel price declines continue to pressure the industry.

SolarWorld reported preliminary total product shipments (modules, mounting systems & inverters) of 382MW, up 11% from around 345MW in the previous quarter. Total product shipments were the highest reported by SolarWorld in several years.

Preliminary revenue for the first quarter was €186 million, up around 13% from the previous quarter when revenue reached €164 million but was down from €213 million in the prior year period, which included lower shipments of 333MW, highlighting product ASP declines.

Hanwha Q CELLS in cash preservation mode as profits and margins crash

Hanwha Q CELLS may have reported record PV module shipments and revenue for 2016 but the underlying strategy for 2017 is cash preservation after its gross profit and margins collapsed in the fourth quarter of 2016.

Hanwha Q CELLS slashed capital expenditures to around US$50 million for 2017, down from US$137.7 million in 2016, with no new in-house capacity expansions planned for the year.

Total revenue-recognized module shipments in 2016 were a record 4,583MW, an increase of 55.0% from 2,956MW in 2015. However, Hanwha Q CELLS guided total module shipments to be in the range of 5,500MW to 5,700MW in 2017, indicating growth was expected to be much lower than last year at around 16%.

Credit PV Cycle

Veolia has opened the first PV module recycling centre in France.

GCL System consolidates position in solar industry 'super league'

China-based PV manufacturer GCL System Integrated Technology has consolidated its position within the 'Silicon Module Super League' (SMSL) ranks after it reported more than 4GW of module shipments in 2016.

With the majority of module shipments supporting sister downstream project developer GCL New Energy in China, which achieved new grid connected solar power plants of over 3.5GW in 2016, which increased by 114% as official Chinese figures were reported to have seen 34.54GW of installs last year. GCL System's shipments almost doubled from 2.1GW in 2015.

GCL System reported full-year 2016 revenue of just over RMB12 billion (US$1.74 billion), compared to RMB6.28 billion in 2015, a 91.31% increase and RMB2.68 billion in 2014, its first year of operation.

Yingli Green Energy avoids bondholder default with US$46 million payment

Struggling China-based PV manufacturer Yingli Green Energy has avoided another bond default with the payment of approximately US$46 million on one of its five-year unsecured medium-term notes (MTNs) due in early May 2017

According to Yingli Green, its subsidiary, Yingli China, which is engaged primarily in PV module manufacturing and downstream product sales, had made the payment to China Government Securities Depository Trust and Clearing Company Limited, as the nominated depositary and custodian of MTN issued in 2012.

Yingli had previously warned of delays in filing its 2016 annual report (Form 20F) with the US Securities and Exchange Commission.

With US$2.2 billion of debt and a US$1.1 billion deficit in working capital, coupled to renewed demands from bondholders, Yingli Green noted that its liquidity issues, debt restructuring and alternative financing plans and going concern warning meant it was unable to file Form 20F on or before the prescribed due date of 1 May 2017.

Suniva victim of Asian panel overcapacity as it files for Chapter 11 bankruptcy

Atlanta-based solar panel manufacturer Suniva has officially filed for Chapter 11 bankruptcy blaming overcapacity due to a mass influx of cheap solar panels in Asia.

When China's Shunfeng International Clean Energy (SFCE) bought a majority stake in the company back in August 2015 for US$58 million, Suniva was one of the top US c-Si manufacturers in terms of total capacity. Shunfeng was also able to circumvent US-China trade duties using Suniva's brand to produce cells in the US.

What started out as a good idea in theory did not quite come to fruition, however. According to Shunfeng's recently published 2016 outlook, the company expects to make an impairment loss of around ¥259 million (US$37.61 million) on its Suniva investment, as well as a provision of around US$33 million "in relation to certain potential financial liabilities of Suniva."

It was Hong Kong-based SFCE, which owns a 63.13% equity interest in Suniva, that made the initial announcement that the manufacturer had filed a Chapter 11 petition for protection with the US Bankruptcy Court in Delaware in late April.

Recycling

Veolia opens France's first PV recycling facility

French waste giant Veolia has opened the first PV recycling facility in France through a partnership with PV Cycle, a not-for-profit take-back and waste management programme for solar in Europe.

The PV panel recycling plant, which is located in Rousset in the Bouches-du-Rhône of southern France, will process 1,400 tonnes of material per year from 2017 and up to 4,000 tonnes by 2021. The secondary raw materials recovered will be used in various other sectors including aluminium, glass and copper.

The processing will help solar plant owners comply with the European Waste Electrical and Electronic Equipment (WEEE) directive, which mandates the recycling of PV panels at end-of-life. The association currently takes on PV modules, inverters, batteries and other equipment subject to the directive.

Credit Yingli Solar

Yingli Solar has avoided another bond holder default with a US$46 million payment to creditors.

Advanced cell and module design for solar LCOE optimization: Is the white glass–glass module the future?

Qiang Huang & **Xinchang Li**, GCL System Integration Technology Co. Ltd. Jiangsu, PR China

ABSTRACT

With the increasing number of solar installations, the PV industry is gradually shifting its focus from \$/W to \$/kWh. The development of advanced solar cells and modules needs to be addressed from a system performance optimization point of view. GCL's specially designed white glass–glass (WGG) module using advanced solar cells is taken as an example in order to demonstrate the 'one-stone-three-bird' methodology, i.e. the use of one product to reduce \$/W cost, to improve system performance, and to increase lifespan, all at the same time. The outlook of the future module design for system optimization is also discussed.

Introduction

The estimated PV system installation capacity in 2016 was ~70GW worldwide [1], as shown in Fig. 1. In fact, the production volume in 2015 was around 200 times that in 2000, with a compound annual growth rate (CAGR) of over 40%. It has recently been noted that as the PV industry matures, the mindset is changing from \$/W to \$/kWh. While \$/W is still a major driving force, the significance of other factors that influence the cost of energy must also be considered. In this regard, PV development is entering the era of \$/kWh-oriented optimization.

> "As the PV industry matures, the mindset is changing from \$/W to \$/kWh."

There is an old Chinese proverb that says, 'kill three birds with one stone'. The nature of solar energy is such that the main factor is the cost of the energy. One of the most important skills in the solar industry is to condense multiple process steps into one in order to maximize the cost reduction. The problem is, can one simultaneously lower the \$/W, increase PV system efficiency, and lengthen the lifespan?

To answer this question, a levelized cost of electricity (LCOE) analysis will be the

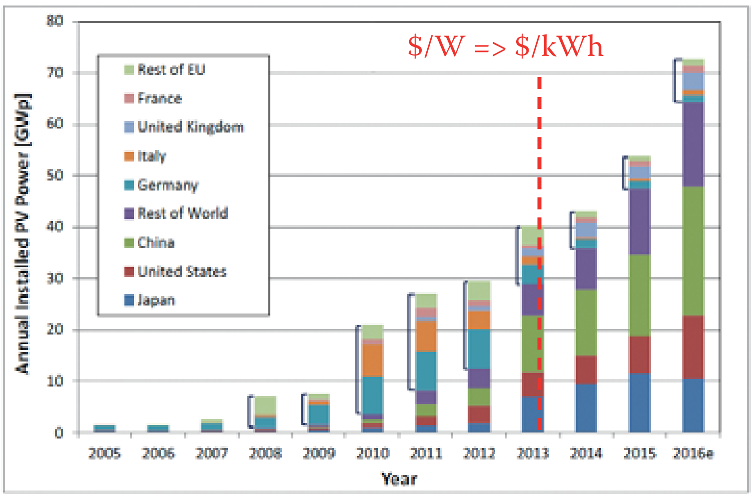

Figure 1. Annual PV system installations from 2005 to 2016 (data taken from Jaeger-Waldau [1]), and the industrial scenario shift from \$/W to \$/kWh.

$$\mathrm{LCOE} = \frac{\text{Total life cycle cost}}{\text{Total lifetime energy production}} \tag{1}$$

$$\mathrm{LCOE} = \frac{\text{Initial investment} - \sum_{n=1}^{N} \frac{\text{Depreciation}^{n}}{(1+\text{Discount rate})^{n}} \times (\text{Tax rate}) + \sum_{n=1}^{N} \frac{\text{Annual cost}^{n}}{(1+\text{Discount rate})^{n}} \times (1-\text{Tax rate}) - \frac{\text{Residual value}}{(1+\text{Discount rate})^{n}}}{\sum_{n=1}^{N} \frac{\frac{\text{Initial kWh}}{\text{kWp}} \times (1-\text{System degradation rate})^{n}}{(1+\text{Discount rate})^{n}}} \tag{2}$$

Equations 1 and 2.

starting point, followed by discussions of innovations along the value chain. A meaningful example – a white glass–glass module – will be used in order to demonstrate the one-stone-three-bird methodology in the optimization of \$/kWh (Fig. 2). The system design outlook will then be discussed.

First principle: optimization of system LCOE

To solve a problem elegantly, experienced engineers begin their analysis with the first principle, i.e. the basic law that governs the issue to be addressed. Here, the objective is the optimization of system LCOE, which is defined by Equation 1 [2]; for solar generation, this equation can be separated into the components indicated in Equation 2 [3].

It can be seen that the LCOE is a function of initial system output, degradation ratio, initial investment, operation and maintenance cost, and depreciation of equipment. It is also related to the financial indices, such as tax rates and the rising interest rates for funds.

To simply the problem, and to focus on the influence of technical improvements on the LCOE, in this paper the loan payment, tax, insurance, discount rate and O&M costs are omitted in the calculations (Fig. 3). Moreover, the residual value at the end of life is always considered to be zero.

To keep it simple, the three most significant factors are:

1. The initial investment, which is linked to module \$/W.
2. PV system performance ratio (PR), which influences the energy yield.
3. Operational lifespan of the system.

The PR is an internationally introduced measure for the degree of utilization of an entire PV system, and is defined in more detail in IEC 61724 [4]. In practical terms, the PR is calculated as follows [5]:

$$PR = E_{specific} / H_{specific} \times 100\% \quad (3)$$

$$E_{specific} = E_{Feed\text{-}in} / P_{STC} \quad (4)$$

$$H_{specific} = H_{POA} / G_{STC} \quad (5)$$

where $E_{Feed\text{-}in}$ is the electricity fed into the grid; P_{STC} is the rated DC power of the modules; H_{POA} is the irradiation sum (energy) in the module plane; and G_{STC} is the irradiation corresponding to the irradiance intensity (1,000W/m^2) in standard test conditions (STC).

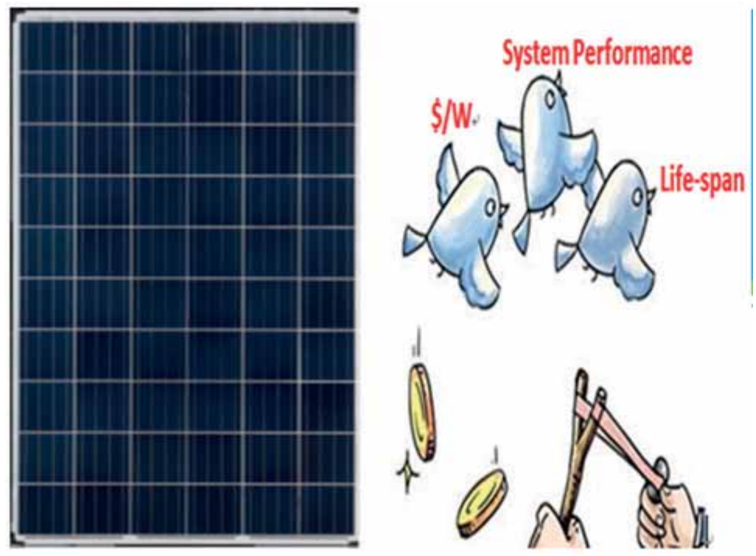

Figure 2. A white glass–glass module from GCL and the one-stone-three bird design methodology to illustrate optimization.

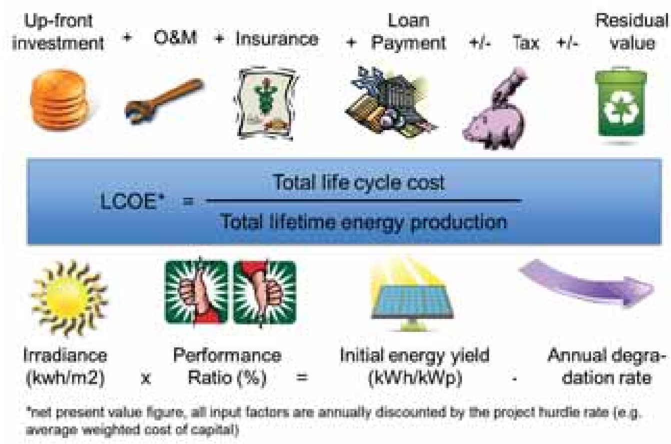

Figure 3. Graphic illustration of LCOE (courtesy of Thomas Reindl).

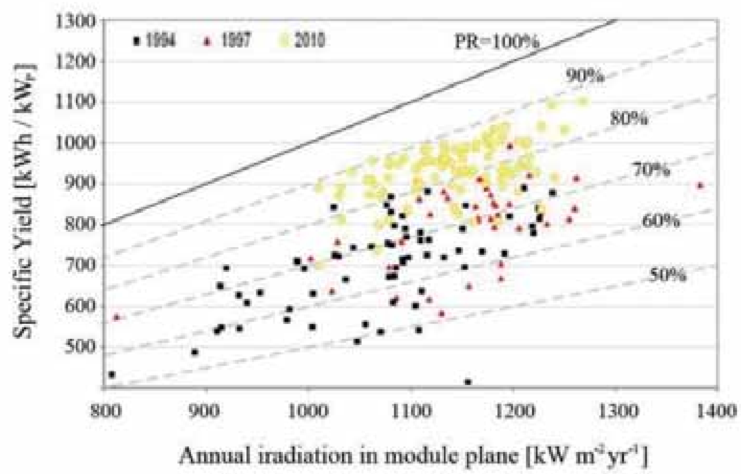

Figure 4. The change in PR values from 1994 to 2010 for German PV systems [5].

For a better understanding, in the case where $H_{specific}$ = 1 (i.e. the in-plane irradiation equals 1,000W/m^2), the PR in Equation 3 reduces to the ratio of system output power to the nameplate power of the panel. The PR represents the overall effect of losses on the PV system's rated output due to array temperature, incomplete utilization of the irradiation, system component inefficiencies or failures.

As shown in Fig. 4, Reich et al. [5] from Fraunhofer ISE have determined the monitored specific yield as a function of total plane-of-array irradiation of PV systems. An improvement in PR with time is clearly seen: the PR is ~65%, 75% and 85% for the years 1994, 1997 and 2010 respectively.

Nobre et al. [6] from the Solar Energy Research Institute of Singapore (SERIS) has demonstrated that the PR is strongly influenced by temperature, soiling, shading, mismatch, etc. If the effects of these factors are reduced, the PR can be improved by ~8%, as shown in Fig. 5.

Innovation along the value chain

The most significant technical innovations that are relevant to Si-based solar technology are listed in Table 1. From this list the best solutions in terms of reducing LCOE have been selected for discussion.

For Si materials, the improved Siemens method is dominant, and companies are seeking locations with lower electricity prices in order to reduce cost. The modified Siemens, fluid-bed reactor (FBR) and metal-Si methods are being launched into mass production by GCL, REC and Elkem respectively. In the case of wafers, larger Si casting blocks (8×8), casting mono (>90% mono), continuous CZ mono (10 silicon rods using one crucible), diamond wire slicing, and direct wafering (e.g. technology from companies such as 1366/Crystal Solar/ Amber Wave) are noted.

For cells, notable innovations include:

- finer lines below 40μm line width;
- five-busbar (5BB);
- multibusbar (MBB, 12–18 busbars);
- black-Si texturing (reactive ion etching, or metal catalyst chemical

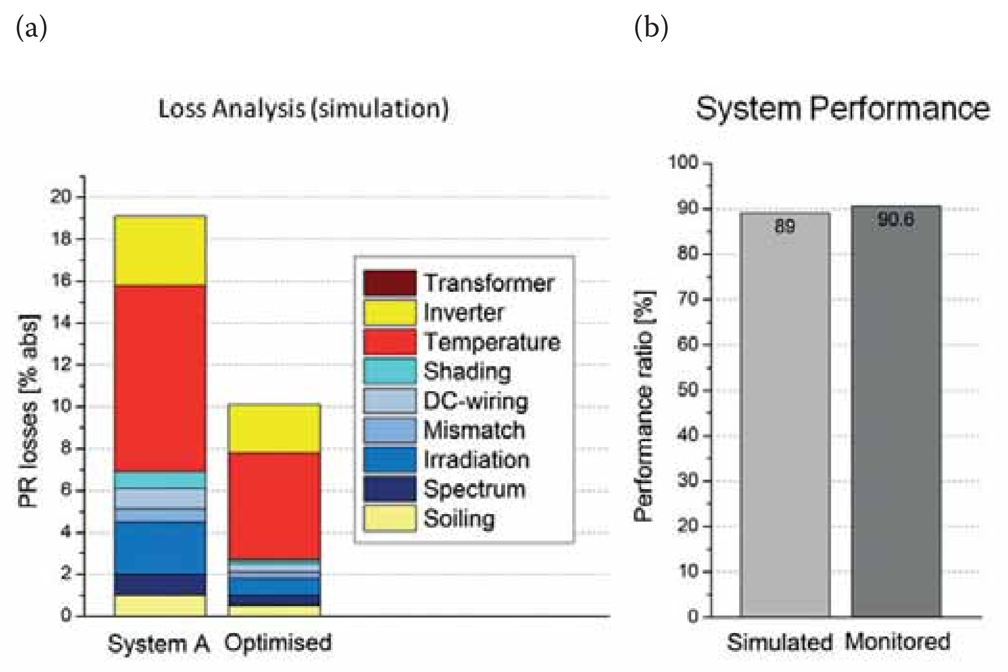

Figure 5. (a) Comparison of the PR for an actual PV system (system A) and a simulated 'optimized' PV system. Also shown is a breakdown of the individual loss factors that influence the PR. (b) Actual system performance of a real-world demonstration system at the Solar Energy Research Institute of Singapore (SERIS). This system has been operating at~90% since 2012 [6].

Si	Wafer	Cell	Module
FBR	Large Si block (8×8)	Fine line/5BB/MBB	**White double-glass**
Siemens Si	Casting mono	**Black – Si texturing**	Bifacial double-glass (n-type, PERC)
Metal-Si	**Diamond wire (DW)**	DW wafer direct texturing	High-voltage (1,500–3,000V)
	Continuous CZ mono	**p-PERC/n-PERL**	**CTM enhancement (twin, high-density)**
	Direct wafer	HJT cells/TOPCon	96× supersize (single-axis tracking)
		Hydrogenation	SMART (MPPT+)
		C-Si tandem cells (e.g. Si+perovskite)	Local (optimized spectrum/ structure)

Table 1. Summary of significant technical innovations along the value chain.

etching) and direct texturing for diamond wire slicing multicrystalline Si wafers;
- p-type passivated emitter rear cell (p-PERC) concepts;
- n-type passivated emitter and rear locally diffused (n-PERL) devices;
- heterojunction cells (HJT) and new TOPCon concept cells;
- hydrogenation, which improves carrier lifetime;
- C-Si/perovskites tandem cell structures.

In the case of modules, notable innovations include:

- white double-glass designs;
- bifacial double-glass designs incorporating n-PERL or p-PERC cells;
- high-voltage modules (1,500–3,000V);
- high-efficiency modules with significant cell-to-module (CTM) power enhancement (half-cut twin-cell modules for 2.5% power enhancement, or high-density modules for 10% power enhancement).

Also listed in Table 1 are 96-cell supersize modules for single-axis tracking, smart modules, and local modules with customized spectrums or structures that are designed for specific locations.

The two hottest topics in recent years – namely diamond wire wafer slicing + black Si, and advanced passivation (p-PERC/n-PERL) – will be used as examples for analysing the impact on LCOE or on $/kWh.

As a rough guide for comparison purposes, a reduction in $/kWh of ~4% is estimated through the use of diamond wire wafer slicing; this reduction mainly arises from the cost saving in $/W for Si materials. The calculation assumes a 20% Si material cost saving from using diamond wire technology as a result of a reduction in line spacing associated with diamond wire; this translates to a $/W saving in module cost of ~8%. If it is assumed that a module constitutes 50% of the initial investment in Equation 2, then the reduction in LCOE or $kWh is ~4% (omitting the influences from financial loan, discount rate, insurance, O&M costs, etc.). In the case of multicrystalline solar cells, only with those solutions listed in Table 2 can diamond wire wafer be used in solar cell production; this introduces some complexity in the production line.

For comparison purposes (and omitting the influences from financial loan, discount rate, insurance, O&M costs, etc.), a reduction in $/kWh of roughly 7% is estimated through the use of advanced passivation of solar cells, such as p-PERC (Fig. 6). From Equation 2, an increase of ~1.5% in solar cell efficiency corresponds to a reduction of ~8% in initial investment. The increase in manufacturing cost (for example resulting from passivation equipment depreciation) is considered to be 2% $/W for a module, or 1% for the initial investment in Equation 2.

No.	Solutions	Cell efficiency	Cost	Sensitivity to wafer process	Market
1	RIE (reactive ion etching) (Dry black Si: wafer surface is bombarded with directional reactive ions to form the texture)	+0.5–0.8%	High ~$2m/line	Not sensitive	High efficiency
2	MCCE (metal catalyst chemical etching) (Wet black Si: Ag, Cu ion-assisted etching to form nano-deep holes. Texture is formed after widening of the holes)	+0.3–0.6%	Low ~$0.5m/line	Sensitive to - grain orientation	Main-stream market
3	Additives (Direct texturing process)	–0.2~0.05%	Zero	Sensitive to - slicing damage	Low cost

Table 2. Comparison of three texturing technologies for diamond wire wafer slicing.

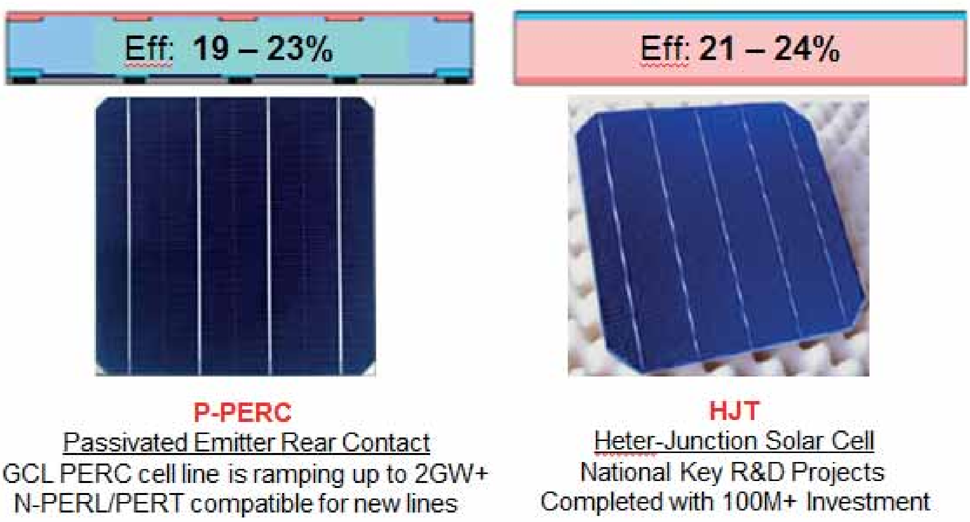

Figure 6. Examples of solar cells with advanced passivation: p-type passivated emitter rear cell (p-PERC) and heterojunction cell (HJT).

An additional advantage of advanced passivation is that the open-circuit voltage of a solar device is improved, such as in the case of PERC. This translates to the optimization of the temperature coefficient of a solar module. For an improvement of 0.02 in the temperature coefficient, the electricity output can be increased by 1% at an environment temperature of 75°C; with reference to Fig. 5, this represents an improvement in the system PR.

From the above analysis, the diamond wire case addresses mainly a $/W cost reduction for the module. In the PERC case, however, not only is there a reduction in $/W, but also the system performance is improved. Nevertheless, a reduction in $/kWh by more than 10% through the use of a single technology would appear to be an extremely difficult task.

An example of the one-stone-three-bird approach

In this section, the third factor that has an impact on LCOE – the lifespan – is considered with reference to GCL's white glass–glass (WGG) module. The reduction in $/kWh for this type of module and its solution packages is estimated to be ~20%.

The advantages of a glass–glass (GG) module, well known in the solar industry [7,8], include:

- Five (or more) years' additional performance warranty (30 years vs. 25 years)
- Lower year-to-year degradation (0.5%/year vs. 0.7%/year)
- Resistance to PID (potential-induced degradation)
- Resistance to power loss caused by dust/snow accumulation
- Lower operation temperature
- Resistance to hot-spot effects, and fireproof properties
- Resistance to microcracks and snail-track defects
- Resistance to friction from airborne sand
- 1,500V system voltage

Most of those advantages will already have been reflected in the commercial terms of the product.

As shown in Fig. 7, the degradation of a standard module over 25 years is 100%, 97.5%, 96.8%, 96.1% … 81.4%, 80.7%. Here, the degradation is 2.5% for year one, mainly due to boron–oxygen (B–O) effects, etc. in the solar cell; for year two onwards, the degradation is 0.7% because of the packaging materials, etc. In comparison, the degradation of a GG module over 30 years is 100%, 97.5%, 97%, 96.5% … 86%, 85.5%, 85%, 84.5%, 84%, 83.5%, 83%; the degradation in this case is 0.5% for year two onwards. Glass is a better packaging material than polymer materials in terms of stability.

A GG module is expected to produce ~21% more electricity as a result of its longer lifespan and lower degradation rate. With reference to Equation 2, an increase of 21% in total energy production in the denominator leads to a decrease in LCOE of 17% (with simplifications of the problem, where financial loan, discount rate, insurance, O&M costs, etc. are not considered).

It is common for no frame to be used in a GG module design; as a consequence, a glass–glass module will be not be susceptible to PID, since this type of degradation is believed to be caused by the potential difference and the short distance between the frame and the solar cells. Moreover, dust or bird droppings usually accumulate along the standard Al frames, causing shading as well as an increase in temperature. For a no-frame glass–glass module, however, dust, bird droppings, or snow in winter can be removed by wind-blowing, gravitational-sliding, or rain-washing effects. In addition, because air can flow more freely and quickly beneath the modules, the temperatures within the modules are lower. As a result of these anti-dust and low-temperature effects, a GG module will increase its electricity output by another 3%.

Because of the mechanical strength and physical properties of glass, a GG module is resistant to microcracks. In fact, lab experiments have been carried out to show that even a person standing on top of a GG module will not cause microcracks, whereas they are easily caused when a normal backsheet module is stepped upon. Glass also has a low water vapour transmission rate. The anti-microcrack and anti-vapour properties prevent the forming of other defects, for example snail-track defects. A GG module is also resistant to hot spots as well as being naturally fireproof. In desert environments, a GG module also demonstrates high resistance to friction from airborne sand.

Last, but not least, because of the excellent isolation properties of glass, the GG modules from GCL are 1,500V voltage ready; this increases the string length by 50% compared with a 1,000V system, further reducing the cost of initial investment (fewer inverters, combiner boxes, cables, etc.) It is estimated that the 1,500V voltage system also helps to increase the power

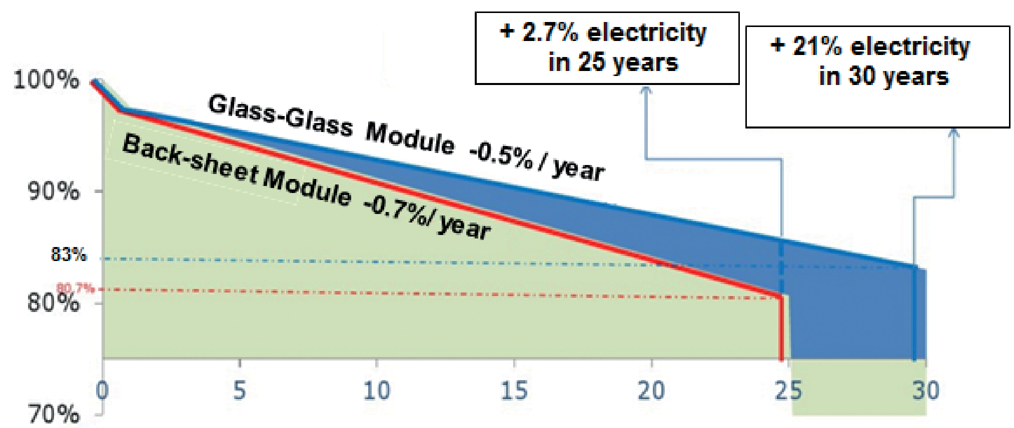

Figure 7. Comparison of the electricity output of a normal backsheet module and a glass–glass module. The degradation value of 0.7% or 0.5% will be specified in the manufacturer's warranty.

output by 1–2% as a result of lower energy losses.

In the case of a GG module with the same $/W cost as a normal module, the LCOE cost reduction is ~ 20% for the GG module (neglecting influences from financial loan, discount rate, insurance, O&M costs, etc.); this is extremely significant in terms of LCOE cost saving.

In the real world, however, the market share of GG modules is only 2–5%, which seems contrary to expectations. Why so small? Three reasons can be identified:

1. The $/W cost is high for a GG module (because of transparency).
2. The installation method is not optimized against breakage.
3. The $/kWh cost is high for a GG module (inadequate system design).

1. Reduction of $/W cost: GCL's white GG design

Transparent GG (TGG) modules are widely used in building-integrated PV (BIPV) as semi-transparent walls, windows or roofs. Because of the losses of light energy, mainly between the solar cells in a TGG module, the $/W cost for a TGG module is ~2–20% higher than that of a normal module. This value depends on the transparency of the TGG module: the higher the transparency, the higher the $/W cost.

> "A WGG module produces at least 5W more power output than a TGG module, while its $/W cost is comparable to that of a standard backsheet module."

The structure of the WGG module developed at GCL is shown in Fig. 8: from top to bottom, glass, transparent EVA, solar cells, white EVA/POE/glaze, and glass are layered one by one. The white EVA (or POE, or ceramic glaze) is used as a reflector to guide the light into the module. White EVA has a better reflection rate than a normal backsheet; instead of a power loss, there is a power gain through using the WGG module design. A WGG module produces at least 5W more power output than a TGG module, while its $/W cost is comparable to that of a standard backsheet module. The first problem has therefore been addressed.

2: Installation optimization: GCL's patented method

Fig. 9 shows the most common installation method for a GG module.

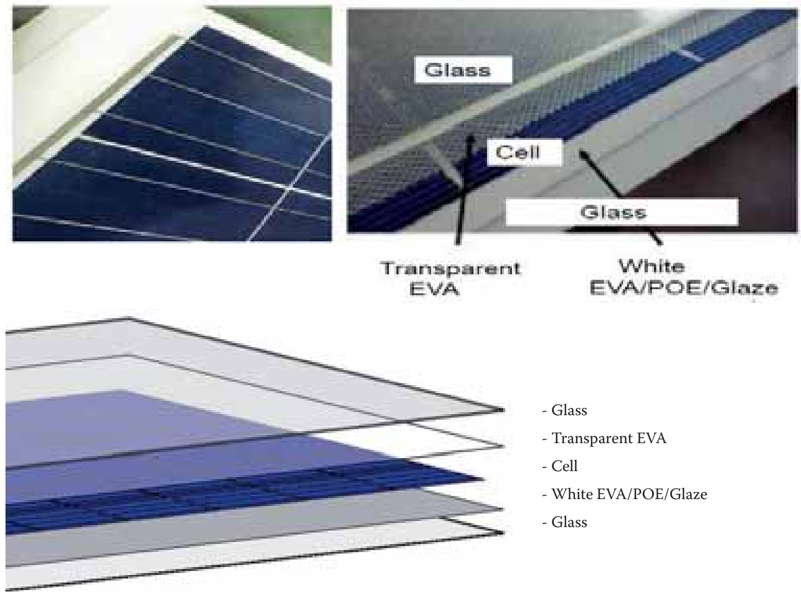

Figure 8. Layered structure of a white glass–glass (WGG) module.

The procedure is simple and convenient for the module manufacturers, but there are some shortcomings:

1. The method is not foolproof: any mistake in installation (e.g. the metal presser directly touching the glass) will lead to glass breakage.
2. Neighbouring modules impinge on each other: if a broken module on the left side drops, the clamping strength is lost for the module on the right side. One broken module can lead to module breakages in the same row.

Fig. 10 shows the patented GCL installation method. The core of this innovation is a module with a metal installation base, which is attached to the GG module by structure glue. There is no stress from metal parts pressing on the side edges of the glass. The installation base is fixed to the cross beam by a fixer; any unevenness of the mechanical stress will be applied only to the regions between the metal installation base and the fixer.

The rubber fixer in the graph is optional and not functionally required. The GG module is safe by design. The new design (Fig. 10) passed a 6,000Pa mechanical loading test for the horizontal installation. The new design also speeds up installation and saves labour, because there are fewer installation steps and a lower level of skill is needed.

Another possible solution is to use the back-side hook concept in a GG module, a technique that is also widespread in the industry. As shown in Fig. 11, the method serves well if there is a good fit between the beam

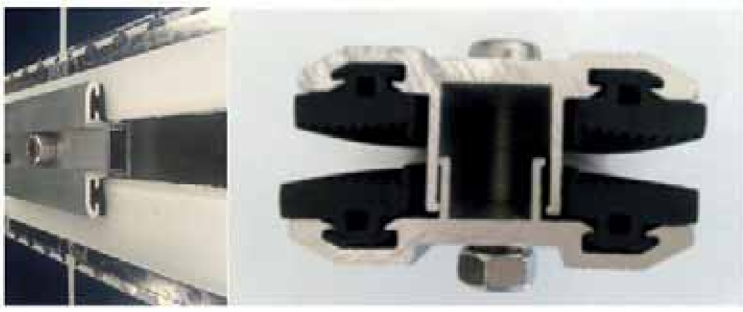

Figure 9. The standard clamps used in common GG installations. This is not a foolproof design, and appropriate skills for proper installation are necessary.

PV Modules

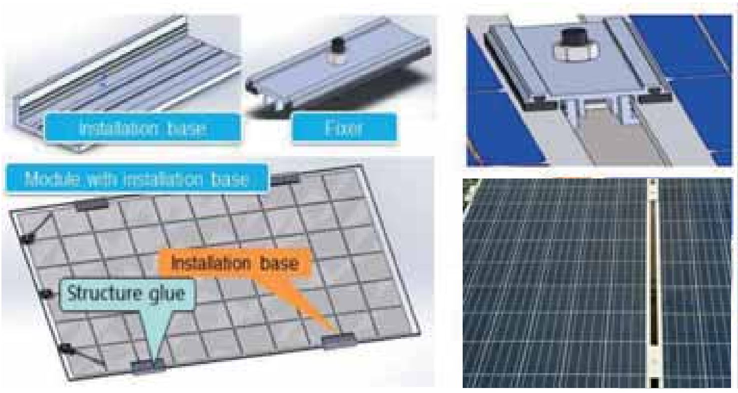

Figure 10. The GCL patented installation method. This foolproof design eliminates breakages resulting from stress to the edges of the glass, as well as increasing the speed of installation at the same time.

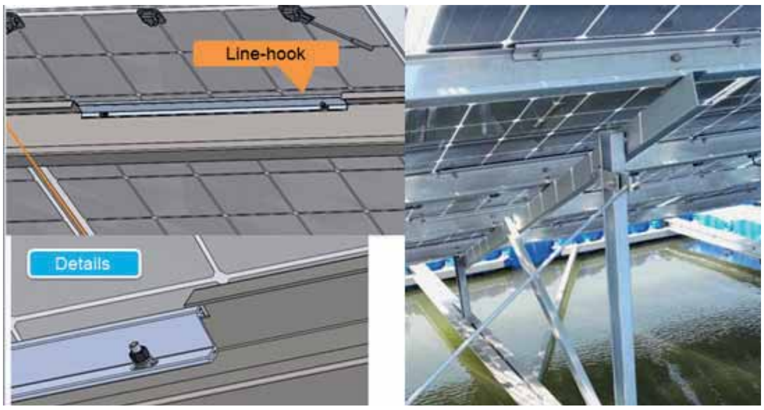

Figure 11. The installation of a GG module by the line-hook (back-side hook) method.

design and the back-side hook module. In the case of any misalignment or changes in the relative position of the beam and the hook, however, the difficulty of installation will increase. The installation using a back-side hook requires the employment of workers with more skills; in addition, this method could not in future be applied to bifacial modules. The GCL-patented GG module with an installation base is therefore considered to be the best solution for tackling the second problem that prevents the GG module from dominating the market.

3. Reduction of $/kWh cost: GCL's system design

There is a natural link between the first and third reasons for the small market share of GG modules. The TGG solution is generally requested by end users, especially for agriculture-related applications, where a certain degree of transparency is necessary for the plants or animals beneath the solar module roof. If the transparency on the module side is provided using the TGG solution, however, the $/W cost and the $/kWh cost are higher.

A fitting solution is to provide the transparency through a systematic combination of a WGG module and a light-splitting plate (LSP), as shown in Fig. 12. First, the WGG modules and LSPs are arranged in an alternating sequence in order to provide a certain degree of transparency. The mini-structures in the LSP guide the light so that it is evenly distributed. Since different plants and vegetation have different light-saturation and light-compensation points, the system design should take these factors into account. LSPs can be constructed using cheap acrylic materials, and so they cost much less than modules.

The combination of the WGG module, the GCL installation method, and the LSP design of the GCL system is a promising solution package for boosting the prevalence of GG modules in the near future. Table 3 summarizes $/W and $/kWh cost-reduction comparisons of diamond wire wafer, advanced passivation and GG modules; it clearly shows that WGG proves superior from a $/kWh point of view.

> "The combination of the WGG module, the GCL installation method, and the LSP design of the GCL system is a promising solution package."

Future design outlook

In order to further reduce the LCOE of a solar power system, more work needs to be done in this direction. One line of investigation, for example, is the use of half cells: the GCL twin module is able to reduce the internal operating joule loss by 75%. An increase in electricity energy output of 2–5% was observed in GCL's experimental solar system set-up on hot days.

In another example, n-PERT bifacial solar cells can increase the electricity energy output by 5–20% under certain conditions, where the back-side reflection of light can be properly utilized. Other examples include the 96-cell supersize module for tracking applications, 3,000V high-voltage modules, and high-density modules, to name a few.

Future innovations may be summarized by separating them into the following categories:

1. System power output optimizations, including trackers, lower concentration design, bifacial cells and module design, 1,500–3,000V systems, smart modules, complementary multiple-energy source systems, etc.

2. Cell efficiency improvement, such as p-PERC, n-PERL, n-PERT bifacial cells, TOPCon cells,

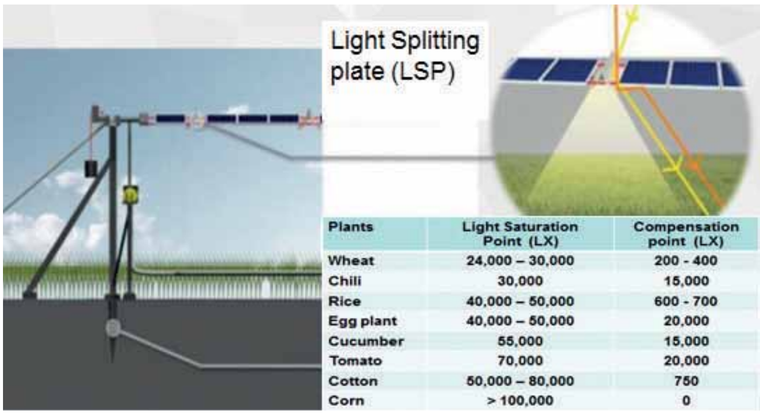

Figure 12. Schematic of a GCL white glass–glass module and light-splitting plate design. Examples of the light-saturation and light-compensation points for various plants are listed [9].

Category	$/W	$/kWh	Dominant factors
Diamond wire	8% ⇩	4% ⇩	Si materials saving
Advanced passivation	2% ⇧	6% ⇩	Cell % efficiency increase
TGG module	2–20% ⇧	10–20% ⇩	Lifetime, and power output
GCL WGG + LSP	2% ⇩	20% ⇩	Lifetime, and power output

Table 3. Changes in $/W or $/kWh for different techniques compared with the diamond wire baseline. (To simplify the problem, the LCOE calculations in this table omit the financial load cost, discount rate, O&M costs and insurance costs [3].)

hydrogenation, and Si/perovskite tandem cells, etc.

3. Module efficiency improvement, including half-cell size modules, high-density modules with 1/3, 1/4, 1/5, 1/6 cell sizes, optical engineering of the modules, and Si/CdTe/perovskite tandem modules.

4. Material cost saving: diamond wire with 35μm diameter using new metal materials, thinner wafers of 100μm thickness, as well as kerf-less direct wafers, etc.

5. Special modules that are designed for different applications, especially for different locations or different climates.

6. Last, but not least, the reduction of O&M, insurance and financial costs is crucial for LCOE reduction.

Because of the limitation on solar cell efficiency, however, the improvements that are seen in the semiconductor or software industries by an order of magnitude (i.e. 10 times better) are not possible in the solar industry. Since solar energy is all about cost, it is still necessary to use a one-stone-three-bird approach for reducing the LCOE. The good news is, most solar technologies are compatible with each other: for example, the WGG module is well suited to PERC, half cells, n-type cells, and bifacial cells (white only in between the cells), as well as to high voltages of 1,500–3,000V. Given this, the authors believe that the one-stone-three-bird WGG module should prove superior in the near future.

References

[1] Jaeger-Waldau, A. 2016, PV Status Report 2016 [http://publications.jrc.ec.europa.eu/repository/handle/JRC103426].

[2] SERIS 2017, "Solar economics handbook" [http://www.solar-repository.sg/solar-economics-handbook/].

[3] SERIS 2017, "LCOE calculator" [http://www.solar-repository.sg/lcoe-calculator/].

[4] IEC 61724:1998 (Edition 1.0, withdrawn), "Photovoltaic system performance monitoring – Guidelines for measurement, data exchange and analysis" (replaced by IEC TS 61724-3:2016, IEC TS 61724-2:2016, IEC 61724-1:2017).

[5] Reich, N.H. et al. 2011, "Performance ratio revisited: Are PR>90% realistic?", *Proc. 26th EU PVSEC*, Hamburg, Germany.

[6] Nobre, A. et al. 2012, "High performing system for tropical regions – Optimization of system performance", *Proc. 27th EU PVSEC*, Frankfurt, Germany, pp. 3763–3769.

[7] Huang, Q. 2017, "The high efficiency twin-cells and white-glass-glass modules", Technical forum for solar top-runner program of Chinese solar industry (Feb.), Zhangjiakou, China.

[8] Wang, H. 2017, "The high efficiency PERC bi-facial glass-glass module", Technical forum for top-runner program of Chinese solar industry (Feb.), Zhangjiakou, China.

[9] Cheng, D. et al. 2017, "The building of 1GW agricultural solar project by GCL", Forum on standards and technologies for agricultural solar applications (Feb.), Beijing, China.

About the Authors

Dr. Qiang Huang is vice president of solar BU for GCL System Integration. Prior to joining GCL, he was vice president at Trina Solar for seven years, and a founding director of State Key Laboratories. He also spent seven years working in semiconductors, mainly at TSMC, and holds a Ph.D. from the National University of Singapore.

Li Xinchang received his bachelor's in automation instrumentation from the University of Shanghai for Science and Technology, and his MBA from Southeast University, China. He is currently a senior module product manager at GCL.

Enquiries

Qiang Huang
Solar BU, GCL System integration Technology Co., Ltd
288#Chenfeng Road, Zhangjiagang
Jiangsu, PR China 215600

Tel: +86 512-5537-8399
Email: huangqiang@gclsi.com

Market Watch

Fab & Facilities

Materials

Cell Processing

Thin Film

PV Modules

Cell modifications for preventing potential-induced degradation in c-Si PV systems

Gaby Janssen[1], **Maciej Stodolny**[1], **Bas Van Aken**[1], **Jochen Löffler**[1], **Hongna Ma**[2], **Dongsheng Zhang**[2] & **Jinchao Shi**[2]

[1]ECN Solar Energy, Petten, The Netherlands; [2]Yingli Green Energy, Baoding, China

ABSTRACT

Potential-induced degradation (PID) in modules is a serious reliability issue for large PV systems. For commercial modules incorporating p-type cells, it has been established that local shunts in the cell are responsible for the degradation. In the case of modules with n-PERT (passivated emitter, rear totally diffused) cells, it has been predicted (and recently confirmed on a laboratory scale) that a different form of PID can occur, i.e. PID by surface polarization. The latest research at ECN has demonstrated the prerequisites for PID-stable n-PERT modules. The susceptibility to PID of n-PERT cells can be drastically reduced by modifications at the cell level, in particular to the anti-reflection coating. In this paper the mechanisms of PID in p-type and n-type cells are compared, as well as mitigation or prevention strategies, which can be either generic or specific to one of the mechanisms. In the concluding section, the implications for other cell architectures based on c-Si are also considered.

Introduction

In recent years, potential-induced degradation (PID) has been recognized as a serious reliability issue for large PV systems, potentially causing efficiency losses of more than 90%, and even failures [1–4]. Such large decreases in efficiency may require the modules in the system to be replaced after just a few years' operation. This has motivated a substantial research effort in the PV community, leading to a better understanding of the phenomenon, as well as to a range of mitigation strategies. A recent publication by Luo et al. gives a comprehensive overview of this research [5].

> "The prevalent degradation mechanism for industrial cells at a negative voltage bias has been found to be the deposition of Na atoms in the front-side emitter of the cell."

PID is caused by a leakage current that is the result of a voltage difference between the frame of a module and the cells it contains. Manifestations of PID are dependent on the sign of the voltage bias, as well as on the cell architecture. The prevalent degradation mechanism for industrial cells at a negative voltage bias has been found to be the deposition of sodium (Na) atoms in the front-side emitter of the cell, resulting in local shunts and a loss in fill factor (*FF*) [6,7]; this mechanism has therefore been termed *PID-s*. Preventive measures against PID-s consist of modifications at the system, module or cell level, mostly aiming to avoid the drift of Na^+ ions into the cell [2,8].

Unlike modules incorporating conventional industrial cells, however, little attention has been paid to PID in modules containing next-generation types of c-Si cell, such as n-PERT (passivated emitter, rear totally diffused) or IBC (interdigitated back contact) cells. Nevertheless, PID in modules with n-type IBC cells at a positive voltage bias has already been reported by SunPower in 2005 [9]; in the same paper it was predicted that n-PERT cells would also be susceptible to PID. Also motivated by recent reports in the literature [10–13], ECN therefore conducted investigations of PID of its bifacial n-Pasha cells, which are mass-produced by Yingli under the Panda brand name [14].

ECN's results confirmed the findings of SunPower and others that the prevalent mechanism for PID in n-PERT cells is surface polarization, a mechanism termed *PID-p* that does not involve sodium atoms [9,10,12,15,16]. At the cell level this degradation predominantly exhibits reductions in short-circuit current density (J_{sc}) and open-circuit voltage (V_{oc}), rather than a decrease in *FF*. In the research carried out at ECN, it was found that PID-p is strongly dependent on the anti-reflection (AR) coating, consisting of non-stoichiometric SiN_x. By using a stack of SiN_x layers instead of a uniform layer, PID-p can be virtually eliminated in n-PERT cells [15,16]. Such modifications do not compromise the AR or passivation properties of the coating.

On the basis of the difference in PID mechanisms, it was also expected that PID might be easier to deal with, or more easily prevented, in systems with n-PERT cells than in systems with industrial p-type cells, including passivated emitter rear cell (PERC) devices. The following sections will first summarize some experimental findings with p-type and n-type modules in the field, as well as giving an outline of PID test methods and their relation to field observations. The mechanisms of PID in both p-type and n-type cells will then be presented and compared, and respective mitigation strategies discussed. The focus will be on modifications for preventing PID that can be made at the cell level.

PID in systems and modules

Observations of PID in the field

Swanson and co-workers from SunPower reported one of the first cases of loss of power in fieldmounted modules in Germany, after only a few months of operation [9]. Interestingly, the degradation seemed to be dependent on the location in the module string, with modules at the highest, positive voltage end of the strings exhibiting the highest degradation rates by far.

PID is observed more often, and is more severe, in locations with high temperatures and high humidity, such as Singapore and Florida, than in drier or cooler places, such as Andalusia, Spain, and Berlin, Germany. On a smaller scale, it has also been observed that PID is more likely to occur near the sea, where salt is present and the humidity is higher.

PID can affect all solar cells in a module, but in the field a distinction is made between *surface* PID and *frame* PID [17]. This distinguishes PID-affected modules on the basis of the degradation pattern: either a selection of cells is degraded in a 'random' pattern, or the degradation occurs mostly, or even solely, in those cells on the outside of the solar panel, in particular the bottom row of cells. As the name implies, frame PID occurs near the edges of the module; it is promoted by a higher conductivity near the bottom edge of the module due to dirt accumulation, which accelerates the degradation of the bottom row of cells relative to the other cells. Alternatively, PID can occur under dry conditions, but only near the four edges of the module. As a result of low humidity, leakage current pathways between the frame and the cells will only be possible close to the frame of the module.

Not only have PV modules been reported to show degradation in the field, but also their recovery has been observed. Hacke (NREL) showed that PID-susceptible p-type modules placed outdoors in Florida at –600V during the daytime exhibited a large power loss of the order of 10 to 30% between July and October; subsequently, between January and April, all of these modules demonstrated a certain amount of recovery [18]. LG reported on the recovery in n-type modules which can take place during a normal day–night sequence [11]; in that paper LG claim that under conditions of strong illumination, i.e. 1000W/m^2, the leakage current is suppressed, and that this prevents the polarization of the cell surface.

Origin and possible limitations of the voltage bias

In a PV array with string inverters the solar panels are connected in series, building up voltage along the string.

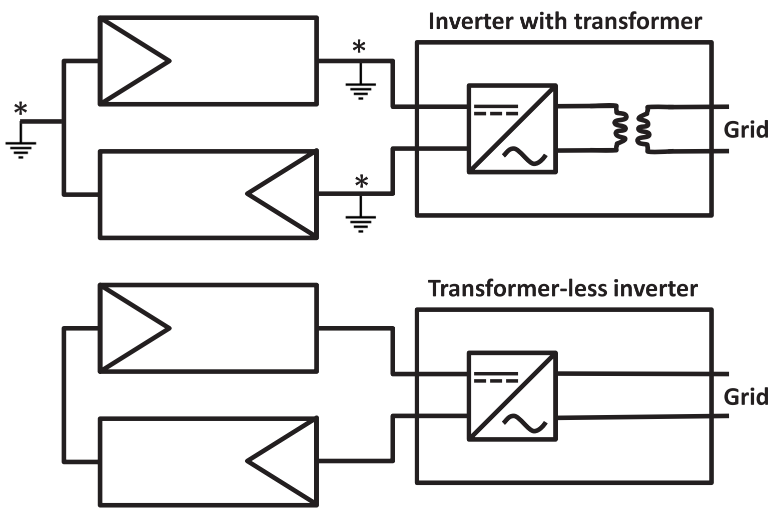

Figure 1. Schematic of a PV system incorporating an inverter with a transformer (top) and a transformer-less inverter (bottom). The locations indicated with an asterisk and a grounding symbol can be selected (one per circuit) for grounding the circuit of the PV system.

A distinction must be made between inverters with transformers and transformer-less inverters that have been coming on the market in recent years. In systems with transformers (Fig. 1, top), there is a galvanic separation between the solar panels and the electricity grid; therefore, one can ground the electric circuit of the PV system at one point, e.g. one of the two poles of the system-side of the inverter. In systems with transformer-less inverters, there is a continuous conducting path from the electricity grid via the inverter and the cabling to the solar cells (Fig. 1, bottom). Grounding a system with transformer-less inverters is no longer possible, as this would lead to a short circuit between the grid and the ground.

In the initial findings reported by SunPower with regard to degradation induced by a positive system voltage, an obvious solution was already indicated. By grounding a PV system that includes an inverter with a transformer, on the positive pole of the DC side of the inverter, the system voltage for all modules in the entire string can only be negative with respect to ground [9]. Similarly, for commercial p-type modules, where degradation occurs in modules at a negative voltage, grounding the system at the negative pole will be an effective preventative measure.

The above mitigation strategy has the disadvantage that it halves the allowed number of modules in a string, as one of the two polarities is out of bounds; it also relies on the system installer (who might install p-type modules one day and n-type modules the next) to ground the system at the appropriate pole. Furthermore, with the emergence of transformer-less inverters, because of their better DC to AC conversion efficiency, this strategy is no longer available.

PID testing and relation to real-life data

The IEC standard 62804-1 has been developed over the past few years as a qualification test for modules. The PID is accelerated at 60° and 85% relative humidity (RH) by applying the maximum intended system voltage, often 1000V, with the appropriate sign(s), for 96h. The voltage is applied between the module frame and the shorted solar cells of the panel. For frameless modules, the voltage is distributed over the front of the solar panel via an Al foil. A pass or fail of the test will be assigned on the basis of the criterion that there is a power loss of less than 5% after 96h under these conditions.

For R&D purposes it is highly desirable to know not just whether the module is susceptible to PID, but also how fast the PID progresses with time. In addition to the qualification test, the progression of PID can be monitored, for example by measuring dark I–V or R_{shunt} (in the dark) at regular intervals during PID exposure or by measuring I–V

curves under illumination at fixed time intervals, such as every 20h. Moreover, to test the PID susceptibility of the cell, single-cell modules are often used.

At the Fraunhofer Centre for Silicon Photovoltaics (CSP) a device that exposes solar cells to PID-like conditions has been developed without the need for encapsulation of the solar cells or for placing the cells in a climate chamber [7].

Data exist in the public domain for PV modules that have been degraded in accelerated PID tests and have been exposed outdoors at high voltage. This enables a connection to be made between the degradation rate indoors and the expected degradation rate outdoors. NREL has published data that show a power loss of 10–20% after around four months during spring and summer in Florida, when −1000V was applied during daytime hours. The same modules exhibited a power loss of approximately twice as much, i.e. 35%, after 60°C/85% RH/−1000V/96h when tested indoors. On the assumption of linear degradation rates, a module that would just pass the IEC standard test would have a degradation rate that is one-seventh that of this module; this corresponds to an extrapolated power loss of between 10 and 20% of its nameplate power after 28 months in Florida [18].

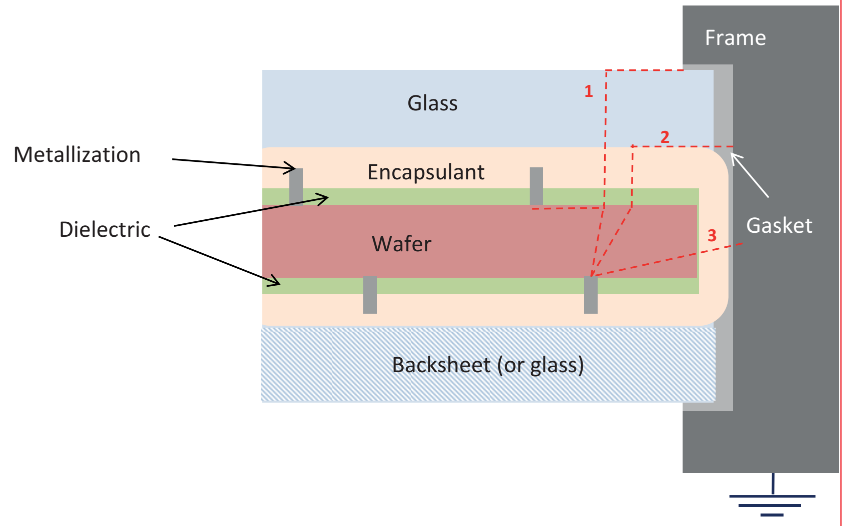

Figure 2. Schematic showing possible leakage current paths (dashed red lines) between the metallization of the cell and the grounded frame (not to scale).

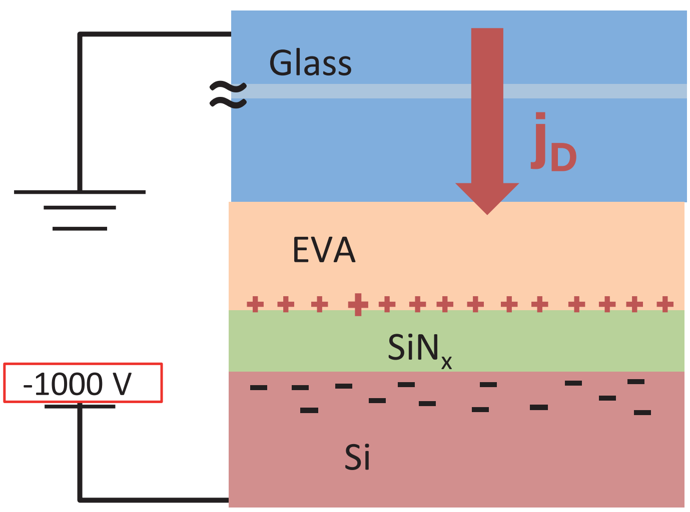

Figure 3. 1D schematic of leakage current at a negative cell bias.

Mechanisms of PID in cells

Root cause of PID: the leakage current

For both PID-p and PID-s the leakage current that arises between the grounded frame and the cell under voltage bias conditions has been identified as the root cause of degradation. Fig. 2 shows several pathways of this leakage current from the frame to the biased cell. In the lateral direction, the pathway along the front glass surface ('1' in Fig. 2) will be favoured, especially in high-humidity conditions, as will the pathway between the encapsulant and the glass ('2' in Fig. 2) [19]. The backsheet usually has a very high resistivity, and the leakage current through the rear of the module will therefore be small.

> "For both PID-p and PID-s the leakage current that arises between the grounded frame and the cell under voltage bias conditions has been identified as the root cause of degradation."

To reach the metallization of the cell, which carries the voltage bias, the current also needs to have a transverse component. This transverse component will not be uniform over the cell area, but it will be present in the sections between the metallization lines, as the doped Si wafer has a high conductivity and can therefore carry current in the lateral direction ('1' in Fig. 2). The transverse leakage current is thought to be responsible for the loss of efficiency in the cells.

Often a simplified 1D scheme like the one shown in Fig. 3 is used to explain the degradation. To reach the cell, the leakage current has to pass the glass, the encapsulant (usually EVA) and a dielectric layer, the AR coating. The local leakage current j_D is the result of the total voltage bias and the resistivity and thickness of these materials. The glass (4mm) and EVA (200µm) are orders of magnitude thicker than the SiN_x coating (only 70nm); hence, the leakage current is mostly determined by the resistivity and thickness of the encapsulant and the glass. The resistivity of both glass and encapsulant strongly depends on temperature and humidity, which means that in PID test conditions the actual local leakage current density is higher than that in most outdoors conditions. Swanson reported a value of 0.6nA.cm^{-2}, while others have reported typical values during testing of up to 10nA.cm^{-2} [9,19]. The voltage drop over the dielectric is of the order of a few volts.

In order for the leakage current to pass through the highly resistive

inter solar
connecting solar business

2,600 EXHIBITORS, 91,000 VISITORS, 6,400 CONFERENCE ATTENDEES, 720 SPEAKERS, 80 PARTNERS AND 165 MEDIA PARTNERS ARE PLACING THEIR TRUST IN US WORLDWIDE.

JOIN THE WORLD'S LEADING EXHIBITION SERIES FOR THE SOLAR INDUSTRY

INTERSOLAR EUROPE
MUNICH, MAY 31–JUNE 2, 2017

INTERSOLAR NORTH AMERICA
SAN FRANCISCO, JULY 11–13, 2017

INTERSOLAR SOUTH AMERICA
SÃO PAULO, AUGUST 22–24, 2017

INTERSOLAR MIDDLE EAST
CONRAD DUBAI, SEPTEMBER 26–27, 2017

INTERSOLAR INDIA
MUMBAI, DECEMBER 5–7, 2017

INTERSOLAR SUMMITS
WORLDWIDE

www.intersolarglobal.com

FOLLOW US

dielectric layer, a large electric field is required. This field will be provided by the accumulation of charges at the interface of the dielectric and the encapsulant; these charges are mirrored by opposing induced charges at the surface of the silicon wafer. There has so far been no discussion of the nature of the accumulated charges or of the species forming the leakage current. In the case of a positive voltage bias, the current and the charges will be electronic in nature; however, a complication arises when the voltage bias is negative, as metal ions (Na^+ ions in particular) are also mobile in the system. The Na^+ ions can originate from the glass (often soda-lime glass is used), or from contaminations of the SiN_x surface or from out of the SiN_x bulk. Both the accumulated charges as well as the leakage current itself can consist of Na^+ ions. In the following sections it will be explained that Na plays a major role in the PID-s mechanism, whereas it is not relevant in the case of PID-p.

Shunting in industrial p-type cells

A negative voltage bias of the cell relative to the frame causes an electric field in the direction of the wafer. By using time-of-flight secondary ion mass spectrometry (TOF-SIMS), high-resolution transmission electron microscopy (TEM) and energy-dispersive X-ray spectroscopy (EDX), Naumann et al. at Fraunhofer CSP have shown that, during PID tests on industrial cells with an n^+-emitter, Na^+ ions drift through the dielectric layer [6]. In the n^+ emitter the Na^+ ions are reduced by the free electrons, and Na atoms then decorate stacking faults in the Si wafer.

The above mechanism is nicely illustrated in Fig. 4, taken from the paper by Naumann [6]. The reduction in Na^+ ions implies that they do not contribute to an opposing charge at the bottom of the dielectric layer, i.e. the drift of Na^+ ions is continued. The Na atoms can thermally diffuse further along the stacking faults, which extend through the emitter into the p-type base. One resulting effect is that a semi-metallic path between the surface of the cell and the base is created, which leads to a local shunt ('process 1' in Fig. 4). A second effect is that the Na atoms form recombination centres in the p-n junction area, leading to an increased ideality factor ('process 2' in Fig. 4). Both effects have a large negative impact on *FF*, and can result in efficiency losses exceeding 90%. The group at CSP have also confirmed, by means of electron beam induced current (EBIC) and dark lock-in thermography (DLIT), the correlation between shunted regions and regions with high Na content [6,7].

Stacking faults occur intrinsically in both monocrystalline and multicrystalline material. It has been reported that these faults are also formed during $POCl_3$ diffusion (extrinsic stacking faults) [6]. It seems not to be entirely clear whether both play a role in PID; moreover, according to recent reports, stacking faults are also induced, or grow, during PID [20]. Naumann et al. attribute a special role to the thin silicon oxide (SiO_x) layer at the SiN_x/Si interface; this thin layer is supposed to facilitate thermal diffusion of Na^+ in the lateral direction, so that the Na can reach the stacking faults [6].

PID in standard PV modules is

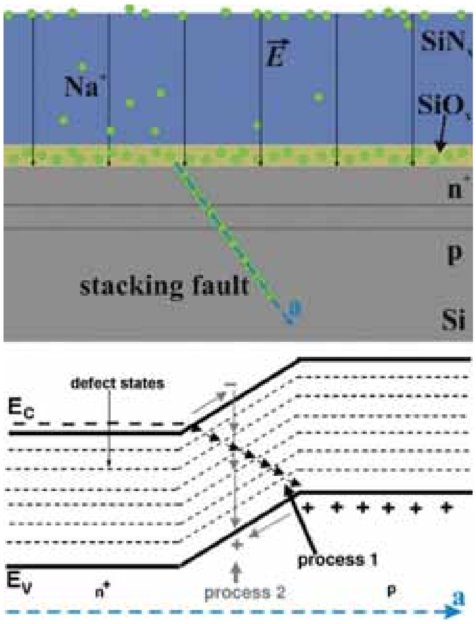

Figure 4. Schematic of a solar cell cross section. Na^+ ions drift, as a result of the dielectric field, towards the Si interface, where diffusion into stacking faults takes place. The bottom graph shows the proposed band structure along a decorated stacking fault. (Reprinted from Naumann et al. [6] with permission from Elsevier.)

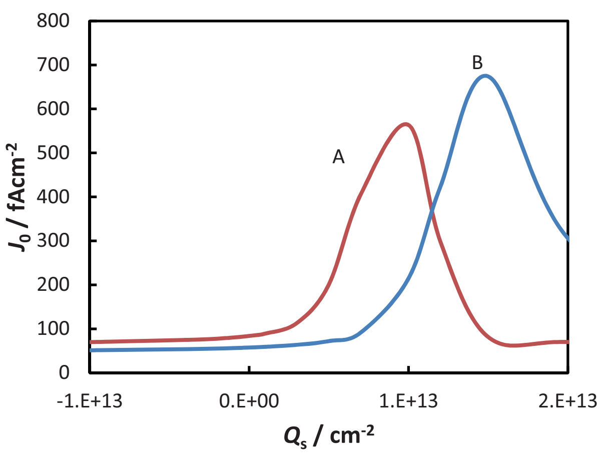

Figure 5. Calculated J_0 values of emitters A and emitter B as a function of an applied external charge Q_s. The recombination velocity *S* at the surface, for holes and electrons, was set to $2000 cm.s^{-1}$

reversible, for example by applying a reverse voltage bias, or the efficiency can be restored at elevated temperatures without a bias. [1,2,21]. Microscopy studies have shown that, after subjecting cells affected by PID-s to a reverse bias or to a thermal process at 250°C, the stacking faults become free of Na, and cell performance is restored [22]. There is still some doubt as to what may be the effect of repeated PID-s exposure/recovery sequences. There are indications that the formation of stacking faults during PID tests is not quite reversible; on the other hand, there are reports that degradation becomes less in subsequent PID tests [5].

Surface polarization of c-Si

Although PID by surface polarization has not been described in great detail in the literature, it is very relevant to next-generation cells, such as IBC and n-PERT. PID-p occurs with a positive voltage bias at n-type surfaces and with a negative bias at p-type surfaces. As pointed out in the discussion of Fig. 3, the electric field across the AR coating results in a space charge in the Si wafer; this means that, as depicted in Fig 3, at a negative voltage bias electrons are attracted to the surface, and holes are repelled from it. In the case of a p-type surface, the result is enhanced surface recombination. At a positive bias, electrons are repelled and holes are attracted, with similar detrimental surface recombination for n-type surfaces (i.e. emitter surface on p-type cells).

In the case of a dielectric with resistivity ρ and dielectric constant ε, the charge density Q seen by the Si wafer is determined by the electric field $E = Q/\varepsilon$, which is in turn determined by the leakage current according to $j_D = E/\rho$, i.e. $Q = j_D \cdot \rho \cdot \varepsilon$. After substitution of appropriate values for the resistivity and dielectric constant, it was calculated that charge density values corresponding to the observed leakage currents can become as large as 10^{12}–10^{13}cm^{-2}, and such high values will impact the surface passivation of emitters.

The effect of this surface polarization can be studied in detail by numerical simulation. Fig. 5 shows the calculations of the recombination parameter J_0 of two typical boron emitter profiles (both ~60Ω/sq.), as a function of an external charge density Q_s, i.e. producing a space charge density $-Q_s$ in the diffused region of the wafer. The total surface recombination is to a good approximation proportional to this parameter J_0. Emitters A and B were both formed in the same diffusion process; in the case of emitter B, however, the 30nm-wide boron depletion zone had been etched way, leading to a higher surface concentration. At a negative external Q_s, holes are attracted to the surface, and surface recombination is actually reduced compared with the zero-charge case. But as Q_s becomes more and more positive, J_0 increases steeply, until it reaches a maximum at the charge density for which the concentrations of holes and electrons are equal. At an even higher charge density, the situation arises that the concentration of holes at the surface is lower than that of electrons, which again leads to improved passivation conditions. Because of the higher surface concentration of emitter B, a large Q_s is required in order to obtain a similar impact on J_0. The J_0 will also depend on the fundamental electron and hole recombination velocity at the surface S, which is proportional to the density of surface states D_{it}.

Numerical device simulations can also illustrate the effect of surface charges on the I–V characteristics of n-PERT cells, which resemble the n-Pasha cells of ECN. With emitter A, assuming good surface passivation, the results in Fig. 6 are obtained. For Q_s values of the order of 10^{12}–10^{13}cm^{-2}, the simulations predict a large effect on J_{sc}, a comparatively smaller but significant effect on V_{oc}, and minor changes in FF. A maximum of 16% loss in cell efficiency is predicted.

These results are in good qualitative agreement with recent experimental results obtained at the ECN laboratory, as well as with those reported by others for n-PERT cells [10,12,15,16]. For the purpose of these experiments, a uniform SiN_x layer with refractive index n = 1.97 was applied as the AR coating to ECN's n-Pasha cells. Fig. 7 demonstrates the significant effect on J_{sc} and V_{oc} of exposure to PID test conditions, thus corroborating the mechanism of enhanced surface recombination. Hara and Bae published external quantum efficiency (EQE) results confirming that the blue response of the cells is diminished [10,12]. The degradation is slower for the cell with emitter B; this is in agreement with Fig. 5, which predicts that higher values of Q_s are required for a similar impact on the J_0 of the emitter. It should be noted that, although the *FF* is not significantly affected by PID-p at the single-cell level, the situation may be different in modules where mismatches in J_{sc} and V_{oc} of cells at different positions along the string can result in module *FF* losses [5,9].

In the case of emitter A, the efficiency loss appears to reach a maximum value at a certain point during the test; this limitation is expected, because the maximum J_0 will be limited, but also because the leakage current j_D will limit the electric field. As j_D is non-uniform over the cell area, and its distribution may even change during testing, it is not possible to say what the limiting factor is in this case. In this respect, PID-p differs from PID-s, where for the latter there is a continuous increase in the amount of Na in the wafer.

In agreement with the PID-p mechanism, the results of PID tests with IBC cells also show mainly effects on J_{sc} and V_{oc}; these effects, however, can be larger than those for n-PERT cells, since IBC cells are more sensitive to front-surface recombination [23,24]. In p-type cells, where a negative bias induces PID-s, a positive bias may induce PID-p. Although there have been some observations suggesting this, it is also expected that, because of the very high surface concentrations of phosphorus emitters, large fields will be necessary in order to see an effect [9]. Since the polarization effect is essentially an electronic effect, it is entirely reversible by removing the bias or by applying a reverse bias [11].

A final question to be asked is: why do Na^+ ions not appear to play a significant role in the PID of n-PERT cells at a negative bias? No Na has ever been reported so far in the p^+

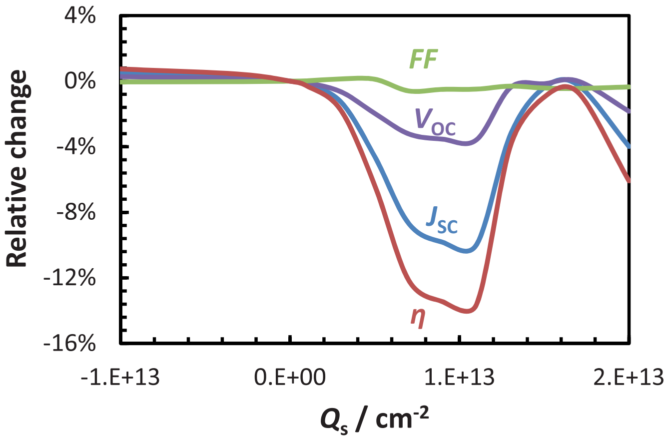

Figure 6. Relative changes in the *I–V* characteristics of an n-PERT cell with emitter A.

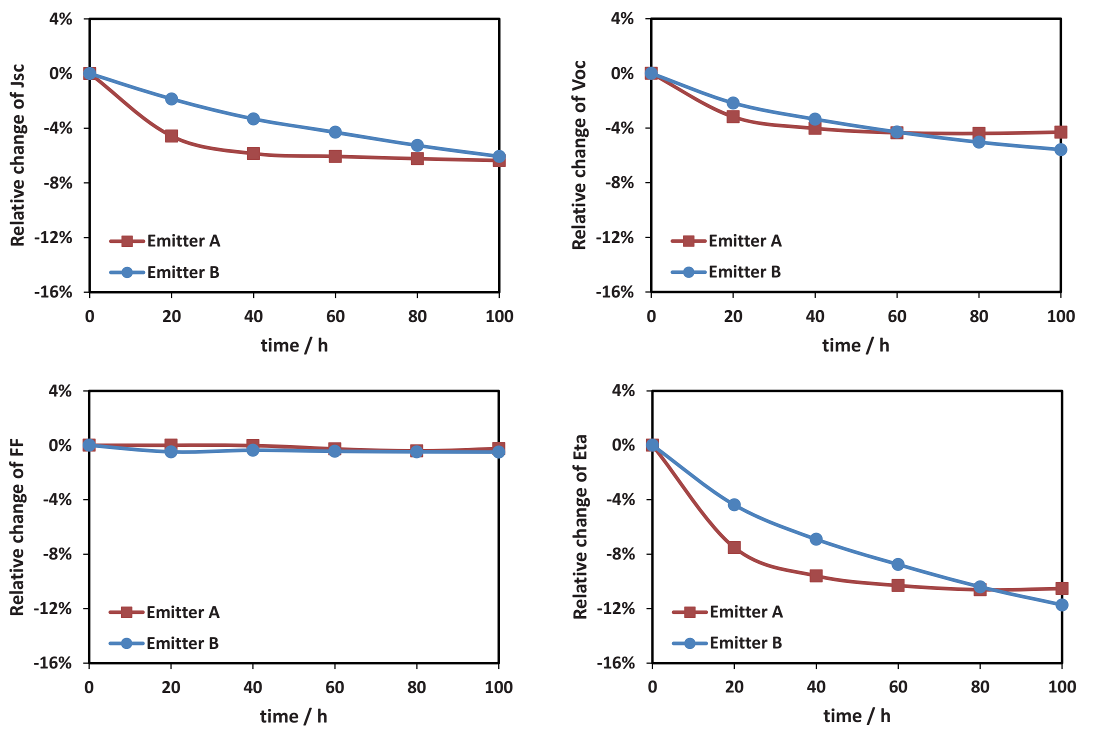

Figure 7. Time evolution of the cell parameters relative to initial values, for n-Pasha single-cell laminates (mini-modules) tested for 100h PID exposure (–1000V, 60°C, 85% RH), with a uniform *n* = 1.97 SiN_x layer on emitters A and B.

emitters after exposure to a negative bias. One explanation could be that at p^+ surfaces Na^+ cannot be reduced, and hence there is no sink for Na^+ ions [5]. Another hypothesis is that stacking faults in boron-doped material are not large enough to accommodate Na [12]. This does not imply that Na^+ cannot accumulate at the interfaces, but in steady-state conditions the Na^+ drift current will be compensated by a diffusion current in the opposite direction.

Corroborating this essential difference between n-type and p-type surfaces are the observations by Yamaguchi et al., who studied an n-PERT cell with a rear junction [25]. At a negative bias, they observed enhanced surface recombination, which cannot be due to polarization, since at a negative bias this would improve the surface passivation; instead, they proposed that Na atoms in the stacking faults form additional recombination centres. Note that, because the emitter is on the other side of the cell, these Na atoms do not cause a shunt or enhanced p-n junction recombination.

Solutions for PID

Generic solutions: reduction of the leakage current

In the earlier discussion of the root cause of PID, it was pointed out that the magnitude of the leakage current, and of the resulting electric field across the dielectric AR layer, is the root cause of PID. As previously discussed in the section on PID in systems and modules, adaptions at the system level to prevent this are costly or impractical. At the module level, however, several solutions have been suggested. These aim to reduce the leakage current by providing a higher electric resistance of the glass and/or encapsulant, which is an effective strategy, since the leakage current is determined by the glass and the encapsulant (see section on root cause of PID).

Alternative glass materials – such as quartz, borosilicate glass and aluminosilicate glass – are available which have volume resistivities that are greater by two to three orders of magnitude. With quartz as the front-side material, it is possible to completely avoid PID-s in conventional modules [26]. One reason for this enhanced resistivity is that glasses of this type contain little or no sodium, which also eliminates an important source of the Na causing PID-s. Nevertheless, a serious drawback of alternative glasses is that they add considerably to the module cost.

A more commonly adopted solution is the replacement of standard EVA with a high-resistivity encapsulant. Silicone, polyolefins and ionomers have volume resistivities of up to two orders of magnitude greater than the resistivity of EVA; moreover, the resistivity of these materials is less dependent on temperature and relative humidity, and their transmittance for visible light is similar to (or better than) that of EVA. Other considerations are mechanical strength, UV stability and adhesion, but these high-resistivity materials seem to be good candidates for replacing EVA; their capacity for reducing PID has been confirmed in several reports [8,26,27]. Again, as in the case of glass, these alternative materials come at a higher cost.

Specific solutions for reducing PID-s

Since it was already suspected at an early stage that Na ions could be the origin of the shunts in industrial cells, the incorporation of Na barriers into the module or the cell has been investigated as a solution, similarly to the Na-lean glass mentioned above. Hara et al. obtained improved PID resistance by inserting a TiO_2 foil between two layers of encapsulant [28]; however, this material results in less visible light reaching the cell, thus reducing the efficiency. Other attempts, including a SiO_2 layer adjacent to the glass, have proved less effective, with similar light absorption losses [26].

It has been widely reported that modifications of the dielectric stack can be effective in reducing PID-s [6,8,29–32], in particular by using a more Si-rich nitride, which is more electronically conductive. On the one hand, this may provide a lateral path for the current to the metal grid, thus by-passing the wafer (see Fig. 2); but perhaps more importantly, it would imply that the transverse degradation current in that layer would be made up more of electronic charges than of Na^+ ions. Indeed, as formulated by Luo et al., the electric field experienced by the Na^+ ions becomes smaller, and hence their flux becomes smaller [5]. The Si-rich, conductive layer, however, will also have a higher refractive index with higher light absorption. To overcome this drawback, Mishina et al. proposed a multilayer SiN_x coating, with the outer, or upper, layer having a low refractive index [31], which resulted in cells with both higher PID resistance and higher initial efficiency.

On the other hand, there have been several reports claiming that the insertion of a SiO_2 or an oxide-rich SiN_x with higher conductivity between the Si wafer and the AR coating provides an efficient Na^+ barrier or Na^+ trapping layer [8,33,34]. The role of the thickness of this layer, as well as its long-term PID resistance, is still a point of debate [5].

Specific solutions for reducing PID-p

PID-p is essentially a surface recombination phenomenon. A logical assumption would therefore be that a reduction of the surface recombination parameters S, i.e. a reduction of D_{it}, would reduce PID-p. Although this is probably true for exceptionally low values of S, according to Fig. 5 a very large J_0 can occur in depletion conditions, even if the S is as low as 2,000cm.s^{-1}, a value lower than that obtained for the 'excellently' passivated boron surfaces [35]. Hence, better surface passivation achieved either by improved S or by increased surface concentration will just slow down the PID but not limit it. A similar result was found at the ECN laboratory, with only a 5% efficiency loss in the 96h PID test after the insertion of a 6nm AlO_x layer between the wafer and the uniform AR layer [16]. While such improvements may in practice be acceptable (e.g. in field conditions where PID only occurs in the morning, which is later reversed when conditions are much drier), they will not always be deemed sufficiently robust.

> “The best prevention strategy for PID-p is the application of non-uniform AR coatings”

The best prevention strategy for PID-p, however, is the application of non-uniform AR coatings [15,16]. Fig. 8 shows the degradation of the n-Pasha cell with emitter A (also shown in Fig. 7). When the 70nm dielectric SiN_x (refractive index n = 1.97) was replaced with a stack of two layers, namely a SiN_x layer of 54nm on top (n = 1.97) and a more conductive 18nm SiN_x layer (n = 2.44) on the bottom (i.e. adjacent to the wafer), a much less pronounced and limited PID was observed. This can be explained by the reduction in the electric field over the more conductive Si-rich layer, and hence the reduction in polarization charge seen by the Si wafer, even when the total leakage current is the same. As explained earlier, the relation between polarization charge Q and leakage current j_D is $Q = j_D \cdot \rho \cdot \varepsilon$. Of course, the Si-rich layer may also result in lower

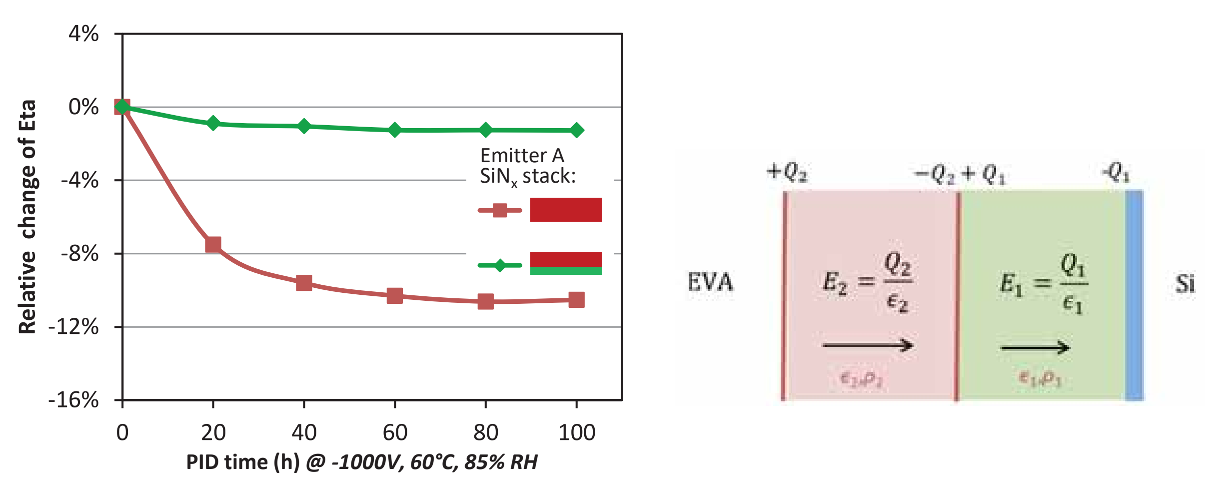

Figure 8. The graph on the left shows that an n-Pasha cell was made PID-resistant by replacing the uniform dielectric coating (red line) by a two-layer stack with a Si-rich conductive layer on the bottom (green line). The equations on the right explain how this improvement is brought about. In the uniform layer with resistivity ρ_2, the wafer would see the charge Q_2, associated with the electric field E_2. By inserting a layer with lower resistivity ρ_1 next to the wafer, a smaller field E_1 is needed to let the current j_D pass, which means that the wafer sees a smaller charge, i.e. Q_1.

D_{it} but, as already indicated in the section on surface polarization of c-Si, this will not be sufficient to limit PID.

In addition, for PID-p the order matters in which the layers with different conductivity are positioned in the dielectric stack. Fig. 9 shows a comparison, for the n-PERT cell with emitter B, of the cases where the more conductive Si-rich layer is adjacent to the wafer, on top, or in the middle of a three-layer stack. In the first case, a minimal and stable efficiency loss can again be seen; in the other two cases, however, a substantial loss is evident. There might be some mitigation in these cases because of a lateral current, but when a more resistive layer is placed adjacent to the Si wafer, then PID is clearly increased. This can be explained using the expressions on the right of the graph in Fig. 8: when the resistivity of the layer adjacent to the Si wafer is higher, the electric field over the layer is higher, and thus the charge Q_1 is now larger than Q_2, resulting in more surface recombination.

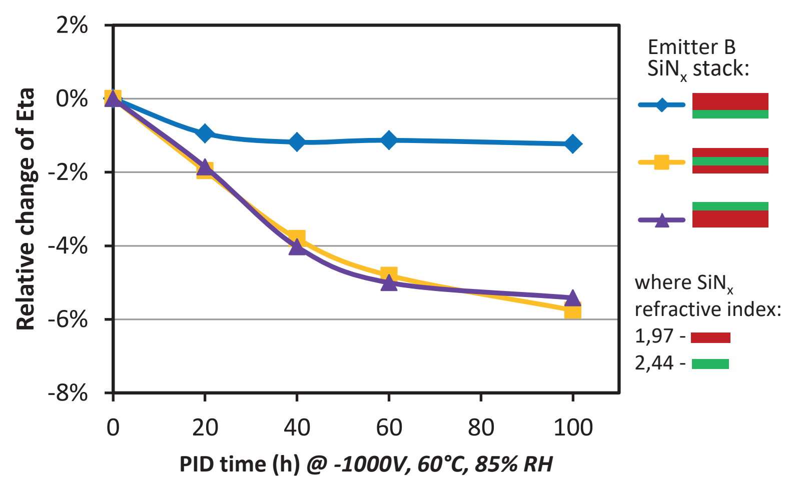

Figure 9. Layer positioning comparison, showing that a PID-resistant cell is only obtained when the Si-rich conductive layer is placed adjacent to the cell. In the other cases, significant degradation is still observed during PID testing.

The mechanism given here is based on ohmic charge transport, which is probably not applicable for very thin oxide layers, where charge transport will take place by tunnelling or through pinholes that have a low resistivity. For charge transport through such layers, the electric field, and hence the required interfacial charge density, will be much smaller. In fact, in all ECN's n-PERT cells, a very thin (~1.5nm) passivating SiO_x layer was formed on the emitter by wet chemical oxidation (NAOS) [36]; however, as shown by the results in Figs. 8 and 9, such a layer does not induce PID. Similarly, PID-resistant n-PERT cells were created at the ECN laboratory using a 6nm AlO_x passivation layer between the emitter and the Si-rich conductive layer of the AR stack [16].

As also pointed out by Mishina [31], the introduction of a thin Si-rich conductive layer next to the Si wafer will not lead to more parasitic absorption when the top layer has a refractive index $n < 2$. The passivation of the cell is even improved by this layer, rather than degraded. Besides providing PID resistance already at the cell level, the described modification of the AR coating requires only minor changes to the standard plasma-enhanced chemical vapour deposition (PECVD) method of SiN_x deposition, and therefore represents a high-throughput, cost-effective solution.

Concluding remarks

As the understanding of PID in c-Si increases, it becomes clear that different mechanisms of PID can apply. In industrial p-type cells the n^+

emitter can be shunted by Na atoms (PID-s), leading to drastic reductions in *FF* and thus in output power. The Na^+ transport is driven by the electric field and Na deposits in stacking faults, thus providing a sink for Na^+ ions which facilitates a continuous Na^+ migration. It must be expected that PERC cells will be similarly affected.

In contrast, cell types based on n-type material are susceptible to PID by surface polarization (PID-p), which manifests itself at the cell level not by a loss in *FF* but by losses in J_{sc} and V_{oc}. At a positive voltage bias, n^+-type surfaces are affected by PID, whereas at a negative bias, p^+-type surfaces are affected. This mechanism does not involve Na ions but only electronic charges, and can therefore show recovery when field conditions change [11]. Moreover, the polarization effect seems to be limited, as it is the magnitude of the leakage current, rather than the accumulated leakage current, that is responsible for the efficiency loss.

The fact that PID-p can occur at both polarities has implications for cells in bifacial modules. Bifacial modules are mostly glass/glass modules, and the cells do not have a fully metallized rear; the rear side may therefore also experience a leakage current and be susceptible to PID. At a negative voltage bias, the direction of the electric field is such that it would reduce surface recombination at the rear of n-PERT cells, but this may be offset by the deposition of Na in the n^+ layer, providing additional recombination centres. At a positive bias the rear will have adverse surface polarization. For PERC+ cells at a negative bias, shunting of the emitter must be expected, as well as enhanced surface recombination at the rear. At a positive bias, the front of PERC+ cells is susceptible to surface polarization.

A better understanding of the mechanisms has promoted solutions at the cell level, in addition to the more expensive solutions that already exist at the system and module levels. Both PID-s and PID-p can be suppressed by modification of the AR coating. As demonstrated here for n-PERT cells, when a multilayer stack with a conductive layer next to the Si wafer is used the polarization effect can be effectively suppressed, resulting in only a 1% degradation over 100h of accelerated PID testing. The literature data suggest that this method is also effective in significantly reducing Na^+ transport to stacking faults in n^+-type regions. The AR and passivation properties of the stack are similar to, or better than, those of a single-layer coating. These cell modifications are easy to implement in the manufacturing process and are therefore cost-effective. Note, however, that although the proposed methods appear to be effective in a laboratory setting, they still need to be proved in field tests.

"The PID-p effect in n-PERT cells can be slowed down by better passivation of the boron emitter."

Another finding at ECN is that the PID-p effect in n-PERT cells can be slowed down by better passivation of the boron emitter. In practice, this may be a useful consequence, since PID-p shows fast recovery, and effects such as high humidity that induce PID-p seem to occur only during part of the day. In fact, this has motivated LG to advocate a module warranty test which includes the recovery behaviour [11]. Furthermore, it must be expected that advanced cell c-Si technologies have very effectively passivated surfaces. Although heterojunction (HJ) cells have been reported to exhibit minimal PID [37], they, as well as other advanced concepts, often feature a TCO layer, which can be susceptible to electrochemical corrosion [5].

References

[1] Berghold, J. et al. 2009, "Potential induced degradation of solar cells and panels", *Proc. 24th EU PVSEC*, Hamburg, Germany, pp. 3753–3759.

[2] Pingel, S. et al. 2010, "Potential induced degradation of solar cells and panels", *Proc. 35th IEEE PVSC*, Honolulu, Hawaii, USA, pp. 002817.

[3] Hacke, P. et al. 2011, "System voltage potential-induced degradation mechanisms in PV modules and methods for test", *Proc. 37th IEEE PVSC*, Seattle, Washington, USA, pp. 000814.

[4] Schneller, E., Shiradkar, N.S. & Dhere, N.G. 2014, "Performance variation of commercially available modules after six months of outdoor system voltage stress testing", *Proc. 40th IEEE PVSC*, Denver, Colorado, USA, pp. 3216.

[5] Luo, W. et al. 2017, "Potential-induced degradation in photovoltaic modules: A critical review", *Energy & Env. Sci.*, Vol. 10, pp. 43.

[6] Naumann, V. et al. 2014, "Explanation of potential-induced degradation of the shunting type by Na decoration of stacking faults in Si solar cells", *Sol. Energy Mater. Sol. Cells*, Vol. 120, pp. 383–389.

[7] Lausch, D. et al. 2014, "Potential-induced degradation (PID): Introduction of a novel test approach and explanation of increased depletion region recombination", *IEEE J. Photovolt.*, Vol. 4, p. 834.

[8] Nagel, H., Metz, A. & Wangemann, K. 2011, "Crystalline Si solar cells and modules featuring excellent stability against potential-induced degradation", *Proc. 26th EU PVSEC*, Hamburg, Germany, pp. 3107–3112.

[9] Swanson, R. et al. 2005, "The surface polarization effect in high-efficiency silicon solar cells", *Proc. 15th Asian PVSEC*, Shanghai, China, pp. 410–411.

[10] Hara, K., Jonai, S. & Masuda, A. 2015, "Potential-induced degradation in photovoltaic modules based on n-type single crystalline Si solar cells", *Sol. Energy Mater. Sol. Cells*, Vol. 140, pp. 361–365.

[11] Kang, K. et al. 2016, "Lifetime warranty test method considering potential induced degradation", *Proc. 32nd EU PVSEC*, Munich, Germany.

[12] Bae, S. et al. 2017, "Potential induced degradation of n-type crystalline silicon solar cells with p^+ front junction", *Energy Sci. Eng.*, Vol. 5, pp. 30–37.

[13] Barbato, M. et al. 2016, "Durability of bifacial solar modules under potential induced degradation: Role of the encapsulation materials", *Proc. 32nd EU PVSEC*, Munich, Germany.

[14] Romijn, I.G. et al. 2013, "Cost effective n-Pasha solar cells with efficiency above 20%", *Photovoltaics International*, 20th edn, pp. 33–40.

[15] Stodolny, M.K. et al. 2016, "PID- and UVID-free n-type solar cells and modules", *Energy Procedia*, Vol. 92, pp. 609–616.

[16] Janssen, G.J.M. et al. 2017, "Minimizing the polarization-type potential-induced degradation in PV modules by cell modifications", *Proc. 7th SiliconPV*, Freiburg, Germany.

[17] Berghold, J. et al. 2015, "PID: From material properties to outdoor performance and quality control counter measures", *Proc. SPIE 9563: Reliab. PV Cells,*

Bifacial Workshop 2017

4th edition of bifiPV
Come and create the PV future with us!

REGISTER NOW!
www.bifiPV-workshop.com

October 25-26, 2017 | Konstanz | Germany

- Sessions on: systems and bankability, cell and module technology, standardization, simulation
- Experts from academy and industry discuss the latest developments
- Podium discussions and networking activities in great atmosphere

bifiPV 2017 workshop takes place subsequent to the metallization WS 2017 in Konstanz. (www.metallizationworkshop.info)

media partners

Mod., Comp., and Syst. VIII, pp. 95630A–956314.
[18] Hacke, P. et al. 2014, "Development of an IEC test for crystalline silicon modules to qualify their resistance to system voltage stress", *Prog. Photovolt: Res. Appl.*, Vol. 22, p. 775.
[19] del Cueto, J.A. & McMahon, T.J. 2002, "Analysis of leakage currents in photovoltaic modules under high-voltage bias in the field", *Prog. Photovolt: Res. Appl.*, Vol. 10, pp. 15–28.
[20] Naumann, V. et al. 2016, "Investigations on the formation of stacking fault-like PID-shunts", *Energy Procedia*, Vol. 92, pp. 569–575.
[21] Pingel, S., Janke, S. & Frank, O. 2012, "Recovery methods for modules affected by potential induced degradation (PID)", *Proc. 27th EU PVSEC*, Frankfurt, Germany, pp. 3379–3383.
[22] Lausch, D. et al. 2014, "Sodium outdiffusion from stacking faults as root cause for the recovery process of potential-induced degradation (PID)", *Energy Procedia*, Vol. 55, pp. 486–493.
[23] Naumann, V. et al. 2014, "Potential-induced degradation at interdigitated back contact solar cells", *Energy Procedia*, Vol. 55, pp. 498–503.
[24] Halm, A. et al. 2015, "Potential-induced degradation for encapsulated n-type IBC solar cells with front floating emitter", *Energy Procedia*, Vol. 77, pp. 356–363.
[25] Yamaguchi, S., Masuda, A. & Ohdaira, K. 2016, "Changes in the current density-voltage and external quantum efficiency characteristics of n-type single-crystalline silicon photovoltaic modules with a rear-side emitter undergoing potential-induced degradation", *Sol. Energy Mater. Sol. Cells*, Vol. 151, pp. 113–119.
[26] Hacke, P. et al. 2011, "Characterization of multicrystalline silicon modules with system bias voltage applied in damp heat", *Proc. 25th EU PVSEC*, Valencia, Spain.
[27] López-Escalante, M.C. et al. 2016, "Polyolefin as PID-resistant encapsulant material in PV modules", *Sol. Energy Mater. Sol. Cells*, Vol. 144, pp. 691–699.
[28] Hara, K. et al. 2014, "Crystalline Si photovoltaic modules based on TiO_2-coated cover glass against potential-induced degradation", *RSC Adv.*, Vol. 4, p. 44291.
[29] Gou, X. et al. 2015, "PID testing method suitable for process control of solar cells mass production", *Int. J. Photoenergy*, Vol. 2015, pp. 1–5.
[30] Wilson, M. et al. 2013, "Importance of defect photoionization in silicon-rich SiN_x dielectrics for high PID resistance", *Proc. 39th IEEE PVSC*, Tampa, Florida, USA, pp. 0218–0222.
[31] Mishina, K. et al. 2014, "Anti-reflection coating with high PID-resistance for crystalline silicon solar cells", *Proc. 29th EU PVSEC*, Amsterdam, The Netherlands.
[32] Mishina, K. et al. 2013, "Investigation on PID-resistant anti-reflection coating for crystalline silicon solar cells", *Proc. 28th EU PVSEC*, Paris, France.
[33] Han, W. et al. 2013, "Ion implantation – An effective solution to prevent C-Si PV module PID", *Proc. 28th EU PVSEC*, Paris, France.
[34] Zhou, C. et al. 2015, "SiO_yN_x/SiN_x stack anti-reflection coating with PID-resistance for crystalline silicon solar cells", *Energy Procedia*, Vol. 77, pp. 434–439.
[35] Black, L.E. et al. 2014, "Effect of boron concentration on recombination at the p-Si-Al_2O_3 interface", *J. Appl. Phys.*, Vol. 115, p. 093707.
[36] Mihailetchi, V.D., Komatsu, Y. & Geerligs, L. J. 2008, "Nitric acid pretreatment for the passivation of boron emitters for n-type base silicon solar cells", *Appl. Phys. Lett.*, Vol. 92, pp. 063510–063513.
[37] Xiong, Z., Walsh, T.M. & Aberle, A.G. 2011, "PV module durability testing under high voltage biased damp heat conditions", *Energy Procedia*, Vol. 8, pp. 384–389.

About the Authors

Gaby Janssen obtained her Ph.D. in quantum chemistry from the University of Groningen in the Netherlands. At ECN she has been working as a research scientist on the simulation, characterization and optimization of materials for energy conversion technologies. Since 2011 she has been focusing on simulation and modelling of PV cells and modules.

Maciej Stodolny received his M.Sc. in applied physics from Gdansk University of Technology in Poland. His Ph.D. research at ECN and the University of Twente dealt with Cr tolerance of solid oxide fuel cells. He now works as a solid state physicist and materials scientist at ECN Solar Energy.

Bas Van Aken received his Ph.D. in solid state chemistry from the University of Groningen, after which he worked as a postdoc at Cambridge University and at the Max Born Institute for Nonlinear and Ultrafast Optics in Berlin. He is currently a researcher in the PV module technology group at ECN, where he focuses on fabrication, reliability and (outdoor) performance of bifacial and back-contact modules.

Jochen Löffler holds a Ph.D. in physics from Utrecht University in the Netherlands, and has been working on PV and related topics since 1998. He joined ECN in 2005 and is currently a senior scientist and project leader in the field of crystalline silicon solar cells, with a focus on industrial high-efficiency cells and modules.

Hongna Ma holds an M.Sc. and has many years' experience in silicon solar cell research. She joined Yingli in 2008 and is currently the leader of the group working on n-type Si solar cells. Her focus is on R&D of solar cells with ion implantation technology.

Dongsheng Zhang has an M.Sc. and joined Yingli in 2004, where he currently leads the battery technology department. His work experience in silicon solar cell research spans many years, and he has acquired an in-depth understanding of all aspects of the crystalline silicon solar cell process.

Jinchao Shi holds an M.Sc. and has worked in silicon solar cell and module research for many years. He joined Yingli in 2006, where he is currently the general manager of the Technology Center. He has extensive experience in lab to fab transference, as well as in cell and module mass production.

Enquiries

Email: janssen@ecn.nl

Systematic PV module optimization with the cell-to-module (CTM) analysis software

Max Mittag & **Matthieu Ebert**, Fraunhofer Institute for Solar Energy Systems ISE, Freiburg, Germany

ABSTRACT

The key to efficient and powerful modules is an optimal cell-to-module (CTM) ratio. Interconnecting solar cells and integrating them into a solar module comes along with different optical and electrical effects. A profound understanding of all factors which influence the module efficiency is essential to derive methods to decrease the losses or to increase the gains caused by module integration. Several CTM calculation methods have been published in the past, mostly not available to a wide number of users in the form of a user-friendly tool. With SmartCal.CTM Fraunhofer ISE has released a software tool available for everybody, allowing to apply the previously published CTM analysis methodology. In this work we present the methodology and the tool, and demonstrate with some case studies how the software can be used to support the module development process.

Introduction

Understanding power losses in technical systems is vital to improve products in every industry and photovoltaic modules present no exception. Losses in solar modules are caused by optical and electrical effects or are determined by simple module geometry through inactive areas [1].

The majority of solar modules contain crystalline silicon solar cells, which can be described by their respective power and efficiency. Usually power and efficiency of the assembled photovoltaic modules do not match those of the initial cells. The ratio of the final module efficiency (or power) and the initial cell efficiency (or power) is called cell-to-module (CTM) ratio and represents an indicator for the performance-tuning of the photovoltaic device.

The importance of the CTM ratio results from the costs linked to the module integration power loss. The ITRPV Roadmap 2017 [2] states a CTM power ratio for modules using alkaline textured mono-si of 98.5%, which means that for every 275Wp-module a CTM loss of more than 4Wp occurs. Using a price of US$0.25/Wp (spot price mono crystalline cells [3]) and therefore loosing US$1 per module, the losses add up to a significant amount of money – for small national module manufacturers as well as for global players. Understanding the CTM losses and reducing them or even turning them into CTM gains therefore is not an academic dalliance but a necessary task to further improve photovoltaic modules.

Gain and loss mechanisms are well known and most of them have been described in detail for common photovoltaic cell and module concepts in several publications [1, 4, 5, 6, 7, 8]. The number of software tools, scripts, methods and algorithms to describe single gain and loss factors is high [9, 10, 11, 12] and every major research institute, university or company has its own set of tools to estimate the cell-to-module-losses. Unfortunately these tools are not accessible for everyone due to their nature as internally used development resources. Scripts without user interfaces, complex Excel-files or software for experts and insiders provide instruments for CTM analysis only to a very limited group of people. It is obvious that the internal nature of these tools leads to a disadvantage for the whole solar community; a transparent comparison of results, concepts and technologies is impossible.

Hädrich et al summarized the work on cell-to-module-analysis and published a comprehensive methodology to analyze contributing gain and loss factors in 2014 [1]. In 2016, Fraunhofer presented the software "SmartCalc.CTM" (www.cell-to-module.com) based on that methodology to allow a precise, convenient and comparable CTM analysis for the entire PV community.

Figure 1. Screenshot of SmartCalc.CTM showing the result of a CTM analysis

PV Modules

The software features a user-friendly graphical user interface (GUI) with several material data input possibilities to allow a detailed CTM analysis of common and novel module and cell concepts. The GUI and the open data import both create the possibility for everyone aside from scientists or experts to perform precise analyses, to accelerate module development and to decrease costs at the same time.

The improvement of existing or the development of new module concepts or materials is an expensive task. Several materials or parameters have to be evaluated, test matrixes grow quickly and single isolated effects are rare. Thus lots of effort and prototyping is necessary to analyze the benefits and impacts of new materials, to find the important factors to focus on and to choose the right development path. SmartCalc.CTM supports the development with virtual prototyping, parameter sweeps and 'what-if' analysis. Simple changes of materials, parameters or components are possible and results only take some minutes: without the need to build a single prototype.

In an iterative development process Smartcalc.CTM saves costs by saving iterations and supporting the selection of promising development paths.

To demonstrate the possibilities of SmartCalc.CTM we improve a module by 21Wp in five simple steps from 287 to 308Wp by using SmartCalc.CTM. An analysis of the initial module is shown in Figure 1.

Software Implementation

Overview

SmartCalc.CTM is a software tool developed by Fraunhofer ISE to calculate and analyze the CTM of photovoltaic modules with crystalline solar cells. Single contributing gain and loss factors relate to physical effects (i.e. electrical resistance) and module components (i.e. interconnector ribbons). Currently 15 different factors are included in the calculation which considers geometrical, optical and electrical gains and losses as well as important module layers and components (Table 1).

Virtual prototyping and module optimization

Prototyping in R&D is expensive. Manufacturing novel modules requires planning, manual labour, complex and new processes, extensive testing, detailed result analyses, qualified personnel and – based on own practical experience – some iterations. Thus R&D prototyping is a costly endeavour and costs are likely to significantly exceed the US$0.40/Wp at which modules are being sold on the market today [2].

Car manufacturing, circuit layout design of computer chips or even architecture have profited from the possibilities of computer aided design or simulation tools (crash tests, thermal dissipation etc.). Prototypes are being virtually constructed, simulations are performed, unfeasible design options are discarded and the focus is put on the best and most promising solutions. With SmartCalc.CTM this product development approach is being enabled for photovoltaic modules.

Why build several modules to find the optimal cell spacing when you can precisely calculate it? Why stop the production and reprogram machinery just to test the potentials of 72 cells per module or 156.75mm solar cells? Simulation software and advanced scientific models allow us to answer questions before the expensive module testing begins. The possibility to change module materials, layers, properties and components with SmartCalc.CTM enables us to virtually build a module and to analyze the module power. By performing parameter sweeps focused optimization is possible.

Figure 2 includes the results of such a parameter sweep for the cell and string spacing (iterations 7 – 10). The cell distance is varied from 2 to 5mm and efficiency and power change accordingly. Variation 5 is the result of a what-if analysis. We asked what would happen if we changed the module layout from 60 to 72 cells. Variation 6 includes a new solar cell, 22% instead of 19% efficiency. In the last iteration we changed the cell design to half-cells.

If a module with more power output is desired the choice is now between three options: 72 cells, higher cell efficiency or half-cells. Simulation

k-factor	Description
Module margin k1	Inactive area at the module margin
Cell spacing k2	Inactive area between cells and strings
Cover reflection k3	Reflection of light at the front interface of the module
Cover absorption k4	Absorption of light in the front cover
Cover/encapsulant reflection k5	Reflection of light at the interface between front cover and encapsulation material
Encapsulant absorption k6	Absorption of light in the encapsulation material
Interconnection shading k7	Shading of the cell by interconnector ribbons
Cell/encapsulant coupling k8	Reduced reflection of the cell due to encapsulation (refractive index matching)
Finger coupling k9	Reflection of light from the cell metallization on the active cell area
Interconnector coupling k10	Reflection of light from the interconnector ribbons on the active cell area
Cover coupling k11	Internal reflection of light at the (rear) cover of the module in the cell spacing area
Cell interconnection k12	Electrical loss in cell interconnector ribbons
String interconnection k13	Electrical loss in cell string interconnectors
Electrical mismatch k14	Deviations in electrical cell parameters and from cell binning
Junction box and cabling k15	Electrical losses in cables and diodes of the junction box

Table 1. Single gain and loss factors of SmartCalc.CTM, loss factors are highlighted black, gains are marked green.

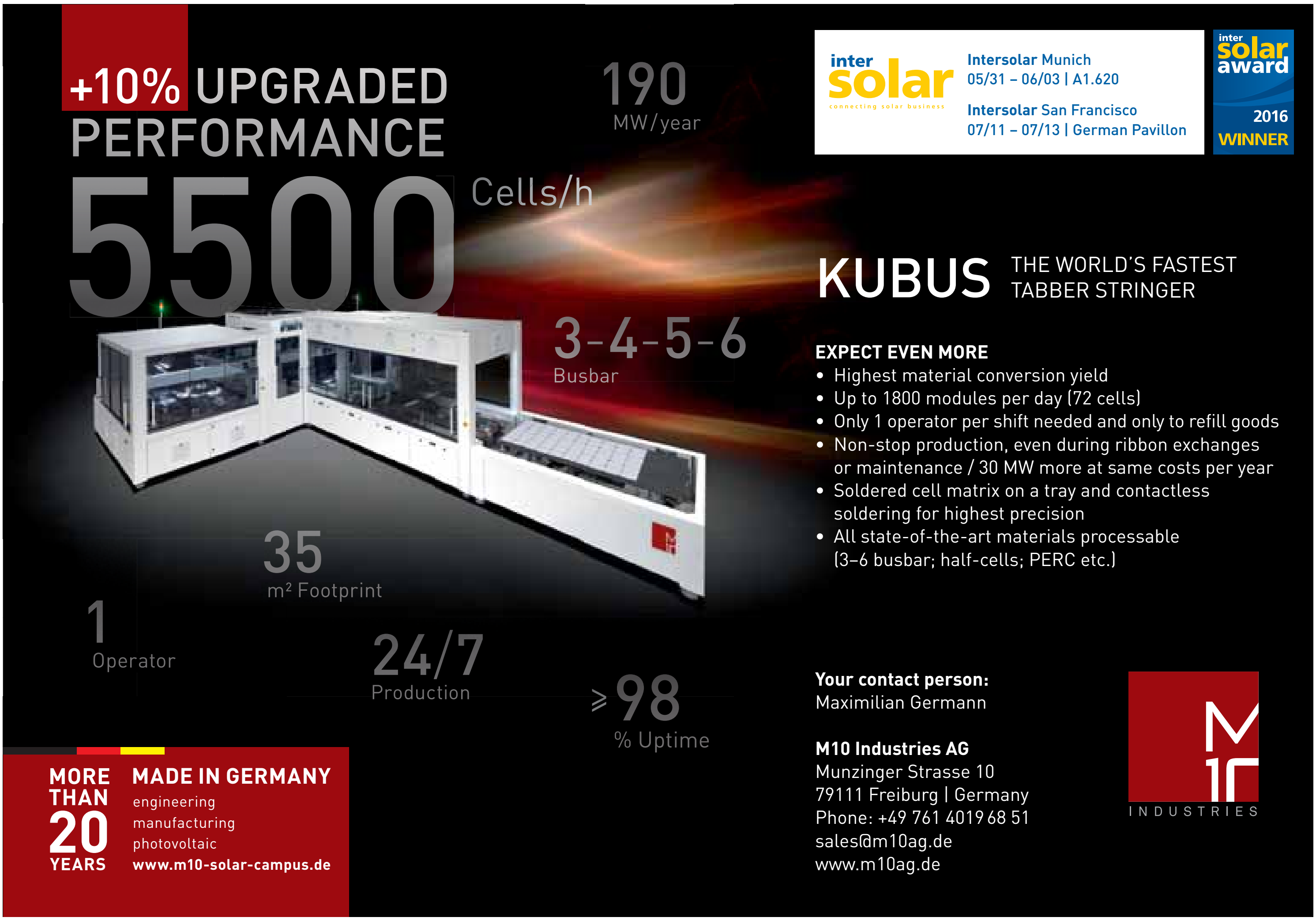

+10% UPGRADED PERFORMANCE
5500 Cells/h
190 MW/year
3-4-5-6 Busbar
35 m² Footprint
1 Operator
24/7 Production
≥98 % Uptime
inter solar connecting solar business
Intersolar Munich
05/31 – 06/03 | A1.620
Intersolar San Francisco
07/11 – 07/13 | German Pavillon
inter solar award 2016 WINNER
KUBUS THE WORLD'S FASTEST TABBER STRINGER
EXPECT EVEN MORE
• Highest material conversion yield
• Up to 1800 modules per day (72 cells)
• Only 1 operator per shift needed and only to refill goods
• Non-stop production, even during ribbon exchanges or maintenance / 30 MW more at same costs per year
• Soldered cell matrix on a tray and contactless soldering for highest precision
• All state-of-the-art materials processable (3–6 busbar; half-cells; PERC etc.)
Your contact person:
Maximilian Germann
M10 Industries AG
Munzinger Strasse 10
79111 Freiburg | Germany
Phone: +49 761 4019 68 51
sales@m10ag.de
www.m10ag.de
INDUSTRIES
MORE THAN 20 YEARS
MADE IN GERMANY
engineering
manufacturing
photovoltaic
www.m10-solar-campus.de

Module concepts & designs	Interconnection technologies	Cell designs
Glass backsheet	Ribbon-based interconnection	Back-contact (IBC, MWT)
Double glass	Round-wire interconnection	Free cell formats (including 5", 6", 6"+ formats, half-cells)
TPedge, NICE	Electrical conductive adhesives (ECA)	Full-square, pseudo-square
Layer properties (thickness, reflection etc.)	Shingled solar cells	Flexible number and position of busbars and pads
Layout (margins, distances, string length etc.)	Serial or parallel string interconnection	Electrical information (eta, ISC, PMPP, etc.)

Table 2. SmartCalc.CTM module design options (excerpt).

PV Modules

with SmartCalc.CTM enabled this quick analysis: without a single module prototype and in only a few hours.

Module, solar cell and interconnector concepts

The variation of cell spacing, glass thickness or spectral information of module layers is a smaller but nonetheless valuable task. Well-equipped R&D departments are capable of evaluating these changes even without simulation-aided development. To evaluate different novel module, solar cell or interconnection concepts a much deeper understanding of CTM effects, advanced and flexible scientific models and sophisticated measurement equipment is necessary. Bypassing scientific models becomes increasingly difficult for advanced concepts.

Comparing module concepts with back-contact solar cells (IBC or MWT), round-wire interconnection (SmartWire or multi-busbar), shingled cells, half-cells or new module topologies (e.g. all strings connected in parallel) is complex and it would be safe to say that most manufacturers do not have the manufacturing equipment to compare all module concepts by prototyping and measurement. When comparing different concepts they are highly dependent on external information. With SmartCalc.CTM a comparison of new concepts is possible and not only module manufacturers but also equipment producers or material suppliers can evaluate new technologies or materials.

While conventional module concepts are well understood and contributing CTM factors are known, the photovoltaic industry has been introducing new concepts to the market recently. Bifacial cells and modules or shingle cell interconnection are only some examples that demonstrate progress. While some technologies like half-cells or electrical conductive adhesives (ECA) do not require new methods for the CTM analysis, other module concepts need new approaches

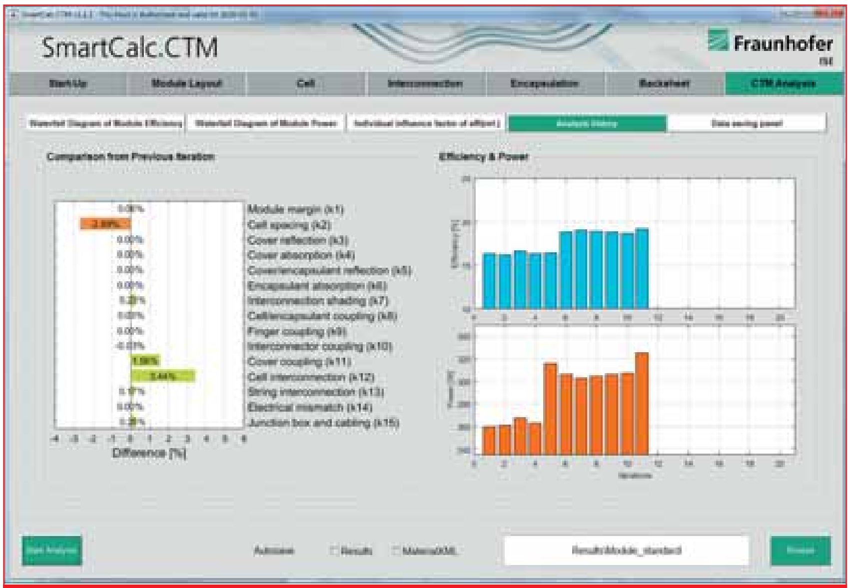

Figure 2. Screenshot of SmartCalc.CTM showing the progress during a module optimization session
Further information is provided at www.cell-to-module.com.

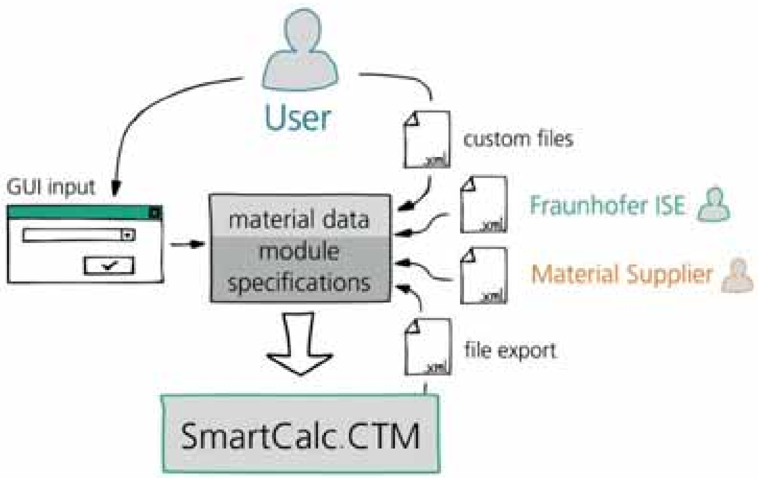

Figure 3. Data input into SmartCalc.CTM.

and a detailed scientific understanding of the resulting CTM changes.

Fraunhofer ISE provides a continued development of loss factors [8] or enhanced algorithms for new concepts (i.e. shingled modules [7]) to guaranty maximum flexibility for SmartCalc.CTM users. New features, concepts

```xml
<Electrical_Information>
  <Efficiency unit="[%]">20.35</Efficiency>
  <Pmpp unit="[W]">5</Pmpp>
  <Impp unit="[A]">8.941</Impp>
  <Isc unit="[A]">NaN</Isc>
  <Isc_gain unit="[%]">-1.9</Isc_gain>
  <Voc unit="[V]">NaN</Voc>
</Electrical_Information>
```

Figure 4. Excerpt of a material data file containing electrical solar cell specifications.

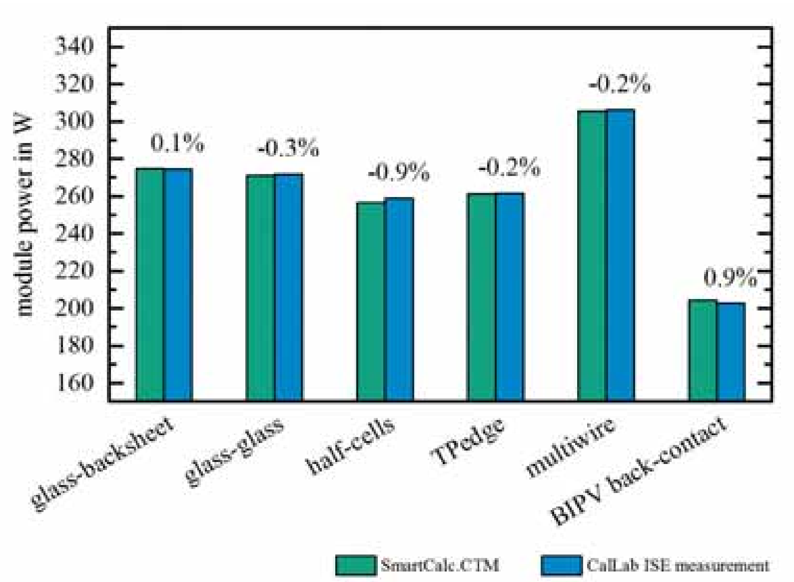

Figure 5. Results of SmartCalc.CTM simulation and measurement.

and calculation options are provided and continuous improvement by Fraunhofer ISE keeps SmartCalc.CTM up to date.

Data input

Key to every precise calculation is a good set of input parameters and material information. Geometrical information, spectral transmission and reflection data and electrical properties are the most important input parameters for solar modules. Data can be entered into SmartCalc.CTM in different ways (Figure 3).

The first and easiest way is to directly enter data into the user interface. Spectral information (reflectance etc.) can be loaded from text files and all inputs can be stored afterwards for later use.

The second possibility is to load previously created data files or to load files provided by external sources. Data is stored in a non-proprietary XML-based text file (Figure 4), which is an open format and can be edited without additional licences. Fraunhofer ISE provides precise measurements and data files, but also material suppliers or in-house R&D departments can create these files.

Fraunhofer ISE also provides assistance for material and component manufacturers to create data files to allow their customers a fast, reliable and easy CTM-analysis. To keep results confidential no web-based services or even an internet connection is required to run SmartCalc.CTM.

Validation

Fraunhofer ISE has been developing new concepts for photovoltaics for more than 35 years. Several innovative modules have been manufactured, evaluated and analyzed at the Fraunhofer ISE Module Technology Centre and of course results and experiences have been used for the development of SmartCalc.CTM. Together with Fraunhofer ISE CalLab PV Modules the development team of SmartCalc.CTM has performed validation measurements on several different photovoltaic modules. Results from selected modules are shown in Figure 5 and prove the flexibility and accuracy of SmartCalc.CTM.

Licensing

SmartCalc.CTM is licensed by Fraunhofer ISE and different packages all including material or component characterization are available. Three options ranging from an extended trial to a premium version can be selected. The premium version guarantees access to feature updates and consulting by Fraunhofer ISE. Upgrades from the extended trial to other versions are possible and the trial fee will be refunded. Fraunhofer ISE also offers the development of specialized or customized features and the accelerated implementation of customer-specific extensions to SmartCalc.CTM.

Module optimization: example

To demonstrate the possibilities of SmartCalc.CTM we perform the optimization of a conventional photovoltaic module and include some typical cases:

a) Switching from a three-busbar cell to a five-busbar cell
b) Evaluating an encapsulant from a different manufacturer
c) Increasing the cell interconnector cross-section
d) Using half-cells instead of full-format wafers
e) Change the cell and string spacing

The module we analyze contains 60 monocrystalline solar cells (full-square, H-pattern, 156.75mm, 20.35%, 5Wp), ribbon interconnection (1.2x0.2mm), commercial EVA foils (0.46mm), a commercial white backsheet and a glass with anti-reflective coating (3.2mm). A junction box with 1m cables (4mm^2) is used.

Results of the initial CTM-analysis are displayed in Figure 1. The module power is 287.3Wp, the efficiency 17.85% and the CTM power ratio is 95.8%.

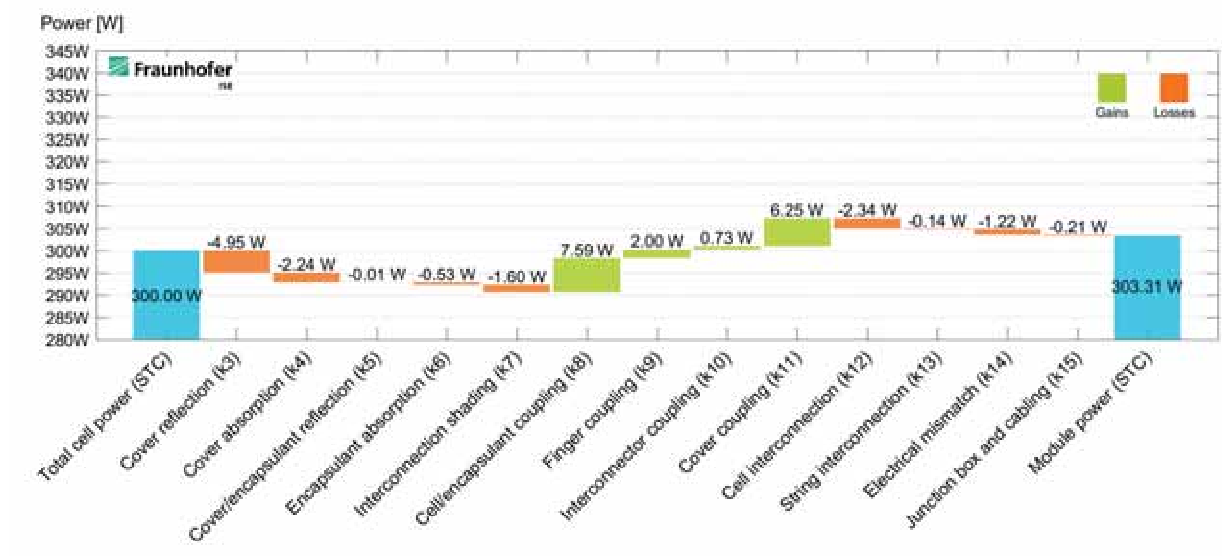

Figure 6. CTM-analysis of a half-cell module.

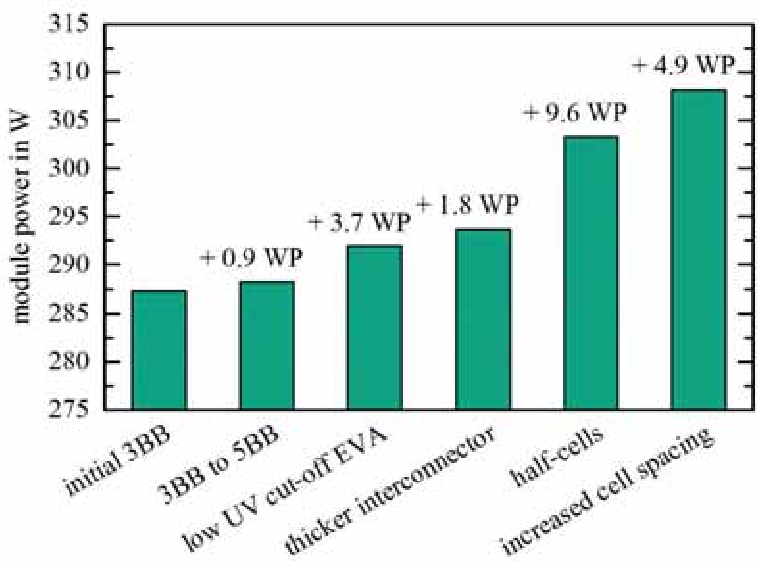

Figure 7. Module power and gain after several optimization steps.

Switching from a three-busbar cell to a five-busbar cell

To evaluate the effects of an increased number of busbars we replace the solar cell with a five-busbar version of the same manufacturer. We change the busbar width from 1.0 to 0.7mm and adapt the position of the busbars. The width of the interconnector ribbons is changed from 1.2 to 0.8mm. The cell performance and other parameters (e.g. cell metallization) remain unchanged.

Results of the analysis show an increase in module efficiency by $0.06\%_{abs}$ which equals a power gain of 0.9Wp (module 288.2Wp).

Evaluating a new encapsulation foil

We perform the comparative CTM analysis with a new encapsulation material offered by the same manufacturer. The new foil features a lower UV cut-off than the initial EVA and a slightly increased transmission. All parameters from the last case are taken and the five-busbar cells are used.

The module power increases by 3.7Wp (291.9Wp). The CTM power ratio is now 97.3% and the module efficiency increased to 18.14%.

Increasing the cell interconnector cross section

The next optimization changes the interconnector height from 0.2 to 0.25mm. As before, we perform this analysis using the same parameters as in the last optimization step. The module therefore includes five-busbar cells and a low UV cut-off EVA. The new interconnector is a copper-based ribbon with a cross-section of 0.8mm x 0.25mm with a coating thickness of 18μm.

The increase of the interconnector cross section increases the module power to 293.7Wp (+1.9 Wp).

Using half-cells instead of full-format wafers

Half-cells have been presented to increase the module power by reducing electrical losses and increasing gains from backsheet reflection. We therefore evaluate this possibility to further optimize our module.

Cell and string distance are kept set to 2mm. The cell parameters change to 2.5Wp and dimensions of 156.75 x 78.375mm. The rear side now only features three pads and the cell current is reduced to 4.48A. Cell strings now have a length of 20 cells each.

Using half-cells increases the module power to 303.3Wp and the efficiency reaches 18.6%, assuming equal cell efficiency. Because the sum of the initial cell power was 300Wp, we have now achieved the goal of having a CTM above 100%. A detailed CTM analysis is shown in Figure 6. The use of half-cells increased the module area due to a larger cell-spacing area.

Change the cell and string spacing

To further increase the gains from backsheet reflection (Figure 6, k11) we change the cell and string spacing from 2 to 4 mm. This increase will raise the gains of k11 but will also lead to higher electrical losses due to longer electrical paths. Also the efficiency will drop because of the larger module area.

Performing the analysis with SmartCalc.CTM we find the module power to be 308.2Wp and the efficiency to be 18.3%. As expected, the backsheet reflection gains increase (5Wp additional gain) as well the electrical losses in the cell interconnection (0.2Wp). The CTM power ratio is now 102.7%.

The initial module featured 287Wp and an efficiency of 17.85%. After performing five optimization steps we are able to achieve 308.2Wp and 18.30%. By using SmartCalc.CTM an increase of module power by 21.2Wp could be accomplished. No prototypes had to be built and therefore no equipment, material or additional process development was necessary. The simulations were performed on an office computer within minutes and could be easily continued for more advanced concepts (i.e. half-cells with round-wire interconnection). Figure 7 displays the progress of the module optimization.

While the introduction of new materials or processes (i.e. cell separation) requires further evaluation (i.e. reliability testing), SmartCalc.CTM supports the development by providing additional information. The gains from the introduction of a new encapsulation foil (+3.7Wp) can be weighted with module cost information (i.e. €0.4/Wp) to get the economic benefit of the new EVA (€1.48/Wp per module). We are now able to compare this to material prices of the new encapsulation foil.

SmartCalc.CTM can successfully participate in supporting decisions regarding the introduction of new materials, components or concepts.

Summary

The precise understanding and analysis of cell-to-module gains and losses are vital to improve photovoltaic modules, cells and materials. Many different approaches are known and several tools, algorithms and methods are used in industry and research to analyze CTM ratios. The access to these tools is limited to a very small group of researchers and experts and no common ground exists to compare results. This missing transparency is a lost opportunity for the photovoltaic community because no comparison of concepts and module components is possible.

Fraunhofer ISE presents SmartCalc. CTM, an accessible, precise and convenient software to perform CTM-analyses. The tool features a graphical user interface, open data interfaces and the possibilities to analyze several solar module concepts.

We use SmartCalc.CTM to optimize a solar module and increase the module power by 21 Wp. We demonstrate the possibilities of SmartCalc.CTM and perform five optimization steps including the change of materials, the change of material properties as well as a change in module design features.

References

[1] I. Haedrich et al. 2014, "Unified methodology for determining CTM ratios: Systematic prediction of module power", *Solar energy materials and solar cells* 131 (2014), pp.14-23, ISSN: 0927-0248, SiliconPV.

[2] ITRPV/ 2017, "International Technology Roadmap for Photovoltaic: 2016".

[3] http://pv.energytrend.com/pricequotes.html, 27.04.2017

[4] E. Fornies et al. 2015, "Cell-to-module losses in standard crystalline PV modules – An industrial approach", *Photovoltaics International*, 29th edition.

[5] I. M. Peters et al. 2014, "Detailed Current Loss Analysis for a PV Module Made With Textured Multicrystalline Silicon Wafer Solar Cells", *IEEE Journal of Photovoltaics*, vol. 4, no. 2, pp.585.

[6] J. P. Singh et al. 2016, "Cell-to-module power loss/gain analysis of silicon wafer-based PV modules", www.pv-tech.org.

[7] M. Mittag et al, "Cell-to-Module (CTM) Analysis for Photovoltaic Modules with Shingled Solar Cells", in 44th IEEE Photovoltaic Specialists Conference (PVSC), to be published, 2017.

[8] M. Mittag et al, "Progress on unified cell-to-module (CTM) determination methodology: systematic calculation of module power", in 44th IEEE Photovoltaic Specialists Conference (PVSC), to be published, 2017.

[9] H. Hamifi et al, "Investigation of cell-to-module (CTM) ratios of PV modules by analysis of loss and gain mechanisms", *Photovoltaics International*, 32th edition, 2016

[10] http://isc-konstanz.de/isc/leistungen/testen-charakterisierung.html

[11] M. Peters et al. 2014, "Full loss analysis for a multicrystalline silicon wafer solar cell PV module at short-circuit conditions", 29th EU PVSEC, Amsterdam.

[12] J. Mueller et al. 2015, "Resistive Power Loss Analysis of PV Modules Made From Halved 15.6 × 15.6 cm2 Silicon PERC Solar Cells With Efficiencies up to 20.0%", *IEEE Journal of Photovoltaics*, pp. 189.

About the Authors

Max Mittag studied industrial engineering and management at the Freiberg University of Mining and Technology. In 2010 he completed his diploma thesis at Fraunhofer ISE and joined the department for photovoltaic modules. His current work includes the cell-to-module efficiency analysis and the development new photovoltaic module concepts.

Matthieu Ebert holds a master degree in renewable energy systems from the University of Applied Science, Berlin. Before joining Fraunhofer ISE in 2011 he completed research stays at the Fraunhofer CSE in Boston and at the Australian National University in Canberra. Since 2011 he has been undertaking research on PV module technology. Since 2015 he has led the module efficiency and new concepts team. His main areas of research are module efficiency and CTM analysis, building-integrated PV and PV for automotive applications.

Enquiries

Email: CTM@ise.fraunhofer.de

Understanding the energy yield of PV modules

Markus Schweiger[1,3], **Werner Herrmann**[1], **Christos Monokroussos**[2] & **Uwe Rau**[3]

[1]TÜV Rheinland Energy GmbH, Cologne, Germany; [2]TÜV Rheinland Co., Ltd., Shanghai, China; [3]IEK5-Photovoltaik, Forschungszentrum Jülich GmbH, Jülich, Germany

ABSTRACT

The output power under standard test conditions (STC) is important for establishing the price at which PV modules are sold. The return on investment, however, is determined by the energy yield of the PV modules in physical outdoor conditions, which depend on the location of the PV system (including daily and seasonal variations) and which are in general substantially different from STC conditions. Furthermore, PV modules which are available on the market exhibit significantly different physical properties, with technology-specific characteristics with regard to the temperature, irradiance behaviour and stability of STC power. The energy yield of PV modules cannot therefore be predicted simply by multiplying the yearly insolation at the plane of the array of a specific location by the rated module output power at STC. Instead, a factor – namely the module performance ratio (MPR), usually significantly smaller than unity – is applied to describe this discrepancy. The MPR facilitates a relative comparison in percentage terms between different technologies with low uncertainty. Independently of PV module efficiency or available solar energy, the MPR makes it possible to investigate all technology-related factors that have an influence on the energy yield of PV modules in different climates.

Introduction

Between 2004 and 2016 a sum of $1,161bn was invested in PV systems [1], and there is currently approximately 200GW of PV capacity installed worldwide. By 2050 a globally installed PV capacity of around 4.6TWp is expected; this in turn implies a global investment market of some $225bn per year on average through 2050 [2].

A major part of this investment is represented by the price of PV modules, which is determined by their output power rated at standard test conditions (STC), specifically an irradiance of 1,000W/m^2, a module temperature of 25°C and a spectral irradiance according to IEC 60904-3. Real outdoor operating conditions, however, are in general considerably different from STC conditions, as demonstrated in Figs. 1 and 2 for optimal mounting conditions. The relevant standards for specifying the energy rating of PV modules are IEC 61853 parts 1 to 4, but not all parts have been published yet [3,4]. The energy yield estimation for various PV module technologies, using simulation tools, exhibits high uncertainties as a result of the limited availability of sufficient PV module performance data.

"It is essential to have a detailed understanding of all the factors that impact on the energy yield performance of PV modules."

It is therefore essential to have a detailed understanding of all the factors that impact on the energy yield performance of PV modules. Such knowledge will provide a scientific basis for making accurate yield estimates for different technologies and for

Figure 1. The test sites operated by TÜV Rheinland for PV module characterization and energy yield measurements (clockwise from left): Cologne (Germany, moderate climate), Tempe (Arizona, dry continental climate), Chennai (India, tropic climate), Thuwal (Saudi Arabia, dry desert climate with sand deposition) and Ancona (Italy, Mediterranean climate).

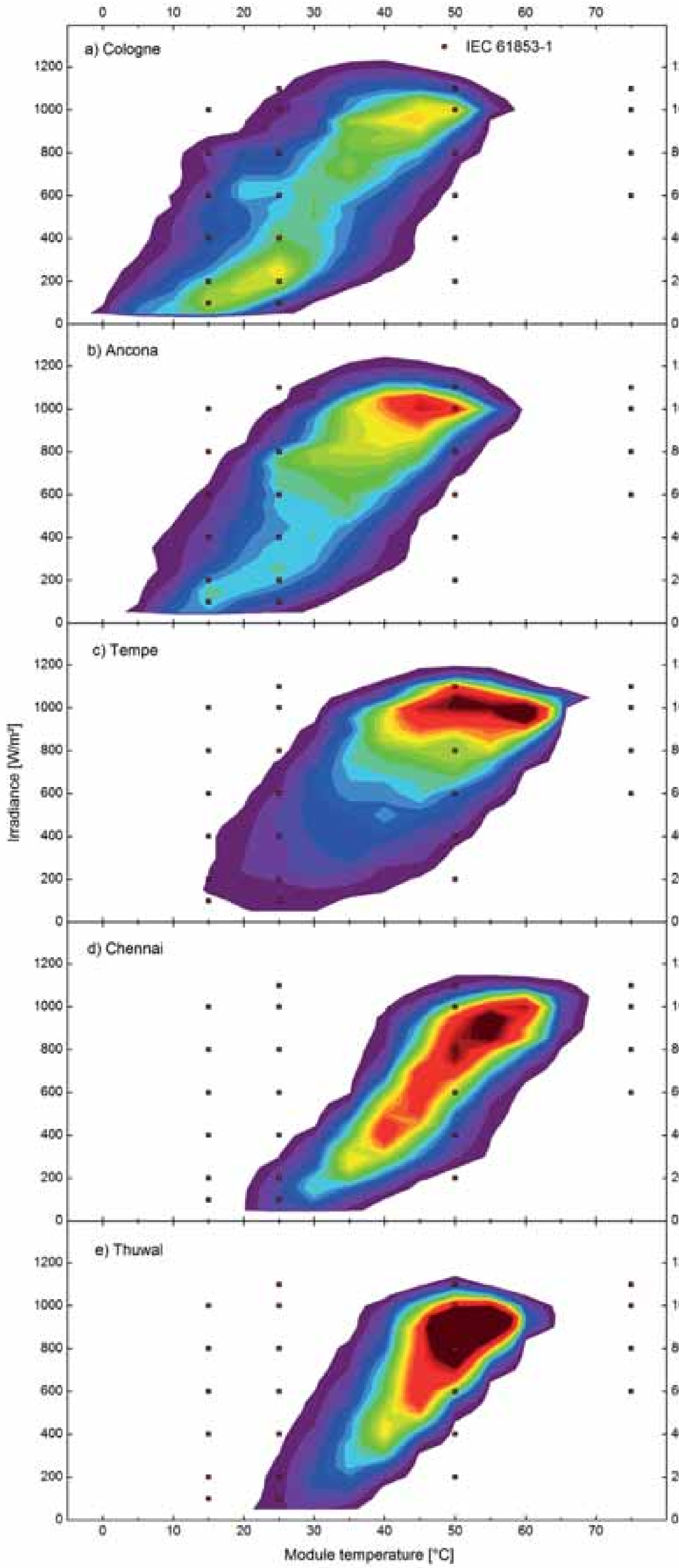

Figure 2. Generated electrical energy of a crystalline PV module in five different climates as a function of module temperature and irradiance on an annual basis, compared with the measuring conditions of IEC 61853-1 energy rating matrix (red dots). Colour range: 0.1–2.6%; colour increment: 0.1%.

optimizing energy yield performance for different climates. For the upcoming multi-GW installations of 125GW/year on average, each percentage of uncertainty results in significant investment uncertainty with regard to capital expenditures.

Energy yield performance as a key factor for the return on a PV investment

Consider a PV power plant with 100MWp nominal power (for STC) at a location with a moderate specific energy yield of 1,500kWh/kWp and a levelized cost of electricity (LCOE) of \$100/MWh; this means \$150,000 extra revenue for each per cent of additional energy yield and year of operation (if emerging interest earnings are neglected). This would essentially mean \$3.75m more revenue per 1% increase in energy yield after 25 years of operation. Furthermore, assuming a new market of around 4.4TWp as mentioned earlier, and while keeping the specific energy yield, lifetime and LCOE constant, the result is an astonishing \$15bn surplus in revenue per 1% of energy yield, which could be achieved by choosing capable PV modules. Besides the chance for investors to maximize their net profit by considering the energy yield performance, this relation also bears a certain investment risk for the PV industry if the long-term performance is lower than expected, and if investors are not able to accurately calculate the expected income.

From absolute yield to specific yield to module performance ratio

The energy yield of PV modules deployed in different climates is a complex topic involving interdisciplinary knowledge of cell physics, module properties and meteorological aspects. To find a pathway to the underlying correlations, some general definitions therefore need to be discussed first.

The absolute energy yield (EY) of PV modules is defined in watt hours (Wh). Because of the different efficiencies and designs of PV modules, it makes sense to calculate the specific energy yield in watt hours per watt peak (kWh/kWp), by dividing EY by the nominal power P_{STC}; this allows a comparison of the energy yield performances of different types of PV module. Besides P_{STC} the second factor dominating energy yield is solar irradiation (H); this strongly depends on geographic location, local mounting conditions of the PV power plant, and annual fluctuations. When choosing a

pyranometer as a reference irradiance sensor, H is almost independent of environment-related impact factors, such as angle of incidence, spectral shifts or temperature. Thus, to compare and elaborate only technology-driven performance factors, the module performance ratio MPR is the best-practice method and can be calculated as:

$$MPR = \frac{EY}{P_{STC}} \cdot \frac{1{,}000\,W/m^2}{H}$$

The MPR is suitable for investigating the efficiency of PV modules in different climates compared with STC efficiency, as well as for comparing different technologies and climates. As the local weather conditions cannot be changed (unlike the global climate), differences with respect to technological origin are of special interest for optimizing PV module performance and for selecting suitable products for a certain climate. The amount by which the value of MPR differs from unity represents the losses in real outdoor operating conditions compared with STC efficiency. The MPR facilitates a relative comparison in percentage terms between different technologies and climates; it includes all the offset relevant influences on energy yield performance due to inaccurate nominal power, temperature losses, non-linear module performance depending on irradiance G (low-irradiance behaviour), and spectral effects, as well as the losses due to soiling and angular behaviour (as illustrated in Fig. 3). The MPR is identical to the performance ratio (PR), commonly used for PV systems, when system losses, such as wiring, module mismatch or invertor losses, are not considered. Uncertainties of less than ±1% can be achieved when choosing P_{STC} as stated by the manufacturers as a constant basis for MPR calculations.

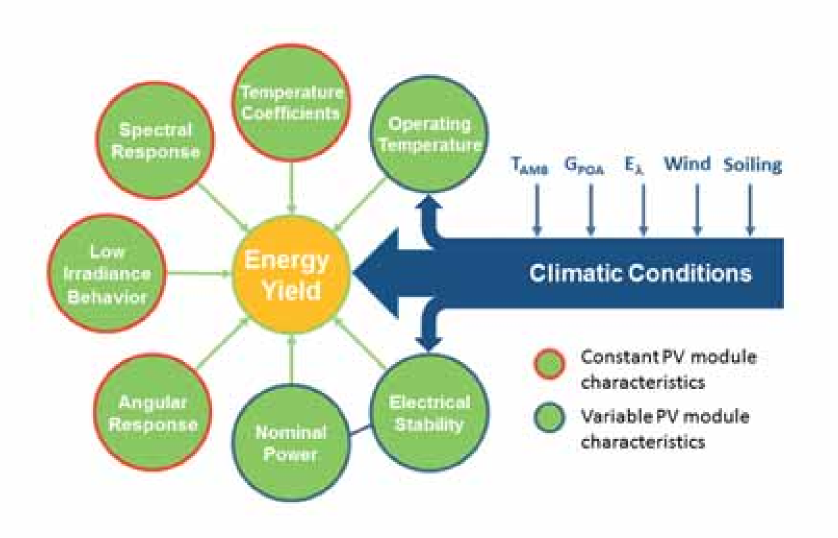

Figure 3. Factors influencing the energy yield of PV modules.

Underlying database and investigations performed

Since 2013 the performance of 15 different PV module types within the nationally founded 'PVKlima' R&D project has been undergoing systematic analysis. The tested modules were:

- Five different crystalline silicon (c-Si) module types from three different manufacturers.
- Four Cu(In,Ga)Se_2 (CIGS) modules from four different manufacturers.
- Three cadmium telluride (CdTe) module types from two different manufacturers.
- Three amorphous silicon (a Si tandem) module variants from three different manufacturers.

The five different c-Si module types comprise three polycrystalline and one monocrystalline PV modules with heterojunction cells, and one monocrystalline module with back-contacted n-type cells. The polycrystalline samples are equipped with different front glasses: one sample with standard float glass, one with an anti-reflection coating and one with deeply structured glass.

Comprehensive tests with regard to energy rating and energy yield were performed in the laboratory and outdoors; five test sites, each in a different climate zone, were therefore constructed (see Fig. 1). The annual in-plane global solar irradiation was 2,386kWh/m^2 in Saudi Arabia, 2,360kWh/m^2 in Arizona, 1,860kWh/m^2 in India, 1,556kWh/m^2 in Italy and 1,195kWh/m^2 in Germany. These test sites allow the generation of the PV module and environmental data sets needed to understand the real-world performance and long-term reliability of PV modules. Thus it was possible to generate an understanding (that so far is unique) of PV module performance under real operating conditions in different climates.

Nominal power at STC and monitoring of electrical stability

To understand the energy yield of PV modules, it is necessary to first begin with the most challenging aspect from the metrology point of view: the determination of STC power and the monitoring of its stability during outdoor operation.

To get a deeper insight into the various seasonal effects on module performance, an elaborate current–voltage (I–V) curve analysis was employed. After the I–V curves of all samples were measured using a sampling rate of 10min, corrections of temperature and irradiance according to IEC 60891 [5] were applied, in combination with a spectral mismatch correction obtained from measured spectral irradiance data according to IEC 60904-7 [6]. These corrections are necessary in order to create constant operating conditions for time series analysis which would not otherwise be achieved outdoors.

Fig. 4 shows the monthly average STC power for four samples representing four technologies. The test site in Italy is used as a model case for the discussion of some fundamental PV module performance characteristics.

With the application of this correction method, all environmental influences are accounted for and can be directly compared. The method allows the influence of temperature and spectral irradiance on fill factor FF, short-circuit current I_{sc}, open-circuit voltage V_{oc} and P_{STC} to be analysed independently of each other.

Starting with c-Si, mostly stable P_{STC} power values were found within more than three years of outdoor exposure for all climates. Typical long-term average degradation rates of less than −0.5% per year can be confirmed. For heterojunction PV modules, higher rates of about −1.0% per year were observed, mainly related to a decrease in V_{oc}. The c-Si 1 sample shown in Fig. 4 exhibits an approximately four per cent lower value than the P_{STC} stated on the label. It is noted that the stated results are subject to a measurement uncertainty of ±2.5%, which should be borne in mind when interpreting the results.

The nominal power of CIGS PV modules revealed significant

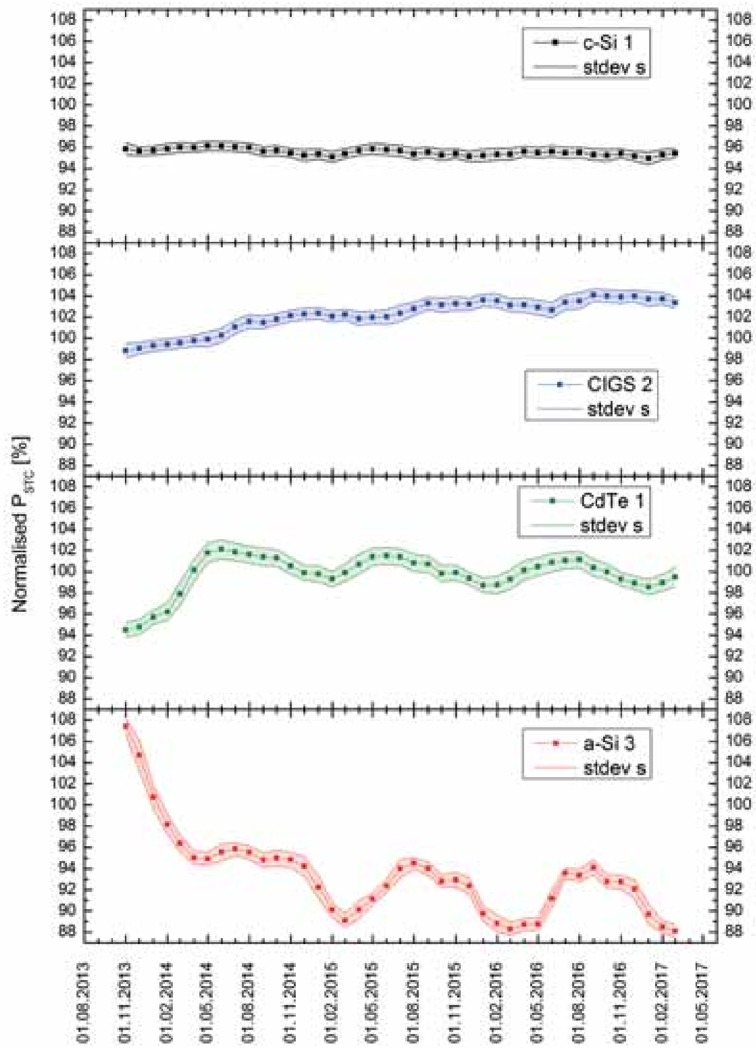

Figure 4. Monthly averages of STC-corrected nominal power for four PV module types, normalized to stated nominal power, for the Ancona test site in Italy (uncertainty: ±2.5%).

performance changes due to metastable cell processes; the consolidation phase of these processes can take longer than a year. Changes in power are related in equal proportions to *FF* and V_{oc}. The depicted CIGS 2 sample in Fig. 4 exhibited an increasing P_{STC} of around +4% compared with the label specification. Some of the other PV module types resulted in more than a –10% deviation from the label value after three years of operation; this depends on the manufacturer and not just on the technology.

The tested CdTe PV modules also revealed metastable processes that significantly affected P_{STC}. After an initial performance increase of up to 8%, which takes several months (depending on local temperature conditions), the nominal power exhibits annealing processes between summer and winter, leading to a P_{STC} oscillation with an amplitude of approximately ±2%; this oscillation disappears in hot climates, such as those found in Tempe or Chennai. The annealing process is assumed to achieve a constant state in these hot locations for the whole year. Changes in power are related mainly to *FF*. The average stabilized P_{STC} of the CdTe 1 sample shown in Fig. 4 fits quite well with the stated P_{STC} values after three years of operation; however, PV module types with more than a –10% deviation from the label value after three years of operation were also found.

The performance of a-Si PV modules revealed the well-known (but not fully understood) Staebler–Wronski effect, with initial stabilization of around –10% to –15%, depending on module type. As in the case of CdTe, the performance reveals a summer and winter oscillation of about ±3%, which could also be observed for hot climates. The time constants of these effects are again temperature driven and mainly related to *FF*. The average stabilized P_{STC} of the depicted a-Si 3 sample is about –9% lower than that stated by the manufacturer. Long-term degradation rates are superimposed onto these metastable effects. One module type completely failed the long-term test: two out of four samples ceased operation after just a few months of operation.

It remains unanswered here whether or not the technology-specific stabilization procedures stated in the new IEC 61215 [7] series of standards are suitable in order to achieve reliable, stabilized P_{STC} values. All the results on stability can be reviewed in Schweiger et al. [8]. Now that the P_{STC} values of all PV modules have been verified, the discussion about climate-related influences can continue.

Origin of climate-related performance differences for PV module technologies and major findings

As mentioned above, PV modules have different low-irradiance behaviours, different temperature coefficients, different operating temperatures, different spectral and angular behaviours and also different soiling behaviours when different front glasses are used. These factors, combined with site-specific climate conditions, result in significant performance differences on the basis of the nominal power measured at STC. As pointed out, the nominal power can deviate significantly up or down from the stated values as a result of binning policies, measuring inaccuracies (±2% in the laboratory) or stability issues, such as light-induced degradation (LID), potential-induced degradation (PID), or metastabilities for thin film.

> "The most important pieces of information for investors are the results based on the pure STC power as stated and sold by the manufacturers."

Given the impact on investment of just one percentage point difference in energy yield performance, the most important pieces of information for investors are the results based on the pure STC power as stated and sold by the manufacturers. Within this project, a significant difference in the energy yield performance was observed between the best- and worst-performing PV module types: up to 23% in India, 21% in Arizona, 14% in Germany and 12% in Italy. After compensating the effects related to nominal power mismatch discussed earlier, an annual difference in yield of 16% in India, 19% in Arizona, 8% in Germany and 9% in Italy remained; the results for Saudi Arabia are still under investigation.

For comparable standard crystalline only, the latest investigation of 24 c-Si samples indicates a technological-origin-related difference of at least 5% (implying again correct and stable nominal power values). This value increases greatly for certain PV modules incorporating special technologies affecting energy yield performance, such as in the case of bifacial PV modules or some thin-film technologies.

Seasonal performance behaviour under investigation

To investigate the origin of the above-mentioned significant differences in annual yield results, an evaluation of short-term MPR values provides a first impression of the physical background. It is a fast and easy way to obtain insights into module performance, which is also the reason why it is used most frequently as a monitoring solution for PV systems, needing just one reference irradiance sensor. The potential, however, is limited, since all influencing factors are superimposed onto just a single value.

For the MPR calculation, the maximum power point was tracked with a sampling frequency of 30s, and a ventilated pyranometer served as a reference irradiance sensor. Fig. 5 shows the monthly average MPR values of representative samples in Italy based on stated P_{STC}, together with the compensated MPR based on measured P_{STC}, as well as temperature losses and spectral irradiance influences. This plot is used again as the model case for the discussion of some fundamental performance characteristics of different PV module technologies.

As discussed earlier, the performance of c-Si PV modules (black dots, Fig. 5) is mostly stable. Nevertheless, the plot of monthly MPR values for c-Si shows the strongest oscillations by season, with maximal MPR values in winter; the reason for this is the high relative temperature coefficient γ, with typical values of –0.35%/K for high-efficiency modules and –0.42%/K for standard cells. The maximum in winter can be reduced for modules of each technology with poor low-irradiance behaviour due to the lower average irradiances on winter days. The influences of spectral effects on c-Si are low. An offset of the MPR curves can occur in the case of PV modules with inaccurately stated nominal power on the label or datasheet.

Almost the same performance behaviour can be observed for CIGS samples (blue dots, Fig. 5); the spectral response signals and temperature behaviour are comparable to those for c-Si. The oscillations between summer and winter can be slightly lower for the samples with better temperature behaviour or poor low-irradiance behaviour. Any potential gains due to a better temperature coefficient can be lost again, however, as a result of higher average operating temperatures. The CIGS 2 module shown in Fig. 5 indicates the effect of an increasing P_{STC} over the years due to metastable behaviour, as demonstrated earlier, which can be either positive or negative for PV modules of this type.

CdTe samples (green dots, Fig. 5) show less oscillation by season, but still exhibit maximum MPR values during the winter months. The reasons for the lower amplitudes can be found in the significantly lower temperature coefficient γ of typically –0.29%/K, and in the spectral gains in summer. The difference between summer and winter is further reduced because of the metastable behaviour, as shown earlier.

In the case of a-Si samples (red dots, Fig. 5), the MPR values during the first few months are dominated by Staebler–Wronski degradation, followed by temperature annealing observed in the summer months. Compared with c-Si,

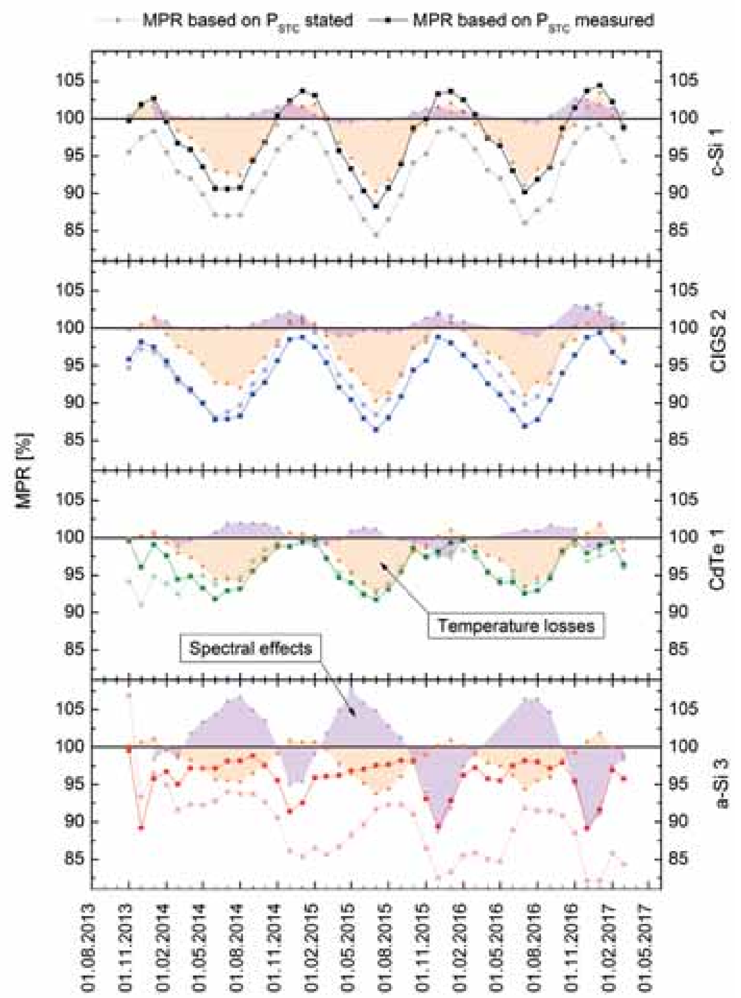

Figure 5. Monthly module performance ratio based on stated P_{STC} for four PV module types, compared with the MPR based on monthly measured P_{STC}, for the Ancona test site in Italy. A deviation from 100% means yield losses or gains; the temperature (orange) and spectral effect (purple) contributions are indicated.

small oscillations between summer and winter are achieved. In contrast to all other cell technologies, the maximum MPR values are reached in summer; the reason is a combination of small temperature losses, again due to low temperature coefficients γ (typically in the range of –0.26%/K to –0.39%/K, depending on manufacturer), gains due to thermal annealing, and significant spectral gains in summer. For some samples, high losses due to poor low-irradiance behaviour in winter were observed. It is noted that the performance of some a-Si samples did not reach a stable level after more than a year of outdoor exposure.

Energy rating of PV modules using linear performance loss analysis

A linear performance loss analysis (LPLA), as described in Schweiger et al. [9], can be used to quickly, accurately and inexpensively predict the MPR of PV modules for different climates. Simple reference environmental data sets and energy rating data, in accordance with the IEC 61853 series, measured in the laboratory serve as input data. An energy yield prediction based on calculated MPR_{Calc}, with a deviation of ±3% from measured $MPR_{Outdoor}$ values, can be achieved, as illustrated in Fig. 6; this deviation is assumed to be mainly due to the influence of P_{STC} measuring uncertainties on the $MPR_{Outdoor}$ results. The approach takes into account all the relevant factors that have an impact on energy yield, such as module temperature, low-irradiance conditions, and spectral and angular effects, as well as soiling.

The approach also allows a quantification and comparison of the various influencing factors for different PV module technologies and for different climates, as illustrated in Fig. 7. The energy yield of PV modules is affected by five individual loss factors; the mechanisms correspond to loss terms ΔMPR for different climates, which can be singled out. The loss mechanisms which influence the MPR of electrically stable PV modules are: temperature (ΔMPR_{TEMP}), low irradiance (ΔMPR_{LIRR}), spectral effects (ΔMPR_{MMF}), angular losses (ΔMPR_{AOI}) and soiling (ΔMPR_{SOIL}).

The losses due to soiling and angular effects are almost constant for PV modules with standard untreated front glass. Soiling losses (ΔMPR_{SOIL}) are highest in Arizona, although higher soiling rates can be expected in Saudi Arabia. The soiling rate is highly dependent on the period under consideration, and long-term averages are needed.

The losses due to angular effects (ΔMPR_{AOI}) are highest, compared with overall available energy, in Cologne, with up to –3.5%. In addition to the advantages gained in light transmission, lower angular losses can be achieved with deeply structured glass (–2.8%) or an anti-reflection coating (–1.6%). For deeply structured glass, however, higher soiling rates must be considered.

Relative losses due to low-irradiance behaviour (ΔMPR_{LIRR}) are also highest

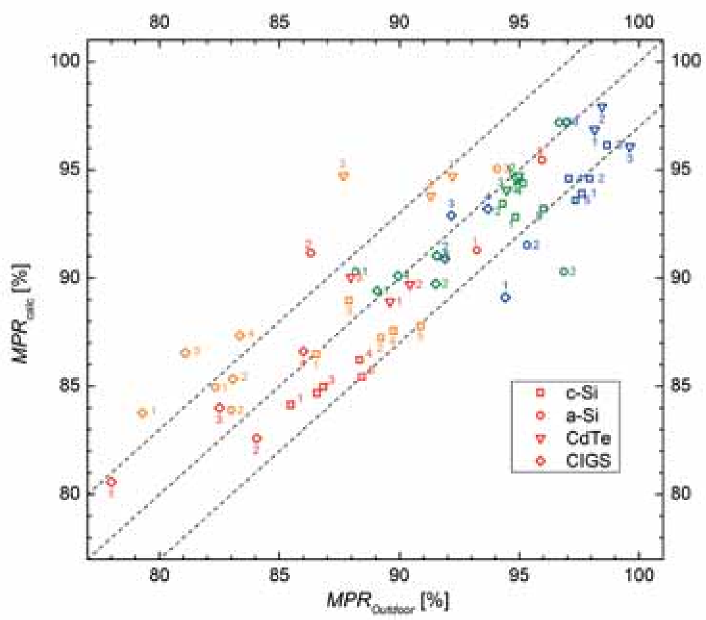

Figure 6. Module performance ratio MPR_{Calc}, calculated using weather data and indoor measurements, plotted versus the measured $MPR_{Outdoor}$ based on energy-weighted average outdoor power (blue: Cologne; green: Ancona; red: Tempe; orange: Chennai).

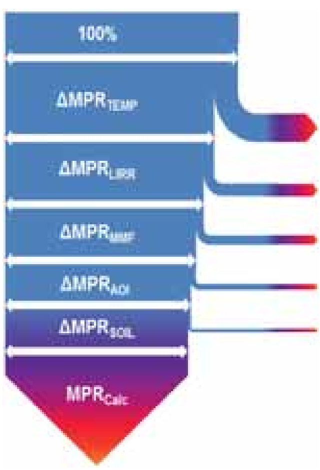

	c-Si 1				CdTe 1				CIGS 2			
	Cologne	Ancona	Tempe	Chennai	Cologne	Ancona	Tempe	Chennai	Cologne	Ancona	Tempe	Chennai
ΔMPR_{TEMP}	-2.3%	-3.9%	-8.9%	-9.6%	-1.5%	-3.5%	-6.7%	-6.2%	-2.9%	-4.5%	-8.8%	-9.1%
ΔMPR_{LIRR}	-1.2%	-0.8%	-0.4%	-0.5%	0.0%	+0.2%	+0.3%	+0.6%	-3.6%	-3.1%	-1.8%	-2.4%
ΔMPR_{MMF}	+1.3%	+0.5%	-0.8%	+1.6%	+2.3%	+0.9%	+1.1%	+5.3%	+1.4%	+0.3%	-1.1%	+1.8%
ΔMPR_{AOI}	-3.5%	-2.4%	-2.0%	-2.9%	-3.5%	-2.4%	-2.0%	-2.9%	-3.5%	-2.4%	-2.0%	-2.9%
ΔMPR_{SOIL}	-0.5%	-0.5%	-3.7%	-2.1%	-0.5%	-0.5%	-3.7%	-2.1%	-0.5%	-0.5%	-3.7%	-2.1%
	-6.2%	-7.2%	-15.9%	-13.5%	-3.1%	-5.4%	-11.1%	-5.3%	-9.1%	-10.3%	-17.4%	-14.7%
MPR_{Calc}	**93.9%**	**92.8%**	**84.1%**	**86.5%**	**96.9%**	**94.6%**	**88.9%**	**94.7%**	**90.9%**	**89.7%**	**82.6%**	**85.3%**

Figure 7. Quantified loss mechanisms influencing the MPR of PV module types c-Si 1, CdTe 1 and CIGS 2 in different climates on an annual basis.

in Cologne, with up to –3.6%. The low-irradiance behaviour for constant spectral irradiance conditions is technology driven, but also depends on the individual manufacturers. The behaviour is dominated by wafer recombination losses, and module internal serial and parallel resistance in combination with operating voltage and current. The performance between different manufacturers may vary significantly. A satisfactory low-irradiance behaviour for constant spectral irradiance conditions means an efficiency drop of less than –5% at 100W/m^2 relative to STC; this can easily be tested in the laboratory.

Losses due to temperature (ΔMPR_{TEMP}) are highest for c-Si, with up to –9.6% in Chennai. Better values can be achieved with thin film when the advantages due to low temperature coefficients are not lost because of higher operating temperatures.

The influence of spectral irradiance (ΔMPR_{MMF}) on c-Si is low on an annual basis. The highest impact on energy yield can be found for CdTe (up to +5.3% in Chennai) and a-Si.

For other mounting conditions with orientations that differ from optimal or those with reduced ventilation, as in the case of building-integrated PV (BIPV), other loss factors must be assumed.

> "A combination of indoor tests and reference climate datasets is sufficient for estimating and comparing the energy yield performance of different PV module technologies."

Conclusions

Because of cost and time pressure, consideration of the energy yield performance of PV systems is often of secondary importance when constructing PV plants. Optimization of the yield is necessary, however, for successful investment. Significant differences were observed in the energy yield of PV modules available on the market – up to 23%, depending on power rating, technology and climate.

The results have shown that a combination of indoor tests and reference climate datasets is sufficient for estimating, within ±3%, and comparing the energy yield performance of different PV module technologies. The long-term stability of electrical power, however, must still be tested in the field.

The ultimate owner of the PV power plant should consider a well-defined module performance ratio before making an investment decision. The competitiveness of solar projects can be enhanced by PV modules with reliable long-term performance and optimal energy yield performance suited to the climate of the installation location.

Acknowledgement

This work was partially funded by the German Federal Ministry for Economic Affairs and Energy (BMWi) as part of Contract Nos. 0325517B and 0325517C.

References

[1] UN Environment and Bloomberg 2017, "Global trends in renewable energy investment" (Apr. 6).

[2] International Energy Agency (IEA) 2014, "Technology roadmap solar photovoltaic energy", 2014 edn.

[3] IEC 61853-1:2011, "Photovoltaic (PV) module performance testing and energy rating – Part 1: Irradiance and temperature performance measurements and power rating".

[4] IEC 61853-2:2013, "Photovoltaic (PV) module performance testing and energy rating – Part 2: Spectral response, incidence angle and module operating temperature measurements" (IEC 82/774/CDV).

[5] IEC 60891:2013, "Photovoltaic devices. Procedures for temperature and irradiance corrections to measured current voltage characteristics".

[6] IEC 60904-7:2009, "Photovoltaic devices – Part 7: Computation of the spectral mismatch correction for measurements of photovoltaic devices".

[7] IEC 61215-1:2016, "Terrestrial photovoltaic (PV) modules – Design qualification and type approval".

[8] Schweiger, M. et al. 2017, "Performance stability of photovoltaic modules in different climates, *Prog. Photovolt: Res. Appl.* [manuscript under review].

[9] Schweiger, M. et al. 2017, "Understanding the energy yield of photovoltaic modules in different climates by linear performance loss analysis", *IET Renew. Power Gen.* [DOI:10.1049/iet-rpg.2016.0682].

About the Authors

Markus Schweiger received the diploma in electrical engineering from the Technical University of Munich and is currently pursuing his doctorate degree in photovoltaics at the RWTH Aachen University. Since 2009 he has been working as a scientist and project engineer in the Solar Innovation Department at TÜV Rheinland. His expertise includes high-precision PV module characterization, performance behaviour of thin-film PV modules, and energy yield of PV module technologies in different climates.

Werner Herrmann studied physics at the Technical University of Aachen and holds a Ph.D. in PV power characterization with solar simulators. Since 1988 he has been working at TÜV Rheinland, and has gained more than 20 years' experience in developing standards for the PV industry. He is the team manager for PV research activities that focus on PV module reliability testing, output power characterization, energy yield assessment, mechanical robustness of PV modules, and PV safety.

Christos Monokroussos is a technical expert for TÜV Rheinland, where his activities focus on R&D, characterization of solar cells and PV modules, quality control of measurement systems, standardization progress and PV module reliability. He earned his doctorate degree in photovoltaics from the Centre for Renewable Energy Systems Technology (CREST) at Loughborough University, UK.

Uwe Rau studied physics at the University of Tübingen, Germany, and at Claude Bernard University Lyon, France. He received his diploma in 1987 and his Ph.D. in 1991 in physics from the University of Tübingen, and also earned his habilitation degree in experimental physics in 2002 from the University of Oldenburg, Germany. Since 2007 he has been the director of the Institute for Energy and Climate Research at Forschungszentrum Jülich, and is a professor at RWTH Aachen University, Germany. His research interests include the physics and technology of thin-film solar cells, and the characterization and qualification of PV components.

Enquiries

Markus Schweiger
TÜV Rheinland Energy GmbH
Am Grauen Stein
51105 Cologne
Germany
Email: markus.schweiger@de.tuv.com

Photovoltaics International

Advertisers & Web Index

SolarWorld isn't all mono yet!

Dedicated monocrystalline integrated PV module manufacturer SolarWorld believes 2017 is a transitional year for the company after announcing a switch to monocrystalline production at the expense of multicrystalline and a full-migration to PERC technology as ASP declines in the second half of 2016 forced a major manufacturing rethink.

Global module ASP declines topped 30% in 2016, yet the real impact occurred with the significant curtailment in China's downstream business in the second half of the year, coupled to ever-increasing module availability in the US from South East Asia that was not subject to anti-dumping and countervailing duties (AD/CVD).

With demand weakness also hitting the booming US market in the fourth quarter, module ASP declines of around 25% were experienced in the second half of the year.

SolarWorld had thought that its module ASP would actually remain relatively flat in 2016, while peak demand in Q3 and Q4 would actually see a slight increase in ASP, while falling back to near ASP levels in Q1.

However, reality was something completely different and the company experienced a sharp 20% ASP decline in the second half of 2016. Revenue began to decline in the second quarter of 2016, from €222 million to €164 million by the fourth quarter of 2016, more than a 25% decline.

Total revenue in 2016 was €803 million, up 5.2% from €764 million in the prior year, driven by increased shipments of modules and kits that reached 1,336MW, up from 1,108MW in 2015. Revenue from modules and kits in 2016 reached €782.3 million, up from €742.9 million in 2015.

What looked like a breakeven year rapidly turned into a race to cut production on inventory build in an effort to stem net losses that reached around €92 million by year-end.

Mono, nothing else!

SolarWorld's new business strategy is centred on stopping all in-house multicrystalline production (ingot/wafer/cell/module) and migrating to monocrystalline production (ingot/wafer/cell/module). As a result, overall in-house capacity will be lowered.

By withdrawing completely from multicrystalline production, SolarWorld is cutting costs both in headcount and production, via plant consolidation. The company summed up the message to investors in the last slide of their latest presentation, noting 'Mono, nothing else!'

However, certainly in 2017, SolarWorld is relying on 300MW of multicrystalline modules under OEM contracts as it plans to increase overall shipments in 2017, while revenue is expected to remain relatively flat, according to new company guidance.

Critically, in tandem with the mono migration is the continued shift to PERC cell technology. Dr. Holger Neuhaus, managing director, SolarWorld Innovations, noted in his presentation at the recently held PV CellTech conference in Penang, Malaysia that the current PERC migration stood at 1,100MW, with full in-house migration to 1,600MW in progress. The higher nameplate capacity than reported in SolarWorld's recently released annual report may be due to the mono and PERC migrations, rather than new capacity.

Dr. Neuhaus also noted that SolarWorld's 25MW p-type mono-PERC pilot line was achieving stable average cell efficiencies of 22.0%, up from 21.8% noted in his presentation at PV CellTech in 2016. SolarWorld is using a five-busbar layout and large-area M2 mono wafers. Mono-PERC modules have achieved 310Wp.

Credit SolarWorld

SolarWorld is undergoing an ongoing transition from multi- to monocrystalline production.

In-house mono ingot/wafer production, which stands at 600MW, will convert to diamond wire sawing in 2017, providing meaningful production cost reductions.

However, mono ingot and wafer slicing operations under its 2017 production consolidation and realignment plans are still performed at different locations. All mono ingot production is located at its Arnstadt facility in Germany, while mono wafer slicing operations are at its facility in Freiburg, Germany.

This is also true of mono-PERC cell production and module assembly. Cells are being made in Arnstadt and modules assembled in Freiburg. SolarWorld's Hillsboro plant will continue with 500MW of p-type mono-PERC cell and module production, although previously planned (250MW) mono-ingot production is off the table in 2017, according to SolarWorld's 2016 annual report.

Clearly, SolarWorld has balanced cell and module production with flexibility built-in with p-type multi module OEM supply. With the migration to mono ingot/wafer production the significant imbalance exists with its in-house cell capacity, highlighting that the company will be meeting more than half its M2 mono wafer requirements from third-party mono wafer producers, predominantly located in Asia.

However, M2 mono wafers are in short supply globally, so this may become an issue on supply or pricing for SolarWorld, should demand remain strong overall in 2017, especially for its high-efficiency products or when further cell expansions may be required.

Of course, SolarWorld could not be making this migration to mono-PERC so quickly if it had not been investing an average of around US$27 million per annum over the last 10 years on R&D and first produced PERC cells in 2012.

The company is banking on the higher efficiency mono-PERC modules holding an ASP premium over commodity multi modules and the opportunity the migration brings in introducing new products such as its 'Bisun' bi-facial modules that could become a mainstream line in the coming years.

The transition to a dedicated high-efficiency mono-PERC manufacturer is underway and according to SolarWorld a return to profitability will take another two years. The slogan if achieved, may well be, 'Profit, nothing else!'

Mark Osborne is Senior News Editor at Solar Media

inter solar
connecting solar business | EUROPE

Various products,Visit us at Intersolar Europe2017!

Date：May 31-June 2
Booth：A1-260

SUNTECH
www.suntech-power.com